Swansea University
Prifysgol Abertawe

Staphylococcus epidermidis, Host Immune Factors
and Medical Device Infections

Nerissa Elise Thomas

Submitted to Swansea University in fulfilment of the requirements for
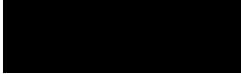the Degree of Master of Research

Swansea University

2022

Summary

Medical device infections, commonly caused by *S. epidermidis* are difficult to treat due to the formation of biofilms on the medical device surface which protect *S. epidermidis* against host immune defences and antibiotics. This project aimed to further our understanding of the interactions between *S. epidermidis*, and fibroblasts or macrophages in the presence of uncoated or whole-blood coated titanium (Ti) and titanium alloy (TiAlV) discs. *S. epidermidis* and fibroblasts/macrophages were co-cultured on Ti or TiAlV discs for 6 and 24 h. The resulting samples were then analysed in one of three ways, 1) supernatant assayed for fibroblast/macrophage cytokine expression; 2) bacterial RNA extracted to analyse transcription of adhesion and biofilm associated genes; 3) samples prepared for visualisation using confocal microscopy and scanning electron microscopy. Cytokine analysis found increased expression of various cytokines involved in the regulation of immune responses to injury and infection, including IL-1β, MCP-1 and MIP-3α or IL-8, MIF, IFN-γ by macrophages and fibroblasts respectively on uncoated Ti, and IL-1α, IL-6 and TNF-α by fibroblasts on pre-coated Ti. RT-qPCR of *S. epidermidis* found that gene transcription differed depending on disc or culturing conditions, indicating that both host cells and surfaces influence attachment and biofilm formation. Microscopy showed the adherence of *S. epidermidis*, macrophages and fibroblasts to discs in monoculture and co-culture, however, by 24 h, fibroblasts detached implying that *S. epidermidis* impacts the ability of fibroblasts to survive on the discs. To conclude, the results suggest that Ti or TiAlV discs, *S. epidermidis* and macrophages/fibroblasts interact with and affect each other during the initial stages of infection, with *S. epidermidis* pathogenesis being further influenced by the presence of host factors. This work is clinically relevant and directly translational to improving the treatment and diagnosis of medical device infections, which remain a burden on the NHS.

Declaration

This work has not previously been accepted in substance for any degree and is not being concurrently submitted in candidature for any degree.

Signed .... Date ....02/03/23...............

This thesis is the result of my own investigations, except where otherwise stated. Where correction services have been used, the extent and nature of the correction is clearly marked in a footnote(s). Other sources are acknowledged by footnotes giving explicit references. A bibliography is appended.

Signed .... Date ....02/03/23.................

I hereby give consent for my thesis, if accepted, to be available for photocopying and for inter-library loan, and for the title and summary to be made available to outside organisations.

Signed .... Date ....02/03/23...................

The University's ethical procedures have been followed and, where appropriate, that ethical approval has been granted.

Signed .... Date ....02/03/23...................

Acknowledgements

Firstly, I would like to thank the Robert Mathys Foundation (Bettlach, Switzerland) for funding my project. I am deeply grateful to my supervisor, Dr Llinos G Harris for her support throughout this project and for taking the time to image the CLSM and SEM samples. I would also like to thank my secondary supervisor, Dr Thomas Wilkinson for his continued guidance with the immunological and cell culture aspects of my project. I feel extremely lucky to have had a supervisory team who believed in me and gave me the opportunity to develop skills and confidence during my time in the lab.

I would like to give a special thanks to the staff of the 5th floor laboratory for their help in the lab and particularly to Dr Josie Parker for allowing me to use the thermocycler for cDNA preparation. A huge thank you also to the Microbiology and Infectious Diseases team, who have been there throughout my research project. I especially want to thank Dr Heather Chick for her help, encouragement, and laughter both inside the lab and out.

Finally, I would like to thank my parents and Harry for their support and motivation throughout the process of researching and writing this thesis.

Contents

List of tables

List of Figures

Abbreviations

Aap	Accumulation associated protein
agr	Accessory gene regulator
AMP	Antimicrobial peptide
ANNOVA	Analysis of Variance
Bp	Base pair
BSA	Bovine Serum albumin
cDNA	Complementary DNA
CFU	Colony forming units
CLSM	Confocal laser scanning microscopy
CoNS	Coagulase negative Staphylococci
CoPS	Coagulase positive Staphylococci
CT	Cycle threshold
DMEM	Dulbecco's Modified Eagle Medium
ECM	Extracellular matrix
EDTA	Ethylenediaminetetraacetic acid
ELISA	Enzyme-linked immunosorbent assay
Embp	Extracellular matrix binding protein
FAK	Focal adhesion kinase
FGF	Fibroblast growth factor
GyrB	Gyrase B
GM-CSF	Granulocyte-macrophage colony stimulating factor
hβD	Human β defensin
HMDS	Hexamethyldisilazane
ICAM-1	Intercellular adhesion molecule 1
IFN	Interferon
IL	Interleukin
IL-1ra	Interleukin-1 receptor agonist

LTA	Lipoteichoic acid
LPS	Lipopolysaccharide
MALDI-TOF	Matrix-assisted laser desorption/ionization coupled to time-of-flight
MCP	Macrophage chemoattractant protein
MEM	Minimum Essential Medium
MSCRAMM	Microbial surface components recognising adhesive matrix molecules
MIF	Macrophage migration inhibitory factor
MIP	Macrophage inflammatory protein
NF-κB	Nuclear factor κB
NHS	National Health Service
NOD-LRR	NOD-like receptor
ODRI	Orthopaedic device related infection
PAMPs	Pathogen associated molecular patterns
PBS	Phosphate buffered saline
PCR	Polymerase Chain Reaction
PGA	Poly-γ-glutamic acid
PIA	Polysaccharide intracellular adhesin
PIPES	2,2-piperazine-1,4-diylbisethanesulfonate
PJI	Prosthetic joint infection
PMA	Phorbol 12-myristate 13-acetate
PRRs	Pathogen recognition receptors
PSM	Phenol soluble modulin
RANTES	Regulated on activation, normal T expressed and secreted
rDNA	Recombinant Deoxyribose nucleic acid
RT-qPCR	Reverse Transcriptase-Quantitative PCR
RNA	Ribonucleic acid
ROS	Reactive oxygen species
RPMI	Roswell Park Memorial Institute medium

S. aureus	*Staphylococcus aureus*
SDS	Sodium Dodecyl Sulphate
SEM	Standard error of the mean
S. epidermidis	*Staphylococcus epidermidis*
TAE	Tris Acetate EDTA
TES	Tris EDTA SDS
TGF-β	Transforming growth factor beta
Ti	Titanium
TiAlV	Titanium Alloy
Ti6Al4V	Titanium-aluminium-vanadium
TLR	Toll-like receptor
TNF	Tumour necrosis factor
TSB	Tryptic soy broth
VCAM-1	Vascular cell adhesion protein 1

Chapter 1. Introduction

1.1 The *Staphylococcus* Genus

The *Staphylococcus* genus was first identified in 1880 when the pus from a knee joint abscess was analysed by the Scottish surgeon, Sir Alexander Ogston in 1880 (translation of original paper, Ogston and Witte, 1984). The name *Staphylococcus* was derived from the Greek words; *staphyle* meaning bunch of grapes and *kokkos* meaning berry due to the bacteria resembling bunches of grapes (translation of original paper, Ogston and Wite, 1984). *Staphylococcus* spp. are Gram-positive spherical bacteria which have an average diameter of 1 μm dependent on culture conditions (Winslow *et al*., 1920; Cowan and Shaw, 1949). In 1884, Friedrich Julius Rosenbach divided the *Staphylococcus* genus into two species; *Staphylococcus aureus,* which formed gold colonies and *Staphylococcus albus,* which produced white colonies (Rosenbach, 1884). The species *S. albus* was later renamed *S. epidermidis* due to its common residency on the human epidermis (Welch, 1891). As more information became available and more species were identified, the system was updated to group *Staphylococcus* species into coagulase-positive Staphylococci (CoPS) and coagulase-negative Staphylococci (CoNS) based on the presence of the enzyme coagulase (Figure 1.1.; Fisk, 1940).
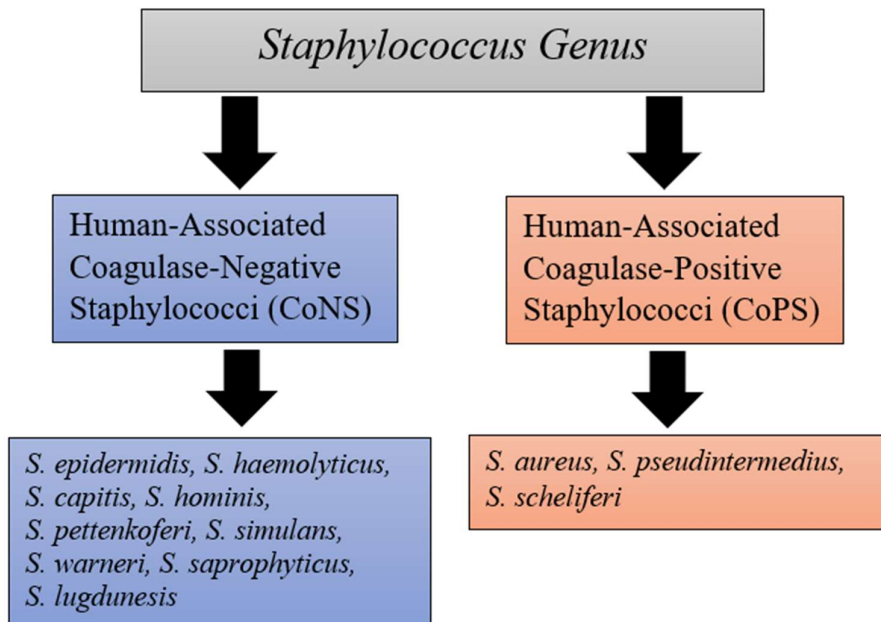
Figure 1.1. Characterisation of a selection of human health related *Staphylococcus* species by the presence of coagulase. Information taken from Becker *et al.* (2014).

Formerly, the coagulase test was used to differentiate between *Staphylococcus* spp. considered pathogenic (coagulase-positive) and non-pathogenic (coagulase-negative) bacteria (Cruickshank, 1937). However, it soon became clear that some CoNS species are capable of causing serious infection (Spink and Vivino, 1942). Coagulase negative Staphylococci have since been associated with a wide range of clinical issues including septic arthritis, orthopaedic medical device infections and shunt device infections (Currey, 1962; Perrin and McLaurin, 1967; Dobbins *et al.*, 1988).

The association between numerous *Staphylococcus* spp. and human infection reinforces the need for accurate Staphylococcal identification in clinical settings (Wieser and Busse, 2000). In previous years, coagulase negative bacteria were identified using a biochemical testing scheme constructed by Kloos and Schleifer (1974) in conjunction with fatty acid analysis (Wieser and Busse, 2000). This however, presented issues differentiating between many CoNS sp. due to similarities between test results and large overlaps in fatty acid composition (Stoakes *et al.*, 1994; Wieser and Busse, 2000). Although 16S DNA sequencing can more accurately identify *Staphylococcus* strains than other techniques, it was considered too expensive

and laborious for routine use (Wiessner and Busse, 2000). Using polymerase chain reaction (PCR) alone or alongside sequence analysis and hybridisation is another successful identification method (Hamels *et al*., 2001). However, this method requires the use of numerous primers which makes multiplex PCR an expensive, complex and lengthy process (Hamels *et al*., 2001). Currently in the UK, clinical laboratories still implement colony identification and coagulase tests as a means of identification for *Staphylococcus* spp. (Public Health England, 2020a). Further analysis of *Staphylococcus* spp. to species level can also be carried out using MALDI-TOF mass spectrometry or next generation sequencing, when required (Public Health England, 2020a). Despite this, the search for more efficient, rapid and inexpensive diagnostic tools for use within clinical environments is continuing and is particularly important to improve the accuracy and cost and time issues associated with current methods (Sah *et al*., 2018).

1.2 *S. epidermidis* and the Human Microbiome

The skin is an important organ of the human body, acting as a barrier and protecting the body from pathogens (Clark, 1926). This barrier is colonised by a variety of bacterial species which vary between individuals and are dependent on the location on the skin site (Grice *et al*., 2009). Collectively, the microbes inhabiting the human skin are referred to as the skin microbiome (Lai *et al*., 2010). Initial studies using culture-based methods to investigate the skin microbiome indicated a strong bias toward Staphylococci spp. (Evans *et al.,* 1950; Grice *et al*., 2009). However, the development and application of molecular approaches has allowed for a better representation of the natural skin flora without culture bias (Turnbaugh *et al*., 2007; Grice *et al*., 2009; Gao *et al*., 2007). Studies have shown that the majority of bacterial species isolated from the skin microbiome belong to the *Corynebacteria, Propionibacteria* and *Staphylococcus* genera (Grice *et al*., 2009).

Staphylococcus epidermidis is a commensal bacterium which is commonly isolated from human skin (Evans *et al*., 1950). In comparison to its pathogenic lifestyle, less is known about the colonising commensal mechanisms of *S. epidermidis* (Otto, 2009). According to Collado *et al*. (2016), *S. epidermidis* makes first contact with the human skin *in utero* where it is present in amniotic fluid. Then, within only a few days of

birth, *S. epidermidis* colonises human skin and becomes a part of the natural flora (Dominguez-Bello *et al*., 2010). Keratinocytes represent one of the most abundant cells in the human skin and are important for skin structure and host immunity (Figure 1.2.; Eckert and Rorke, 1989; Pivarcsi *et al*., 2004). Upon contact with the skin, peptidoglycan, or lipoproteins from *S. epidermidis* are recognised by toll-like receptor (TLR) 2 which is present on keratinocytes (Baker *et al*., 2003). This recognition results in a host protective immune response and induces host cell production of antimicrobial peptides (AMPs) such as human β defensin (hβD)- 2 and hβD-3 to inhibit bacterial growth (Lai *et al*., 2010). For pathogenic bacterial species, this activation of TLRs would result in an increase production of proinflammatory cytokines, leading to an inflammatory response (Lai *et al*., 2009). However, as a commensal species, *S. epidermidis* uses host immune evasion mechanisms to inhibit this inflammatory response (Lai *et al*., 2009). Following TLR activation, *S. epidermidis* negatively regulates TLR signalling using lipoteichoic acid (LTA) (Lai *et al*., 2009). This process involves the LTA-TLR2 suppression of TLR3 using the negative regulatory factor, TNF receptor-associated factor 11 (Lai *et al*., 2009). Overall, this reduces the release of cytokines from keratinocytes, thereby allowing *S. epidermidis* to successfully colonise the skin without triggering an inflammatory immune response (Lai *et al*., 2009).
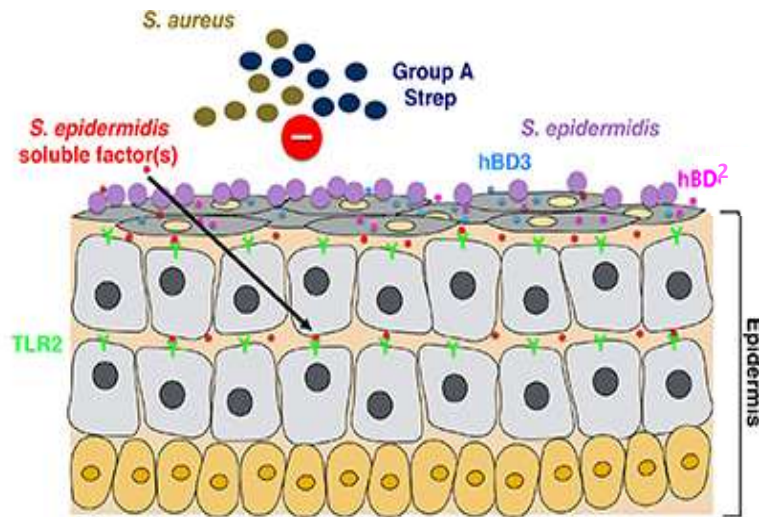
Figure 1.2. **The host keratinocyte response to *S. epidermidis* colonisation.** Peptidoglycans or soluble factors such as lipoproteins from *S. epidermidis* interact with and bind to TLR2 receptors on keratinocytes. This in turn, initiates the production of antimicrobial peptides such as hβD-2 and hβD-3 by host cells which have a prevent colonisation of the skin by other bacteria such as *S. aureus* and *Streptococcus* spp. Image taken from Nguyen *et al.* (2017).

As a commensal species, *S. epidermidis* aids the skin's resistance to specific bacterial infections by both increasing keratinocyte expression of AMPs and by producing and secreting its own AMPs (Lai *et al*., 2010; Cogen *et al*., 2010a.). One of the main forms of AMP produced by *S. epidermidis* are phenol soluble modulins (PSMs) which act to enhance the antibacterial activity of the skin's surface (Cogen *et al*., 2010a.). In particular, Cogen *et al*. (2010b) noted that *S. epidermidis* PSM-δ and PSM-γ peptides both interact with host AMPs and exhibit antibacterial action by causing the membrane leakage of other bacterial species. Another antibacterial mechanism of *S. epidermidis* is the hydrolysation of sebum triglycerides to produce free fatty acids which have antibacterial activity against many bacterial species (Götz *et al*., 1998; Georgel *et al*., 2005). In addition to this, some free fatty acids including lauric acid and palmitic acid also trigger the production of hβD-2 which further enhances the skins antimicrobial activity (Nakatsuji *et al*., 2010). *S. epidermidis* also produces bacteriocins such as the lantibiotics; epidermin, Pep5 and epilacin K7 (Sahl and Brandis, 1981; Van De Kamp *et al*., 1995; Bierbaum *et al*., 1996). Some bacteriocins secreted by *S. epidermidis* are particularly beneficial as they can inhibit a wide range of bacterial species including *S. aureus* (Jang *et al*., 2020). According to Iwase *et al*. (2010), *S. epidermidis* is known to secrete serine proteases such as Esp, which can interfere with *S. aureus* colonisation and biofilm production by degrading essential proteins. *S. epidermidis* also secretes a thiolactone-containing peptide which inhibits the *S. aureus* accessory gene regulator (*agr*) quorum sensing system and controls the production of many *S. aureus* virulence factors (Otto *et al*., 1999). Alongside impacting *S. aureus* colonisation, Xia *et al.* (2016) stated that *S. epidermidis* also prevents skin inflammation caused by *Propionibacterium epidermidis* through the induction of a single stranded non-coding RNA sequence, miR-143, which regulates gene expression. As a result, the anti-inflammatory properties of *S. epidermidis* are now being explored as possible treatments for numerous inflammatory conditions such as Acne vulgaris (Xia *et al*., 2016).

In order to protect itself against the host immune response, *S. epidermidis* has developed numerous protective strategies (Lai *et al*., 2010). According to Lai *et al*. (2007), one protective measure is the production of metalloprotease, SepA, which can degrade the host AMP, Dermcidin. In addition, *S. epidermidis* utilises a three-component AMP sensing system to protect against the action of hβDs (Lai *et al*.,

2010). This sensing system allows *S. epidermidis* to alter the net charge of the cell membrane, thus repelling positively charged host AMPs (Lai *et al*., 2010). A further protective strategy of *S. epidermidis* against the host immune system is the formation of biofilms (Le *et al*., 2018).

1.3 *S. epidermidis* Adhesion and Biofilm Formation

It has long been known that *S. epidermidis* forms biofilms on a wide range of surfaces including those of medical devices and host cells (Khoury *et al*., 1992; Le *et al*., 2018). The formation of a biofilm involves a sequence of processes including adherence, accumulation, maturation, and detachment (Figure 1.3.; Fey and Olson, 2010). Firstly, *S. epidermidis* cells attach to a surface through direct binding or receptor-mediated binding mechanisms (Yao *et al*., 2005). The initial adhesion of *S. epidermidis* to a surface is influenced by the hydrophobicity and charge of the bacterial cell surface and is mediated by several surface proteins (Gilbert *et al.,* 1991; Vacheethasanee *et al*., 1998). Specifically, cell surface proteins such as microbial surface components recognising adhesive matrix molecules (MSCRAMM) allow for attachment to surfaces by forming non-covalent interactions with host tissues or proteins (Patti *et al*., 1994). For *S. epidermidis* proteins including Aae (Heilmann *et al*., 2003), AtlE (Heilmann *et al*., 1997) Embp (Williams *et al*., 2002), Fbe (Nilsson *et al*., 1998), GehD (Bowden *et al*., 2002) SdrF (McCrea *et al*., 2000) and SdrG (McCrea *et al*., 2000) allow binding to extracellular matrix (ECM) proteins such as fibronectin, vitronectin and collagen.

The second step in biofilm formation is accumulation (Yao *et al*., 2005). During accumulation, *S. epidermidis* cells proliferate and accumulate alongside extracellular matrix molecules to build a structured biofilm (Yao *et al*., 2005). For some *S. epidermidis* strains, biofilm accumulation is associated with the production of polysaccharide intracellular adhesin (PIA) (Mack *et al*., 1996; Heilamann et al, 1996). Polysaccharide intracellular adhesin is an unbranched homopolymer of N-acetylglucosamine residues produced by the *icaADBC* operon which allows for attachment between *S. epidermidis* cells (Mack *et al*., 1996). In PIA-dependent *S. epidermidis* strains, PIA has been described as one of the major virulence factors and is thought to significantly contribute to the chronic nature of the biofilms (Vuong

et al., 2004). In addition to its role in biofilm accumulation, PIA also acts as a haemagglutinin, as a mediator of biocide resistance and as an inhibitor of neutrophil-dependent killing (Mack *et al*., 1999; Vuong *et al*., 2004; Begun *et al*., 2007).

It has however, been noted that PIA is not essential for *S. epidermidis* biofilm formation and that strains deficient in *ica* genes are still able to form functional biofilms (Francois *et al*., 2003). While PIA-dependent biofilm strains are most common clinically, Rohde *et al*. (2007) reported that 27% of analysed clinical strains produced protein-dependent biofilms. These protein-dependent biofilms are reliant on various proteinaceous factors such as accumulation-associated protein (Aap) (Rohde *et al*., 2005) and extracellular matrix-binding protein (Embp) (Williams *et al.,* 2002). Accumulation associated protein is a 220 kDa protein which is processed through protein cleaving by bacterial and host proteases into its active form (Rohde *et al*., 2005). In its active form the Aap B domain forms Zn^{2+} -dependent dimers with neighbouring bacterial cells (Rohde *et al*., 2005). This, therefore, allows for intercellular adhesion and biofilm aggregation. In embp-dependent biofilms, the 1 MDa protein utilises FIVAR and FIVAR-GA domains not only for binding to fibronectin but also for intercellular adhesion during biofilm accumulation (Christner *et al*., 2010; Le *et al*., 2018).

During maturation, channels and mushroom-like structures are formed which allow nutrients to be delivered to bacteria in all layers of the biofilm (Hermanowicz, 2001). The production of these channels is mediated through quorum sensing which utilises PSMβ peptides as major factors (Wang *et al*., 2011). The detachment of singular cells or cell clusters from the biofilm, allows *S. epidermidis* to spread and colonise new sites (Yao *et al*., 2005). According to Vuong *et al*. (2004b) biofilm detachment is dependent on the *agr* gene and is involved with the production of PSMs. Specifically, PSM-γ, also known as δ-toxin is thought to strongly contribute to the detachment of cells from an *S. epidermidis* biofilm (Vuong *et al*., 2003).
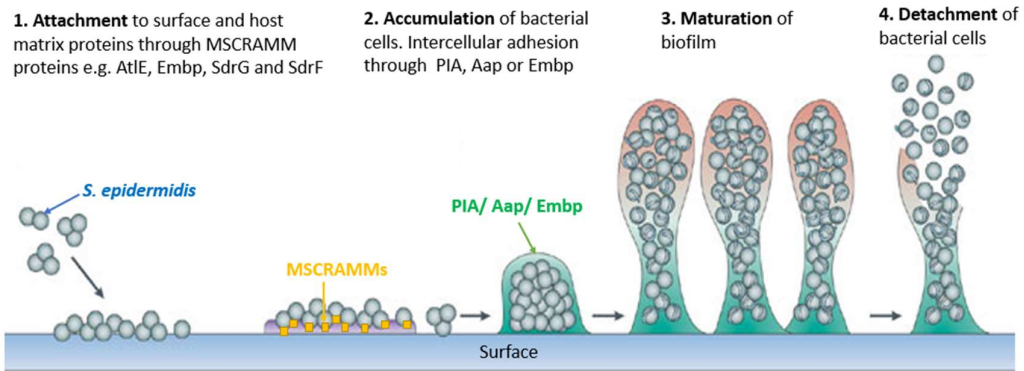
Figure 1.3. *S. epidermidis* **biofilm formation.** The process occurs in four steps: attachment, accumulation, maturation, and detachment. Initially, the bacterial cells will attach to the polymer surface or to host matrix proteins through MSCRAMM proteins including AtlE, Embp, SdrG and SdrF. The cells will then proliferate and adhere to one another within a polysaccharide- or protein-based extracellular matrix. *S. epidermidis* cells will then mature forming channels and mushroom-like structure for nutrient delivery. Finally, detachment of *S. epidermidis* cells allows for bacterial colonisation of new sites. Image adapted from Otto (2009).

In many biofilms, quorum sensing plays an integral role by providing a means of 'communication' within the bacterial community (Hammer and Bassler, 2003). In *Staphylococcus* species, two quorum sensing systems, the *agr* system and the LuxS/AI-2 system, are associated with biofilm formation (Vuong *et al.,* 2003; Xu *et al.*, 2006). The *agr* system is composed of a two-component signalling system and a pheromone production system and is particularly important in the regulation of numerous virulence factors (Vuong *et al.*, 2003). Olson *et al.* (2014) noted that *S. epidermidis* has three types of *agr* system, *agr* type I, type II and type III and thus has three autoinducing peptide signals. Investigations by Olson *et al.* (2014) have revealed cross talk between the *agr* type I and II systems, and type I and III systems. However, there is no evidence to suggest cross talk between *agr* type II and III systems despite similarities in signals (Olson, *et al.*, 2014). The *agr* locus consists of the *agrBDCA* operon which encodes for the machinery essential to detect and produce autoinducing peptides (Olson *et al.*, 2014). The *agrBDCA* operon is important for the production and detection of autoinducing peptide signals and includes two promoters, P_2 and P_3 (Olson *et al.*, 2014). Promoter P_3 is particularly significant as it promotes the expression of *RNAIII* which in turn acts as the main effector of the system and encodes for the production of PSMγ (Olson *et al.*, 2014). Overall, the *agr* system demonstrates a regulatory effect on *S. epidermidis* colonisation and primary attachment during

biofilm formation by influencing AtlE and PSMγ production (Vuong *et al*., 2003). It has been noted that disabling the *agr* system in *S. epidermidis* leads to increased biofilm formation and function by increasing adhesion through AtlE and decreasing PSMγ-mediated biofilm detachment (Vuong *et al*., 2003).

The LuxS/AI-2 system is present in many Gram-positive and -negative species and species and is thought to allow for 'communication' between bacterial species (Winans and Bassler, 2002). In *S. epidermidis* specifically*,* the *luxS* gene regulates *ica* gene transcription which results in PIA production (Xu *et al*., 2006). Similar to the *agr* system, the LuxS/AI-2 system has a repressive effect on *S. epidermidis* biofilm formation, and thus, *S. epidermidis* strains deficient in the LuxS/AI-2 system show increased biofilm formation (Xu *et al*., 2006).

Biofilms improve the ability of *S. epidermidis* to survive in a range of otherwise hostile environments (Yao *et al*., 2005). The increased biofilm formation of *S. epidermidis luxS* and *agr* gene mutants is known to result in increased virulence (Xu *et al*., 2006). Within biofilms *S. epidermidis* strains can alter their gene expression, allowing for better adaptation to extreme environments (Yao *et al*., 2005; Gomes *et al*., 2011). For example, *S. epidermidis* biofilms on the human skin have adapted to extremes of salinity by producing osmoprotective factors which protect bacterial cells (Yao *et al*., 2005). Bacteria in biofilms also have increased resistance to antibiotics and immune responses (Nickel *et al*., 1985; Darouiche *et al*., 1994). This, in part, could be due to decreased diffusion of some antibiotics and solutes through the biofilm's polysaccharide matrix (Stewart, 1998; Daraouiche *et al*., 1994). However, it has been noted that many antibacterial agents are sufficiently able to diffuse into the biofilm and thus additional resistance mechanisms are likely in place (Dunne *et al*., 1993; Rani *et al*., 2005).

1.4 *S. epidermidis* Medical Device Infections

The infection of medical devices such as intravenous catheters, heart valves, shunts and joint prosthesis is strongly associated with morbidity and mortality (Harris *et al*., 2016). As an opportunistic pathogen, *S. epidermidis* is strongly associated with medical device infections such as orthopaedic device related infections (ODRIs; Welch, 1891; Post *et al*., 2017). According to Trampuz and Zimmerli (2005) CoNS

are responsible for up to 43% of prosthetic joint infections (PJIs). A recent study of sonication fluid from 97 PJI patients identified *S. epidermidis* in 13 % of samples (Street *et al*., 2017).

The occurrence of ODRIs is known to be influenced by a large range of patient factors such as immunosuppression, diabetes, renal failure, smoking, heart or lung disease and obesity and surgical factors including the surgical site and procedure (Hoekman *et al*., 1991; Berbari *et al*., 1998; Hansen and Rand, 1998; Saleh *et al*., 2002). In the past, PJIs were recorded in 1.5% and 2.5% of patients undergoing total hip arthroplasty and total knee arthroplasty respectively (Hanssen and Rand, 1998). However, in recent years, PJI infections in Europe have decreased to 1.4% (Marang-Van de Mheen *et al*., 2017). Despite this, the requirement for revision surgery due to orthopaedic device related infections has increased by 2.3-fold for total hip arthroplasties and 2.5-fold for total knee replacements between 2003 and 2014 (Lenguerrand *et al*., 2017a; Lenguerrand *et al*., 2017b). This has resulted in a high burden on the national health service (NHS). In 2012, the NHS spent approximately £27.4 million on total knee arthroplasty revision surgery alone (Kallala *et al*., 2015). Overall, the prevalence of ODRIs in the United States varies between 2.0-2.4%, however, ODRI prevalence is rising due to increasing requirement for orthopaedic device implantation (Kurtz *et al*., 2012). Patients with PJIs often present with pain, swelling and heat at the implant area alongside increased inflammatory markers (Sanzen and Carlsson, 1989; Public Health England, 2020b). Despite this, diagnosing ODRIs can be challenging (Metsemakers *et al*., 2018). Therefore, a combination of medical history, host physiology, clinical presentation, laboratory tests and a biopsy culture are often required for accurate diagnosis (Metsemakers *et al*., 2018). The establishment of biofilms of medical device surfaces is integral to the role of *S. epidermidis* as an opportunistic pathogen (Figure 1.4.; Vuong and Otto, 2002).
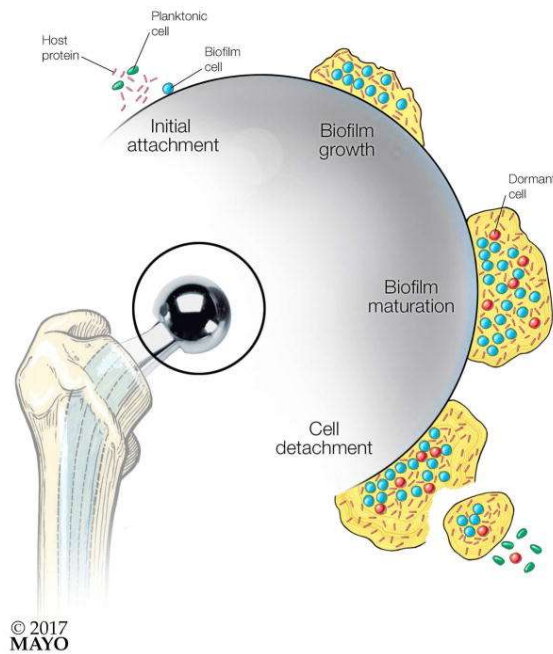
Figure 1.4. The stages of development of an *S. epidermidis* biofilm on a prosthetic joint. *S. epidermidis* planktonic cells colonise the prosthetic joint and begin to accumulate. The biofilm matures, allowing for the protection of biofilm bacteria against many host factors and antibiotics. Finally, cells detach from the biofilm and spread to infect other surfaces within the host. Image taken from Wi and Patel (2018).

Once a biofilm has established on the medical device surface, treatment of the infection can become challenging (Lorenzetti *et al*., 2015). Often, the removal of the infected device and the long-term prescription of antibiotics is the only successful method to treat medical device infections (Lorenzetti *et al*., 2015). Difficulty treating medical device infections has been amplified in recent years due to the emergence of numerus antibiotic resistant strains, such as methicillin-resistant *S. epidermidis* (Knafl *et al*., 2017). Diekema *et al*. (2001) noted that within United States hospitals approximately 75-90% of *S. epidermidis* isolates are methicillin resistant. Additional challenges in the treatment of medical device infection treatment arise due to the presence of bacterial biofilms (Nickel *et al*., 1985). These biofilms can increase antibiotic resistance or reduce susceptibility to a variety of antibiotic treatments (Nickel *et al*., 1985). Within the biofilm, *S. epidermidis* shows a higher rate of horizontal gene transfer which aids the spreading of antibiotic resistance genes (Yoda *et al*., 2014). For example, in patients with ODRIs who were not cured after 26 months, *S. epidermidis* isolates had a higher prevalence of accessory genes such as the biofilm

associated *bhp* gene and the antiseptic resistance *qacA* gene (Post *et al.*, 2017). Despite this, numerous studies have demonstrated successful treatment of *S. epidermidis* medical device infections using a combination of antibiotics such as rifampin, vancomycin, clindamycin, cephalothin, teicoplanin and ofloxacin (Monzón *et al.*, 2002; Vergidis *et al.*, 2011). To improve medical device infection treatment, new methods are currently in development, and include pre-coating medical device surfaces, nanotechnology, and anti-biofilm AMPs aimed to target quorum sensing, break down the biofilm matrix and increase antibiotic penetration into the biofilm (Li *et al.* (2021).

Medical devices are commonly constructed from titanium (Ti) or titanium alloy (TiAlV) as they provide superb mechanical properties, resistance to corrosion and biocompatibility (Cao *et al.*, 2018). However, these surfaces are still susceptible to colonisation by bacteria such as *S. epidermidis* (Figure 1.5.)*,* resulting in medical device infections (Cao *et al.*, 2018).
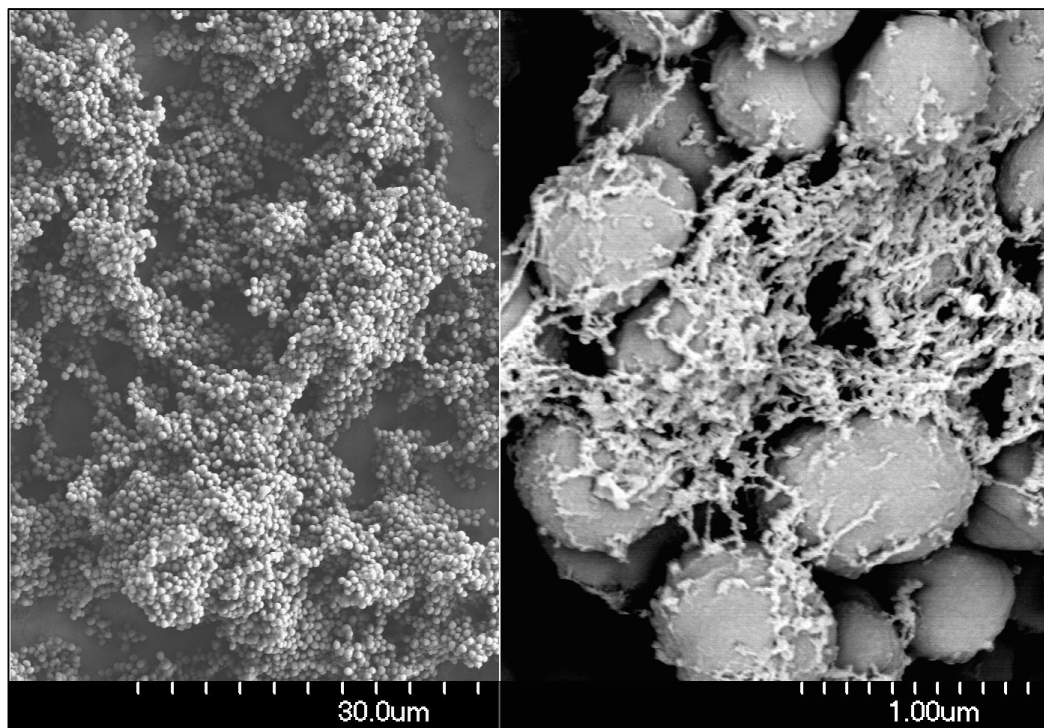
Figure 1.5. Scanning electron microscopy images of an *S. epidermidis* 1457 biofilm with PIA on Ti surface. Images obtained from Dr Llinos G Harris.

Despite the risk of other complications such as lack of integration, inflammation and total rejection, bacterial colonisation remains the largest cause for medical device

removal (Oliveria *et al*., 2018). Most commonly, bacteria colonise and contaminate the medical device's surface prior to or during surgical insertion, likely originating from the microbiome of the patient or healthcare worker or from the surgical environment (McCann *et al*., 2008; Zheng *et al*., 2018). To overcome this issue, bactericidal implants which use antimicrobial agents on device surfaces have been trialled to prevent bacterial colonisation (Cao *et al*., 2018). However, this has not proven successful for long term medical devices as the antimicrobial agent depletes over time (Cao *et al*., 2018). Previous studies have investigated a variety of coatings on implant surfaces such as hydrophobin (Artini *et al*., 2017), trimethylsilane plasma (Ma *et al*., 2012), polyastaxanthin derivatives (Weintraub *et al*., 2018) and silver (Kuehl *et al*., 2016) to successfully reduce *S. epidermidis* biofilm formation. Although, they present significant drawbacks such as increased antibiotic resistance and poor long-term stability (Weintraub *et al*., 2018).

1.5 The Host Immune Response

One of the first defences against infection is the human skin, which acts as a protective barrier against pathogens (Clark, 1926). Damage to this barrier for example through wounding, triggers the host immune response (Coates *et al*., 2018). The immune system is widely described as two arms, the innate immune system and the adaptive immune system which work cooperatively to generate a host protective response (Takeda and Akira, 2005; Turvey and Broide, 2010). Both arms of the immune system play integral roles in pathogen elimination through the identification of microbial pathogens as non-self and the activation of immune responses (Figure 1.6.; Takeda and Akira, 2005).
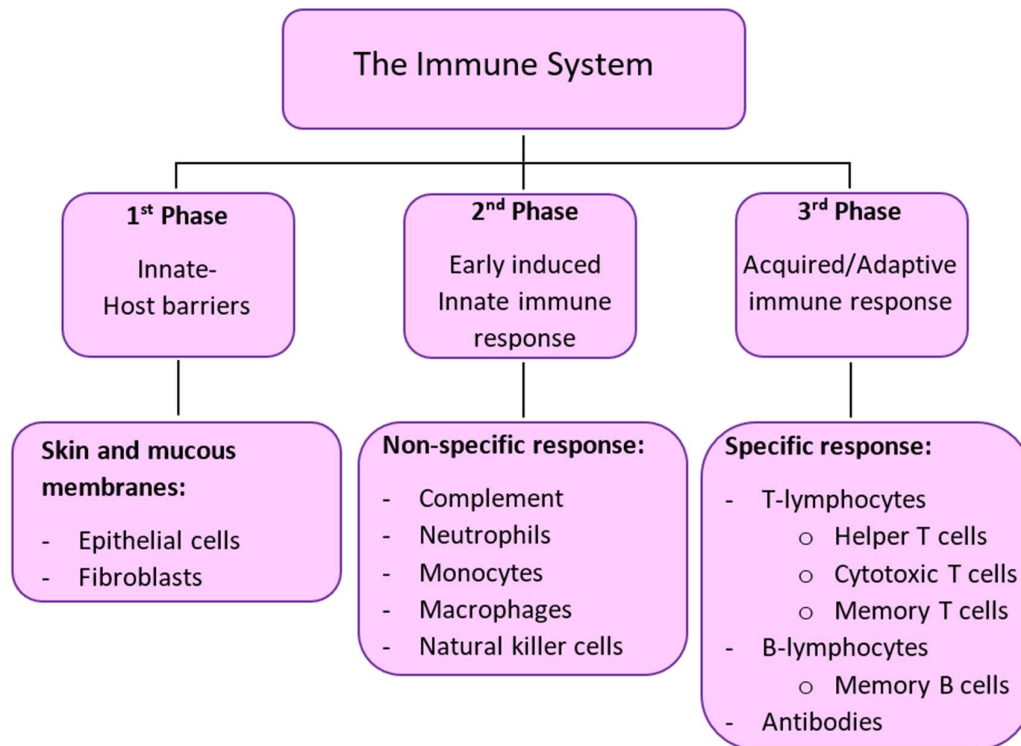
Figure 1.6. **A schematic of the three main phases in the host immune response**. Skin and mucous membranes act as the first barriers to infection by inducing an innate immune response. This is followed by the induction of an innate immune response including the induction of the complement cells, natural killer cells and phagocytic cells such as neutrophils and macrophages. The final phase of the immune response is induction of the adaptive immune response. This is a specific response mediated by subsets of T-lymphocytes, B-lymphocytes, and antibodies.

Initially during the innate immune response, pathogen associated molecular patterns (PAMPs) are recognised by pathogen recognition receptors (PRRs) present on host cells such as monocytes, macrophages, neutrophils, dendritic cells, fibroblasts and endothelial cells (Mizel *et al*., 2003; Fournier and Philpott, 2005). These PRRs include Toll-like receptors (TLRs) and NOD-like receptors (NOD-LRRs). As gram-positive bacteria, *Staphylococcus* spp. are primarily detected by TLR-2 which recognises PAMPs such as lipoproteins and peptidoglycan or NOD-2 which also detects peptidoglycan (Girardin *et al*., 2003; original paper cited in Fournier and Philpott 2005). This results in signal transduction leading to the production of inflammatory cytokines and chemokines through the activation of nuclear factor κB (NF-κB), the activation of monocytes or macrophages and the initiation of the adaptive immune response (Fournier and Philpott, 2005).

Cytokines and chemokines play a critical role in the immune response by acting as signalling molecules allowing intercellular communication between a numerous cells including monocytes, macrophages, fibroblasts and endothelial cells (Arango Duque and Descoteaux, 2014). Cytokines produced in response to infection bind to receptors on target cells, initiating a signalling cascade which, in turn alters cellular function (Arango Duque and Descoteaux, 2014). Many cytokines such as tumour necrosis factor (TNF), interleukin (IL)-1, IL-6, IL-8 and IL-12 have pro-inflammatory effects such as initiating recruitment of inflammatory cells, production of acute inflammatory response proteins, fever and vascular permeability (original papers cited in Arango Duque and Descoteaux, 2014). Meanwhile, other cytokines including, IL-1 receptor agonist (IL-1ra), IL-4, IL-10 and transforming growth factor beta (TGF-β) have anti-inflammatory effects such as supressing the effect or production of inflammatory cytokines, supressing antigen presentation and supressing activation of macrophages (Opal and Depalo, 2000; Arango Duque and Descoteaux, 2014). Chemokines have many functions but are notably responsible for the migration of immune cells to target areas using chemotaxis (Comeford and McColl, 2011; Arango Duque and Descoteaux, 2014). For example, macrophage inflammatory protein-2α (MIP)-2α secreted by macrophages plays a role in the recruitment of neutrophils to the area of infection (original papers cited in Arango Duque and Descoteaux, 2014).

Another important aspect of the innate immune system is the complement system which can be activated through three pathways; the classical pathway, the lectin pathway and the alternative pathway (Janeway *et al*., 2001). Some complement proteins such as C3a and C5a are peptide mediators of inflammation which can act as a chemoattractant by recruiting phagocytes to the site of the infection (Janeway *et al*., 2001). During *S. epidermidis* infection by PIA-dependent strains, increased expression of both C3a (Kristian *et al*., 2008) and C5a (Rand *et al*., 2015) have been observed, suggesting a role for PIA in complement activation. Other complement proteins including C3b can bind to receptors pathogens including *S. epidermidis* and opsonise it for engulfment by phagocytes (Janeway *et al*., 2001; Kristian *et al*., 2008). Finally, complement proteins such as C5b, C6, C7, C8 and C9 have a particularly important role in the development of the membrane-attack complex which creates pores in the cell walls of Gram-negative bacteria, causing cell lysis (Janeway *et al*., 2001).

1.5.1 Macrophages and the Host Immune Response

In the late 19th century, the macrophage was first identified by Ilya Metchnikoff as an evolutionary conserved phagocyte (Metschnikoff, 1887). Phagocytic cells such as monocytes, macrophages, neutrophils play a key role in the removal of pathogenic cells by engulfing microbial pathogens and initiating the adaptive immune response (Greenberg and Grinstein, 2002; Gasteiger *et al*., 2017). Monocytes are typically derived from stem cells in the bone marrow before circulating in the blood with a half-life of approximately 70 hours (Arango Duque and Descoteaux, 2014). Within the blood, monocytes act as immune effector cells and migrate to areas of infection upon activation of PRRs or chemokine receptors on other immune cells (Geissmann *et al*., 2010). Upon reaching areas of high inflammation, monocytes differentiate into macrophages which have many functions such as monitoring surrounding tissue, maintaining homeostasis, cytokine production and phagocytosis of pathogenic cells (Gasteiger *et al*., 2017). The activity of these macrophages is determined through further activation of differentiated M0 macrophages into M1 (classically activated) macrophages which play a role in removal of pathogenic bacteria or M2 (alternatively activated) macrophages which reduce inflammation and initiate tissue repair (Figure 1.7.; Orekhov *et al*., 2019).
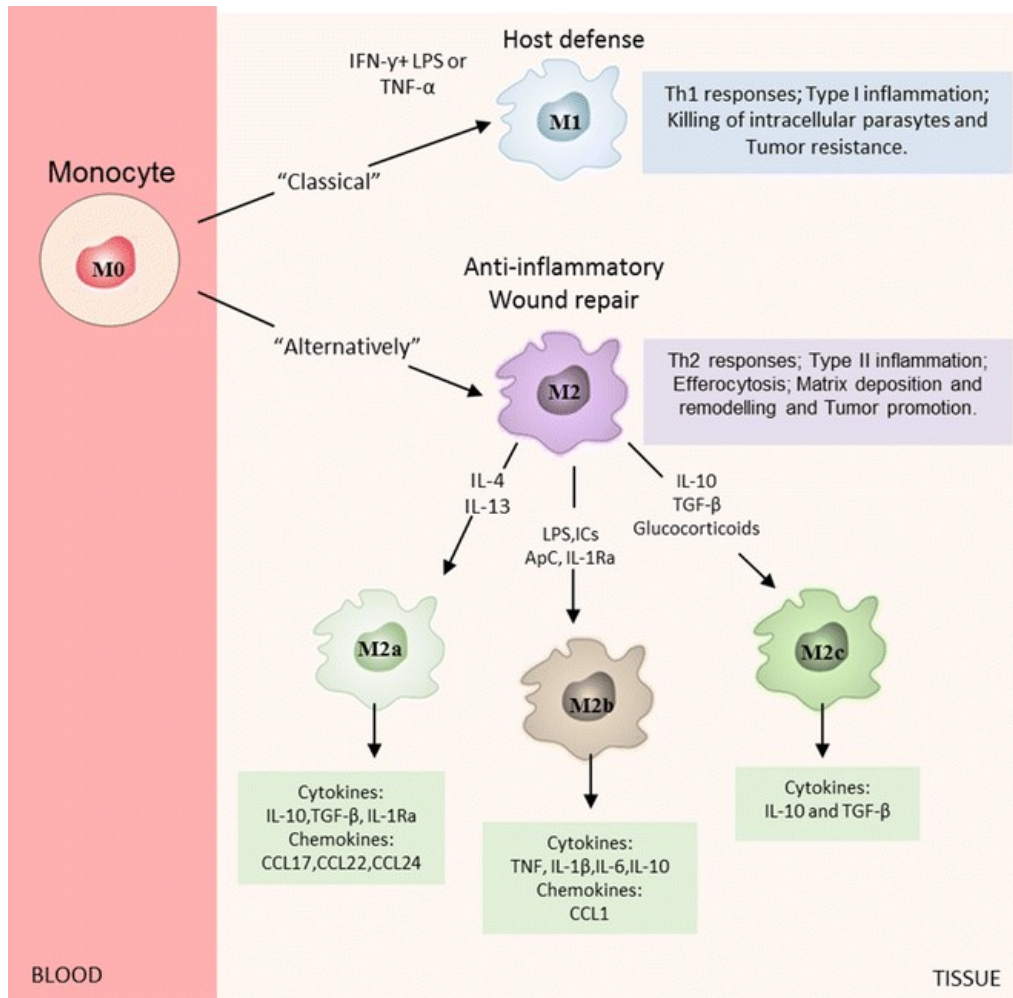
Figure 1.7. The differentiation of M0 macrophages into M1 and M2 macrophages in host tissue. M0 macrophages are classically activated into M1 macrophages by LPS, IFN-ɣ and TNF-α. M1 macrophages display host protective responses including increased inflammation, antitumour activity and antimicrobial activity. M0 macrophages can also be alternatively activated into M2 macrophages by IL-4 and IL-13 (M2a), LPS, immune complexes (ICs), antigen presenting cells and IL-1ra (M2b) and IL-10, TGF-β and glucocorticoids (M2c). Activated M2 macrophages display anti-inflammatory and wound healing activity within the host. Image taken from Navegantes *et al.* (2017).

Upon initiation of the innate immune response and the release of cytokines such as IFN-γ, TNF-α by T helper 1 cells or the presence of bacterial components including LPS or peptidoglycan, M0 macrophages are activated into M1 macrophages (Ma *et al.*, 2003). The presence of *S. epidermidis* bacterial cells results in increased macrophage expression of pro-inflammatory cytokines such as TNF-α, IFN-γ, IL-1, IL-6, IL-8, GM-CSF and IL-13, which alert other immune cells to the infection and

also encourage differentiation into M1 cells (Cerca *et al.,* 2011; Spiliopoulou *et al*., 2012). One of the main functions of M1 macrophages is the removal of pathogens through phagocytosis and the synthesis of nitric oxide (Mosser, 2003). Phagocytosis is a complex process which varies depending on the response of the pathogen being ingested (Aderem and Underhill, 1999). Firstly, macrophage recognition of PAMPS through receptors including scavenger receptors, complement receptors and Fc receptors triggers the internalisation of the pathogen within a phagosome (Aderem and Underhill, 1999). The phagosome then binds with lysosomes, becoming a phagolysosome, in which the pathogen is killed through decreased pH, lysis, reactive oxygen species (ROS) and antimicrobial peptides (Aderem and Underhill, 1999). This, however, is not always an efficient method as pathogens such as *S. aureus* and *S. epidermidis* employ immune evasion strategies to survive within macrophages and escape cell death (Figure 1.8.; Shiau and Wu, 1998; Schommer *et al*., 2011; Thurlow *et al*., 2011).

Macrophage *S. aureus* killing mechanisms
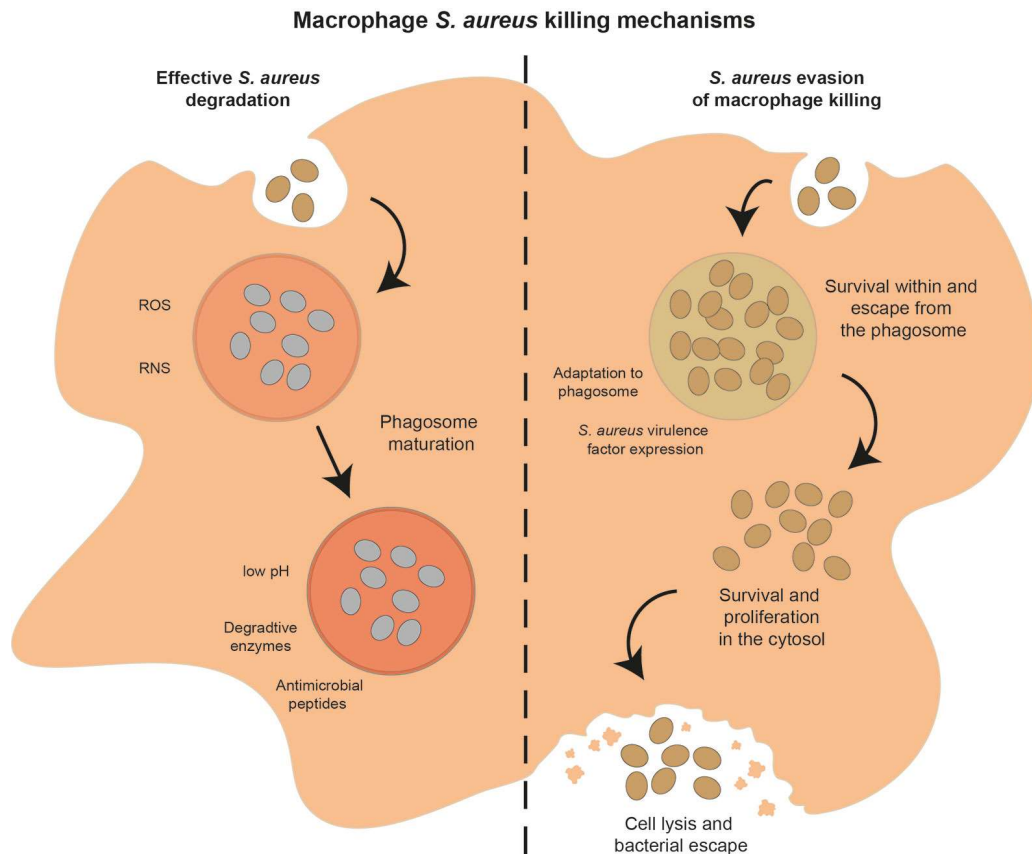
Figure 1.8. The effective and ineffective phagocytosis of *S. aureus* cells by macrophages. *S. aureus* cells are effectively degraded in the phagosome through reactive oxygen species (ROS), reactive nitrogen species (RNS), low pH, degradative enzymes, and antimicrobial peptides (left). However, some *S. aureus* cells can evade phagocytosis by surviving in the phagosome, proliferating within the cytosol, and escaping the macrophage cell (right). Image taken from Pidwill *et al*. (2021).

In addition to roles within the innate immune response, macrophages also activate the adaptive immune response by acting as antigen presenting cells (Navegantes *et al*., 2017). According to Baker *et al*. (2002), macrophages act as the main antigen presenting cells responsible for clearing both necrotic and apoptotic matter in areas of inflammation. Following phagocytosis of a pathogen, macrophages present pathogen-derived peptides through major histocompatibility complex class II, which in turn leads to the activation of naïve T-cells and B-cells through T-cell and B-cell receptors (Underhill *et al*., 1999; Kaiko *et al*., 2008). Upon activation, both T-cells and B-cells play critical roles in clearing infected cells and producing memory cells which protect the host from future infection (den Haan *et al*., 2014).

Depending on location and microenvironment, macrophages differentiate into site-specific cells such as Kuppfer cells in the Liver, alveolar macrophages in the lungs, histiocytes in connective tissue or Langerhans cells in the skin (Italiani and Boraschi, 2014). While many tissue macrophages are derived from differentiated monocytes, some macrophages originate from macrophage precursors, developed during embryonic development (Mass *et al*., 2016). These resident macrophages show variation in functions depending on location. For example, in the skin, Langerhans cells are primarily involved in immune homeostasis and wound repair, whereas in the liver, Kupffer cells remove not only respond to microbial infection but also dead red blood cells from the blood stream (Willekens *et al*., 2005; West and Barnett, 2018).

1.5.2   Fibroblasts and the host immune response

Fibroblasts are spindle or fusiform shaped cells which were first identified in the 19th century (Original papers cited in Fernandes *et al*., 2016). Fibroblasts are mesenchymal cells which can be found throughout the body in tissues and organs associated with the ECM (McAnulty, 2007). Overall, fibroblasts have numerous roles within the body including in wound healing, regulating inflammation and the immune response (Smith *et al*., 1997; Kalluri and Zeisberg, 2006). However, fibroblast function is known to differ and alter depending on its environment within the body (Driskell *et al*., 2013). Even within the skin, the function of fibroblasts differs between those isolated from different areas, with upper dermal fibroblasts being involved with hair follicle formation, and lower dermal fibroblasts demonstrating increased ECM formation and involvement with wound healing (Driskell *et al*., 2013).

Wound healing is dependent upon three processes: inflammation, proliferation and remodelling, which are all reliant on the presence of fibroblasts (Figure 1.9.; Gurtner *et al*., 2008). Upon injury to the epidermis, the coagulation cascade is initiated to decrease blood loss and a fibrin matrix is formed by fibroblasts as a scaffold for wound healing and migrating cells (Gurtner *et al*., 2008). Simultaneously, cellular debris and dead cells are removed from the area of injury through the initiation of inflammation and the migration of immune cells (Gurtner *et al*., 2008). Next, new tissue is formed by the proliferation of cells and the development of new blood vessels through angiogenesis (Gurtner *et al*., 2008). Some fibroblasts migrate from the edge of the

wound and differentiate into myofibroblasts, allowing the contraction and closure of the wound, while the remaining fibroblasts and myofibroblasts secrete ECM components to form a mature scar (Gurtner *et al*., 2008). Finally, the wound is remodelled and strengthened though the secretion of matrix metalloproteases by fibroblasts, macrophages and endothelial cells (Gurtner *et al*., 2008).
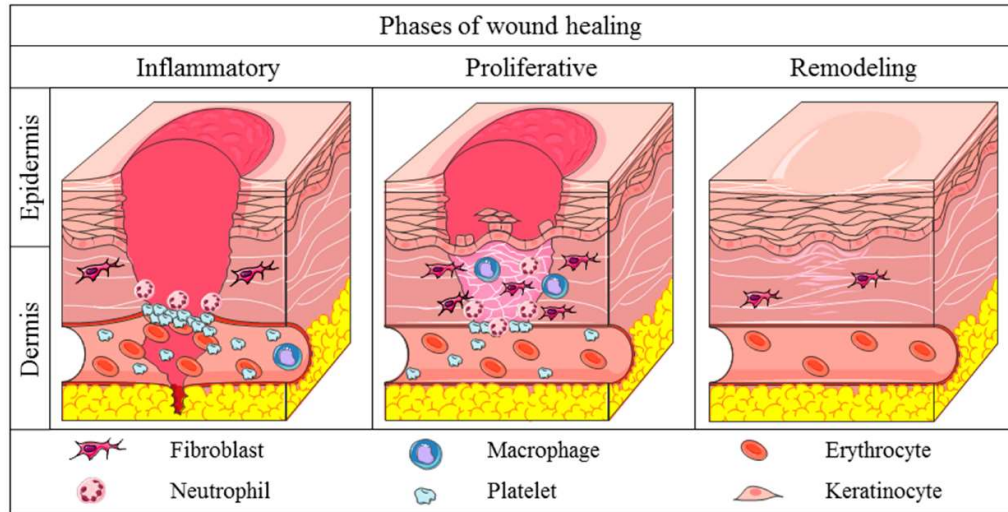
Figure 1.9. The three stages of wound healing. During the inflammatory phase, fibroblasts release pro-inflammatory cytokines and chemokines to induce homeostasis, acute inflammation and recruit other immune cells to the wound. In the proliferative phase, fibroblasts increase ECM production while immune cells, fibroblasts, keratinocytes and epithelial cells proliferate within the wound. Finally in the remodelling phase, extracellular matrix remodelling occurs, and cells involved with wound healing apoptose. Image taken from Gushiken *et al* (2021).

Despite being previously thought of as only structural cells, fibroblasts have since proven to contribute to immune function (Correa-Gallegos *et al*., 2021). Fibroblasts are sentinel cells which act to recognise microbial pathogens and initiate an immune response (Smith *et al*., 1997). As confirmed by Yao *et al*. (2015), dermal fibroblasts express TLRs on their cell surface which, upon activation by microbial components, stimulate the production and secretion of cytokines and chemokines. Following activation, fibroblasts secrete a range of inflammatory cytokines including IL-6, IL-8, TNF-α and IFN-γ to trigger the inflammatory response (Yao *et al*., 2015; Correa-Gallegos *et al*., 2021). In addition to this, fibroblasts also secrete chemokines including MIP-2 and macrophage chemoattractant protein 1 (MCP-1) which recruit other immune cells to the site of infection (Smith *et al*., 1997; Yao *et al*., 2015). Fibroblasts also continue to interact with immune cells such as monocytes and macrophages

through increased expression of adhesion molecules, intercellular adhesion molecule 1 (ICAM-1) and vascular cell adhesion protein 1 (VCAM-1) (Steinhauser *et al*., 1998). In addition to aiding immune clearance of pathogens, fibroblasts also play a role in the replenishment of resident immune cells through the expression of chemokines such as MIP-1α and MCP-1 (Gaga *et al*., 2008; Correa-Gallegos *et al*., 2021). This, therefore, solidifies the role of fibroblasts not only during wound healing but also in maintaining haemostasis (Correa-Gallegos *et al*., 2021).

1.5.3 Host Cell Adhesion Mechanisms

The adhesion of fibroblasts and macrophages to surfaces, the ECM and neighbouring cells is essential to their roles within immunity, wound healing and cell survival (Prieto *et al*., 1994; Richards *et al*., 1997). Macrophages and fibroblasts use a number of cellular adhesion mechanisms such as attachment through integrins, ICAM-1 and VCAM-1 (Prieto *et al*., 1994; Buhl *et al*., 1995; Chrzanowska-Wodnicka and Burridge, 1996; Richards *et al*., 1997; Wiesolek *et al*., 2020). The host ECM is composed of proteins, proteoglycans and glycoproteins which exhibit a range of functional and structural properties to create a 3D structure (Badylak, 2002). The host ECM is important for many processes including inflammation, angiogenesis, vasculogenesis, cell migration, cell proliferation, immune responses and wound healing (Richards *et al*., 1997; Badylak, 2002). In addition, the ECM provides a matrix for cellular attachment through the cell cytoskeleton, focal adhesions and integrins (Figure 1.9; Schoenwaelder and Burridge, 1999; Zamir and Geiger, 2001; Kaverina *et al*., 2002). Binding to the ECM proteins can occur directly through actin filament bundles at focal adhesions sites, or through transmembrane links via integrin receptors (Schoenwaelder and Burridge, 1999; Zamir and Geiger, 2001; Kaverina *et al*., 2002). Integrins are large glycoproteins, composed of an α and β subunit which act as receptors to a wide range of ligands including ECM proteins such as fibrinogen, fibronectin, paxillin and vitronectin, ICAM-1, and complement proteins such as C4b and iC3b (Figure 1.10.; Yakubenco *et al*., 2006).
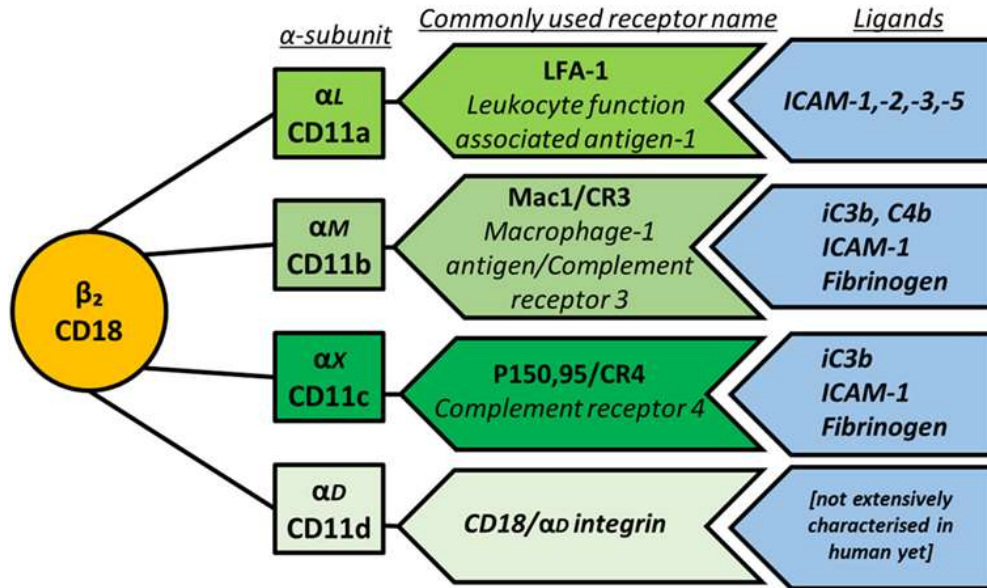
Figure 1.10. Examples of CD18 integrin receptors expressed by macrophages and the ligands to which they bind. Image taken from Schittenhelm *et al*. (2017).

Within the cell cytoskeleton, integrin receptors are bundled into structures called focal adhesions or focal complexes, located at the ends of actin filaments (Schoenwaelder and Burridge, 1999). For this reason, the interactions between the focal adhesion complexes and ECM components are termed focal contacts (Figure 1.11.; Richards *et al*., 1997; Schoenwaelder and Burridge, 1999). The development of these focal adhesions and actin stress filaments is mediated by the GTPase, Rho, kinase phosphatase pathways and Ca^{2+} influxes (Buhl *et al*., 1995; Chrzanowska-Wodnicka and Burridge, 1996; Yamada and Geiger, 1997). Focal contacts allow not only for ECM attachment but also cell motility (Izzard and Lochner, 1976). Cell migration and motility is mediated through the induction of tension in the actin cytoskeleton (Chrzanowska-Wodnicka and Burridge, 1996). This is followed by retraction of mature focal adhesions whereby integrins disperse and focal adhesions disassemble (Chrzanowska-Wodnicka and Burridge, 1996). Cell adhesion and motility is known to be influenced by a range of mechanical, chemical and electrical stimuli (Chung *et al*., 2001; Snyder *et al*., 2017; Ross *et al*., 2013). A number of signalling proteins are located at focal contacts including α-actin, vinculin, zyzin, paxillin and focal adhesion kinase (FAK; Ren *et al*., 2000). Focal adhesion kinase (FAK) is a tyrosine phosphorylated protein, which is an important factor in cell migration (Ren *et al*., 2000; Mitra *et al*., 2005). As reported by Ren *et al*. (2000), FAK inhibits Rho, thereby

decreasing focal contacts and increasing cell migration. Overall, this continuous process of contraction and retraction of focal adhesions allows for the movement of cells (Chrzanowska-Wodnicka and Burridge, 1996).
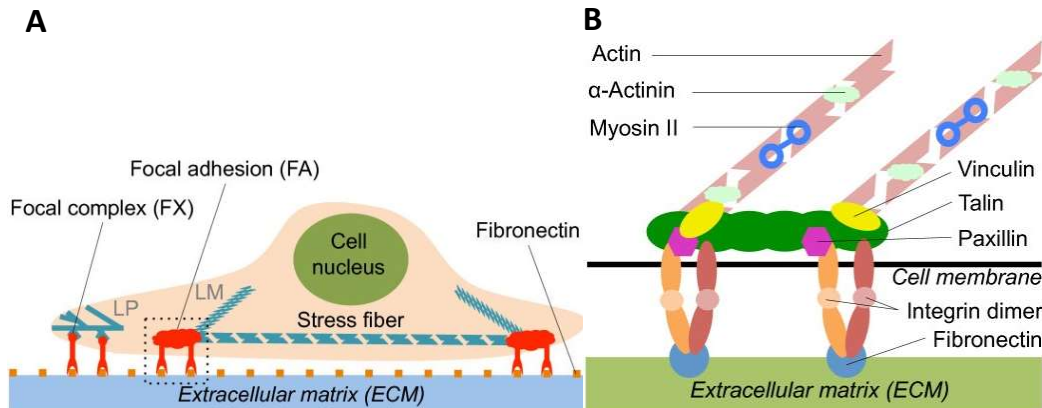
Figure 1.11. Schematics of cellular adhesion to the extracellular matrix. Adhesion to proteins including fibronectin can occur directly or indirectly through focal adhesions and focal complexes (**A**). The main components of cellular adhesion through integrin receptors at focal contacts (**B**). Image taken from Hoffmann and Schwarz (2013).

For both macrophages and fibroblasts, ICAM-1 and VCAM-1 play critical roles in cell-to-cell adhesion between host cells such as epithelial cells or other immune cells (Marlin and Springer, 1987; Diamond *et al*., 1991; Wiesolek *et al*., 2020). The attachment of fibroblasts to cells such as macrophages and lymphocytes is mediated through the expression of ICAM-1 on cell surfaces (Marlin and Springer, 1987; Diamond *et al*., 1991). This attachment is controlled by binding of ICAM-1, expressed by fibroblasts, to integrins such as macrophage adhesion ligand 1 and lymphocyte function-associated antigen 1 (Marlin and Springer, 1987; Diamond *et al*., 1991). In addition, fibroblasts can also bind to immune cells such as macrophages through VCAM-1 which binds to the integrins VLA-4 and VLA-5 (Elices *et al*., 1990; Hart and Greaves, 2010). These adhesion mechanisms allow fibroblasts to interact with immune cells, alerting them to the presence of damage or pathogens, and thus enabling the initiation of an immune response (Steinhauser *et al*., 1998).

1.6 The Host Immune and Inflammatory Response to Medical Devices

The effectiveness of a medical device is reliant upon the biocompatibility of the medical device surface, alongside the ability of the immune system to elicit a 'normal' immune response following implantation (Shiels *et al*., 2020). The immune response to a biocompatible foreign surface is shown in Figure 1.12.
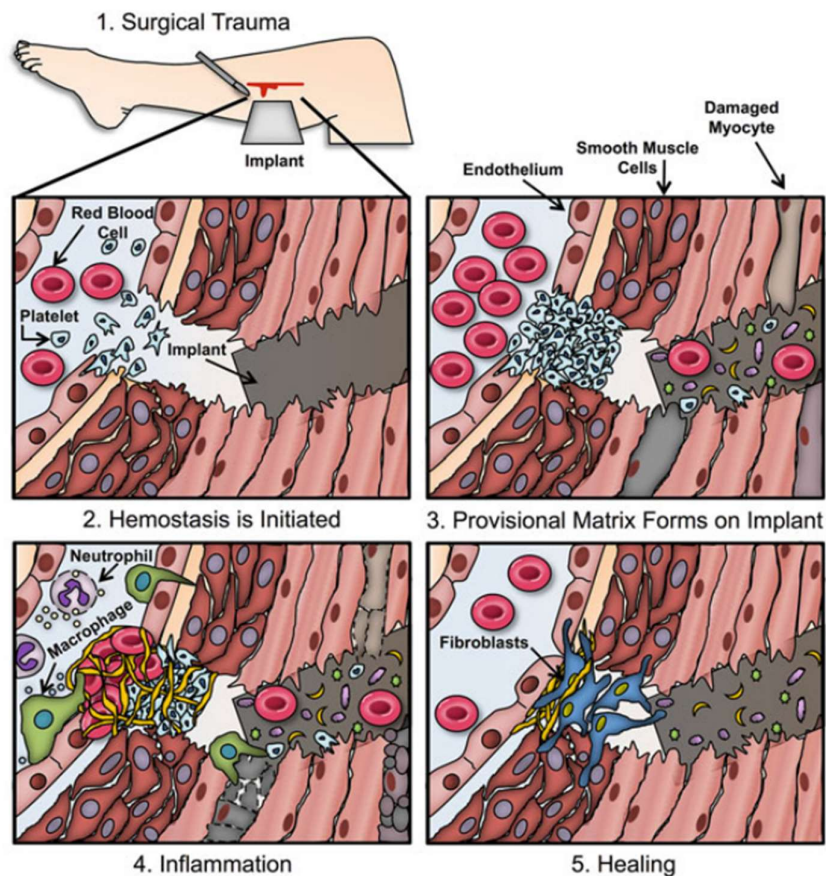
Figure 1.12. The sequence of events following the insertion of a medical device into a patient. 1. Upon implantation, damage occurs to tissue surrounding the medical device. 2. The coagulation cascade is initiated due to damage surrounding the medical device causing the formation of a platelet-fibrin-red blood cell clot. 3. Host proteins such as fibronectin, vitronectin and albumin from the blood and surrounding fluid coat the medical device. 4. The medical device and damage to the host causes an inflammatory response. Neutrophils, monocytes, and macrophages are recruited to the site of implantation to aid in the clearing of debris. 5) Healing of the tissue surrounding the medical device is initiated. Image taken from Corradetti *et al.* (2017).

Upon implantation of the medical device, damage to surrounding tissue initiates the coagulation cascade and the formation of a fibrin-platelet clot (Corradetti *et al.,* 2017).

Within the host, the medical device surface is coated with host proteins such as fibronectin, vitronectin and albumin alongside host cells (Hamlet and Ivanovski, 2017). Damage to surrounding cells causes the release of inflammatory cytokines such as IL-1β, IL-8 and TNF-α, chemokines such as MCP-1 and RANTES and the recruitment of neutrophils, monocytes, and macrophages to the area of implantation (Corradetti *et al.*, 2017). These host cells work to clear cellular debris and damaged cells during the acute inflammatory response, which usually clears within 3 to 5 days (Corradetti *et al.*, 2017). Finally, the implantation site is healed through the formation of granulation tissue, a complex characterised by the presence of ECM and proliferation of fibroblasts, keratinocytes and endothelial cells (Reinke and Sorg, 2012; Corradetti *et al.*, 2017; Alhajj and Goyal, 2021). During granulation, motile fibroblasts proliferate and synthesise and secrete molecules such as collagen, fibronectin, and proteoglycans to create and remodel the ECM of the granulation tissue (Reinke and Sorg, 2012). In addition to this, the development of capillaries by endothelial cells provides the granulation tissue with nutrition and a means of waste disposal (Reinke and Sorg, 2012).

When developing biomaterials for orthopaedic device use, factors such as biocompatibility, strength, resistance to corrosion and osteointegration must be considered (Pennem *et al*., 1991). As orthopaedic devices are often subject to heavy loads, repetitive motions and high friction, the biomaterial must be of adequate strength to prevent device failure (Engh *et al*., 1992). In addition, the longevity of the device is dependent upon high biocompatibility, measured by the host response to biomaterials alongside the degradation of the biomaterial within the host environment (Simon and Fabry, 1991). The degradation of biomaterials within the host leads to the release of particles, detected by macrophages (Nich *et al*., 2013). Once detected, macrophages act to remove any particles through phagocytosis, initiate an inflammatory response and activate the adaptive immune system (Nich *et al*., 2013). To combat larger particles or biomaterials, macrophages fuse to form a foreign body giant cell (Sheikh *et al*., 2015). Foreign body giant cells contribute to inflammation and the initiation of the immune response through the release of cytokines such as TNF-α and IL-1β (Hernandez-Pando *et al*., 2000). Foreign body macrophages use two main methods of biomaterial removal; engulfment and degradation (Figure 1.13.; Sheik *et al.,* 2015). During engulfment, the foreign body giant cell surrounds the

biomaterial and actively work to digest the device and may remain for the duration of the device life (Anderson, 2000). Alternatively, foreign body giant cells may secrete mediators of degradation such as reactive oxygen species, degradative enzymes, or acid (original papers cited in Anderson *et al.*, 2008).
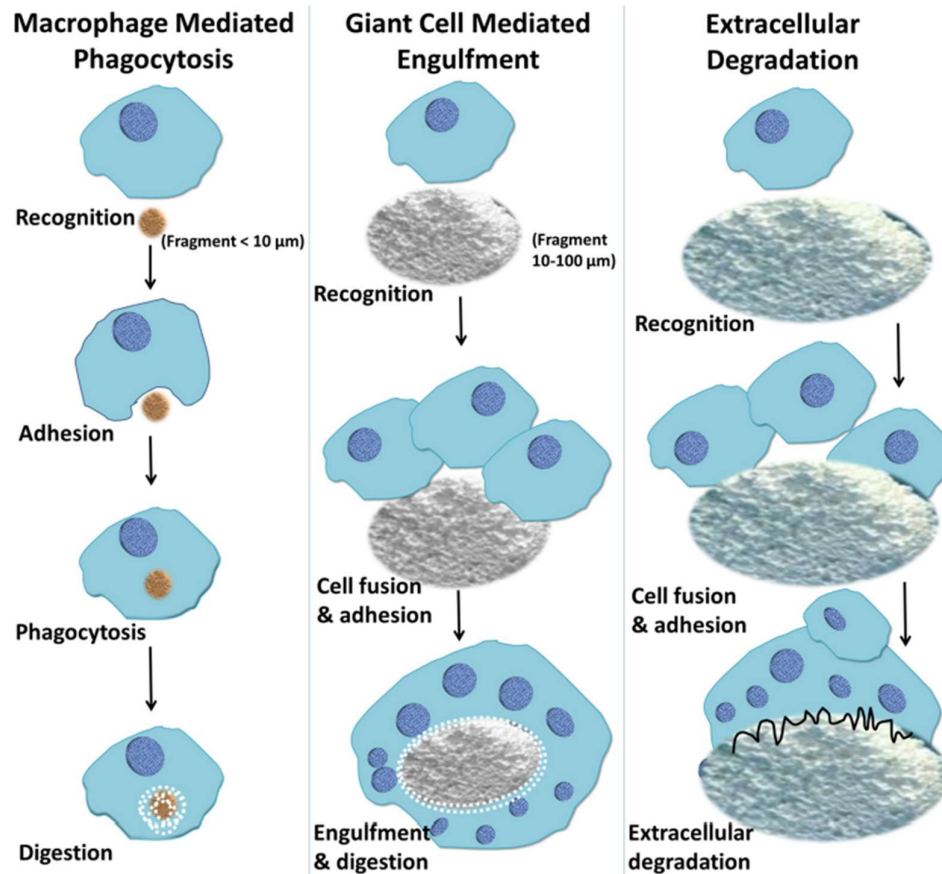
Figure 1.13. A schematic of the three foreign body responses by macrophages. Macrophage mediated phagocytosis allows for the recognition and removal of small particles released from the foreign device. In instances where particles are too large to be phagocytoses, macrophages form foreign body giant cells. These foreign body giant cells remove the foreign body by engulfment and digestion of the large biomaterial, or through the degradation of the biomaterial. Image taken from Sheik *et al.* (2015).

Within orthopaedics, polymers such as poly(methyl methacrylate) and ultrahigh-molecular-weight polyethylene and ceramics such as alumina, zirconia and hydroxyapatite, are widely used to produce implants for low load-bearing implants such as bone remodelling or for joint arthroplasty (Paital and Dahotre, 2009). In addition, due to their high biocompatibility, high strength and resistance to corrosion

titanium, titanium alloys and stainless-steel have worldwide applications within load-bearing implants such as osteosynthesis implants (Harris and Richards, 2006). In comparison to pure Ti, titanium alloys such as titanium-aluminium-vanadium (Ti6Al4V) are stronger and harder, thus increasing durability within the host (Zhu *et al*., 2003). However, the loss of aluminium or vanadium particles from the Ti6AlV surface can have a cytotoxic effect on host cells, leading to eventual device failure (Haydar *et al*., 2021). As a result of this, orthopaedic device composition is consistently under revision in order to optimise both biocompatibility and strength. The effects of surface composition and surface coatings have been explored for Ti and Ti alloy biomaterials. These studies have explored the use of elements such as boron, niobium, nickel, zirconium, hafnium and tantalum, molybdenum, iron and tin (Oliveria *et al.,* 1998; Zhu *et al*., 2003, Van Hove *et al*., 2015, Guillemot *et al*., 2004, Xu *et al*., 2020). In addition, surface topography studies of existing Ti and Ti alloy surfaces have also been explored to improve biocompatibility and osteogenesis (Damitri *et al*., 2018). Altering surface topography through plasma spraying has been demonstrated to increase both solidity, bioactivity, resistance to corrosion and surface roughness of Ti alloy surfaces (Ganpathy *et al*., 2015; Singh *et al*., 20202). Zhou *et al*. (2020) noted that modifying the Ti biomaterial through surface coating with silicon micropore/microsphere topography, not only increased surface roughness but also adhesion, proliferation and osteogenic differentiation of host cells. This therefore increases osteogenesis and the biocompatibility of the device within the host system (Zhou *et al*., 2020). However, despite the benefits of host cell-biomaterial interactions, increased surface roughness can also increase bacterial adhesion, thus resulting in increased chance of medical device infection (Harris and Richards, 2004; Pier-Francesco *et al*., 2006).

1.7   The Host Immune Response to *S. epidermidis* Medical Device Infections

In comparison to *S. aureus*, a much smaller pool of research is available regarding the interaction between *S. epidermidis* and the host immune system (Nguyen *et al*., 2017). Following implantation of the medical device, host and bacterial cells compete to be the first colonisers of the device surface in 'the race for the surface' (Gristina *et al*., 1988). The outcome of this colonisation plays a critical role in the development of a medical device infection (Shiels *et al*., 2020). Initial colonisation by *S. epidermidis*

results in biofilm formation and thus the emergence of a medical device infection (Subbiahdoss *et al.,* 2009; Shiels *et al*., 2020). In comparison to this, initial colonisation by host cells has been found to reduce the likelihood of a medical device infection, improve the likelihood of implant survival and increase patient recovery (Subbiahdoss *et al.,* 2009; Shiels *et al*., 2020).

Bacterial species employ a range of immune evasion strategies to avoid detection and elimination by the host immune response. In the case of *S. epidermidis,* the host immune response is not sufficient enough to overcome these immune evasion strategies and thus, medical device infections often persist (Nguyen *et al*., 2017). As reviewed by Le *et al.* (2018), *S. epidermidis* uses a number of immune evasion strategies both as a commensal and pathogenic species, a large number of which rely on the production of a biofilm. In particular, biofilm producing *S. epidermidis* strains have been noted to down-regulate the production of pro-inflammatory cytokines including IL-1β, IFN-γ and IL-12 and increase the production of anti-inflammatory cytokines such as IL-13, thus decreasing the inflammatory response (Spiliopoulou *et al*., 2012). As demonstrated by Spiliopoulou *et al*. (2012), biofilm *S. epidermidis* is less susceptible than planktonic cells to immune clearing mechanisms, including killing by macrophages. This in turn is aided by the ability of *S. epidermidis* to persist intracellularly within host immune cells such as fibroblasts and osteoblasts (Parez and Patel, 2018). The host's innate immune system reacts to a staphylococcal infection through the activation of effector cells and the complement system (Le *et al*., 2018; Nguyen *et al*., 2017). However, this is an unsuccessful strategy against *S. epidermidis* biofilms due to the ability of the biofilm to decrease the accumulation and efficiency of C3b and immunoglobulin (Kristian *et al*., 2008). Within the biofilm, some *S. epidermidis* strains produce poly-γ-glutamic acid (PGA) and PIA which aid protection against host defences (Shiau and Wu, 1998; Vuong *et al*., 2004a; Kocianova *et al*., 2005). The pseudopeptide polymer, PGA not only assists *S. epidermidis* resistance to neutrophil phagocytosis and AMPs but is also protective against high salinity environments (Kocianova *et al*., 2005). It has also been noted that PIA dependent biofilms can decrease the action of neutrophil killing, complement deposition, immunoglobulins and AMPs (Vuong *et al*., 2004a; Cerca *et al*., 2006; Kristian *et al*., 2008). In PIA-independent biofilms, proteinaceous factors, Aap and Embp also show similar functions in decreasing effector-cell mediated killing of *S.*

epidermidis (Schommer *et al*., 2011). Unlike *S. aureus* which produces a wealth of toxins, *S. epidermidis* toxin production is more limited and mainly involves PSMs (Otto, 2009). These PSMs play various roles in immune evasion through catalytic activity against neutrophils or by reducing markers of inflammation (Cheung *et al*., 2010).

1.8 Aims and Objectives

The main aim of this study is to develop a 3D co-culturing method to gain further understanding of the interactions between *S. epidermidis* and immune cells in the presence of titanium (Ti) and titanium alloy (TiAlV) surfaces. This aim is split into four objectives:

- **Objective 1-** to develop a method allowing for the co-culture of *S. epidermidis* with fibroblasts or macrophages on Ti and TiAlV surfaces.
- **Objective 2-** to explore the effects of co-culturing *S. epidermidis* with THP-1 macrophages on cellular adhesion and *S. epidermidis* gene expression or macrophage cytokine expression in the presence of Ti or TiAlV surfaces.
- **Objective 3-** to explore the effects of co-culturing *S. epidermidis* with human dermal fibroblasts (1BR.3.G fibroblasts) on cellular adhesion and *S. epidermidis* gene expression or fibroblast cytokine expression in the presence of Ti or TiAlV surfaces.
- **Objective 4-** To investigate the effects of pre-coating Ti or TiAlV surfaces on cellular adhesion and gene expression of *S. epidermidis* or cytokine expression by fibroblasts in co-culture.

Understanding the interactions between *S. epidermidis* and immune cells during medical device infection will allow us to gain better insight to the immune response during a medical device infection.

Chapter 2. Materials and Methods

In general, all chemicals and reagents were of analytical grade and were purchased from Sigma Aldrich (Gillingham, UK), Thermo Fisher Scientific (Loughborough, UK) or Oxoid (Basingstoke, UK) unless otherwise stated.

2.1 Media

2.1.1 Bacterial Culture Media

Unless otherwise stated, bacterial culture media was prepared using distilled water (dH$_2$O) and was sterilized by autoclaving at 15 p.s.i for 20 min.

2.1.1.1 Columbia Agar with Horse Blood

Pre-poured Columbia Agar with 5% Horse Blood plates were purchased from Oxoid (Basingstoke, UK).

2.1.1.2 Tryptic Soy Broth (TSB)

Tryptic Soy Broth	30 g/L
H$_2$O	1 L

2.1.1.3 Tryptic Soy Broth (TSB) agar

Tryptic Soy Broth	30 g/L
H$_2$O	1 L
Oxoid Agar technical (no. 3; 1% (w/v) agar)	10 g/L

2.1.2 Cell Culture Media

2.1.2.1 Dulbecco's Modified Eagle Medium (DMEM)

500 ml 1 X Dulbecco's Modified Eagle Medium (DMEM) with D-glucose, L-glutamine and pyruvate

50 ml (10%) Foetal Bovine Serum, Qualified

5 ml (1%) L-glutamine 200 mM (100X)

5 ml (1%) Minimum Essential Media Non-Essential Amino Acids (100X)

5 ml (1%) Penicillin Streptomycin (Pen Strep) 10,000 units/ml Penicillin, 10,000 µg/ml Streptomycin.

For bacterial work, antibiotic-free media was used.

2.1.2.2 Minimum Essential Medium (MEM)

500 ml Minimum Essential Medium (MEM) Alpha Medium (1X) without Ribonucleosides and Deoxyribonucleosides

50 ml (10%) Foetal Bovine Serum, Qualified

5 ml (1%) L-glutamine 200 mM (100X)

5 ml (1%) Minimum Essential Media Non-Essential Amino Acids (100X)

5 ml (1%) Penicillin Streptomycin (Pen Strep) 10,000 units/ml Penicillin, 10,000 µg/ml Streptomycin.

For bacterial work, antibiotic-free media was used.

2.1.2.3 Roswell Park Memorial Institute (RPMI) Medium

500 ml Roswell Park Memorial Institute (RPMI) medium 1640 (1X) with L-Glutamine

50 ml (10%) Foetal Bovine Serum, Qualified

5 ml (1%) L-glutamine 200 mM (100X)

5 ml (1%) Penicillin Streptomycin (Pen Strep) 10,000 units/ml Penicillin, 10,000 µg/ml Streptomycin.

For bacterial work, antibiotic-free media without Pen Strep was used.

2.1.3 1% Agarose Gel for Electrophoresis

Electrophoresis grade agarose (1% w/v)	0.05 g
1 × TAE	50 ml

2.2 Buffers, Stocks and Solutions

2.2.1 0.1% Crystal Violet

Crystal Violet >99% (0.1% w/v)	0.1 g
Sterile H_2O	100 ml

2.2.2 Glycerol

>99% Glycerol was purchased from Sigma Aldrich (Gillingham, UK) and diluted to 50% in sterile H_2O.

Glycerol	10 ml
Sterile H_2O	10 ml

2.2.3 Phosphate Buffered Saline (PBS)

Phosphate buffered Saline (PBS) tablets were purchased from VWR Life Science (Leicestershire, United Kingdom).

Phosphate Buffered Saline (PBS) tablets	1 tablet
Distilled H_2O	100 ml

2.2.4 Sodium (Meta)periodate

Sodium (meta)periodate, >99%	0.21 g
Sterile H_2O	10 ml

2.2.5 50× Tris Acetate EDTA (TAE) Buffer

TRIZMA Tris base was purchased from Sigma Aldrich (Gillingham, UK) and Glacial Acetic acid >99.85% was purchased from VWR life sciences (Leicestershire, UK).

TRIZMA Tris base	242 g
Glacial Acetic acid	57.1 ml
0.5 M EDTA (pH 8.0)	100 ml
Distilled H_2O	842.9 ml

Before use, the 50X TAE was diluted 1:50 to make 1X TAE.

2.2.6 0.1% Triton X-100

Triton X-100	20 µl
PBS	20 ml

2.2.7 Cell Culture Buffers, Stocks and Solutions

2.2.7.1 Phosphate Buffered Saline (PBS) for Cell Culture

Phosphate Buffered Saline pH 7.4 (1X) without $CaCl_2$ and $MgCl_2$ was used for all cell culture work.

2.2.7.2 Phorbol 12-myristate 13-acetate (PMA)

Phorbol 12-myristate 13-acetate (PMA) purchased from Thermo Fisher Scientific (Loughborough, UK). The PMA powder was dissolved in 1 ml Dimethyl Sulfoxide (DMSO) and was stored as 20 µl aliquots -20° C. The PMA was diluted to 100 nM in RPMI medium before use.

2.2.7.3 TrypLE™ Express

Dissociation reagent, TrypLE™ express (1X) without phenol red was used for cell culture work.

2.2.8 Microscopy Buffers, Stocks, and Solutions

2.2.8.1 2.5% Glutaraldehyde in PIPES

25% Glutaraldehyde	2 ml
0.4 M PIPES (pH 7.4)	5 ml
Distilled H_2O	13 ml

2.2.8.2 2% Osmium Tetroxide

Osmium tetroxide 0.25g ampoules were purchased from Agar Scientific (Essex, UK).

Osmium tetroxide	0.25 g
Distilled H_2O	12.5 ml

The osmium tetroxide was dissolved in water using sonication and then filter sterilized using a Millipore filter (Sigma Aldrich; Gillingham, UK) and was stored at 4 °C in the dark for up to 3 weeks.

2.2.8.3 1% Osmium Tetroxide in PIPES

2% Osmium tetroxide	10 ml
0.4 M PIPES (pH 6.8)	5 ml
Distilled H_2O	5 ml

2.2.8.4 10% Paraformaldehyde

Paraformaldehyde powder, 95%	2 g
Distilled H_2O	20 ml

2.2.8.5 4% Paraformaldehyde in 0.4 M PIPES

10% Paraformaldehyde	2 ml
0.4 M PIPES (pH 7.4)	2.5 ml
Distilled H_2O	2.5 ml

2.2.8.6 2,2-piperazine-1,4-diylbisethanesulfonate (PIPES) O.4 M

PIPES, 98% powder	12 g
Distilled H_2O	100 ml

Drops of NaOH were added until cloudy solution became clear. The solution was stirred until the desired pH was reached and was stored for up to 3 weeks at 4 °C.

2.2.9 RNA Extraction Buffers, Stocks, and Solutions

2.2.9.1 Buffer RLT

Supplied in the Qiagen RNeasy Miniprep kit, details not provided.

2.2.9.2 Buffer RW1

Supplied in the Qiagen RNeasy Miniprep kit, details not provided.

2.2.9.3 Buffer RPE

Supplied in the Qiagen RNeasy Miniprep kit, details not provided. Buffer RPE was reconstituted in 44 ml of >99% ethanol prior to use.

2.2.9.4 DNase Kit

RNase-Free DNase Set was purchased from Qiagen (Manchester, UK). Lyophilised DNase I was dissolved in 550 µl nuclease free H_20 and stored as 20 µl aliquots at -20 °C. Buffer RDD was stored at 4 °C.

2.2.9.5 Ethylenediaminetetraacetic acid (EDTA; 0.5 M)

Ethylenediaminetetraacetic acid powder	74.44 g
Distilled H_2O	250 ml

Adjusted to pH 8.0 using sodium hydroxide pellets.

2.2.9.6 Lysostaphin

Lysostaphin, from *Staphylococcus staphylolyticus* was purchased from Sigma Aldrich (Gillingham, UK) and was resuspended in 1 ml nuclease free H_2O. Lysostaphin was stored as 20 µl aliquots at -20 °C.

2.2.9.7 Magnesium chloride (0.5 M)

Magnesium chloride	4.76 g
Distilled H_2O	1 L

2.2.9.8 Mutanolysin

Mutanolysin from *Streptomyces globisporus* ATTC 21553 was purchased from Sigma Aldrich (Gillingham, UK) and was resuspended in 1 ml of dH_20 containing 10 µl of 1 mM $MgCl_2$ and 50 µl of 0.05 M TES buffer. Mutanolysin was stored as 20 µl aliquots at -20 °C.

2.2.9.9 RNAprotect™

RNAprotect™ was supplied from Qiagen (Manchester, UK), details not provided.

2.2.9.10 10% Sodium Dodecyl Sulphate (SDS)

Sodium Dodecyl Sulphate (10% w/v)	10 g
Distilled H_2O	100 ml

2.2.9.11 Tris (1 M)

TRIZMA Tris base	2.36 g
Tris hydrochloride	2.7 g
Distilled H_2O	100 ml

Adjusted to pH 8.0 using Sodium hydroxide pellets and solution autoclaved before use.

2.2.9.12 Tris EDTA SDS (TES) Buffer

1 M Tris (pH 8)	10 µl
0.5 M EDTA (pH 8)	20 µl
10% SDS	100 µl
Distilled H_2O	9.87 ml

2.2.10 ELISA Buffers, Stocks, and Solutions

2.2.10.1 ELISA Block Buffer (1% BSA in PBS)

Bovine Serum Albumin (1% w/v)	0.5 g
Distilled H_2O	50 ml

2.2.10.2 ELISA Colour Solution (Sure Blue™)

KPL SureBlue™ TMB Microwell Peroxidase Substrate (1-Component) was purchased from Sera Care (Milford, Massachusetts, United States) and was stored at 4 °C.

2.2.10.3 ELISA Capture Antibody

Capture Antibody was supplied in the DuoSet ELISA kit and was reconstituted in 0.5 ml PBS.

2.2.10.4 ELISA Detection Antibody

Detection Antibody was supplied in the DuoSet ELISA kit and was reconstituted in 1 ml of Reagent Diluent.

2.2.10.5 ELISA Reagent Diluent (0.1% BSA in PBS)

Bovine Serum Albumin (0.1% w/v)	0.05 g
Distilled H_2O	50 ml

2.2.10.6 ELISA Standard

The Standard was supplied in the DuoSet ELISA kit and was reconstituted in 0.5 ml distilled H_2O.

2.2.10.7 ELISA Stop Solution (1 M Hydrochloric Acid)

37% Hydrochloric acid	41.5 ml
Distilled H_2O	458.5 ml

2.2.10.8 ELISA Wash buffer (0.05% Tween 20 in PBS)

Tween 20	0.5 ml
Phosphate Buffered Saline	1000 ml

2.2.11 Proteome Profiler Array Buffers, Stocks, and Solutions

2.2.11.1 Array Buffer 4/6

Array buffers 4 and 6 were supplied in the Proteome Profiler Human Cytokine Array Kit, details not provided.

Array Buffer 4	4 ml
Array Buffer 6	8 ml

2.2.11.2 Chemi Reagent Mix

Chemi reagents 1 and 2 were supplied in the Proteome Profiler Human Cytokine Array Kit, details not provided.

Chemi Reagent 1	2 ml
Chemi Reagent 2	2 ml

2.2.11.3 Detection Antibody Cocktail

Detection Antibody Cocktail was supplied in the Proteome Profiler Human Cytokine Array kit, details not provided. Detection Antibody Cocktail was reconstituted in 200 μl distilled H_2O prior to use.

2.2.11.4 Streptavidin-HRP

Streptavidin-HRP was supplied in the Proteome Profiler Human Cytokine Assay Kit, details not provided.

Streptavidin-HRP	1 μl
Array Buffer 6	1999 μl

2.2.11.5 Wash Buffer

Wash buffer concentrate was supplied in the Proteome Profiler Human Cytokine Assay Kit, details not provided.

Wash Buffer Concentrate	40 ml
Distilled H_2O	960 ml

2.3 Antibodies and Fluorophores for Immunolabelling

Monoclonal antibodies and fluorophores were purchased from Invitrogen (Thermo Fisher Scientific; Loughborough, UK; Table 2.1.).

Table 2.1. A list of antibodies used for immunolabelling.

Antibody	Target	Species	Excitation/ Emission	Fluorophore
Phalloidin	F-actin	*Amanita phalloides* 'Death Cap' Mushroom	581/ 609 nm (red)	Alexa Fluor™ 594
Gram-positive Bacteria LTA Monoclonal Antibody (G35C)	Lipoteichoic acid	Mouse	N/A	Unconjugated N/A
Anti-mouse IgG	Mouse IgG	Goat	499/520 nm (Green)	Alexa Fluor™ 488

Lyophilised Alexa Fluor™ 594 Phalloidin was dissolved in 150 µl of Dimethyl Sulfoxide (Sigma Aldrich; Gillingham, UK) to make a 400× solution and was stored at -20 °C. Gram-positive Bacteria LTA Monoclonal Antibody was supplied at 0.1 mg/ml in PBS and 0.1% Sodium azide. Alexa Fluor 488™ Goat Anti-mouse IgG was supplied at 2 mg/ml in PBS and 5 mM sodium azide. Both Gram positive LTA Monoclonal Antibody and Alexa Fluor 488™ Goat Anti-mouse IgG were stored at 4 °C.

2.4 Titanium (Ti) and Titanium Aluminium Vanadium (TiAlV) Discs

Ti discs are composed of Titanium Grade 4 metal and TiAlV discs are composed of Titanium alloy vanadium Grade 5 metal, both from Dynamic Metals Ltd (Leighton Buzzard, UK). The Ti and TiAlV discs were vibratory grinded, precleaned, etched, final cleaned, controlled and packaged by KKS Ultraschall AG (Steinen, Switzerland). Finally, the discs were gamma sterilized by Synergy Health (Däniken AG, Switzerland).

2.5 Bacterial Culture

2.5.1 Bacterial Strains

Two biofilm-positive *Staphylococcus epidermidis* bacterial strains were chosen for laboratory work: *S. epidermidis* 1457 which was isolated from an infected intravenous catheter and is *icaADBC* and PIA positive (Mack *et al*., 1992), and *S. epidermidis* 5179-R1 which is derived from an infected CSF-shunt and produces an Aap-dependent, PIA negative biofilm (Rohde *et al*., 2005).

2.5.2 *S. epidermidis* Glycerol Stock Preparation

S. epidermidis strains 1457 and 5179-R1 were streaked from freezer stocks onto Columbian horse blood agar plates (Section 2.1.1.1). The streaked plates were incubated for 24 h at 37 °C in a Genlab incubator (Cheshire, UK). Following incubation, a single colony from the overnight cell culture plate was used to inoculate 700 µl of TSB broth in a 1.5 ml microcentrifuge tube. Next, 300 µl of 50% glycerol was added to the microcentrifuge tube. The glycerol stock was pulse vortexed on a Genius 3 vortex (IKA®; Oxford, UK) and stored at -80 °C in a Thermo Fisher Scientific TSX Series Freezer (Loughborough, UK).

2.5.3 *S. epidermidis* Mono-culture

S. epidermidis 1457 and 5179-R1 were streaked onto Columbian horse blood agar plates and incubated at 37 °C overnight in a Genlab incubator. From the streak plate, one to five colonies were selected and suspended in 3 ml TSB broth in a 7 ml Bijou tube. The bacterial suspension was incubated with shaking at 37 °C for 3 h in a Kuhner shaker X incubator (Basel, Switzerland). Following incubation, each sample was centrifuged at 200 x g for 3 min in a MiniSpin benchtop centrifuge (Eppendorf; Madrid, Spain) and the supernatant was disposed. The pellet was resuspended in PBS and the optical density at 600 nm was measured using a Jenway 7200 spectrophotometer (Staffordshire, UK). The sample was diluted to desired OD_{600} using desired media (Section 2.1).

2.6 Cell Culture

2.6.1 Eukaryotic Cells

Human Skin Fibroblasts (1BR.3.G; ECACC 90020507) were purchased from Public Health England (Porton Down, Salisbury, UK) and were frozen in liquid nitrogen upon arrival. 1BR.3.G fibroblasts were cultured in MEM medium and supplemented as in Section 2.1.2.2

Human monocytic cells (THP-1) were obtained from the Microbiology and Infectious Diseases cell collection library at Swansea University. THP-1 human monocytic cells were originally obtained from the blood of a 1-year-old boy with acute monocytic leukaemia (Tsuchiya *et al.*, 1980). THP-1 cells were cultured in RMPI medium supplemented as described in Section 2.1.2.3

All cells were incubated at 37 °C with 5% CO_2 in a NuAire Incubator (Plymouth, UK).

2.6.2 Recovery of Cells

1BR.3.G fibroblasts and THP-1 monocytes were removed from liquid nitrogen and immediately thawed. The cell suspension was removed and layered onto 20 ml of corresponding cell media in a conical tube. The cell suspension was centrifuged at 220 xg for 5 min at room temperature in a Megafuge 16R centrifuge (Thermo Fisher, Scientific; Loughborough, UK). The supernatant was then discarded, and the cells were resuspended in 12 ml fresh corresponding media. The cell suspension was aliquoted into a T-75 flask and was incubated at 37 °C with 5% CO_2 until ready to be sub-cultured.

2.6.3 Calculating Cell Viability

1BR.3.G and THP-1 cells were mixed 1:2 with trypan blue by adding 10 µl cell suspension to 10 µl 0.4 % trypan blue (Thermo Fisher Scientific, Loughborough, UK) in a 0.2 ml microcentrifuge tube. Next, 10 µl of the mixture was added to each side of a Countess™ cell counting chamber slide (Thermo Fisher Scientific; Loughborough, UK). Cells were counted using the Countess 3 Automated Cell Counter (Thermo Fisher Scientific; Loughborough, UK). Cell seeding was calculated as:

$$(Average\ no.cells\ \times 10000) \times 2 = X\ cells/ml$$

$$\frac{Desired\ cell/ml}{X} = N\ (dilution\ factor)$$

$$\frac{Volume\ (ml)}{N} = Z\ ml\ cell\ suspension$$

$$Volume\ (ml) - Z = Y\ ml\ fresh\ cell\ media$$

2.6.4 Sub-culturing THP-1 monocyte Cells

THP-1 suspension cells were grown to 8-9.5 $\times 10^5$ cells/ml in a T-75 cell-culture flask. Once at the desired confluency, the cell suspension was removed from the flask, added to a 50 ml conical tube and centrifuged at 200 xg for 5 min at room temperature. Following centrifugation, the supernatant was removed from the conical tube and the pellet was resuspended in 12 ml RPMI cell culture media with supplement (Section 2.1.2.3). Cell viability was determined, and the cell suspension was diluted to 1×10^6 cells/ml as described in Section 2.6.3. Finally, 20 ml of diluted THP-1 cell suspension was added to a new T-75 cell culture flask and incubated at 37 °C with a 5% CO_2.

2.6.5 Sub-culturing 1BR.3.G Fibroblasts

1BR.3.G cells were grown to 70-80% confluency in a T-75 cell culture flask. Once at the desired confluency, the cell culture media was removed, and the flask was washed three times with 5 ml of PBS. Next, 5 ml of TryplE express was added and the flask was incubated at 37 °C in a 5% CO_2 atmosphere for up to 10 min. The detachment of the 1BR.3.G cells was monitored using a light microscope. Following incubation, the cell suspension was added to a 50 ml centrifuge tube containing 10 ml of supplemented MEM cell culture media (Section 2.1.2.2) and centrifuged at 200 xg for 5 min at room temperature in the Megafuge 16R. Then, the supernatant was removed from the centrifuge tube and the pellet was resuspended in 12 ml of supplemented MEM cell culture media. The cells were split into new T-75 flasks using a 1:10 dilution and incubated at 37 °C in 5% CO_2.

2.6.6 Co-culture of THP-1 macrophages with *S. epidermidis*

THP-1 monocytes were centrifuged and resuspended in 12 ml RPMI antibiotic free medium as described in section 2.6.4. Next, the cell viability was determined, and the cell suspension was diluted to 5×10^5 cells/ml as described in Section 2.6.3. In 24-well cell culture plates, Ti or TiAlV discs were added to wells using sterile forceps. Then,

1 ml of diluted cell suspension containing 100 nM Phorbol 12-myristate 13-acetate (PMA) was added to each well and the 24-well plate was incubated at 37 °C with a 5% CO_2 for 24 h. The following day, *S. epidermidis* 1457 and 5179-R1 cultures were prepared and diluted to OD_{600}=0.05 in RPMI (antibiotic free) as described in Section 2.5.3. Following incubation, the media was removed from the 24-well cell culture plates containing differentiated THP-1 cells and replaced with 1 ml of *S. epidermidis* cell suspension. Control wells with no Ti/TiAlV discs, *S. epidermidis* only, THP-1 macrophages only, THP-1 monocytes only and THP-1 macrophages with LPS were also included. The 24-well plate was incubated for 6 h or 24 h at 37 °C in 5% CO_2. Following incubation, the media was removed from the wells and centrifuged at 14k rpm for 5 min in an Eppendorf MiniSpin Centrifuge. The supernatant was then stored in a 1.5 ml microcentrifuge tube at -20 °C for cytokine analysis. Titanium and Titanium alloy discs were immediately processed for immunostaining, RNA extraction or scanning electron microscopy (SEM).

2.6.7 Co-culture of 1BR.3.G fibroblasts with *S. epidermidis*

1BR.3.G fibroblasts were washed, centrifuged, and resuspended in 12 ml of MEM antibiotic free media as described in Section 2.6.5. Next, cell viability was determined, and the cell suspension was diluted to 5×10^4 cells/ml as described in Section 2.6.3. In 24-well cell culture plates, Ti or TiAlV discs were added to wells using sterile forceps. Then, 1 ml of diluted cell suspension was added to each well and the 24-well plate was incubated at 37 °C with a 5% CO_2 for 48 h. *S. epidermidis* 1457 and 5179-R1 cultures were prepared and diluted to OD_{600}=0.05 in MEM (antibiotic free) as in Section 2.5.3. Following incubation, the media from the 24-well cell culture plates was removed by pipetting and replaced with 1 ml MEM containing *S. epidermidis* cells. Control wells with no Ti/TiAlV discs, *S. epidermidis* only and 1BR.3.G cells only and 1BR.3G. cells with lipopolysaccharide (LPS) were also included. The 24-well plate was incubated for 6 h or 24 h at 37 °C with a 5% CO_2. Following incubation, the media was removed from the wells and centrifuged at 14,000 rpm for 5 min in an Eppendorf MiniSpin Centrifuge. The supernatant was then stored in a 1.5 ml microcentrifuge tube at -20 °C for cytokine analysis. Titanium and Titanium alloy discs were immediately processed for immunostaining, RNA extraction or scanning electron microscopy (SEM).

2.7 Whole Blood Model

2.7.1 Acquisition of Whole Blood

Whole blood was acquired from healthy volunteers using the Joint Clinical Research Facility at Swansea University. Prior to acquiring the blood, consent was given by all volunteers and ethical approval was gained for the collection of the blood by a trained nurse. The collection of blood is a project (13/WA/0190) assessed by the local ethics committee (Wales Rec 6) at Swansea University Medical School. From each donor, one 9 ml tube containing heparin was collected and used on the day of donation.

2.7.2 Pre-coating Ti/TiAlV Discs with Whole Blood

In 24-well cell culture plates, Ti or TiAlV discs were added to wells using sterile forceps. Next, 200 µl of whole blood was added to each disc and the 24-well plates were incubated at 37 °C with 5% CO_2 for 2 h. Following incubation, whole blood was removed from discs by pipetting and the wells were washed three times with PBS. 1BR.3.G fibroblasts were co-cultured on the pre-coated discs with *S. epidermidis* 1457 or 5179-R1 as described in Section 2.6.7. In addition, 1 ml *S. epidermidis* 1457 and 5179-R1 diluted to OD_{600}=0.05 in MEM antibiotic free media (Section 2.5.3) was added to pre-coated discs and incubated at 37 °C with 5% CO_2 for 6 h and 24 h. Following incubation, the media was removed from the wells and centrifuged at 14,000 rpm for 5 min in an Eppendorf MiniSpin Centrifuge. The supernatant was then stored in a 1.5 ml microcentrifuge tube at -20 °C for cytokine analysis. Titanium and Titanium alloy discs were immediately processed for RNA extraction or SEM.

2.8 Phenotypic Analysis

2.8.1 Initial CFU/ml Counts for *S. epidermidis*

S. epidermidis 1457 and 5179-R1 were prepared to OD_{600}= 0.01, 0.05, 0.1 and 0.5 in TSB as described in Section 2.5.3. Next, samples were serially diluted in PBS to 10^7. Then, 20 µl of each dilution and the original suspension was added to a TSB plate and incubated at 37 °C overnight. Following incubation, the number of colonies on were counted on each plate and the CFU/ml for each sample was calculated using the formula below:

$$CFU/ml = \frac{no.\,colonies \; \times dilution\,factor}{0.02}$$

2.8.2 Growth Curve Assay

S. epidermidis 1457 and 5179-R1 cultures were prepared and diluted to OD_{600}=0.05 in TSB, DMEM, MEM and RPMI as in Section 2.5.3. Then, 200 µl aliquots of each sample were added to a Nunc™ 96-well plate (Thermo Fisher Scientific; Loughborough, UK). The optical density of each well was measured hourly for 24 h at 570 nm using the FLUOstar Omega plate reader (BMG Labtech, Aylesbury, UK).

2.8.3 Biofilm Assay

S. epidermidis cultures were prepared were prepared and diluted to OD_{600}=0.05 in TSB, DMEM, MEM and RPMI as in Section 2.5.3. Then, 200 µl aliquots of each sample were added to a Nunc™ 96-well plate. To select wells, 1 µl Proteinase K (Qiagen; Manchester, UK) or 40 µl Sodium (meta) periodate was added with TSB media. The 96-well plate was then incubated at 37 °C for 24 hours. After incubation, the media was removed, and the wells were washed three times with 200 µl of PBS before airdrying at room temperature overnight. The next day, bacteria adherent to the wells were stained with 150 µl 0.1% Crystal Violet for 15 min in the dark. The excess stain was removed by flicking the plate. The plate was washed five times with water before airdrying at room temperature overnight. The optical density of the biofilms was measured at 570 nm using the FLUOstar Omega plate reader. Biofilms were characterised as strong ($OD_{570} > 0.7$), positive (OD_{570} 0.5-0.69), weak (OD_{570} 0.2-0.49) or negative ($OD_{570} < 0.19$) as described by Harris *et al*., 2017.

2.8.4 Biofilm Assay of Adherent *S. epidermidis* on Ti Discs

S. epidermidis 1457 and 5179-R1 cultures at OD_{600}=0.05 in TSB and MEM were prepared as above in Section 2.5.3. Next, 1 ml of diluted *S. epidermidis* culture was added to a 24-well cell culture plate (Thermo Fisher Scientific; Loughborough, UK) with wells containing Ti discs. The samples were then incubated for 2 h, 4 h, 6 h and 24 h at 37 °C. After incubation, the media was removed from the wells and wells were washed with 500 µl of PBS three times before air drying at room temperature overnight. Following this, bacteria adherent to the discs were stained with 500 µl 0.1% crystal violet for 15 min in the dark. The excess crystal violet was removed by pipetting and the samples were air dried at room temperature overnight. The next day, 500 µl of 100% ethanol was added to the well and was incubated at room temperature for 30 min with the lid on. Following this, 200 µl of each sample was added in triplicate

to a 96-well plate. The optical density of the biofilm was measured at 570 nm using the FLUOstar Omega plate reader.

2.8.5 Total Viable Counts

S. epidermidis 1457 and 5179-R1 co-cultures with 1BR.3.G and THP-1 cells were prepared as in Sections 2.6.6 and 2.6.7 respectively, before incubating with 5% CO_2 for 2, 4, 6 or 24 h. At each time point, the supernatant was removed from each well. Next, 500 µl of PBS was added to the well and the bacteria adherent to the Ti discs was removed using a cell scraper. The cell suspension was added to a 2 ml microcentrifuge tube containing 500 µl 0.1% Triton-X 100 and samples were serially diluted to a dilution of 10^7. Then, 20 µl of each dilution and the original suspension was added to a TSB plate and incubated overnight at 37 °C. Following incubation, the number of colonies on each plate were counted and the CFU/ml for each sample was calculated using the formula in Section 2.8.1.

2.9 Microscopy analysis

2.9.1 Sample fixation for SEM

Samples were cultured on Ti/TiAlV discs as in Sections 2.6.6, 2.6.7. and 2.7.2. The wells containing Ti or TiAlV discs were rinsed with 500 µl of 0.1 M PIPES (pH 7.4). Next, 500 µl of 4% formaldehyde in 0.1 M PIPES (pH 7.4) was added to the well as primary fixation. The plate was covered with parafilm and incubated at 4 °C overnight. The following day, 500 µl of 0.1 M PIPES (pH 7.4) was added to each well for 2 min before discarding. For secondary fixation, 500 µl of 2.5% glutaraldehyde in 0.1 M PIPES (pH 7.4) was added to each well and incubated at room temperature for 5 min. Then, 500 µl of 0.1 M PIPES (pH 7.4) was added to each well for 2 min, three times. The Ti and TiAlV discs were postfixed by adding 500 µl of 1% osmium tetroxide in 0.1 M PIPES (pH 6.8) and incubated in the dark for 60 min. The wells were then rinsed three times by adding 500 µl of double distilled water for 2 mins. The Ti and TiAlV discs were dehydrated using an ethanol and ethanol:HMDS series. To each well 500 µl of 50% ethanol was added and incubated for 5 min at room temperature before removing. This was repeated for 70%, 96% and 100% ethanol, followed by 1:2, 1:1 2:1 and 100% HMDS in ethanol, in sequence. Each disc was removed from the well and placed on filter paper in a petri-dish to dry overnight. The next day, the discs were

mounted onto SEM stubs and coated with conductive silver paint (Agar Scientific; Essex, UK) before coating with 10 nm chromium. Due to COVID-19, all samples were imaged by Dr Llinos G Harris. The samples were imaged with a Hitachi S-4800 Field Emission Scanning Electron Microscope (FESEM; Oxon, UK) and operated using the upper or mix secondary electron (SE) detector with a L.A.5 BSE bias. The microscope was operated at accelerating voltages 1 kV, with an emission current of 10 µA and a working distance of 8 mm.

2.9.2 Immunostaining *S. epidermidis* Co-cultures

Samples were cultured on Ti and TiAlV discs as described in Sections 2.6.6 and 2.6.7. Next, the 24-well plates were washed with 500 µl PBS to remove non-adherent bacteria and debris. Then, 500 µl of 4% formaldehyde in PBS was added to each well and incubated at room temperature for 10 min before being removed. After this, 500 µl of the permeabilizing buffer 0.1% Triton X-1000 in PBS was added to each well and incubated at 37 °C for 5 min. Following incubation, the Triton X-1000 was removed and disposed before 500 µl of 1% BSA and 500 µl of 0.1% Tween 20 in PBS was added for 5 min to block nonspecific antigenic sites. To each well 400 µl of 1:100 Gram-positive Bacteria LTA Monoclonal Antibody (G43J) in PBS was added and incubated for 1 h at room temperature. Following incubation, the samples were washed three times with 500 µl of 0.1% Tween 20 in PBS for 2 min. Then 200 µl of 1:1000 Anti-Mouse AlexaFluor488 and 200 µl 1:100 Alexa594 conjugated Phalloidin was added to the well before incubating the sample in the dark at room temperature for 1 h. After incubation, the wells were washed 3 times with 500 µl of PBS. The discs were removed from the well and mounted onto labelled glass slides. One drop of VECTASHIELD® Hard Set™ Antifade Mounting Medium (2BScientific; Oxfordshire, UK) was applied to the disc and a coverslip was placed on the sample. Due to COVID-19, all samples were imaged by Dr Llinos G Harris. The slide was visualised using the Zeiss LSM710 Confocal Microscope (Carl Zeiss AG; Oberkochen, Germany) using Carl Zeiss™ Immersol™ immersion oil (Thermo Fisher Scientific; Loughborough, UK).

2.10 RNA Extraction and Reverse Transcriptase-Quantitative PCR

2.10.1 RNA extraction

RNA was extracted from *S. epidermidis* 5179-R1 co-cultures using the Qiagen RNeasy Mini Kit (Manchester, UK). Samples were cultured in triplicate on Ti and TiAlV discs as described in Sections 2.6.6, 2.6.7. and 2.7.2.

S. epidermidis 5179-R1 adherent to the Ti/TiAlV discs was removed by adding 500 µl PBS and harvesting using a CytoOne® Cell Scraper with 10 mm Pivoting Blade (Starlab; Milton Keynes, UK). The bacterial suspension from three identical wells was removed and added to a 2 ml microcentrifuge tube before centrifuging at 14,000 rpm for 5 min. The supernatant from each microcentrifuge tube was removed and discarded and the pellet was resuspended in 500 µl PBS and   1000 µl of RNAprotect. The microcentrifuge tube was vortexed gently for 5 seconds and incubated at room temperature for 5 min before centrifuging at 5k rpm for 10 min. The supernatant was then discarded, and the pellet was stored at -80 °C.

The RNA extraction method was adapted from the Qiagen RNeasy kit protocol. Firstly, the pellet was thawed and resuspended with 500 µl of 1× TE buffer (Thermo Fisher Scientific; Loughborough, UK) and pipetted into a 1.5 ml microcentrifuge tube. The sample was centrifuged for 5 min at 4,000 rpm and the supernatant was removed. The pellet was resuspended in 200 µl 1× TE buffer containing 40 µl lysostaphin (200 µg/ml), 20 µl mutanolysin (400 µg/ml) and 1 µl proteinase K (Qiagen; Manchester, UK; 100 µg/ml) and incubated on a rotary wheel at 37 °C for 1 h. Following incubation, 350 µl of RLT buffer was added to the suspension and vortexed vigorously for 10 s. Then, the sample was centrifuged for 2 min at 10,000 rpm. The supernatant was applied to a QIAshredder spin column and centrifuged at 12,000 rpm for 2 min. The spin column was discarded and 250 µl of 100% ethanol was added and mixed by pipetting. The suspension and precipitate were added to a RNeasy mini spin column and centrifuged at 10,000 rpm for 15 s before the flow through was discarded. Eighty microlitres of DNase treatment containing 10 µl DNase 1 and 70 µl DNase buffer was added to the spin column and incubated at room temperature for 30 min. Following incubation, the sample was centrifuged at 10,000 rpm for 15 s. The flow through was discarded and the spin column was transferred to a new collection tube. Then, 500 µl of RW1 solution was added to the spin column and centrifuged for 15 s at 10,000 rpm. The flow through was discarded and the spin column was transferred to a new

collection tube. Next, 500 µl of RPE was added to the spin column and centrifuged at 10,000 rpm for 15 s. Again, the flow through was discarded and the spin column was transferred to a new collection tube. The sample was then centrifuged at 12,000 rpm for 2 min and the spin column was transferred to a 1.5 ml microcentrifuge tube. Finally, 50 µl of nuclease free water was added to the spin column. The spin column was left to stand for 1 min and then centrifuged at 10,000 rpm for 1 min. The RNA (ng/µl) was quantified using the Nanodrop Spectrophotometer (Thermo Fisher Scientific; Loughborough, UK) and was stored at -80 °C.

2.10.2 cDNA Synthesis

The qPCRBIO cDNA Synthesis Kit (PCR Biosystems; London, UK) was used for all cDNA synthesis reactions. Ribonucleic acid was converted to cDNA as per the qPCRBIO cDNA Synthesis Kit product datasheet. The S1000™ Thermocycler (Bio-Rad; Hertfordshire, UK) was used for cDNA reactions. In a 0.2 ml PCR tube, 4 µl of 5× cDNA synthesis mix, 1 µl of 20× Reverse transcriptase for cDNA synthesis mix, 12 µl of nuclease free water and 3 µl of *S. epidermidis* RNA (2 µl/ml) was added. Conditions for cDNA synthesis were as stated in the qPCRBIO cDNA synthesis kit product data sheet and were as follows:

Step 1: *Incubate at 42 °C for 30 min for reverse transcription*

Step 2: *Incubate at 85 °C for 10 min to denature reverse transcriptase*

Step 3: *Hold at 4 °C*

Once completed, the cDNA was stored at -20 °C and used within 2 weeks.

2.10.3 Reverse Transcriptase-Quantitative PCR

2.10.3.1 Reverse Transcriptase-Quantitative PCR Primers

Primers for RT-qPCR were purchased from Eurofins (Wolverhampton, UK) and are listed in Table 2.2. New primers were created using Primer3 (v4.1.0; Whitehead Institute for Biomedical Research).

Table 2.2. A list of primers used.

Primer Name	Sequence (5' to 3')	Annealing Temperature	Source
icaAR1	F: TGTATCAAGCGAAGTCA R: GGCAGTAACATCCAGCAAGG	56.5 °C 57.3 °C	Knobloch *et al.*, 2004
aapR1	F: ATGGGCAAACGTAGACAAGG R: GCTTTCGCTTCATGGCTACT	57.3 °C 57.3 °C	Rohde *et al.*, 2004
EmbpR3	F: GCAACTAACGGATGGTGTAAATC R: GCCAATAATAGCCGCAACTTC	58.9 °C 57.9 °C	Christner *et al.*, 2010
atlE	F: AACAACCACAGAATCAGTCTAATC R: TTGAACTTGGGTAGGGTCTTG	57.6 °C 57.9 °C	Rohde *et al.*, 2004
sdrG	F: GACGGCCCTTTCATCAGTAA R: GTTGAACCTTCATCGCCATT	57.3 °C 55.3 °C	Designed for project
SdrF2	F: AATACTCGTGGGTGCTACGTT R: GGTGACAGAGAACGACTTCAAA	57.9 °C 58.4 °C	Designed for project
RNA3	F: GTTATGATGGCAGCAGA R: GGATGGCTCAACAACAACT	50.0 °C 58.0 °C	Harris *et al.*, 2017
gyrB	F: CTGACAATGGCCGTGGTATTC R: GAAGATCCAACACCGTGAAGAC	59.8 °C 60.3 °C	Knobloch *et al.*, 2004

Primers were reconstituted in nuclease free water to a concentration of 100 pmol/µl, aliquoted into 10µl aliquots and stored at -20 °C.

2.10.3.2 Reverse Transcriptase-Quantitative Polymerase Chain Reaction (RT-qPCR) Using SYBR Green

RT-qPCR using SYBR green was carried out to amplify the genes of interest and housekeeping gene (Table 2.2.). For each reaction, 12.5 µl of SensiMix SYBR No-ROX (Meridian Bioscience, Tennessee, USA), 8.5 µl nuclease free water, 0.5 µl forward primer, 0.5 µl backward primer and 3 µl of *S. epidermidis* cDNA (Section 2.10.2) was added. Reactions were run in 0.2 ml PCR tubes or in the Rotor-Disc 72 (Qiagen; Manchester, UK), and heat sealed with Rotor-Disc heat sealing film (Qiagen; Manchester, UK) on the Roto-Disc heat sealer (Qiagen; Manchester, UK). For each run, samples were amplified in triplicate and non-template controls were added for each primer. The RT-qPCR reaction was run on the Corbett Rotorgene 6000 RT-qPCR instrument (Qiagen, UK) using the following conditions:

Step 1: Hold at 95 °C for 10 min

Step 2: Denature at 95 °C for 20 s and anneal at 55 °C for 20 s. Repeat 40 times

Step 3: Extend at 72 °C for 30 s

Step 4: Melt by increasing temperature from 72 °C to 95 °C by increasing 1 °C each step. Wait 90 s on pre-melt condition first step and wait 5 s for each step following.

Following RT-qPCR, cycle threshold (CT) values were recorded. The fold-difference in gene expression between samples was determined using the $2^{-\Delta\Delta C_T}$ method as described in Livak and Schmittgen (2001). The fold differences were calculated as below:

$$Gene\ CT_1 - Housekeeping\ CT_1 = \Delta CT_1$$

$$Gene\ CT_2 - Housekeeping\ CT_2 = \Delta CT_2$$

$$\Delta CT_1 - \Delta CT_2 = \Delta\Delta CT.$$

$$2^{-\Delta\Delta CT} = Fold\ difference$$

2.10.4 Gel Electrophoresis

Gel electrophoresis was used to verify the RT-qPCR products and controls. A 1% small agarose gel was produced by heating 50 ml 1 X TAE with 0.05 g electrophoresis grade agarose until fully dissolved and then adding 5 µl Sybr® Safe DNA gel stain (Invitrogen, Thermo Fisher Scientific; Loughborough, UK). The gel was cast in a gel mould box with a gel comb and left to cool for 20 min. During this time, samples were prepared by mixing 10 µl PCR product with 2 µl of 6× Blue/Orange DNA loading dye (Promega; Madison, Wisconsin, USA). The DNA ladder was also prepared by adding 5 µl 100 kb DNA ladder (Promega; Madison, Wisconsin, USA) to 2 µl DNA loading dye. Next, the gel comb was removed from the set gel and the gel was moved to the gel tray. Then, 10 µl of PCR samples and 7 µl of DNA ladder was added to the wells of the gel and the gel tray was filled with 1 X TAE. The gel was run at 60 V for 60 min. Finally, the gel was imaged using the Chemidoc Imaging System (Bio-rad; Hertfordshire, UK).

2.11 Cytokine analysis

2.11.1 Proteome Profiler Arrays

The Proteome Profiler Human XL Cytokine Array (R&D systems; Minneapolis, UK) and Proteome Profiler Human Cytokine Array (R&D systems; Minneapolis, UK) were used for cytokine analysis of samples as prepared in Sections 2.6.6, 2.6.7 and 2.7.2. Reagents were prepared as per the manufacturer's instructions. Both cytokine arrays were carried out as per the product data sheets. Cytokines are listed in Appendices A and B. Membranes were imaged using the Chemidoc (Bio-rad; Hertfordshire, UK). ImageJ software (1.53k; Rasband, 2018) was used to determine average pixel density. Negative control spots were utilised to determine background pixel density. The membranes were adjusted to equal contrast for comparable results.

2.11.2 IL-8 ELISA

The DuoSet ELISA IL-8 kit (R&D systems; Minneapolis, UK) was used to analyse the production of IL-8 by samples as prepared in 2.6.6, 2.6.7 and 2.7.2. Cell samples incubated with LPS for 4 h were included as positive controls. A Grenier Bio-One half area 96-well plate (Sigma Aldrich; Gillingham, UK) was used for the IL-8 ELISA and all reagents used were half the volume of the manufacturers protocol except for the stop solution. As per the manufacturers protocol, the blocking buffer was 1% BSA in PBS and the reagent diluent was 0.1% BSA in PBS. The stop solution used was 1 M HCl and SureBlue™ was used as the colour solution.

Firstly, the capture antibody was diluted to the appropriate working concentration in 5.5 ml of PBS without carrier protein in a 50 ml conical tube and vortexed. Next, 50 µl of diluted capture antibody was added to wells in the half area plate. The half area plate was covered in parafilm and incubated overnight at room temperature. The next day, the capture antibody was discarded, and the plate was washed three times. To wash, approximately 200 µl of wash buffer was added to each well using a squirt bottle and removed by flicking the plate. After the last wash, excess liquid was removed by inverting the plate and blotting it against paper towels. Then, 150 µl of Blocking Buffer was added to each well, before covering the plate with parafilm and incubating at room temperature for an hour. During this time, standards were prepared by performing a seven-point two-fold serial dilution of the High Standard into the

Reagent Diluent in 1.5 ml microcentrifuge tubes. In one 1.5 ml microcentrifuge tube, 250 µl of Reagent Diluent was prepared as a blank. To prepare the samples, a two-point ten-fold serial dilution in the reagent diluent was performed in 1.5 ml microcentrifuge tubes. Following an hour incubation, the Blocking Buffer was removed from the plate and the wells were washed as above. After washing, 50 µl of the prepared standards, blank and samples were added in duplicate to the plate. The plate was covered with parafilm and incubated for 2 h at room temperature. Following incubation, the samples were removed, and the plate was washed as above. Next, the Detection Antibody was diluted to the working concentration in 5.5 ml of Reagent Diluent and 50 µl of the diluted Detection Antibody was added to each well. The plate was then covered with parafilm and incubated for 2 h at room temperature. After incubation, the Detection Antibody was removed from the plate and the plate was washed as above. The Streptavidin-HRP was diluted to the working concentration and 50 µl was added to each well before incubating in the dark for 20 min at room temperature. After incubation, the Streptavidin-HRP was removed, and the plate was washed as above. To each well 50 µl of SureBlue™ TMB Microwell Peroxidase Substrate Kit (SeraCare, Massachusetts) was added, and the plate was incubated in the dark for 20 min. Next, 50 µl of stop solution, HCl was added to each well and the plate was tapped to mix the samples. The optical density of each well was immediately determined at 570 nm using the BMG plate reader. Using the BMG Mars data analysis software (v3 02R2) the optical densities of standards and samples were blank corrected. A 4-paramater fit was applied to the data to generate a standard curve from which the R^2 value and sample concentrations were calculated.

2.12 Statistical Analysis

Statistical analysis was performed with Graph Pad Prism version 7 (La Jolla, California, USA). All data was firstly tested for normality using the Shapiro-Wilks normality test. Data not normally distributed was analysed using Mann-Whitney tests, or Kruskal-Wallis while normally distributed data was analysed using parametric T-tests, one-way ANOVA, or two-way ANOVA. Significant differences were determined when $p<0.05$.

Chapter 3. Results

3.1 Optimisation

As a result of the COVID-19 pandemic, only one biological replicate of optimisation experiments could be completed within the time frame.

3.1.1 Initial CFU/ml of *S. epidermidis*

Studies have previously used CFU/ml values between 1×10^6 to 1×10^7 CFU/ml to represent an *S. epidermidis* medical device infection (Wang *et al*., 2009; Siverino *et al*., 2021). For this reason, it was decided to develop a co-culturing method in which 5×10^6 CFU/ml was added to each well. As OD_{600} readings were utilised to dilute bacterial cultures before co-culture, the OD_{600} which represented 5×10^6 CFU/ml was determined in all culture media used for co-culture. To achieve this, *S. epidermidis* 1457 and 5179-R1 cultures were diluted to starting OD_{600} of 0.01, 0.05, 0.1 and 0.5 in TSB, MEM, DMEM and RPMI media. Then, 20 μl of this suspension was cultured on TSB agar overnight, before CFU/ml values were calculated the next day (Section 2.8.1).

Figure 3.1 displays a positive correlation between the OD_{600} and CFU/ml of *S. epidermidis* 1457 and 5179-R1 in all media. No obvious differences in CFU/ml were identified between media at all OD_{600} dilutions. As expected, the lowest CFU/ml was seen with OD_{600} of 0.01 (2.4×10^3 to 4.6×10^4 CFU/ml) and the highest with OD_{600} of 0.5 (4.8×10^7 to 1.41×10^8 CFU/ml), with OD_{600} 0.05 and 0.1 ranging between 2.4×10^6 and 3.3×10^7 (Figure 3.1.). As *S. epidermidis* CFU/ml values were in the desired range of approximately 55×10^6 CFU/ml in all media at an OD_{600} of 0.05, OD_{600} 0.05 was chosen as the most appropriate dilution to use for further experiments.
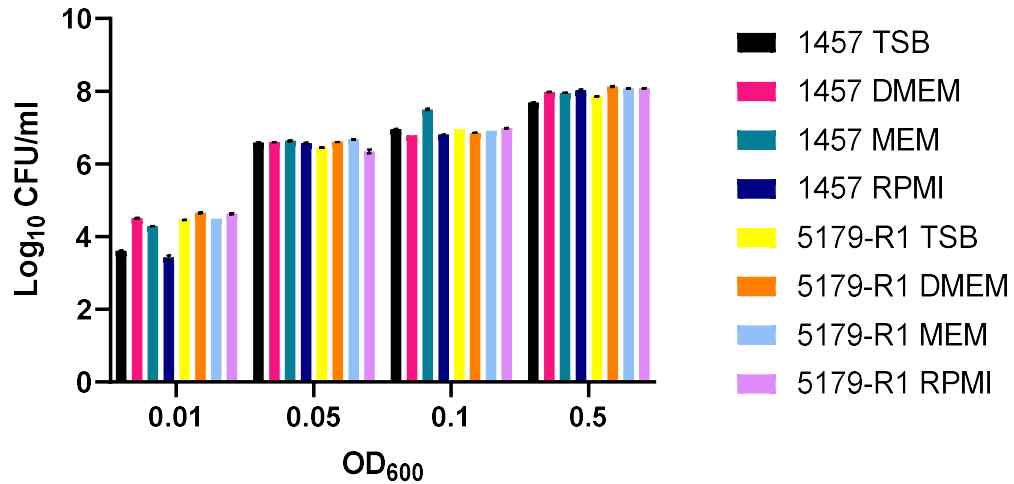
Figure 3.1. Log CFU/ml values of *S. epidermidis* 1457 and 5179-R1 in bacterial and cell culture media. *S. epidermidis* cultures were diluted to starting OD_{600} values of 0.01, 0.05, 0.1 and 0.5 in TSB, MEM, DMEM and RPMI before log CFU/ml values were recorded. Results show the mean average +/- the standard error of the mean for 2 technical replicates.

3.1.2 *S. epidermidis* Growth

For a successful co-culturing method to be developed, the growth of *S. epidermidis* in the associated cell culture media was essential. To assess the ability of *S. epidermidis* 1457 and 5179-R1 to grow over 24 h in DMEM, MEM and RPMI cell culturing media, growth curve assays were performed as in Section 2.8.2. Both *S. epidermidis* strains were diluted to OD_{600}=0.05 in TSB, DMEM, MEM or RPMI before optical density at 570 nm was recorded using the BMG plate reader over 24 h.

As displayed in Figure 3.2., *S. epidermidis* 1457 showed growth in all media. *S. epidermidis* 1457 grew best in TSB with a mean OD_{570} of 1.14 by 5 h. In DMEM, *S. epidermidis* 1457 grew slower than in TSB but achieved a comparable OD_{570} of 0.99 after 11 h. When grown in RMPI, *S. epidermidis* 1457 reached an optimal OD_{570} of 0.72 by 4 h. Finally, when grown in MEM, *S. epidermidis* 1457 grew to a mean OD_{570} of 0.78 by 5 h but after 6 h, the OD_{570} of *S. epidermidis* 1457 decreased to an OD_{570} of 0.296 by 24 h whilst other media remained above 0.5.
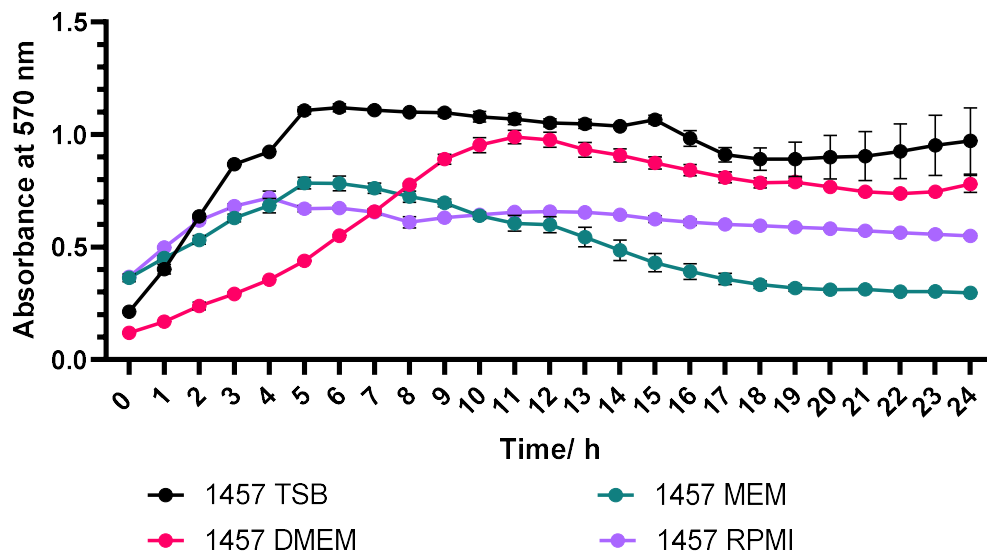
Figure 3.2. Growth curve assay showing the effect of TSB, DMEM, MEM and RPMI on the growth of *S. epidermidis* 1457 over 24 h. Results show the mean +/- the standard error of the mean for 3 replicates.

Similar to *S. epidermidis* 1457, *S. epidermidis* 5179-R1 displayed growth in all media (Figure 3.3.). *S. epidermidis* 5179-R1 grew best in TSB with a mean OD_{570} of 0.72 by 4 h. In DMEM, *S. epidermidis* 5179-R1 grew slower than in TSB but achieved a comparable OD_{570} of 0.8 after 13 h. When grown in RMPI, *S. epidermidis* 5179-R1 reached an optimal OD_{570} of 0.40 by 5 h. Finally, when grown in MEM, *S. epidermidis* 5179-R1 grew to a mean OD_{570} of 0.69 by 10 h but after 10 h, the OD_{570} of *S. epidermidis* 1457 decreased to an OD_{570} of 0.36 by 24 h whilst other media remained above 0.4.
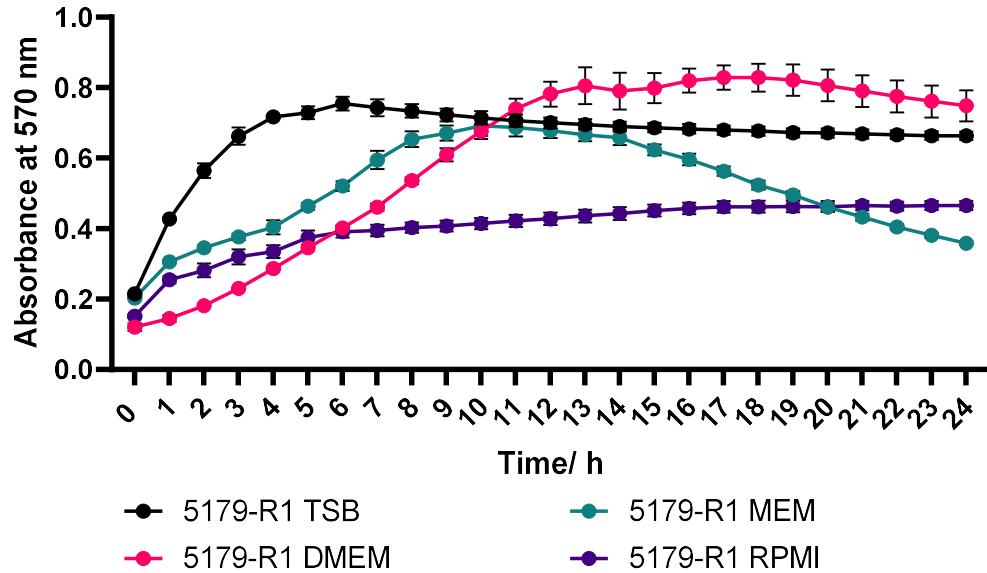
Figure 3.3. Growth curve assay showing the effect of TSB, DMEM, MEM and RPMI on the growth of *S. epidermidis* 5179-R1 over 24 h. Results show the mean +/- the standard error of the mean for 3 replicates.

3.1.3 *S. epidermidis* Biofilm Formation

To confirm the biofilm formation mechanisms of *S. epidermidis* 1457 and 5179-R1, a biofilm assay in TSB with proteinase K or sodium (meta)periodate was performed. *S. epidermidis* biofilms were grown at 37 ˚C in TSB with proteinase K or sodium (meta)periodate for 24 h, before staining with crystal violet and recording optical density at 570 nm with the BMG plate reader (Section 2.8.3.). Sodium (meta)periodate is known to break up polysaccharide-based biofilms through periodate oxidation, whilst proteinase K can disperse protein-based biofilms (Rhode *et al*., 2005). This, therefore, allows for the differentiation between PIA-dependent and protein-dependent biofilm formation mechanisms.

As shown in Figure 3.4., *S. epidermidis* 1457 produced strong biofilms in both TSB and TSB with Proteinase K but in the presence of sodium (meta)periodate a negative phenotype was seen. Similarly, *S. epidermidis* 5179-R1 also produced a strong biofilm in TSB and TSB with Sodium (meta)periodate, however, a biofilm negative phenotype when grown in TSB with Proteinase K. This confirms that both *S. epidermidis* 1457 and 5179-R1 have the correct phenotypes.
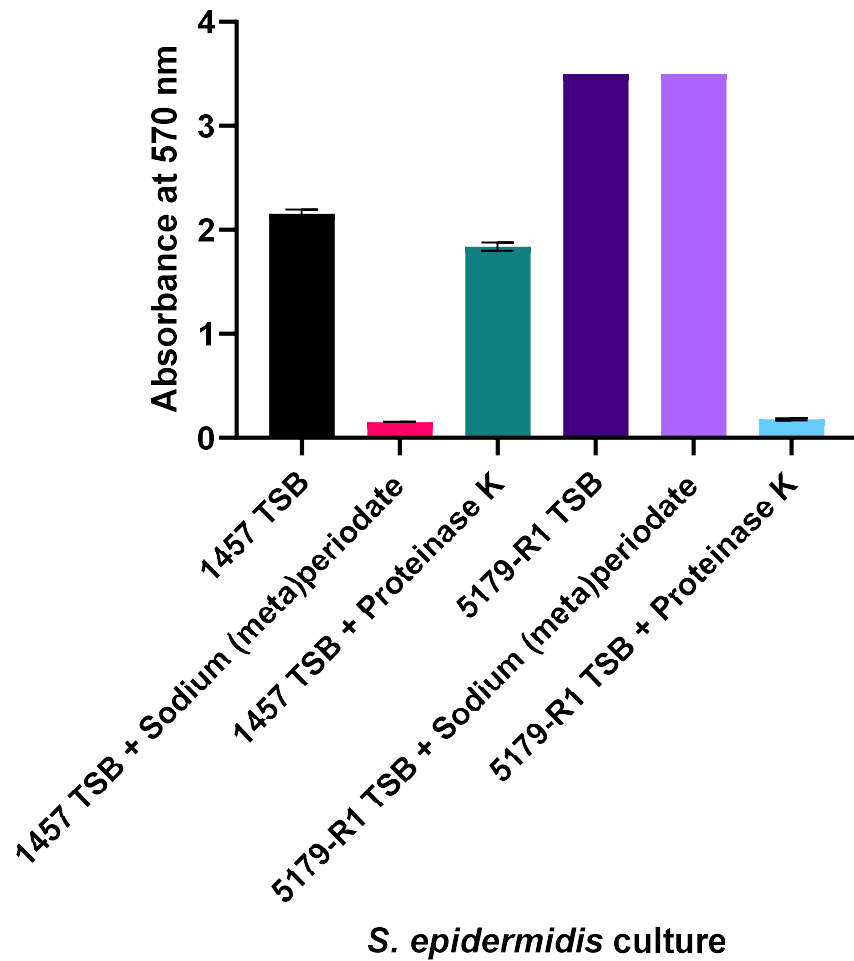
Figure 3.4. Biofilm assay showing the effect of TSB, sodium (meta)periodate and proteinase K on *S. epidermidis* 1457 and 5179-R1 biofilm production. Results show the mean average +/- the standard error of the mean for 3 technical replicates.

Another important component in the development of an *S. epidermidis* co-culturing method, is the ability of *S. epidermidis* to form biofilms in the required cell-culture media. To investigate the ability of *S. epidermidis* 1457 and 5179-R1 to produce biofilms in DMEM, MEM and RPMI, a further biofilm assay was conducted as described in Section 2.8.3. *S. epidermidis* biofilms were grown at 37 ˚C in TSB, DEMEM, MEM and RPMI for 24 h, before staining with crystal violet and recording optical density at 570 nm with the BMG plate reader.

As shown in Figure 3.5., *S. epidermidis* 5179-R1 produced strong biofilms when grown in both TSB and DMEM (OD_{570} 3.50 and OD_{570} 2.71 respectively), while in RPMI the biofilm strength decreased (OD_{570} 0.66) and in MEM only a weak biofilm formed (OD_{570} 0.25). Similar to *S. epidermidis* 5179-R1, *S. epidermidis* 1457 also produced a strong biofilm when grown in TSB (OD_{570} 3.50) but produced only a weak biofilm in RPMI (OD_{570} 0.24) and had a negative phenotype in both MEM and DMEM (OD_{570} 0.06 and OD_{570} 0.10 respectively).
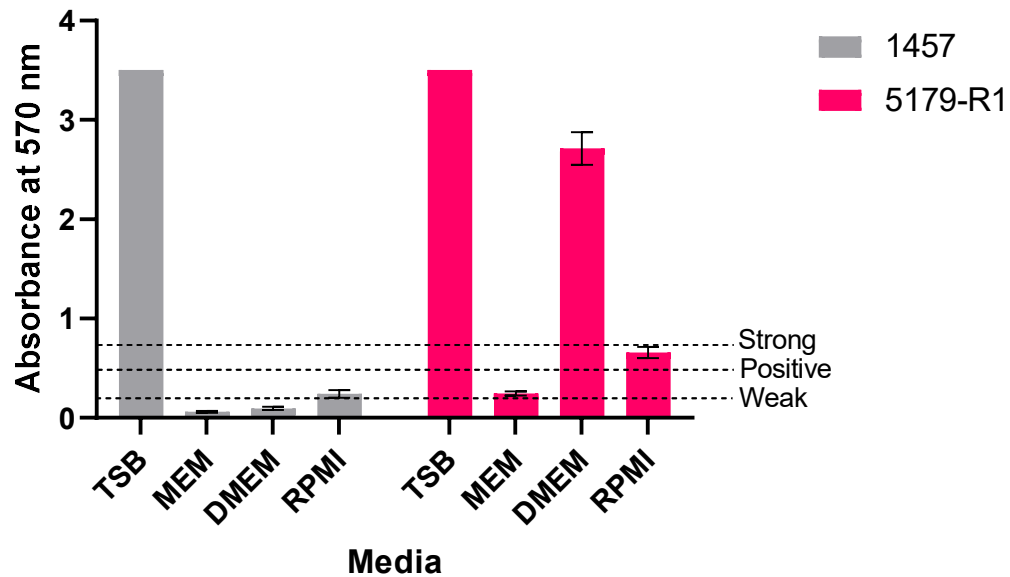
Figure 3.5. Biofilm assay showing the effect of TSB, MEM, DMEM and RPMI on *S. epidermidis* 1457 and 5179-R1 biofilm production. Results show the mean average +/- the standard error of the mean for 3 technical replicates.

In co-culture, *S. epidermidis* biofilms may be influenced by the presence of a Ti or TiAlV surface. To confirm the ability of *S. epidermidis* 1457 and 5179-R1 to produce biofilms on the Ti disc, when in TSB or MEM, the cell culture media required for fibroblast culture a biofilm assay was performed over 24 h in MEM and TSB (Section 2.8.4). *S. epidermidis* strains were cultured on Ti surfaces in TSB or MEM for 24 h at 37 ˚C for biofilm formation. Following incubation, biofilms were washed and stained with crystal violet. Ethanol was then added to absorb the colour of the crystal violet-stained biofilm before the absorbance was read with the BMG plate reader.

When grown on Ti discs in TSB, the thickness of *S. epidermidis* 1457 and 5179-R1 biofilms increased over the 24 h in a time-dependent manner (Figure 3.6.). In MEM,

S. epidermidis 5179-R1 biofilms were weaker than when grown in TSB but increased in strength in a time-dependent manner over the 24 h period. In contrast to when grown in TSB, *S. epidermidis* 1457 biofilm production in MEM remained weak at all time points (OD_{570} 0.279). Despite this, as biofilm formation of both *S. epidermidis* strains was confirmed in MEM on Ti, the use of this cell culturing media was continued.
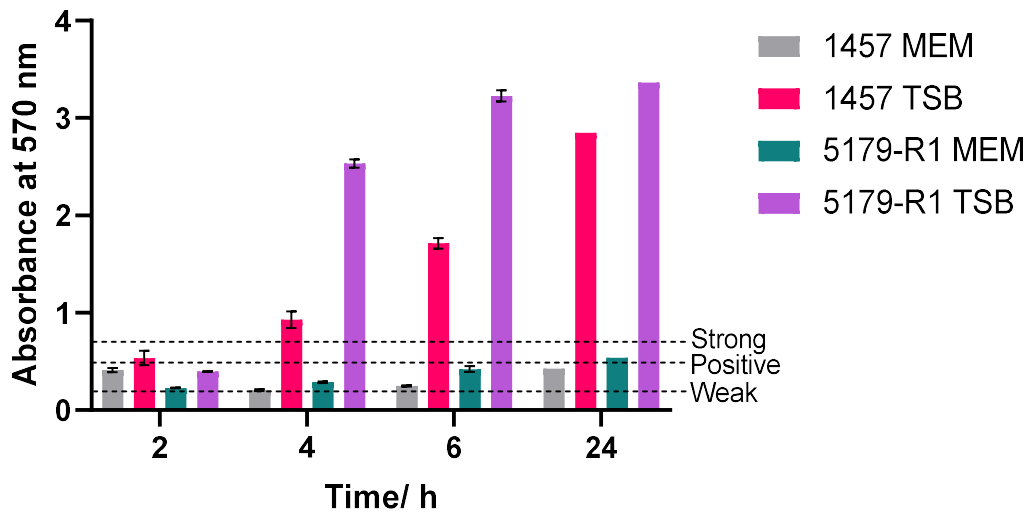
Figure 3.6. Biofilm assay showing the effect of TSB and MEM on *S. epidermidis* 1457 and 5179-R1 biofilm formation on Ti discs. Results show the mean average +/- the standard error of the mean for 3 technical replicates.

3.1.4 Scanning Electron Microscopy (SEM)

To determine the adherence of THP-1 monocytes and 1BR.3.G fibroblasts to Ti/TiAlV discs in mono-culture or co-culture with *S. epidermidis* 1457 or 5179-R1, the cultures were visualised using SEM.

3.1.4.1 Co-culturing THP-1 monocytes with *S. epidermidis* on Ti

Bacterial cell components and the secretion of cytokines such as GM-CSF or IL-4 are known to be triggers for monocyte differentiation into macrophages (Ohradanova-Repic *et al*., 2016). For this reason, SEM was used to visualise whether the presence of *S. epidermidis* would cause differentiation of THP-1 monocytes, and thus adhesion to the Ti surface. Firstly, *S. epidermidis* was allowed to attach to the Ti surface for 4 h before co-culturing with THP-1 monocytes for 24h. To achieve this, 500 µl *S.*

epidermidis 1457 and 5179-R1 diluted to OD_{600} of 0.1 in RPMI (Section 2.5.3) was added to Ti discs and incubated for 4 h at 37 °C with a 5% CO_2. Following incubation, 500 µl of THP-1 monocytes (500,000 cells/ml) were added to the culture and incubated for a further 24 h at 37 °C with a 5% CO_2. Co-cultures were then fixed for SEM as described in Section 2.9.1.

Following mono-culture of THP-1 monocytes, cellular debris was observed on the Ti disc (Figure 3.7. A). However, no differentiation or adhesion of monocytes was observed. Both *S. epidermidis* 1457 and 5179-R1 adhered to the Ti surface in mono-culture, with clear clusters of coccoid bacteria present (Figure 3.7.B and C). After co-culturing with THP-1 monocytes, bacterial aggregations of *S. epidermidis* 5179-R1 were present with cellular debris between cells (Figure 3.7.D). In comparison, *S. epidermidis* 1457 co-cultures with THP-1 monocytes showed less cellular debris surrounding bacteria (Figure 3.7.E). Results demonstrated that the presence of *S. epidermidis* did not cause differentiation and adhesion of THP-1 monocytes (Figure 3.7.D. and 3.7.E.).
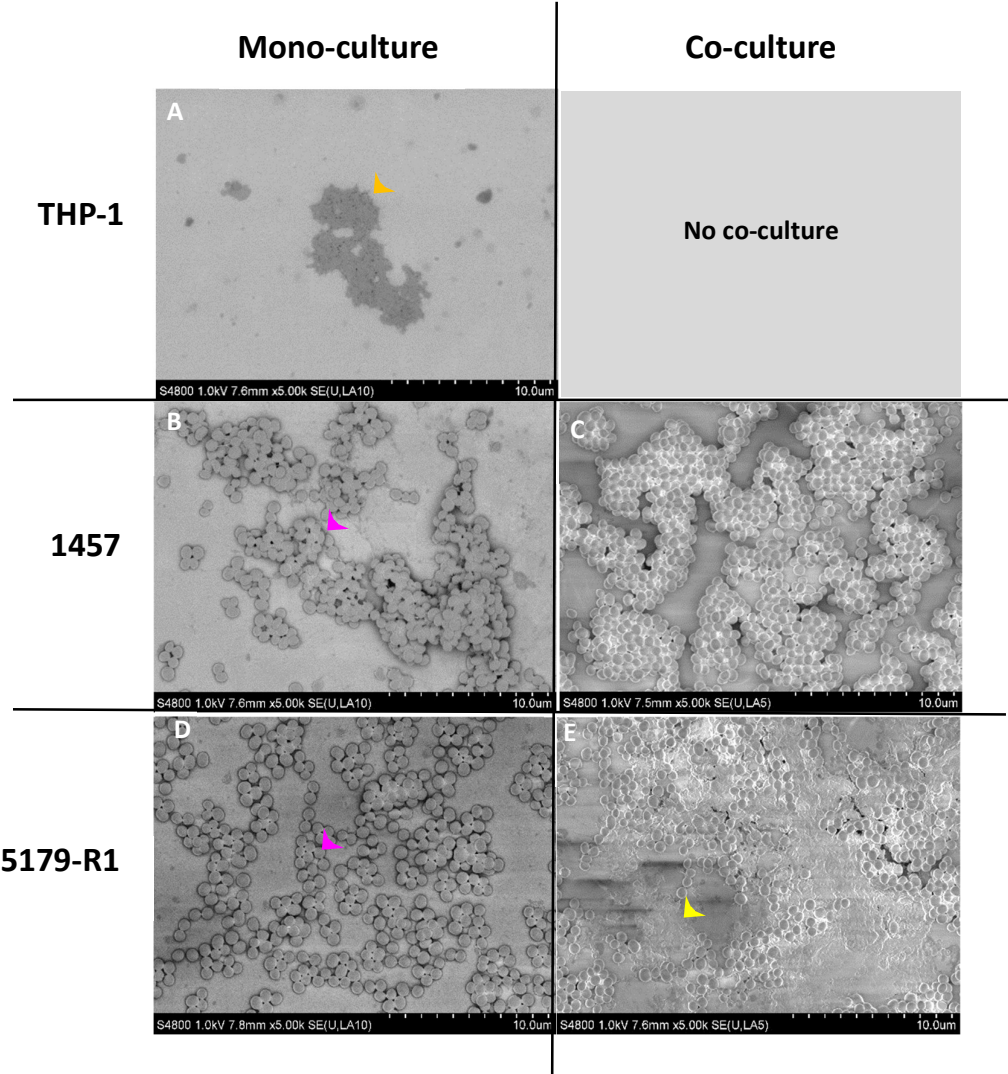
Figure 3.7. **SEM images of Ti discs cultured with THP-1 monocytes or *S. epidermidis* in mono- or co-culture**. A) mono-cultured THP-1 monocytes for 24 h, B) mono-cultured *S. epidermidis* 1457 for 4 h, C) *S. epidermidis* 1457 for 4 h co-cultured with THP-1 monocytes for 24 h, D) mono-cultured *S. epidermidis* 5179-R1 for 4 h, E) *S. epidermidis* 5179-R1 for 4 h and THP-1 monocytes for 24 h. Arrowheads show examples of monocytes (orange), *S. epidermidis* cells (purple) and cellular debris (yellow).

To further investigate the ability of *S. epidermidis* to differentiate THP-1 monocytes into macrophages, THP-1 monocytes were allowed to establish on the Ti surface prior to incubating with *S. epidermidis* for an incubation period of either 4 h or 24 h. THP-1monocytes were seeded at 500,000 cells/ml on Ti and incubated for 24 h at 37 °C with a 5% CO_2. Following incubation, *S. epidermidis* 1457 and 5179-R1 diluted to OD_{600} of 0.1 in RPMI (Section 2.5.3) was added to each sample and incubated further for 4 h or 24 h before fixation (Section 2.9.1).

In mono-culture at 4 h, clusters of *S. epidermidis* 1457 and 5179-R1 were observed (Figure 3.8.A and E). Following 24 h incubation, larger aggregates of bacteria were present for both strains (Figure 3.8.C and G). Similar to mono-culture samples, larger aggregates of bacterial cells were observed in co-culture at 24 h compared to 4 h (Figure 3.8.B, D, F and H). Cellular debris of THP-1 monocytes was observed in all co-culture conditions with both *S. epidermidis* strains (Figure 3.8.B, D, F and H). However, the differentiation of monocytes and subsequent adhesion to the Ti surface was not observed under any co-culture condition (Figure 3.8.B, D, F and H).

Due to the absence of monocyte attachment to Ti discs and the lack of differentiation of THP-1 monocytes to macrophages in the presence of *S. epidermidis* (as seen with SEM), THP-1 monocytes were differentiated to macrophages prior to the addition of *S. epidermidis* for the duration of this project. In addition, as a result of the CFU/ml data (Figure 3.1.) in conjunction with SEM images, *S. epidermidis* OD_{600} was decreased from 0.1 to 0.05 from this point.
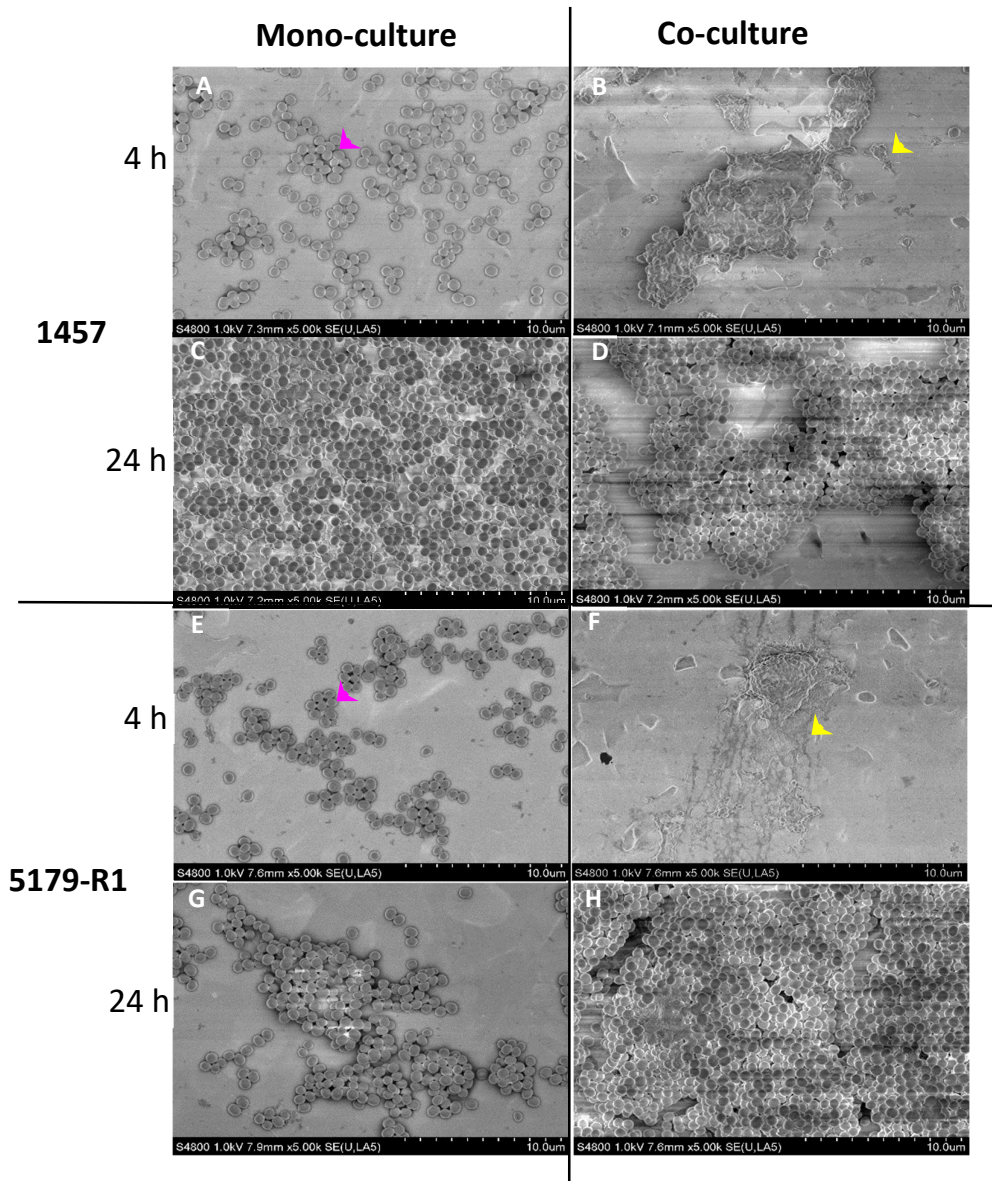
Figure 3.8. SEM images of Ti discs cultured with THP-1 monocytes or *S. epidermidis* in mono- or co-culture for 4 or 24 h. Ti discs cultured with *S. epidermidis* 1457 (top panel) or *S. epidermidis* 5179-R1 (bottom panel) for 4 h (A, B, E and F) or 24 h (C, D, G and H) in mono-culture (left panel) or in co-culture with THP-1 monocytes (right panel). THP-1 monocytes were cultured for 24 h prior to the addition of *S. epidermidis* in co-culture samples. Arrowheads show examples of *S. epidermidis* cells (purple) and cellular debris (yellow).

3.1.4.2 Co-culturing 1BR.3.G Fibroblasts with *S. epidermidis* on Ti

To identify an appropriate growth media and seeding value for the co-culture of 1BR.3.G fibroblasts and *S. epidermidis,* mono-cultures and co-cultures were prepared on Ti or TiAlV surfaces, before fixing for SEM visualisation (Section 2.9.1). Firstly,

1BR.3.G fibroblasts were seeded at 20,000 cells/ml on Ti discs for 48 h in DMEM or MEM. SEM imaging showed the presence of 1BR.3.G fibroblasts on the Ti disc, however, confluency was not reached in either medium (Figure 3.9).
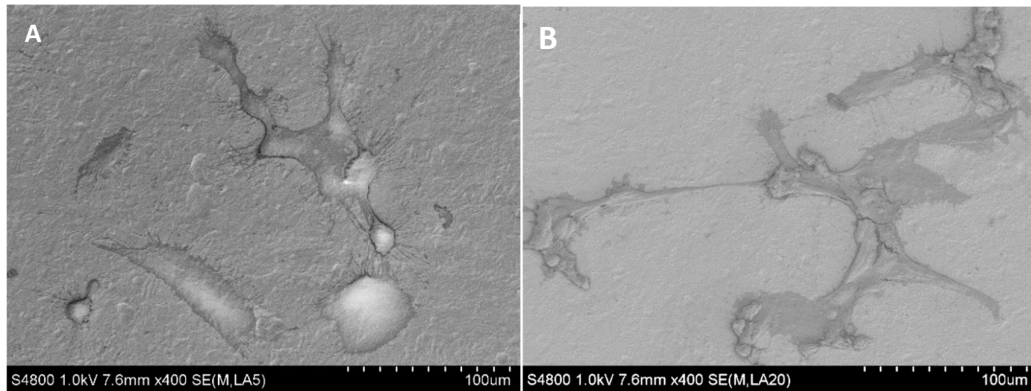
Figure 3.9. SEM images of 1BR.3.G fibroblasts seeded at 20,000 cells/ml on Ti discs. Images show 1BR.3.G fibroblasts cultured in A) DMEM and B) MEM for 48 h.

To obtain a higher confluency, 1BR.3.G fibroblasts were seeded at 50,000 cells/ml in DMEM and MEM. When cultured in DMEM, 1BR.3.G fibroblasts did not develop a confluent layer on the Ti discs, however, in MEM a higher confluency of 1BR.3.G fibroblasts was obtained (Figure 3.10). For this reason, 1BR.3.G fibroblasts were seeded at 50,000 cells/ml in MEM and incubated for 48 h prior to co-culture with *S. epidermidis* strains in future experiments.
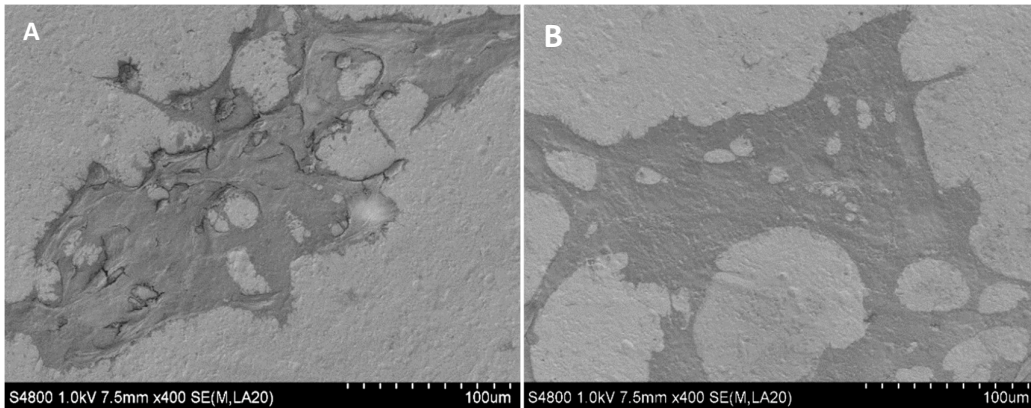
Figure 3.10. SEM images of 1BR.3.G fibroblasts seeded at 50,000 cells/ml on Ti discs. Images show fibroblasts cultured in A) DMEM and B) MEM for 48 h.

To confirm that 1BR.3.G fibroblasts could be co-cultured with *S. epidermidis,* samples were prepared as described in Section 2.6.7 and then fixed for SEM (Section 2.9.1).

In co-culture both 1BR.3.G fibroblasts and *S. epidermidis* 5179-R1 were visualised however, fewer clusters of *S. epidermidis* 5179-R1 were present on the Ti discs than expected (Figure 3.11.). For this reason, it was decided to increase *S. epidermidis* incubation time from 4 h to 6 h for all future experiments.
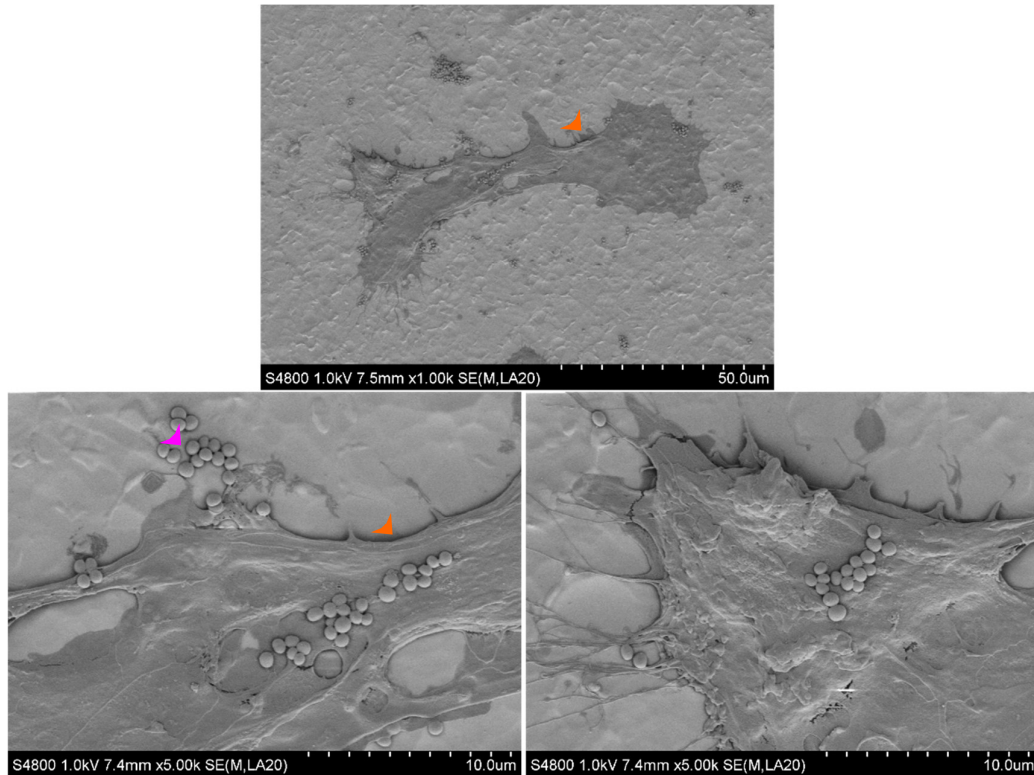
Figure 3.11. SEM images of 1BR.3.G fibroblasts co-cultured with *S. epidermidis* 5179-R1 for 4 h on Ti. Arrowheads show examples of 1BR.3.G fibroblasts (orange) and *S. epidermidis* cells (purple).

3.1.5 Total Viable Counts

To confirm that the presence of 1BR.3.G fibroblasts or THP-1 macrophages did not have an impact on *S. epidermidis* cell viability when co-cultured on Ti discs, total viable counts were performed over 24 h as in Section 2.8.5. To achieve this, *S. epidermidis* was co-cultured with 1BR.3.G fibroblasts or THP-1 macrophages over 24 h. Next *S. epidermidis* cells adherent to the Ti surface were cultured on TSB agar and CFU/ml values were calculated.

Results showed an increase in viable *S. epidermidis* 1457 and 5179-R1 cells when co-cultured with THP-1 macrophages over 24 h (Figure 3.12.A). At 2 h, 9.85×10^3 CFU/ml of *S. epidermidis* 1457 and 1.05×10^4 CFU/ml of *S. epidermidis* 5179-R1 were

recorded, with numbers increasing to 9.15×10^6 CFU/ml for *S. epidermidis* 1457 and 9.8×10^5 CFU/ml for *S. epidermidis* 5179-R1 by 4 h. At 6 h, *S. epidermidis* 1457 and 5179-R1 had further increased in numbers to 9.10×10^7 and 9.30×10^6 CFU/ml respectively and finally, by 24 h *S. epidermidis* 1457 reached 1.27×10^8 and *S. epidermidis* 5179-R1 reached 1.09×10^8 CFU/ml.

Comparatively, in co-culture with 1BR.3.G fibroblasts, *S. epidermidis* 1457 and 5179-R1 CFU/ml values increased over time (Figure 3.12.B). At 2 h CFU/ml values of 3.4×10^6 for *S. epidermidis* 1457 and 2×10^7 CFU/ml for *S. epidermidis* 5179-R1 were recorded, while at 4 h, both *S. epidermidis* 1457 and 5179-R1 CFU/ml increased to 5.1×10^6 and 5×10^7 CFU/ml respectively. This further increased by 6 h to 8.25×10^6 CFU/ml for *S. epidermidis* 1457 and 9.125×10^7 CFU/ml for *S. epidermidis* 5179-R1. Finally, at 24 h, both strains reached the CFU/ml values of 2×10^7 CFU/ml for *S. epidermidis* 1457 and 4×10^8 CFU/ml for *S. epidermidis* 5179-R1. This demonstrates that co-culture conditions are not having a negative impact on the viability of *S. epidermidis* 1457 and 5179-R1 across the culture duration.
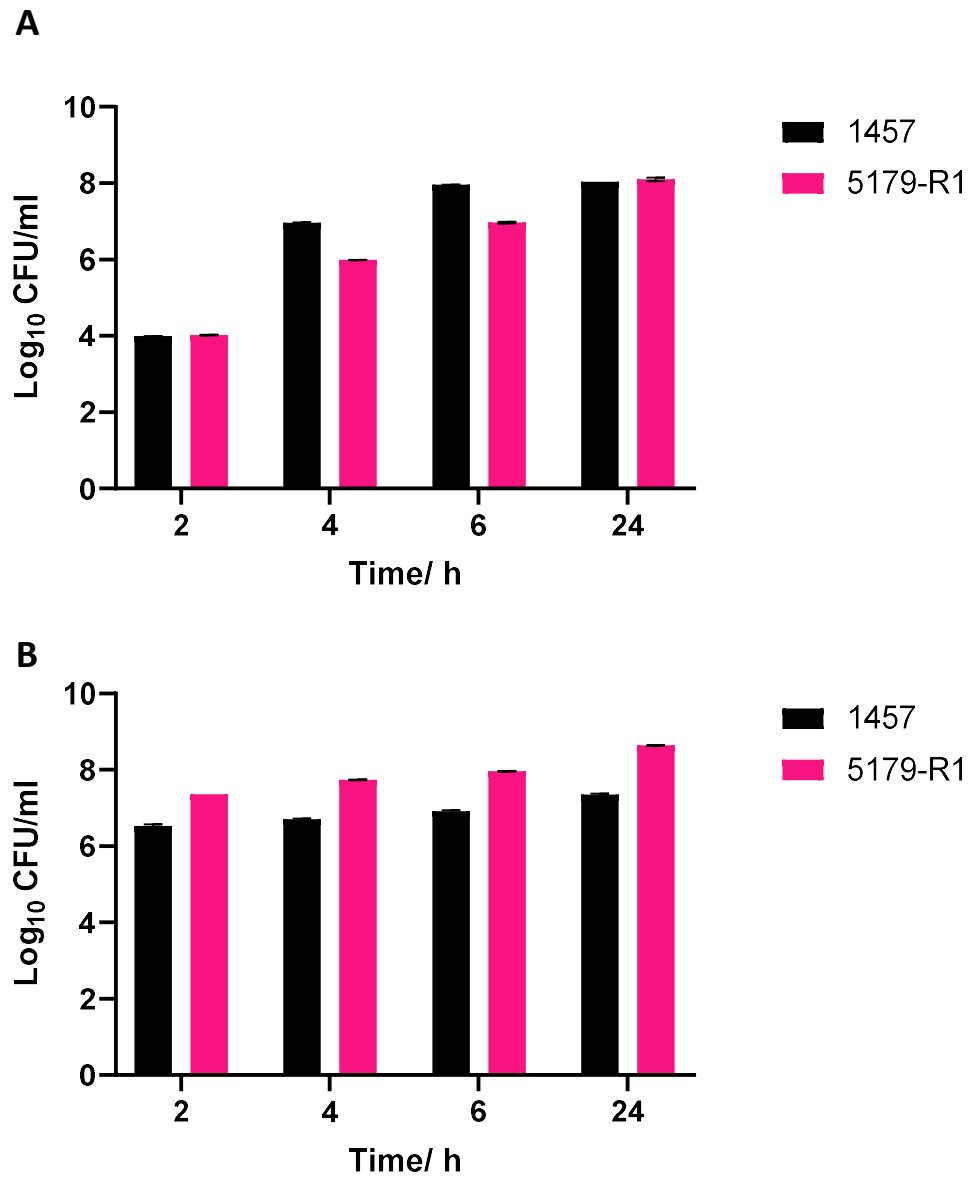
Figure 3.12. Total viable counts of *S. epidermidis* 1457 and 5179-R1 co-cultured with A) THP-1 macrophages or B) 1BR.3.G fibroblasts on Ti discs over 24 h. Results show the mean +/- the standard error of the mean for 3 technical replicates.

3.1.6 Primer Optimisation for *S. epidermidis* Transcription Analysis

To analyse the transcription of biofilm and accumulation genes, RNA was extracted from *S. epidermidis* following mono- and co-culture with 1BR.3.G fibroblasts or THP-1 macrophages on Ti or TiAlV discs. Initial RNA extractions from a single *S. epidermidis* co-culture provided a low yield of RNA. This likely was related to the low biofilm production on the metal surface (Figure 3.6). To overcome this, *S. epidermidis* cells from three Ti or TiAlV discs were pooled together for a single RNA extraction. This provided a higher yield of *S. epidermidis* 5179-R1 which could be utilised for cDNA synthesis and subsequent RT-qPCR reactions. Despite this, the yield of 1457 in MEM remained low. Due to the low yield of RNA from *S. epidermidis* 1457 and a shortage of time, transcriptional studies were not carried out for this strain. Thus, for this study, the gene expression of *S. epidermidis* 5179-R1 only will be discussed. Preparation for RT-qPCR reactions was carried out as described in Section 2.10. RNA was extracted from *S. epidermidis* 5179-R1 and converted to cDNA before RT-qPCR reactions were carried out using SYBR green.

Figure 3.13. shows an example RT-qPCR reaction using the gene *sdrG* and housekeeping gene *gyrB* for *S. epidermidis* 5179-R1 samples in mono-culture or co-culture with THP-1 macrophages on TiAlV. From Figure 3.13.A, it is clear that all *S. epidermidis* 5179-R1 samples amplified correctly, confirming the function of both *sdrG* and *gyrB* primers. The *sdrG* primer no template control showed no amplification over the course of 40 cycles, while the *gyrB* primer no template control amplified toward the end of the PCR reaction, at cycle 32, but was deemed a late false positive result.

To confirm the results, the melt curve was analysed (Figure 3.13.B) and shows all *S. epidermidis* 5179-R1 samples with the primer *sdrG* displayed one major peak at approximately 79 ˚C, while the *sdrG* primer no template control showed no peak. For the primer *gyrB*, one major peak was recorded at 82 ˚C. The *gyrB* no template control did not peak at the same temperature as the 5179-R1 samples, confirming that the late amplification seen is a false positive (Figure 3.13.A).
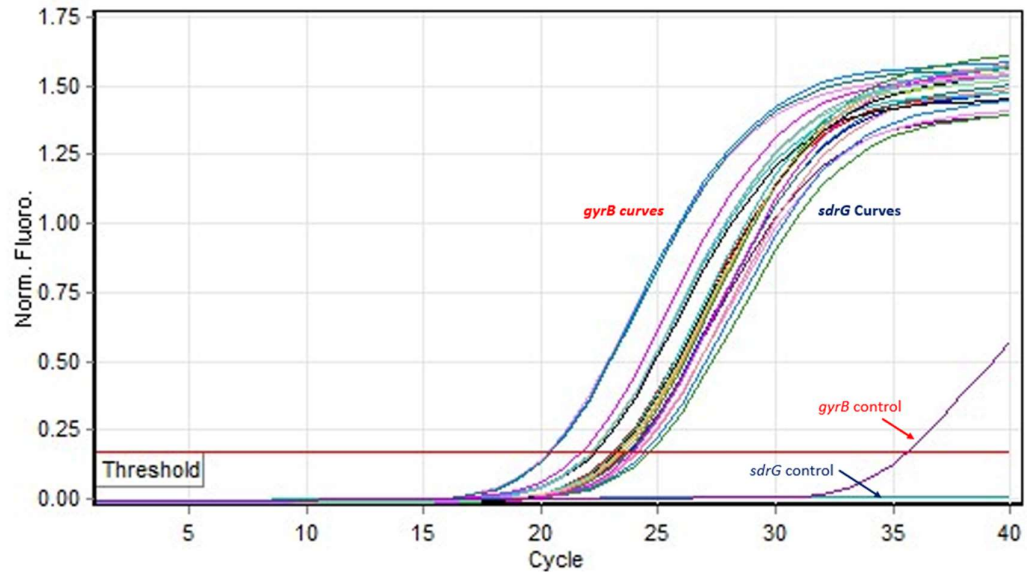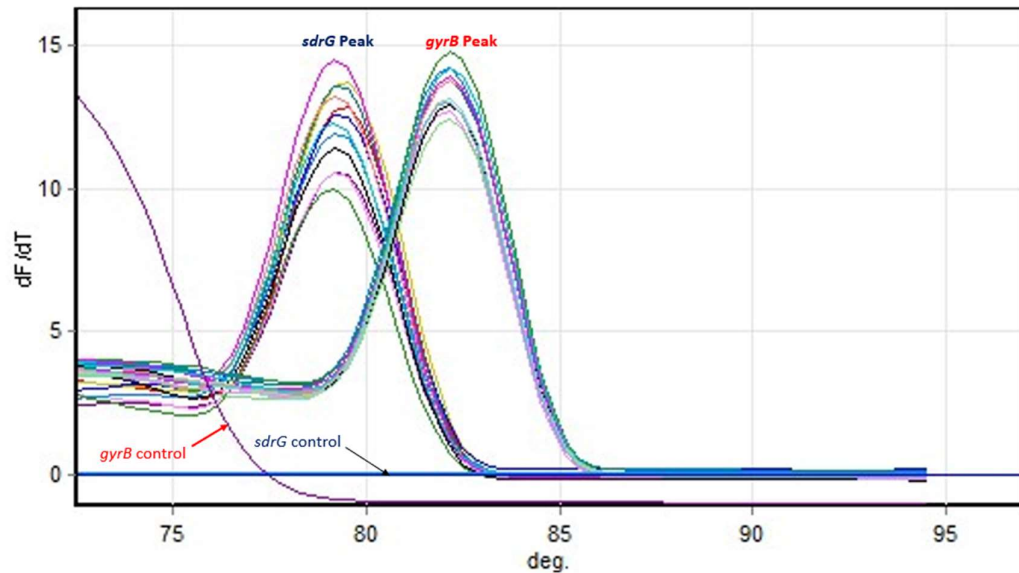
Figure 3.13. Example RT-qPCR output of *S. epidermidis* 5179-R1 *sdrG* and *gyrB* expression. *S. epidermidis* samples were cultured in mono-culture or co-culture with THP-1 macrophages for 6 or 24 h on TiAlV discs. **A:** the cycling green curve and **B:** the melt curve for the RT-qPCR reaction.

To further confirm primer function, PCR gels (Section 2.10.4) were run using the RT-qPCR products. As seen in Figure 3.14., products were produced at the appropriate base pairs for all PCR reactions with *S. epidermidis* samples. For genes *aap, icaA, atlE, sdrG* and *embp,* no bands were visible for the no-template controls, thus confirming that there was no amplification within these samples. As expected, a light

band was identified for the *gyrB* no-template control, corresponding with the late false positive result in the PCR data (Figure 3.13.). For both *RNAIII* and *sdrF*, no-template control products did not show bands at the same bp as *S. epidermidis* products, thus confirming the function of these primers. However, lighter bands below the expected base pairs were visible, possibly due to primer dimers or single primers.
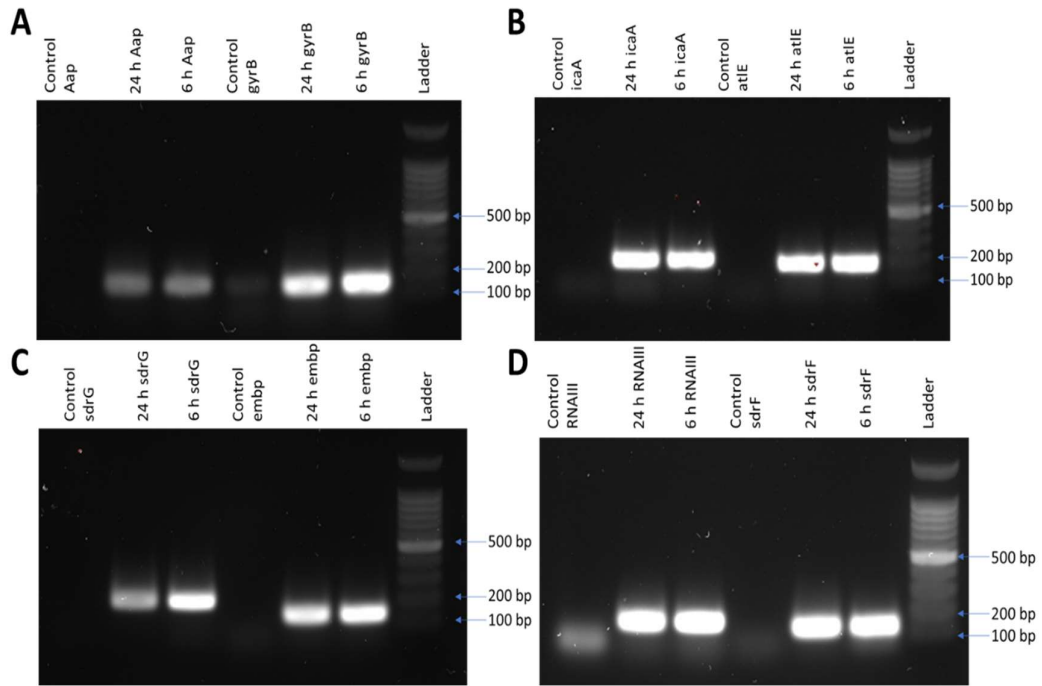
Figure 3.14. Gel electrophoresis of RT-qPCR products. Where A) *aap* and *gyrB,* B) *ica* and *atlE,* C) *sdrG* and *embp* and D) *RNAIII* and *sdrF.* Products include no-template control and *S. epidermidis* 5179-R1 cultured on TiAlV for 6 h or 24 h.

.

3.2 The Co-culture of THP-1 Macrophages with *S. epidermidis* 1457 and 5179-R1 on Ti and TiAlV Discs

3.2.1 Confocal Laser Scanning Microscopy (CLSM)

To better distinguish between eukaryotic and *S. epidermidis* cells through red/green fluorescence, and gain a 3D picture through stacked images, CLSM was chosen for further microscopy analysis. Firstly, as THP-1 monocytes did not adhere or differentiate in the presence of *S. epidermidis,* PMA was added to differentiate cells prior to co-culture. The differentiation and adhesion of THP-1 monocytes was visualised by immunostaining and fixing cells to the Ti or TiAlV discs (Section 2.9.2.). In mono-culture, confluent THP-1 macrophages were seen on both the Ti and TiAlV discs at 48 h (Figure 3.15.), indicating they had successfully differentiated from THP-1 monocyte cells. Stacking of THP-1 macrophage cells was clear on both discs as seen in Figure 3.15.
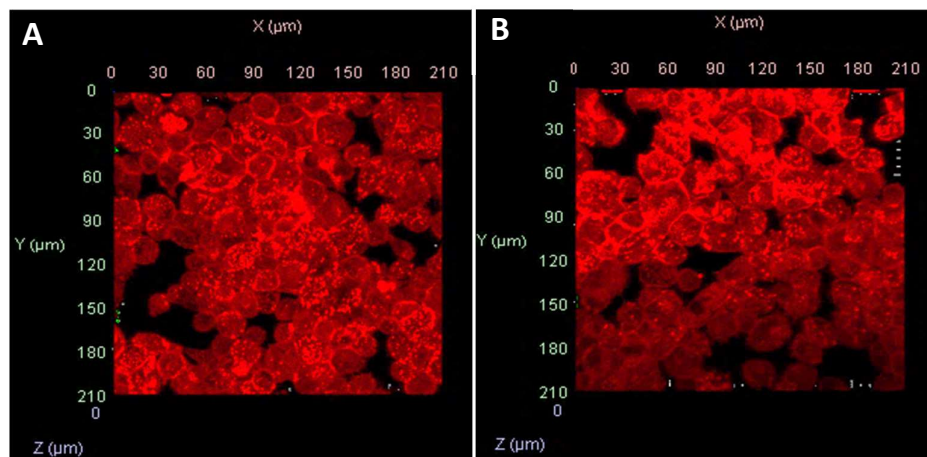
Figure 3.15. 3D CLSM images of THP-1 macrophages on A) Ti and B) TiAlV discs.

Next, to confirm the presence and attachment of *S. epidermidis* cells, *S. epidermidis* 1457 and 5179-R1 were cultured on Ti or TiAlV discs for 6 h or 24 h, before immunostaining (Section 2.9.2). When visualised with CLSM, aggregates of *S. epidermidis* 1457 and 5179-R1 cells were observed on both Ti and TiAlV discs (Figure 3.16.). For both strains, the density of bacteria on the Ti and TiAlV discs increased between 6 h and 24 h, as expected.
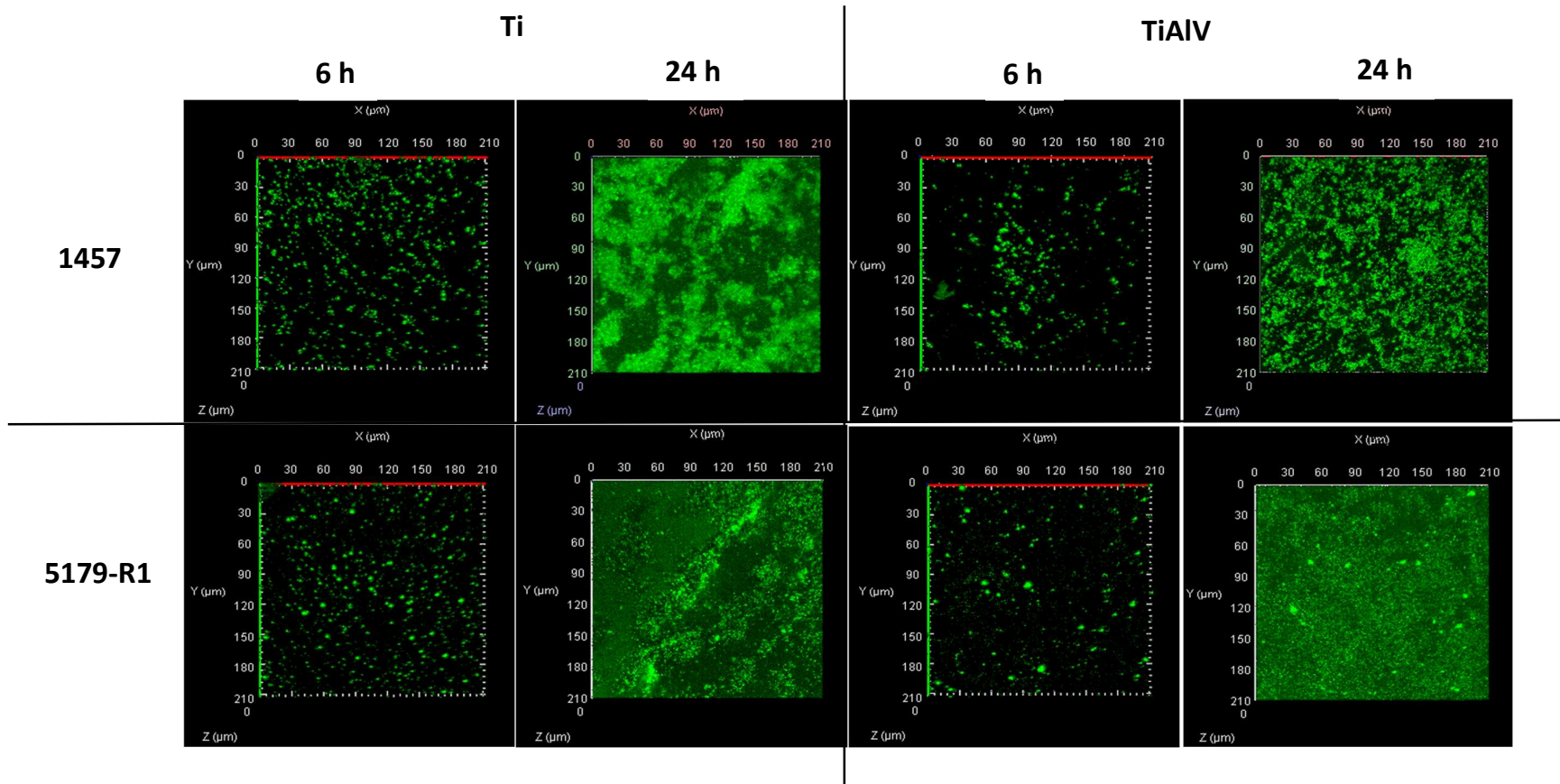
Figure 3.16. 3D CLSM images of *S. epidermidis* 1457 and 5179-R1 on Ti and TiAlV discs. *S. epidermidis* 1457 was cultured on Ti (left panel) and TiAlV (right panel) for 6 and 24 h – top panel; and *S. epidermidis* 5179-R1 was cultured on Ti (left panel) and TiAlV (right panel) for 6 and 24 h – lower panel.

Finally, to visualise the cellular adhesion of both THP-1 macrophages and *S. epidermidis* in co-culture at 6 h or 24 h, co-cultures were immunostained and visualised with CLSM (Section 2.9.2). The co-culture of *S. epidermidis* 1457 and 5179-R1 with THP-1 macrophages for 6 h showed the presence of both bacterial cells and THP-1 macrophages on the Ti and TiAlV discs (Figure 3.17.). In co-culture, THP-1 macrophages showed a lower confluency on both discs compared to when in mono-culture. The density of *S. epidermidis* at 6 h was higher in co-culture than in mono-culture on both discs. There were no notable differences between growth and biofilm formation of 1457 or 5179-R1 on each disc. Clusters of *S. epidermidis* 1457 and 5179-R1 were observed both on the Ti and TiAlV discs but also on the THP-1 macrophage cells.
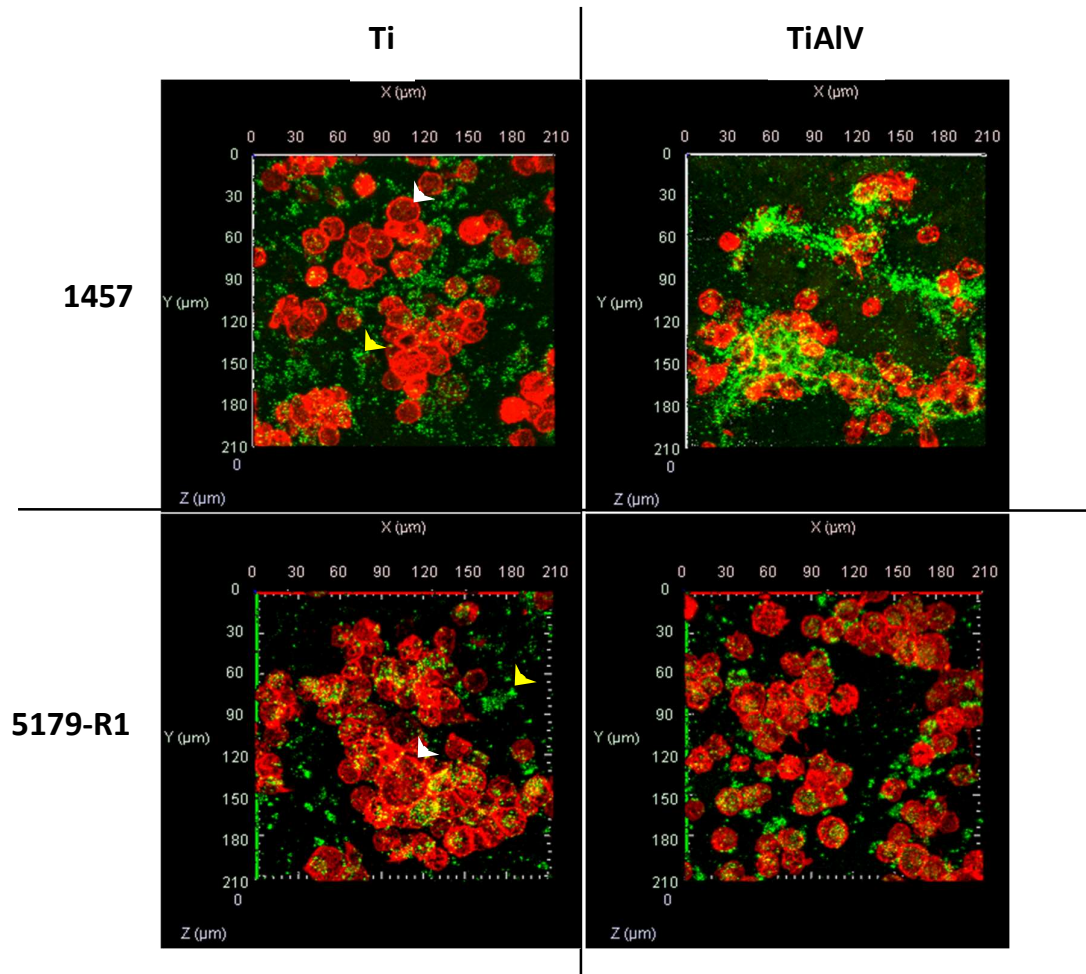
Figure 3.17. 3D CLSM images of *S. epidermidis* co-cultured with THP-1 macrophages for 6 h on Ti and TiAlV discs. *S. epidermidis* 1457 (top panel) and 5179-R1 (bottom panel) co-cultured for 6 h on Ti (left panel) and TiAlV (right panel) with THP-1 macrophages. Arrowheads show examples of THP-1 macrophages (white) and *S. epidermidis* cell clusters (yellow).

At 24 h on the Ti disc, both THP-1 macrophages and *S. epidermidis* 1457 or 5179-R1 were present and adherent to the disc (Figure 3.18.A and C). The confluency of THP-1 macrophages was higher at 24 h than 6 h irrespective of being in co-culture with either *S. epidermidis* 1457 or 5179-R1. Similarly, *S. epidermidis* numbers were also higher at 24 h compared to the 6 h and showed biofilm formation both on the Ti disc and directly on the THP-1 macrophages. (Figure 3.18.A and C). On TiAlV, *S. epidermidis* 1457 and 5179-R1 numbers also increased at 24 h compared to the 6 h, with biofilms visible on the TiAlV disc (Figure 3.18.B and D). However, THP-1 macrophages were not adhered to the TiAlV disc at 24 h, despite the presence of cellular debris.
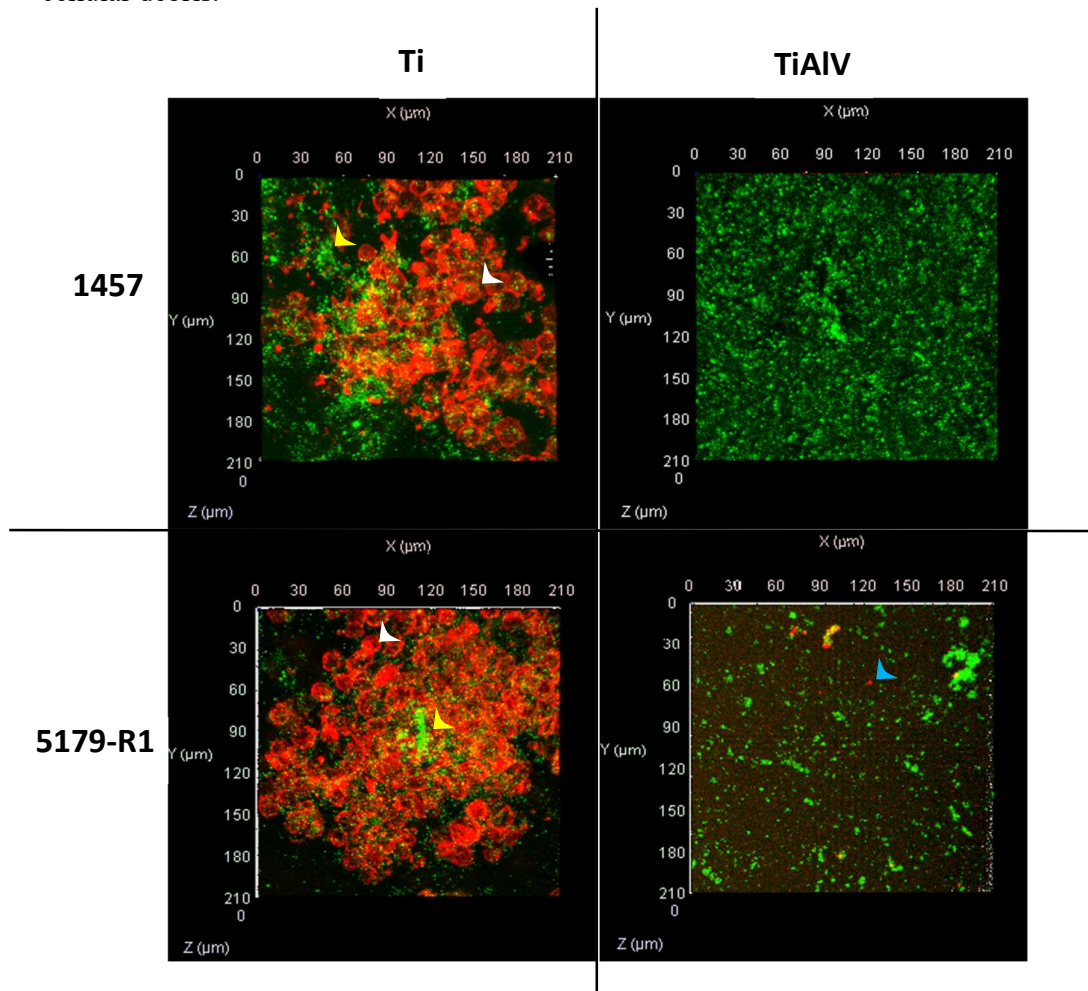
Figure 3.18. 3D CLSM images of *S. epidermidis* co-cultured with THP-1 macrophages for 6 h on Ti and TiAlV discs. *S. epidermidis* 1457 (top panel) and 5179-R1 (bottom panel) cultured for 6 h on Ti (left panel) and TiAlV (right panel) with THP-1 macrophages. Arrowheads show examples of THP-1 macrophages (white), *S. epidermidis* cell clusters (yellow) and cellular debris (blue).

3.2.2 *S. epidermidis* 5179-R1 Gene Expression

To investigate the transcription of *S. epidermidis* 5179-R1 genes when in mono-culture or co-culture with THP-1 macrophages for 6 or 24 h on Ti or TiAlV discs, RNA was extracted from adherent cells, and cDNA was synthesised. This cDNA was used to carry out RT-qPCR reactions and to determine fold-differences between culture conditions (Section 2.10).

Overall, the expression of *S. epidermidis* 5179-R1 adhesion and biofilm associated genes varied depending on culture condition and sample disc (Figure 3.19. and 3.20.). A 3-fold difference in $2^{-\Delta\Delta Ct}$ was used as a cut-off point for gene transcription up- and down-regulation between 6 and 24 h and between mono-cultured and co-cultured samples. Results showed no down-regulation of any accumulation or biofilm genes across culture-conditions (Figures 3.19. and 3.20.). No differences in the expression of *icaA*, *aap* and *atlE* between 6 h and 24 h were observed when cultured alone or in presence of THP-1 macrophages on Ti discs (Figure 3.19.A), while an increase in expression was seen for *embp* and *sdrG* under both culturing conditions. An increase in expression was also observed for *sdrF* when cultured on Ti disc alone but not in the presence of THP-1 macrophages, whilst the opposite can be said for *RNAIII* which showed the opposite trend. Similar to Ti, there was no difference in gene expression of *icaA, aap* and *atlE* between 6 h and 24 h for either culture condition on TiAlV (Figure 3.19.B). In addition, the expression of *embp* and *RNAIII* also remained constant between time points, while the expression of *sdrG* and *sdrF* was increased only in *S. epidermidis* cultured alone. Statistically no differences (p>0.05) were observed between culture conditions for each gene as a great variation in expression was seen between experimental replicates.

Comparing gene expression between *S. epidermidis* cells cultured alone and in co-culture with THP-1 cells on Ti at 6 h, the only gene showing an increase in expression was *atlE* (Figure 3.20.A), while the expression of all other genes remained constant. At 24 h, however, an increase in expression was seen for all genes, except *aap* and sdrF (Figure 3.20.A). Interestingly, on the TiAlV discs, the expression of all genes remained constant in *S. epidermidis* cultured alone and in co-culture at both 6 h and 24 h time points (Figure 3.20.B). There were no statistical differences in expression between time points due to variation within sample sets (p>0.05).
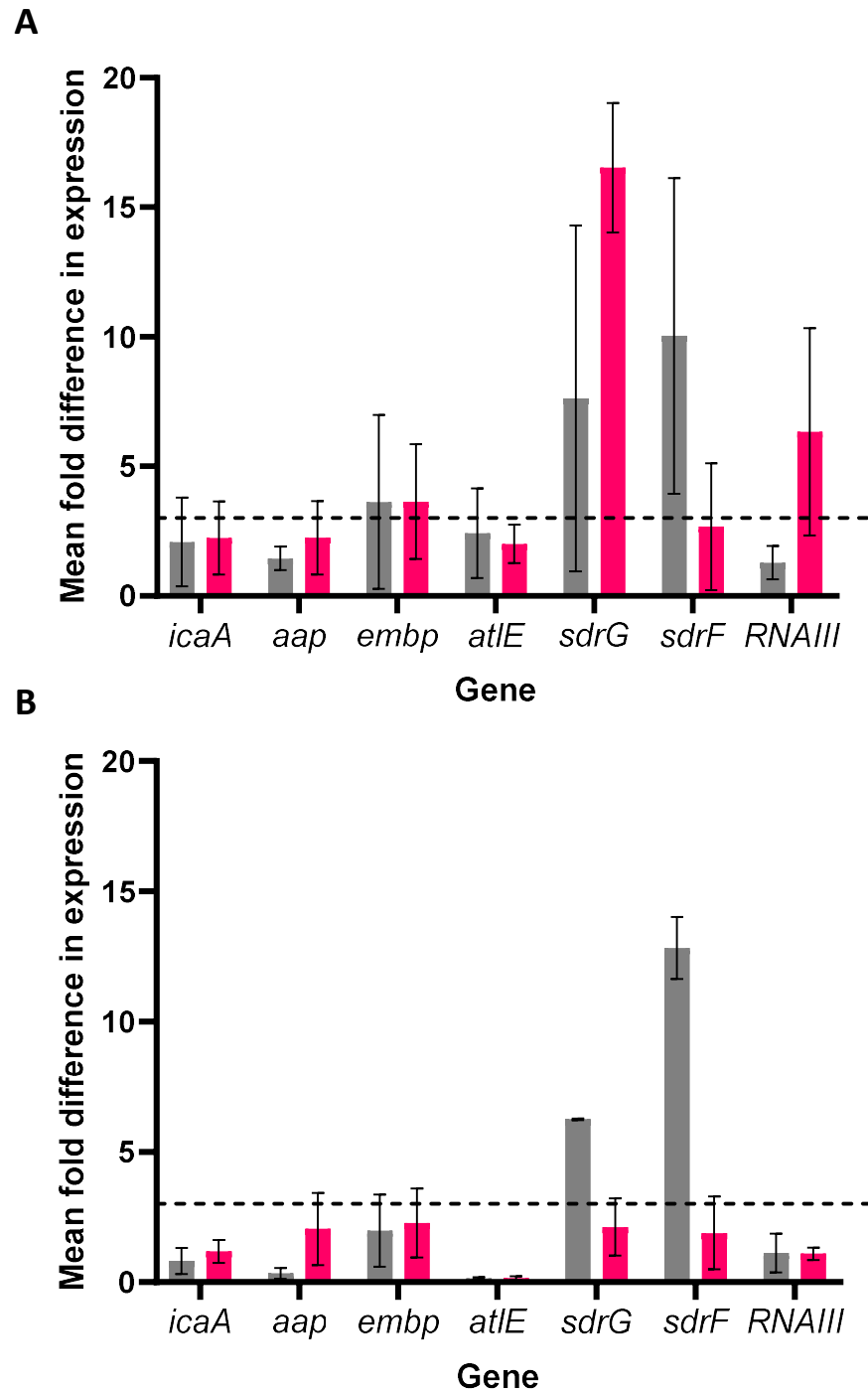
Figure 3.19. The mean fold difference in expression of *S. epidermidis* genes between 6 h and 24 h on Ti and TiAlV in mono- or co-culture with THP-1 macrophages. The mean fold difference in expression of *S. epidermidis* genes; *icaA, aap, embp, atlE, sdrG, sdrF* and *RNAIII*, between 6 h and 24 h when cultured on A) Ti or B) TiAlV discs in mono-culture (grey) or co-culture with THP-1 macrophages (pink; n=3 biological replicates). Results show the mean average +/- the standard error of the mean and hashed line represents the 3-fold threshold.
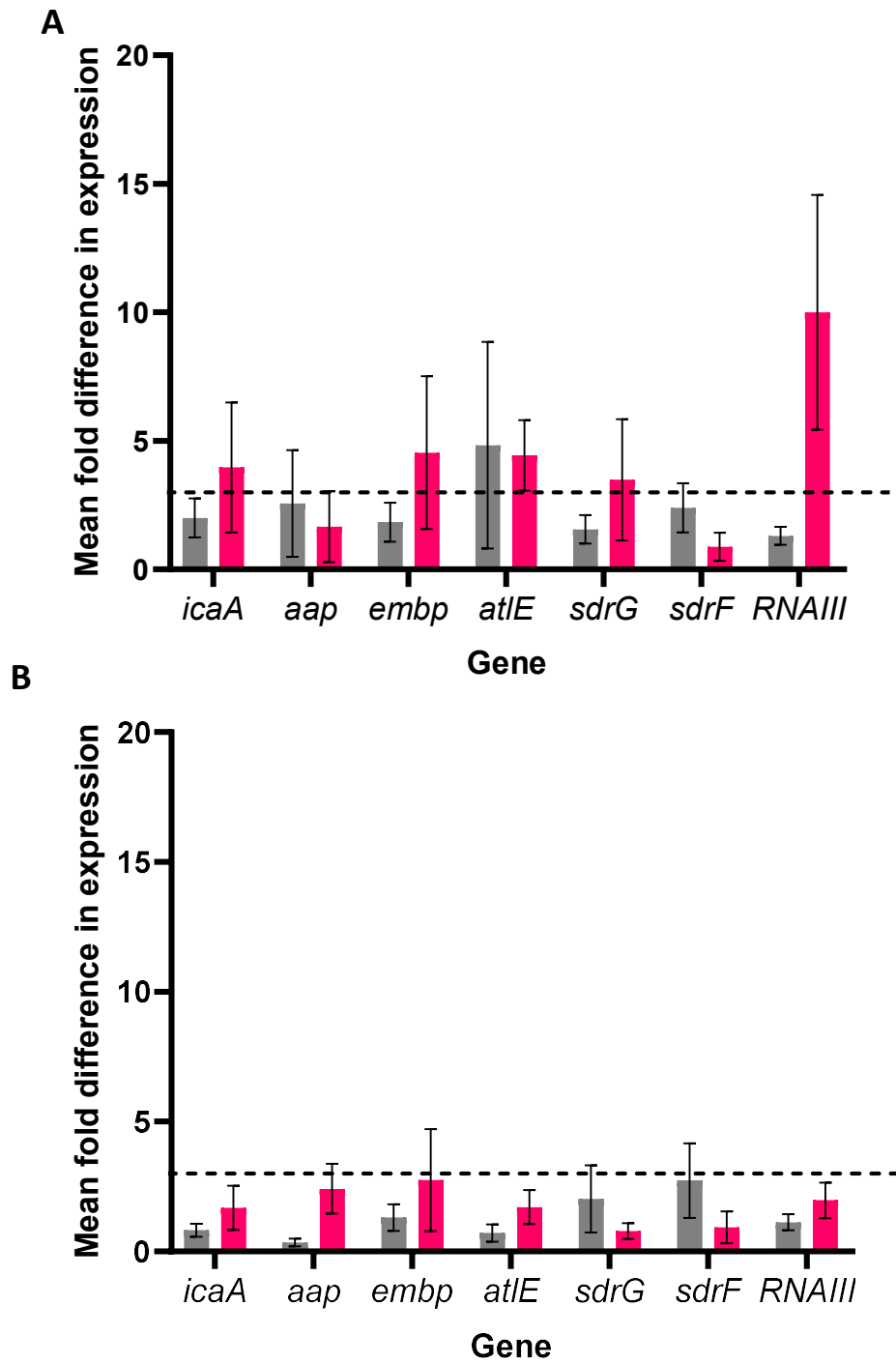
Figure 3.20. The mean fold difference in expression of *S. epidermidis* genes between mono-culture and co-culture with THP-1 macrophages on Ti and TiAlV. The mean fold difference in expression of *S. epidermidis* genes; *icaA, aap, embp, atlE, sdrG, sdrF* and *RNAIII*, between mono-culture and co-culture with 1BR.3.G fibroblasts A) Ti or B) TiAlV discs at 6 h (grey) or 24 h (pink; n=3 biological replicates). Results show the mean average +/- the standard error of the mean and hashed line represents the 3-fold threshold.

3.2.3 Cytokine Analysis

As IL-8 is a well-known inflammatory marker and is known to be influenced by *S. epidermidis* biofilm presence, it was decided to investigate the expression of IL-8 by eukaryotic cells using ELISA (Spiliopoulou *et al.*, 2012). The impact of the presence of *S. epidermidis,* Ti discs or TiAlV discs on IL-8 expression by THP-1 macrophages was explored. To achieve this, THP-1 macrophages were prepared in mono-culture or co-culture with *S. epidermidis* in the absence or presence of Ti or TiAlV discs. The cell supernatants from these cultures were collected and analysed using DuoSet IL-8 ELISA (Section 2.11.2).

As expected, THP-1 macrophages stimulated with LPS expressed IL-8 on both Ti and TiAlV discs (Figure 3.21.). In mono-culture on Ti and TiAlV discs, the expression of IL-8 by THP-1 macrophages was approximately increased by two-fold compared to THP-1 macrophages cultured without a metal disc. Following co-culture for 6 h and 24 h on Ti and TiAlV, the mean IL-8 concentration was higher than that of mono-cultured THP-1 macrophages but was not statistically different ($p > 0.05$). Co-cultured THP-1 macrophages showed similar expression of IL-8 at both 6 h and 24 h, with no obvious difference in expression between disc material. Statistically, there were no differences in IL-8 expression between culture conditions ($p > 0.05$).
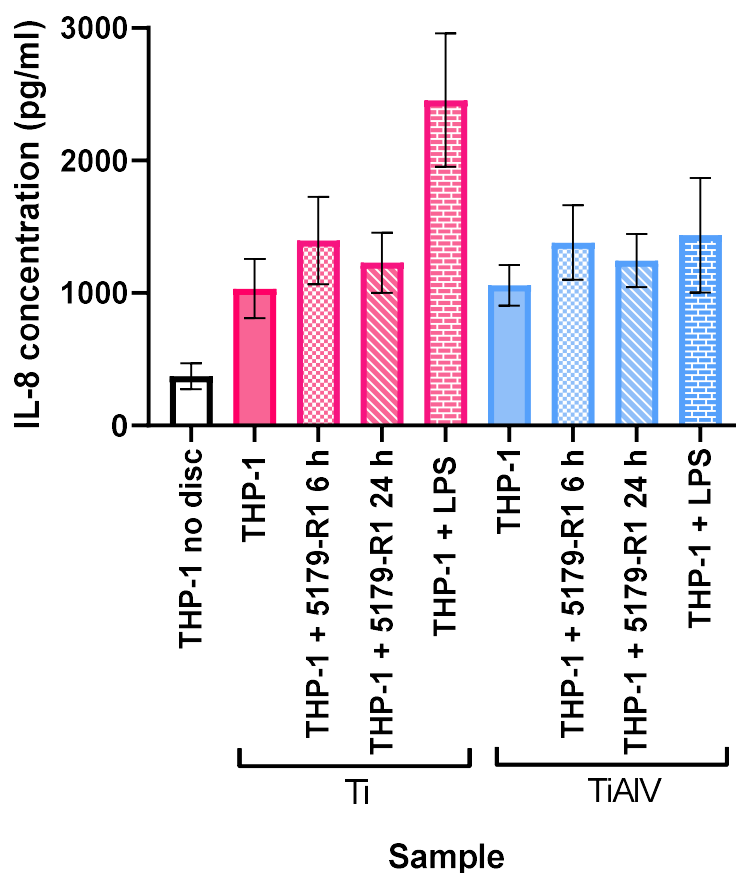
Figure 3.21. The effects of culture condition on THP-1 macrophage expression of IL-8 in mono- or co-culture with _S. epidermidis_. The expression of IL-8 by THP-1 macrophages is shown in mono-culture or co-culture with _S. epidermidis_ 5179-R1 in the absence or presence of Ti or TiAlV discs (n=3 biological samples, 2 technical replicates). Results show the mean average +/- the standard error of the mean.

Unfortunately, due to time constraints, further analysis of IL-8 expression could only be undertaken one time. Despite this, results showed no variation in IL-8 expression between THP-1 macrophages and monocytes both with and without Ti or TiAlV discs. Similar to THP-1 macrophage samples, IL-8 expression by THP-1 monocytes also increased in the presence of Ti and TiAlV discs. In co-culture with _S. epidermidis_ 5179-R1, THP-1 macrophages cultured without metal discs showed high expression of IL-8 with no obvious difference between IL-8 concentration at 6 h or 24 h. THP-1 macrophage expression of IL-8 in co-culture was similar at both 6 h and 24 h despite the presence or absence of the metal discs.
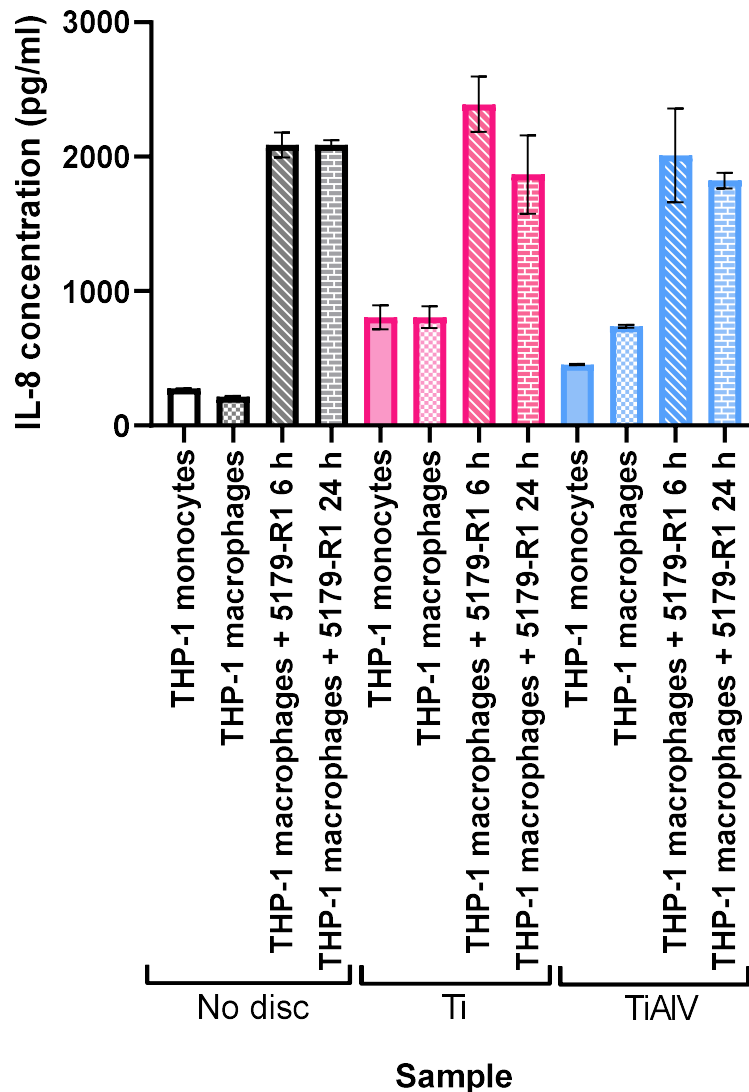
Figure 3.22. The effects of culture condition on THP-1 macrophages and monocytes expression of IL-8 in mono- or co-culture with *S. epidermidis.* The expression of IL-8 by THP-1 macrophages or monocytes is shown in mono-culture or co-culture with *S. epidermidis* 5179-R1 in the absence or presence of Ti or TiAlV discs (n=1 biological sample, 2 technical replicates). Results show the mean average +/- the standard error of the mean.

To further explore cytokine expression, human proteome profiler arrays containing 36 cytokines or human proteome profiler XL arrays containing 105 cytokines were used to determine THP-1 macrophage expression in mono-culture or co-culture with *S. epidermidis* 5179-R1 in the presence or absence of Ti discs (Section 2.11.1 and Appendix A and B). These arrays provide a strong method for screening a wealth of cytokines using a single sample, however, due to their expense, only a small selection

of these arrays could be purchased. For this reason, only 1 array could be analysed for each condition. Membrane images are shown in Figure 3.23., and all membranes showed obvious positive control spots with high pixel density (orange circles), and negative control spots (blue circles) showing no change in pixel density. The mean pixel density was calculated by subtracting the pixel density from the background pixel density and averaging the two values as each cytokine spot is duplicated on the membrane. All cytokines expressed by THP-1 macrophages in both mono- and co-culture conditions are displayed in Appendix C.
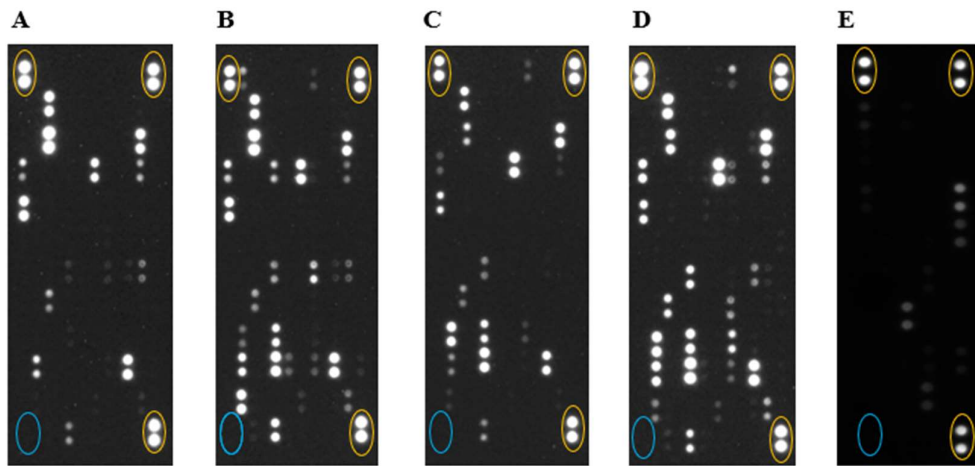
Figure 3.23. Human Proteome Profiler Array membranes of THP-1 macrophages in mono-culture or co-culture with *S. epidermidis.* Cytokine Array membranes show the expression of 36 (E, small membrane) or 105 (A-D, large membranes) human cytokines for samples A) THP-1 macrophages with no disc, B) THP-1 macrophages on Ti, C) THP-1 macrophages cultured with *S. epidermidis* 5179-R1 for 6 h on Ti, D) THP-1 macrophages cultured with *S. epidermidis* 5179-R1 for 24 h on Ti and E) THP-1 macrophages and *S. epidermidis* 5179-R1 cultured with no disc. Positive and negative control spots are circled in orange and blue respectively.

Table 3.1 shows the effect of Ti discs on the expression of cytokines by THP-1 macrophages in either mono-culture or co-culture with *S. epidermidis* 5179-R1. In mono-culture, the addition of the Ti surface resulted in increased expression of CD14, EMMPRIN, GRO-α, ICAM-1, IGFBP-3, IL-1ra, IP-10, MCP-1, MIF, MIP-1α/MIP-1β, MIP-3α, SDF-1α, Serpin E1, TNF-α and VEGF, while also causing a decrease in expression of Complement factor D and IFGBP-2. In comparison, when a Ti disc was added to THP-1 macrophages in co-culture with *S. epidermidis* 5179-R1, the expression of G-CSF, GM-CSF, GRO-α, ICAM-1, IL-1α, IL-1β, IL-1ra, IL-4, IL-8,

IL-17A, IL-27, MCP-1, MIF and RANTES, while only IP-10 expression was decreased.

The impact of co-culture with *S. epidermidis* 5179-R1 in the absence of a Ti disc on THP-1 cytokine expression can also be determined from Table 3.1. Compared to mono-culture, the expression of GRO-α, ICAM-1, IL-1β, IP-10, MIP-1α/MIP-1β and TNF-α were increased in co-culture with *S. epidermidis* for 24 h. In addition, co-culture also led to decreased expression of complement factor D, IL-1ra, IL-8, IL-17A, MIF and RANTES by THP-1 macrophages.

Table 3.1. The effect of *S. epidermidis* 5179-R1 or Ti discs on cytokine expression by THP-1 macrophages in mono- or co-culture conditions (n=1). Detected with the Human Proteome Profiler XL Array or Human Cytokine Array Kit.

Cytokine	THP-1 No Ti	THP-1 With Ti	THP-1 + 5179-R1 No Ti	THP-1 + 5179-R1 With Ti
CD14	×	+	n/a	n/a
Complement factor D	+++	++	×	×
EMMPRIN	+	++	n/a	n/a
G-CSF	×	×	×	+
GM-CSF	×	×	×	+
GROα	×	+	+	+++
ICAM-1	×	+	+	+++
IGFBP-2	+	×	n/a	n/a
IGFBP-3	+	+++	n/a	n/a
IL-1α	×	×	×	+++
IL-1β	×	×	+	+++
IL-1ra	+	++	×	++
IL-4	×	×	×	+
IL-8	+++	+++	++	+++
IL-17A	+	+	×	+
IL-27	×	×	×	+
IP-10	×	++	++	+
MCP-1	×	+++	×	+
MIF	+	+++	×	+++
MIP-1α/MIP-1β	+	+++	+++	+++
MIP-3α	×	+++	n/a	n/a
RANTES	+++	+++	+	+++
SDF-1α	×	+	×	+
Serpin E1	×	+++	×	+
TNF-α	×	++	+	+++
VEGF	×	+++	n/a	n/a

× = no expression (mean pixel density <10), + = low expression (mean pixel density = 10-50), ++ = positive expression (meal pixel density = 51-100), +++ = High expression (mean pixel density >101) and n/a= not present on cytokine array.

To investigate the effect of *S. epidermidis* 5179-R1 on the expression of cytokines by THP-1 macrophages on Ti discs, differences in THP-1 cytokine expression were recorded in Table 3.2. Following 6 h co-culture with THP-1 macrophages on Ti, THP-1 macrophages displayed decreased expression of numerous cytokines including CD14, complement factor D, Cystatin C, EMMPRIN, ICAM-1, IGFBP-3, IP-10, MCP-1 and Serpin E1, while only GRO-α, IL-1β and TNF-α expression was increased. Despite this, by 24 hours in co-culture with *S. epidermidis* 5179-R1, THP-

1 macrophage expression of Angiopoietin-1, CD40 ligand, complement factor D, DKK-1, EMMPRIN, Endoglin, FGF-19, G-CSF, GM-CSF, GRO-α, ICAM-1, IL-1α, IL-1β, IL-4, IL-24, IL-27, TNF-α and Vitamin D BP had all increased compared to expression in mono-culture. Meanwhile, 24 h co-culture with *S. epidermidis* decreased THP-1 expression of CD14, Cystatin C, IGFBP-3, IP-10, MCP-1 Serpin E1 and SHBG.

Table 3.2. The effect of *S. epidermidis* 5179-R1 on cytokine expression by THP-1 macrophages in mono- or co-culture conditions on Ti discs (n=1). Detected with the Human Proteome Profiler XL Array or Human Cytokine Array Kit.

Cytokine	THP-1 with Ti	THP-1 + 5179-R1 6 h With Ti	THP-1 + 5179-R1 24 h With Ti
Angiopectin-2	×	×	+
CD14	+	×	×
CD40 ligand	×	×	+
Complement factor D	++	+	+++
Cystatin C	++	×	+
Dkk-1	×	×	+
EMMPRIN	++	+	+++
Endoglin	×	×	+
FGF-19	+	+	+++
G-CSF	×	×	+
GM-CSF	×	×	+
GROα	+	++	+++
ICAM-1	+	×	+++
IGFBP-3	+++	×	×
IL-1α	×	×	+++
IL-1β	×	+	+++
IL-4	×	×	+
IL-24	×	×	+
IL-27	×	×	+
IP-10	++	×	+
MCP-1	+++	×	+
Serpin E1	+++	×	+
SHBG	×	×	+
TNF-α	++	+++	+++
Vitamin D BP	×	×	+

× = no expression (mean pixel density <10), + = low expression (mean pixel density = 10-50), ++ = positive expression (meal pixel density = 51-100), +++ = High expression (mean pixel density >101)

3.3 The Co-culture of 1BR.3.G Fibroblasts with *S. epidermidis* 1457 and 5179-R1 on Ti and TiAlV Discs

3.3.1 Confocal Laser Scanning Microscopy (CLSM)

CLSM was used to visualise the attachment of both 1BR.3.G fibroblasts and *S. epidermidis* cells to the Ti or TiAlV surface in the co-culture model. Firstly, to ensure the adhesion of 1BR.3.G fibroblasts in mono-culture, mono-cultures were prepared and fixed for CLSM analysis (Section 2.9.2). Figure 3.24. shows confluent 1BR.3.G fibroblasts on both the Ti and TiAlV discs when in mono-culture for 72 h. 1BR.3.G fibroblasts showed expected morphology with collagen fibrils visible on both discs.
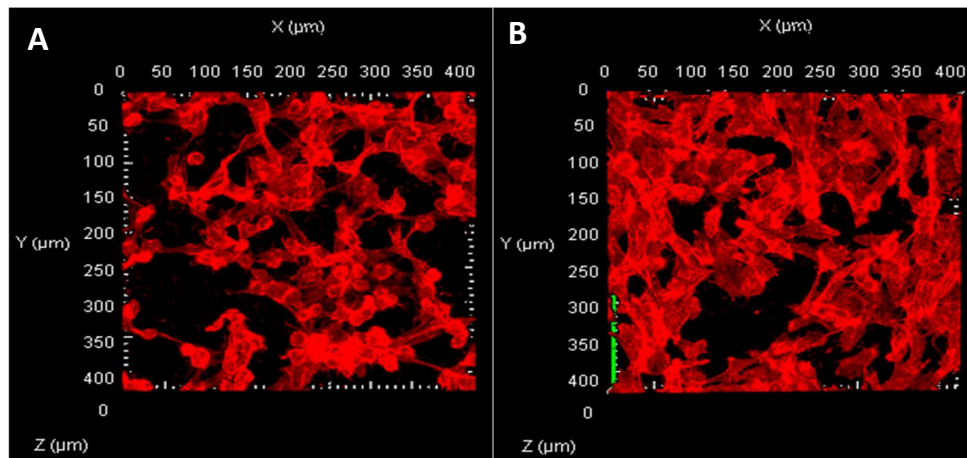
Figure 3.24. 3D CLSM of 1BR.3.G fibroblasts in mono-culture on A. Ti and B. TiAlV discs.

To visualise the adherence and attachment of 1BR.3.G fibroblasts and *S. epidermidis* on Ti and TiAlV discs, samples were co-cultured (Section 2.6.7) and then immunostained for visualisation with CLSM (Section 2.9.2). The co-culture of *S. epidermidis* 1457 and 5179-R1 with 1BR.3.G fibroblasts for 6 h showed adhesion of both bacterial cells and 1BR.3.G fibroblasts to the Ti and TiAlV discs (Figure 3.25.). 1BR.3.G fibroblasts were confluent on both discs and were comparable in morphology to mono-culture (Figure 3.24.). Clusters of *S. epidermidis* were observed both on Ti and TiAlV discs but also on the fibroblast cells. There were no notable differences between 1BR.3.G fibroblast growth on each disc.
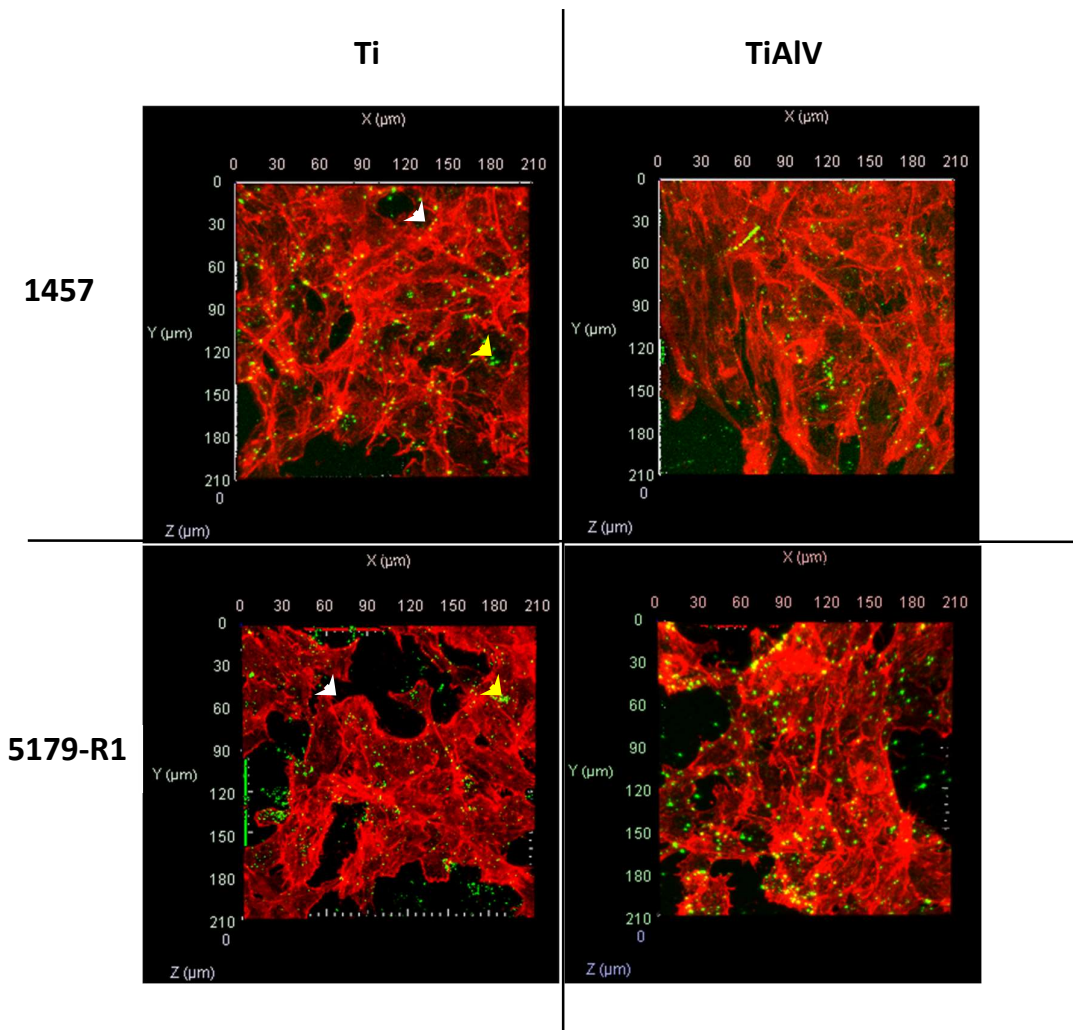
Figure 3.25. 3D images of *S. epidermidis* 1457 and 5179-R1 co-cultured with 1BR.3.G fibroblasts for 6 h on Ti or TiAlV discs. *S. epidermidis* 1457 (top panel) and 5179-R1 (bottom panel) co-cultured with 1BR.3.G fibroblasts for 6 h on Ti (left panel) and TiAlV (right panel). Arrowheads show examples of 1BR.3.G fibroblasts (white) and *S. epidermidis* cell clusters (yellow).

At 24 h in co-culture, CLSM images showed detachment of 1BR.3.G fibroblasts from the Ti and TiAlV discs, whereas both *S. epidermidis* 1457 and 5179-R1 adhered to the Ti and TiAlV discs and produced biofilms (Figure 3.26.). Some cellular debris remained on both discs; however, remaining 1BR.3.G fibroblasts were clustered together and were morphologically different to that of co-cultured cells at 6 h (Figures 3.25. and 3.26.). The numbers of *S. epidermidis* 1457 and 5179-R1 were increased at 24 h compared to 6 h on both discs.
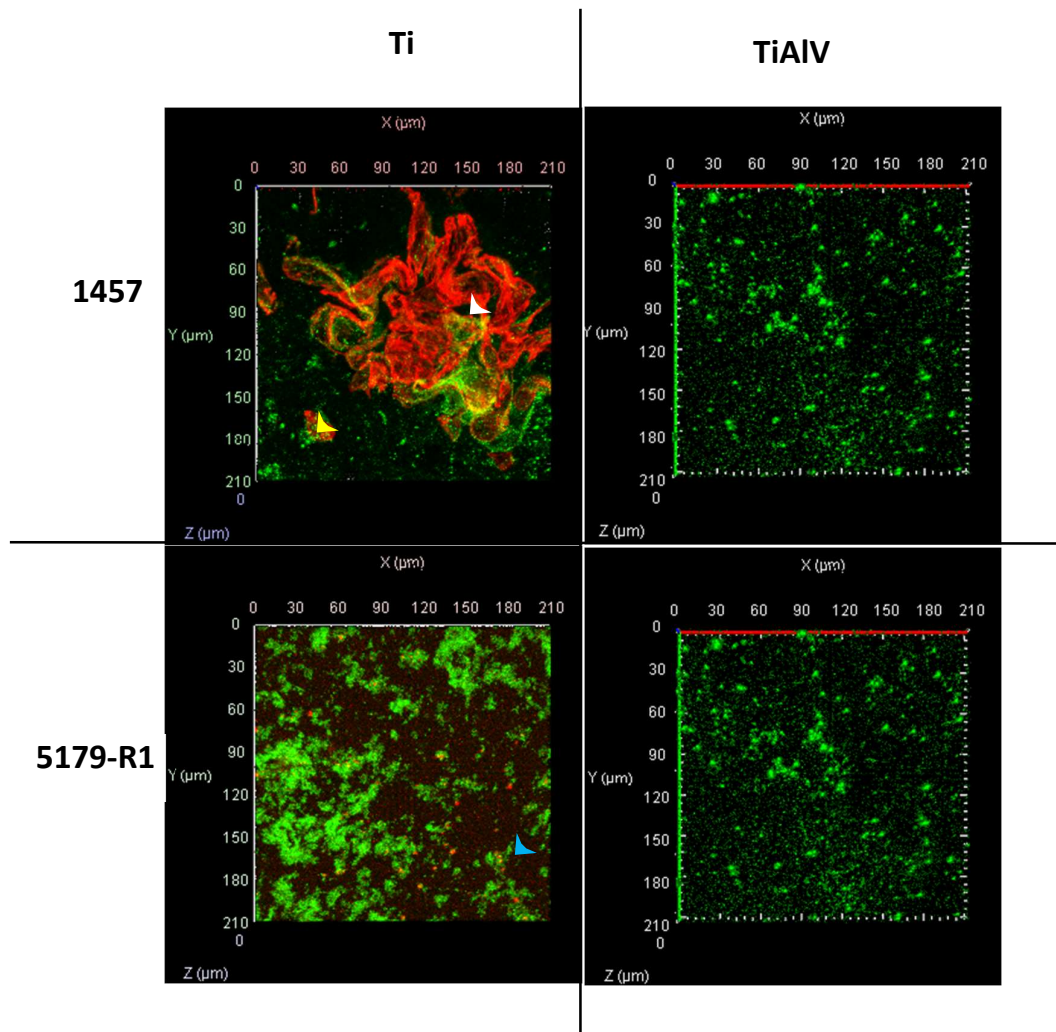
Figure 3.26. 3D images of *S. epidermidis* 1457 and 5179-R1 co-cultured with 1BR.3.G fibroblasts for 24 h on Ti or TiAlV discs. *S. epidermidis* 1457 (top panel) and 5179-R1 (bottom panel) co-cultured with 1BR.3.G fibroblasts for 24 h on Ti (left panel) and TiAlV (right panel). Arrowheads show examples of 1BR.3.G fibroblasts (white), *S. epidermidis* cell clusters (yellow) and cellular debris (blue).

3.3.2 *S. epidermidis* 5179-R1 Gene Expression

To investigate the transcription of *S. epidermidis* 5179-R1 genes when in mono-culture or co-culture with 1BR.3.G fibroblasts for 6 or 24 h on Ti or TiAlV discs, RNA was extracted from adherent cells, and cDNA was synthesised. This cDNA was used to carry out RT-qPCR reactions and to determine fold-differences between culture conditions (Section 2.10).

Overall, the expression of *S. epidermidis* 5179-R1 adhesion and biofilm associated genes varied depending on culture duration and sample disc but were not influenced

by the presence of 1BR.3.G fibroblasts in co-culture (Figure 3.27.). Overall, no down-regulation of accumulation and biofilm genes was noted across culture conditions (Figures 3.27. and 3.28.). Results showed no differences in the expression of *atlE* and *RNAIII* between 6 and 24 h when cultured on Ti discs, while *sdrG* and *sdrF* expression was increased in both culture conditions (Figure 3.27.A). An increase in expression of *icaA, aap* and *embp* was also observed, but only in co-culture conditions on Ti. The expression of *atlE* and *embp* remained constant between time points under both culture conditions, while *sdrG* and *sdrF* expression was increased on TiAlV discs (Figure 3.27.B). Unlike on Ti discs, the expression of *aap* also remained constant under both culture conditions, whereas the expression of *icaA* and *embp* increased in co-culture conditions only. Statistically no differences ($p>0.05$) were observed between culture conditions for each gene due to variation in expression between experimental replicates.

On both Ti and TiAlV discs, there were no differences in gene expression of *S. epidermidis* cells cultured alone or in co-culture at both time points (Figure 3.28.). No statistical differences in expression were found between samples at 6 h or 24 h ($p> 0.05$).
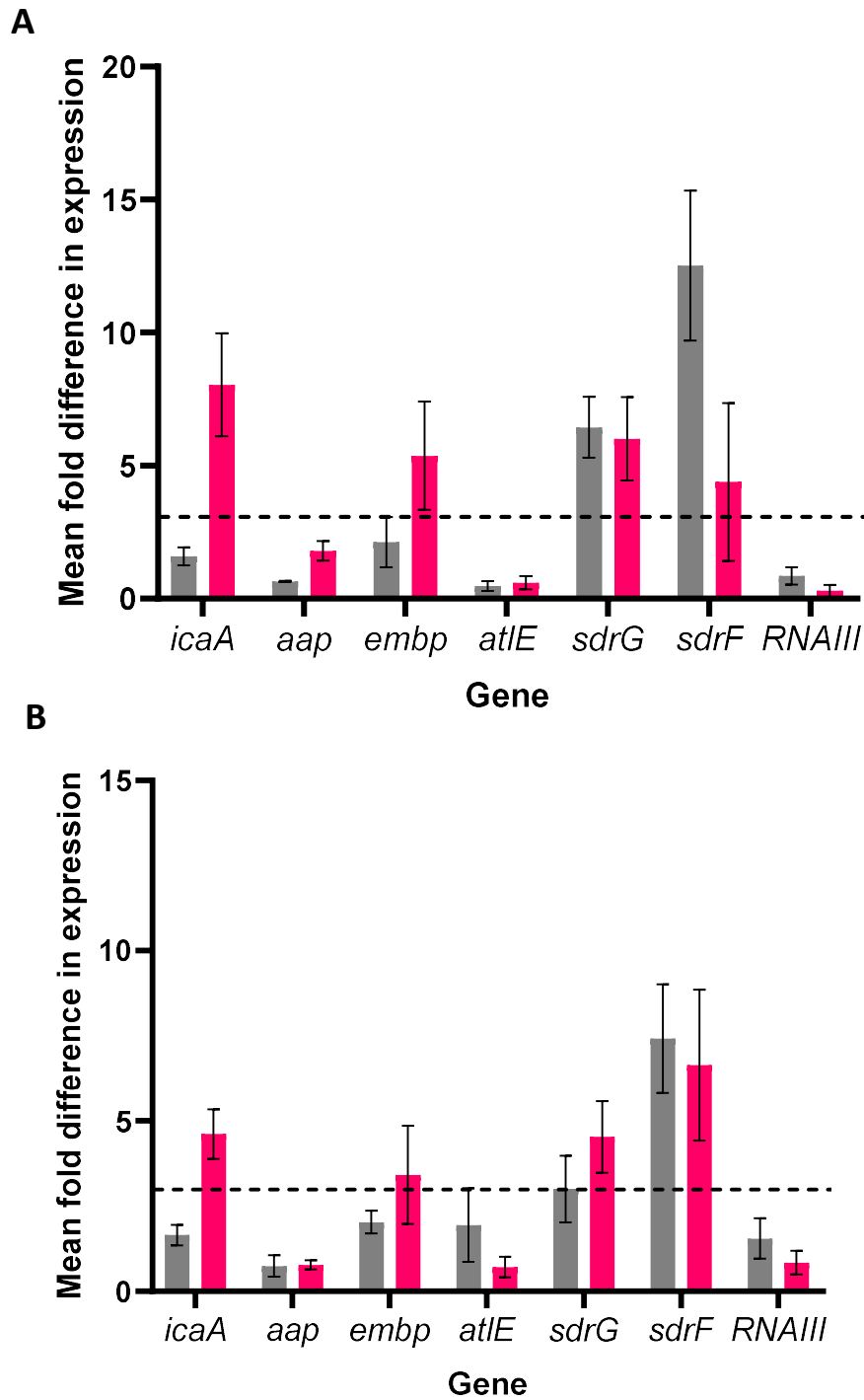
Figure 3.27. The mean fold difference in *S. epidermidis* gene expression between 6 h and 24 h on Ti and TiAlV in mono- or co-culture with 1BR.3.G fibroblasts. The mean fold difference expression of *S. epidermidis* genes; *icaA, aap, embp, atlE, sdrG, sdrF* and *RNAIII* between 6 h and 24 h when cultured on A) Ti; and B) TiAlV discs in mono-culture (grey) or co-culture with 1BR.3.G fibroblasts (pink; n=3 biological replicates). Results show the mean average +/- the standard error of the mean and hashed line represents the 3-fold threshold.
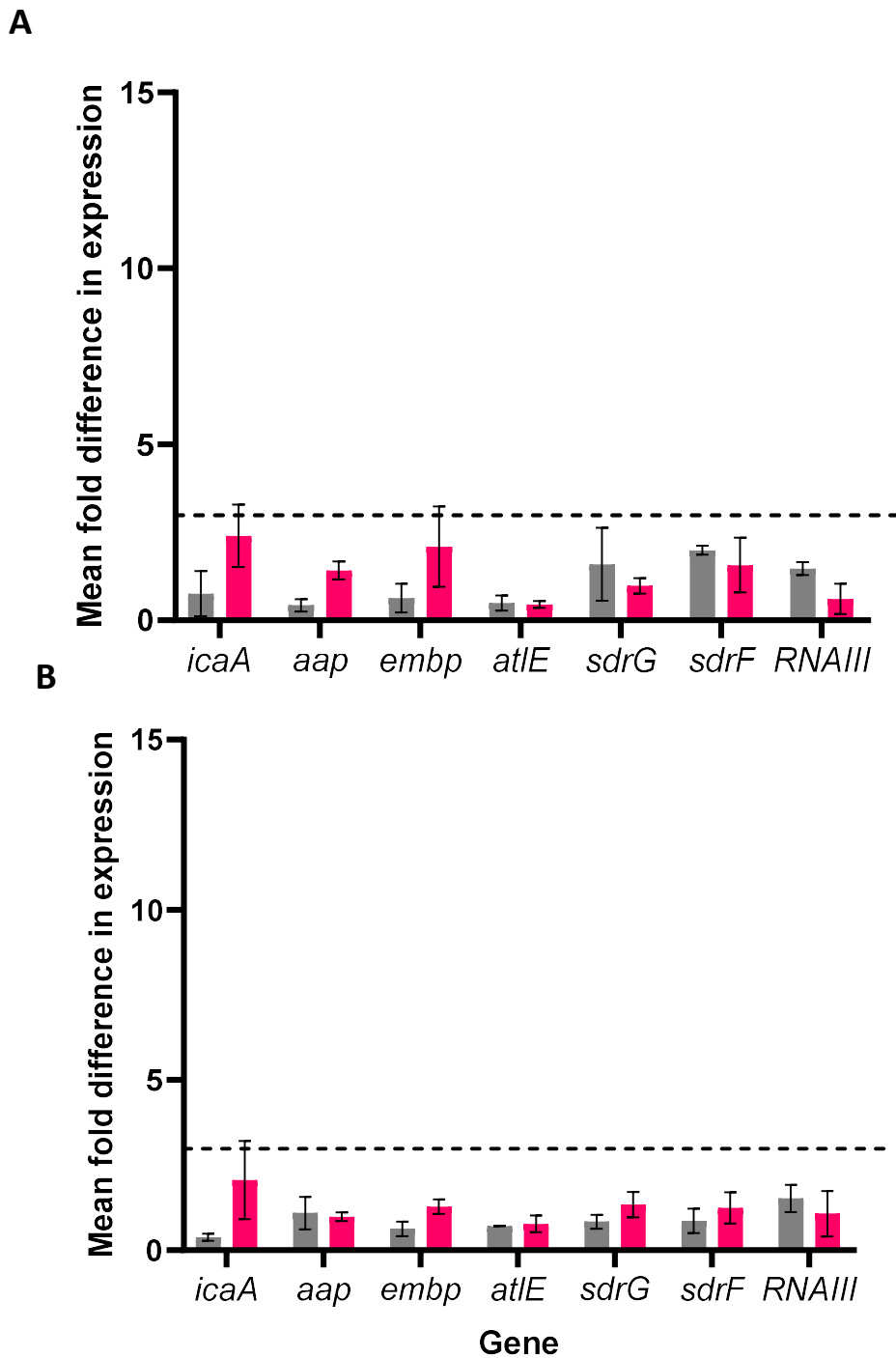
Figure 3.28. The mean fold difference in *S. epidermidis* gene expression between mono- and co-culture with 1BR.3.G fibroblasts on Ti and TiAlV. The mean fold difference in expression of *S. epidermidis* genes; *icaA, aap, embp, atlE, sdrG, sdrF* and *RNAIII*, between mono-culture and co-culture with THP-1 macrophages A) Ti or B) TiAlV discs at 6 h (grey) or 24 h (pink; n=3 biological replicates). Results show the mean average +/- the standard error of the mean and hashed line represents the 3-fold threshold.

3.3.3 Cytokine Analysis

To investigate the effect of *S. epidermidis* 5179-R1 and Ti or TiAlV discs on the expression of IL-8 by 1BR.3.G fibroblasts, a DuoSet IL-8 ELISA was carried out on the cell supernatant from mono- or co-cultures (Section 2.11.2).

As displayed in Figure 3.29. 1BR.3.G fibroblasts stimulated with LPS successfully expressed IL-8 on both Ti and TiAlV discs. Compared to 1BR.3.G fibroblasts in mono-culture with no disc, 1BR.3.G fibroblasts in mono-culture on Ti or TiAlV discs showed increased expression of IL-8 but were not statistically different ($p > 0.05$). 1BR.3.G fibroblast expression of IL-8 was similar in both mono-culture and co-culture with *S. epidermidis* 5179-R1 at 6 h. However, following 24 h in co-culture, IL-8 expression by 1BR.3.G fibroblasts was increased on both Ti and TiAlV discs and was significantly different to that of 1BR.3.G fibroblasts in mono-culture with no disc ($p=0.001$ and $p=0.028$ respectively), but was not statistically different to cultures on Ti or TiAlV discs ($p>0.05$). Overall, there was no obvious difference in IL-8 expression between 1BR.3.G fibroblasts cultured on Ti and TiAlV discs ($p>0.05$).
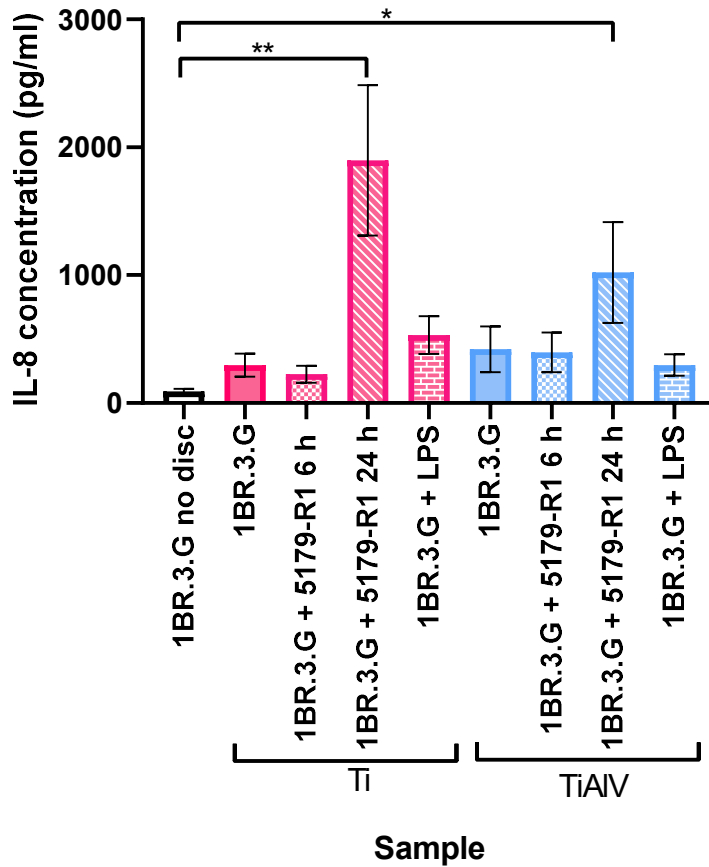
Figure 3.29. The effects of culture condition on 1BR.3.G fibroblast expression of IL-8 in mono-culture or co-culture with *S. epidermidis*. The expression of IL-8 by 1BR.3.G fibroblasts is shown in mono-culture or co-culture with *S. epidermidis* 5179-R1 in the absence or presence of Ti or TiAlV discs (n=3 biological samples, 2 technical replicates). Results show the mean average +/- the standard error of the mean. Asterisks represent significant difference between samples where *=p<0.05 and **=p<0.1.

Unfortunately, due to time constraints, further analysis of IL-8 expression could only be undertaken one time. Despite this, ELISA data showed an increase in 1BR.3.G fibroblast expression of IL-8 when *S. epidermidis* 5179-R1 was added both in the presence and absence of Ti and TiAlV discs (Figure 3.30.). In the absence of a metal disc, IL-8 expression by 1BR.3.G fibroblasts in co-culture increased by 8-fold at 6 h and by 10-fold at 24 h. The expression of IL-8 by 1BR.3.G fibroblasts in co-culture was similar in the presence and absence of metal surfaces at 6 h but was increased in the presence of the metal surfaces by 24 h.
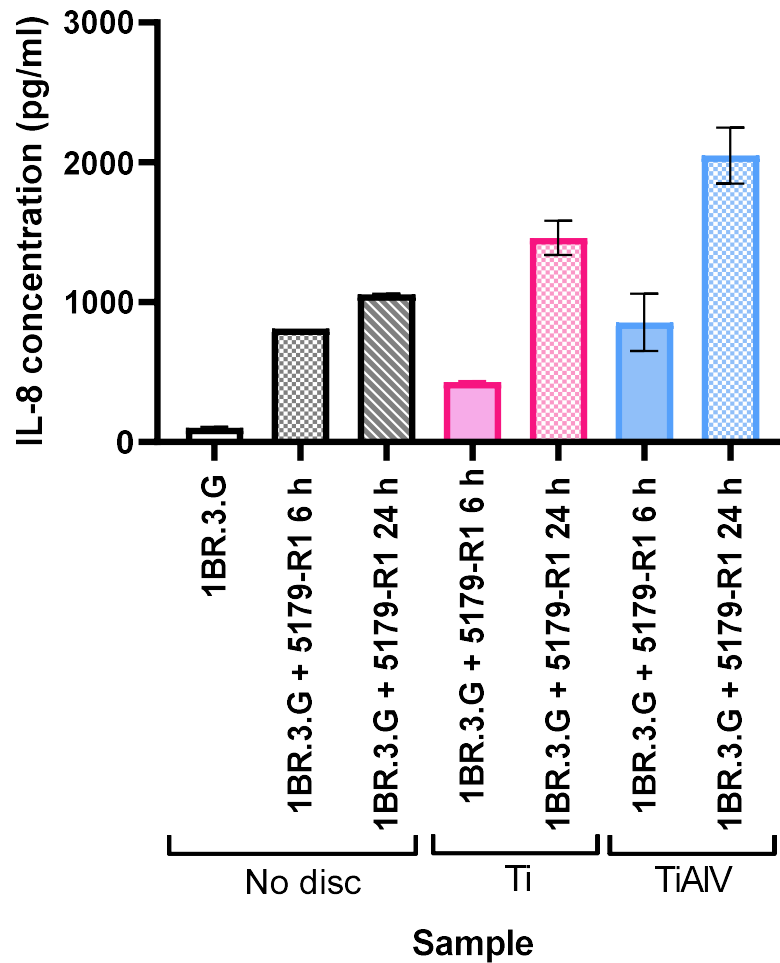
Figure 3.30. The effects of Ti and TiAlV disc presence on 1BR.3.G fibroblast expression of IL-8 in mono-culture or co-culture with *S. epidermidis.* The expression of IL-8 by 1BR.3.G fibroblasts in mono-culture or co-culture with *S. epidermidis* 5179-R1 in the absence or presence of Ti or TiAlV discs (n=1 biological sample, 2 technical replicates). Results show the mean average +/- the standard error of the mean.

To further explore cytokine expression, a human proteome profiler array XL containing 105 cytokines was used to analyse cytokine expression of 1BR.3.G fibroblasts in mono-culture or co-culture with *S. epidermidis* 5179-R1 in the presence or absence of Ti discs (Section 2.11.1 and appendix A). Results are shown in Figure 3.31., and on all membranes positive control spots (orange circles) with high pixel density, and negative control spots (blue circles) showing no change in pixel density were seen, confirming that the membranes were successful. All cytokines expressed

by THP-1 macrophages in both mono- and co-culture conditions are displayed in Appendix D.
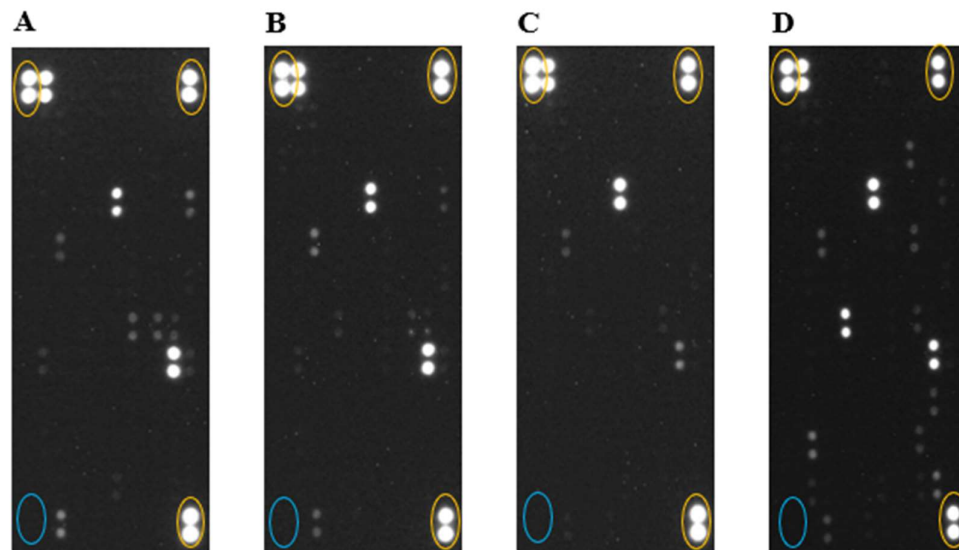
Figure 3.31. Human Proteome Profiler Array membranes of 1BR.3.G fibroblasts in mono-culture or co-culture with *S. epidermidis*. Membranes show the expression of 105 human cytokines for samples A) 1BR.3.G fibroblasts cultured with no disc, B) 1BR.3.G fibroblasts cultured on Ti, C) 1BR.3.G fibroblasts co-cultured with *S. epidermidis* 5179-R1 for 6 h on Ti, D) 1BR.3.G fibroblasts co-cultured with *S. epidermidis* 5179-R1 for 24 h on Ti. Positive and negative control spots are circled in orange and blue respectively.

In mono-culture, the presence of the Ti disc resulted in increased expression of Angiopoietin-2, BNDF, Cystatin C, IFN-γ, MIF, Pentraxin 3 and Vitamin D BP by 1BR.3.G fibroblasts (Table 3.3). Meanwhile, the expression of Angiogenin, IGFBP-3 and IL-17A was decreased. Interestingly, when co-cultured with *S. epidermidis* for 6 h on Ti, 1BR.3.G fibroblasts did not increase the expression of any cytokines compared to when in mono-culture on the Ti surface. However, expression of Angiogenin, BDNF, Cystatin C, Pentraxin 3, SDF-1α, Thrombospondin-1 and Vitamin D BP was decreased. In contrast to this, 1BR.3.G fibroblasts in co-culture on Ti for 24 h showed increased expression of numerous cytokines including DPPIV, EMMPRIN, Endoglin, FGF basic, IL-17A, MIC-1, GRO-α, MIF, uPAR and VEGF when compared to fibroblast expression in mono-culture on Ti. Differences were further observed through the decrease in expression of Angiopoitenin-2, BDNF, Cystatin C, IFN-γ, SDF-1α, Thrombospondin-1 and Vitamin D BP by 1BR.3.G fibroblasts in co-culture for 24 h.

Table 3.3. The effect of *S. epidermidis* 5179-R1 or Ti discs on cytokine expression by 1BR.3.G fibroblasts in mono- or co-culture conditions (n=1). Detected with the Human Proteome Profiler XL Array or Human Cytokine Array Kit.

Cytokine	1BR.3.G No Ti	1BR.3.G With Ti	1BR.3.G + 5179-R1 6 h With Ti	1BR.3.G + 5179-R1 24 h With Ti
Angiogenin	++	+	×	+
Angiopoietin-2	×	+	+	×
BDNF	×	+	×	×
Cystatin C	×	+	×	×
DPPIV	×	×	×	+
EMMPRIN	×	×	×	++
Endoglin	×	×	×	++
FGF basic	×	×	×	++
IFN-γ	×	+	+	×
IGFBP-3	++	×	×	×
IL-17A	+	×	×	+
MIC-1	×	×	×	+
GROα	×	×	×	+
MIF	×	+	+	+++
Pentraxin 3	+	++	+	++
SDF-1α	++	++	+	+
Thrombospondin-1	+	+	×	×
uPAR	×	×	×	++
VEGF	×	×	×	+
Vitamin D BP	×	+	×	×

× = no expression (mean pixel density <10), + = low expression (mean pixel density = 10-50), ++ = positive expression (meal pixel density = 51-100), +++ = High expression (mean pixel density >101)

3.4 The Co-culture of 1BR.3.G Fibroblasts with *S. epidermidis* 1457 and 5179-R1 on Ti and TiAlV Discs Pre-coated with Whole Blood

Due to the COVID-19 pandemic, whole blood samples were difficult to obtain. For this reason, only one biological replicate of experiments involving whole blood could be completed for this project.

3.4.1 Scanning Electron Microscopy (SEM)

As whole blood contains numerous eukaryotic cells, which if present would also be stained by the Alexa Fluor™ 594 Phalloidin, it was decided to use SEM to give a clear differentiation between the eukaryotic cell morphologies. To visualise the adherence of 1BR.3.G fibroblasts and *S. epidermidis* on Ti discs pre-coated with whole blood, samples were prepared as described in Section 2.7.2 and fixed for SEM (Section 2.9.1).

Following coating with whole blood, cellular debris and red blood cells were visible on the Ti disc (Figure 3.32.A). In mono-culture, confluent 1BR.3.G fibroblasts, red blood cells and cellular debris were seen on the discs at 72 h (Figure 3.32.B). Red blood cells were observed adhering to both the Ti disc and to the fibroblast cells.
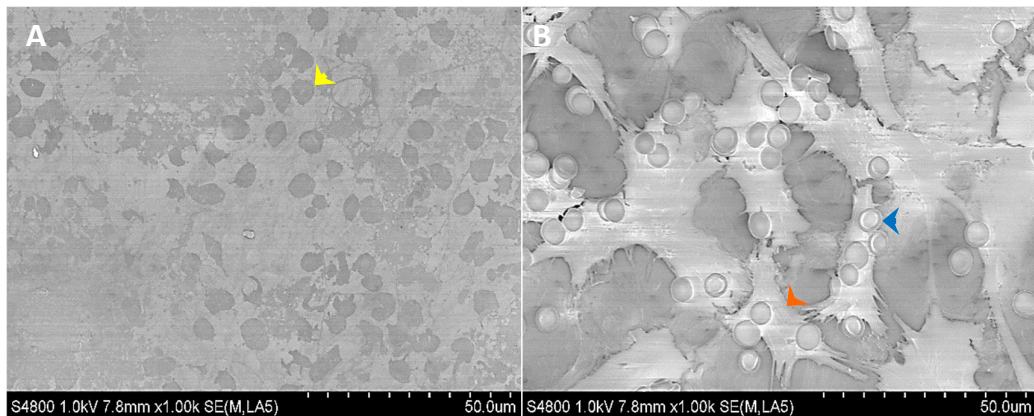
Figure 3.32. SEM images of pre-coated Ti discs in the absence (A) or presence (B) of 1BR.3.G fibroblasts. Arrowheads show examples of 1BR.3.G fibroblasts (orange), red blood cells (blue) and cellular debris (yellow).

When mono-cultured on the pre-coated discs, aggregates of *S. epidermidis* 1457 were observed at both 6 and 24 h surrounded by cellular debris and red blood cells (Figure

3.33.). The presence of bacteria increased between 6 h and 24 h with charging visible in images at both time points.
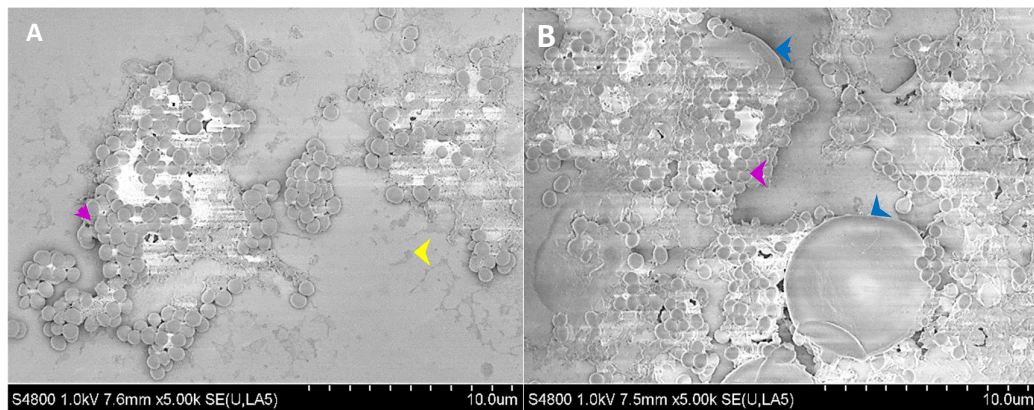
Figure 3.33. SEM images of *S. epidermidis* 1457 cultured on whole blood coated Ti discs for A) 6 h and B) 24 h. Arrowheads show examples of *S. epidermidis* clusters (purple), red blood cells (blue) and cellular debris (yellow).

In co-culture, 1BR.3.G fibroblasts, *S. epidermidis* cells, cellular debris and red blood cells were seen on the pre-coated Ti discs at both time points (Figure 3.34.). At 6 h, red blood cells showed typical biconcave morphology, however, by 24 h acanthocytes and echinocytes were also observed. Both *S. epidermidis* 1457 and *S. epidermidis* 5179-R1 aggregates were observed in co-cultures at 6 h and 24 h on pre-coated Ti discs, and comparable to in mono-culture, the presence of *S. epidermidis* 1457 and 5179-R1 cells increased between 6 h and 24 h. Confluent 1BR.3.G fibroblasts were observed in co-culture at 6 h, however, confluency decreased by 24 h comparable to uncoated discs (Fig 3.26). Despite this, more 1BR.3.G fibroblasts remained adherent to the pre-coated Ti surface in co-culture at 24 h compared to uncoated surfaces.
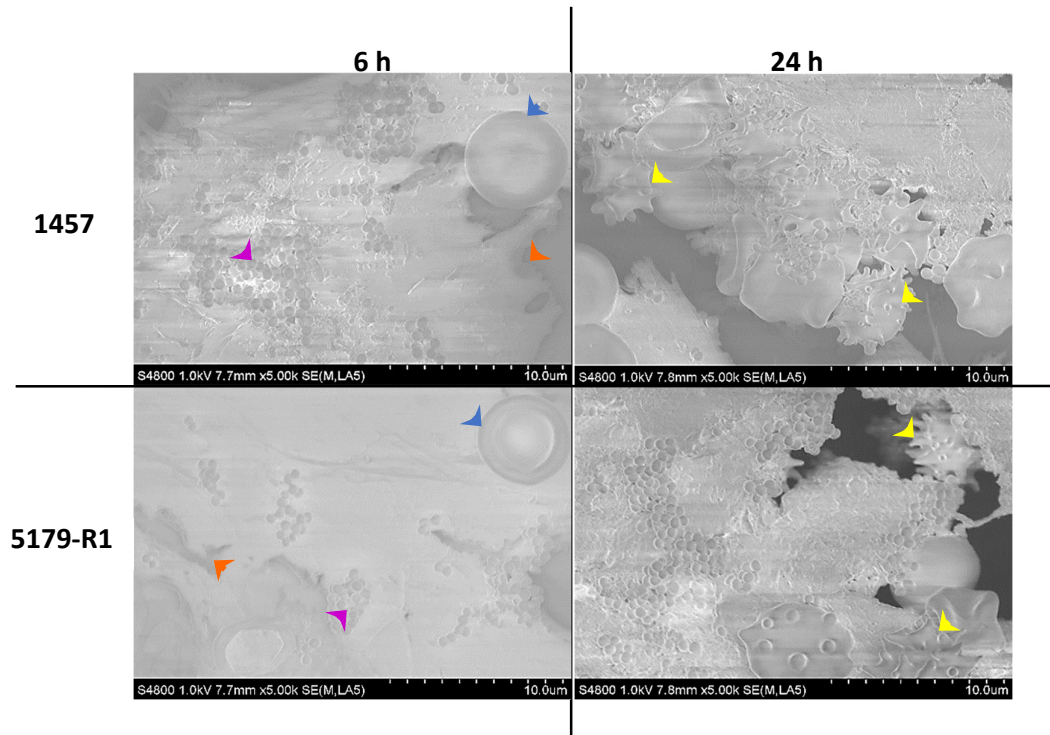
Figure 3.34. SEM images of 1BR.3.G fibroblasts co-cultured with *S. epidermidis* on whole blood coated discs. 1BR..3.G fibroblasts co-cultured with *S. epidermidis* 1457 (top panel) and 5179-R1 (bottom panel) for 6 h (left panel) or 24 h (right panel) on Ti discs pre-coated with whole blood. Arrowheads show examples of 1BR.3.G fibroblasts (orange) and *S. epidermidis* cell clusters (purple), biconcave red blood cells (blue) and echinocytes/acanthocytes (yellow).

3.4.2 *S. epidermidis* 5179-R1 Gene Expression

To investigate the transcription of *S. epidermidis* 1579-R1 genes when in mono-culture or co-culture with 1BR.3.G fibroblasts on Ti or TiAlV discs pre-coated with whole blood, RNA was extracted from adherent cells, and cDNA was synthesised. This cDNA was used to carry out RT-qPCR reactions and to determine fold-differences between culture conditions (Section 2.10).

Overall, the expression of *S. epidermidis* 5179-R1 adhesion and biofilm associated genes varied depending on culture time and sample disc but were not influenced by the presence of 1BR.3.G fibroblasts in co-culture (Figure 3.35.). No down-regulation of any accumulation or biofilm genes was identified across culture conditions (Figures 3.35. and 3.36.). On pre-coated Ti discs, results showed no difference in expression of *aap*, *atlE* and *RNAIII* between 6 h and 24 h when cultured alone of in the presence of 1BR.3.G fibroblasts (Figure 3.34.A). Whereas the expression of *icaA, embp*, *sdrG* and

sdrF increased under both culture conditions on the pre-coated Ti discs. On pre-coated TiAlV discs, the expression of *icaA*, *aap*, *atlE*, *sdrG* and *RNAIII* remained constant between time points under both culture conditions (Figure 3.35.B). In contrast, an increase in expression of both *embp* and *sdrF* was observed, but only when cultured alone on the pre-coated TiAlV discs. On both pre-coated Ti and TiAlV discs, there was no difference in gene expression when comparing *S. epidermidis* cultured alone or in co-culture with 1BR.3.G cells at 6 or 24 h (Figure 3.36.).
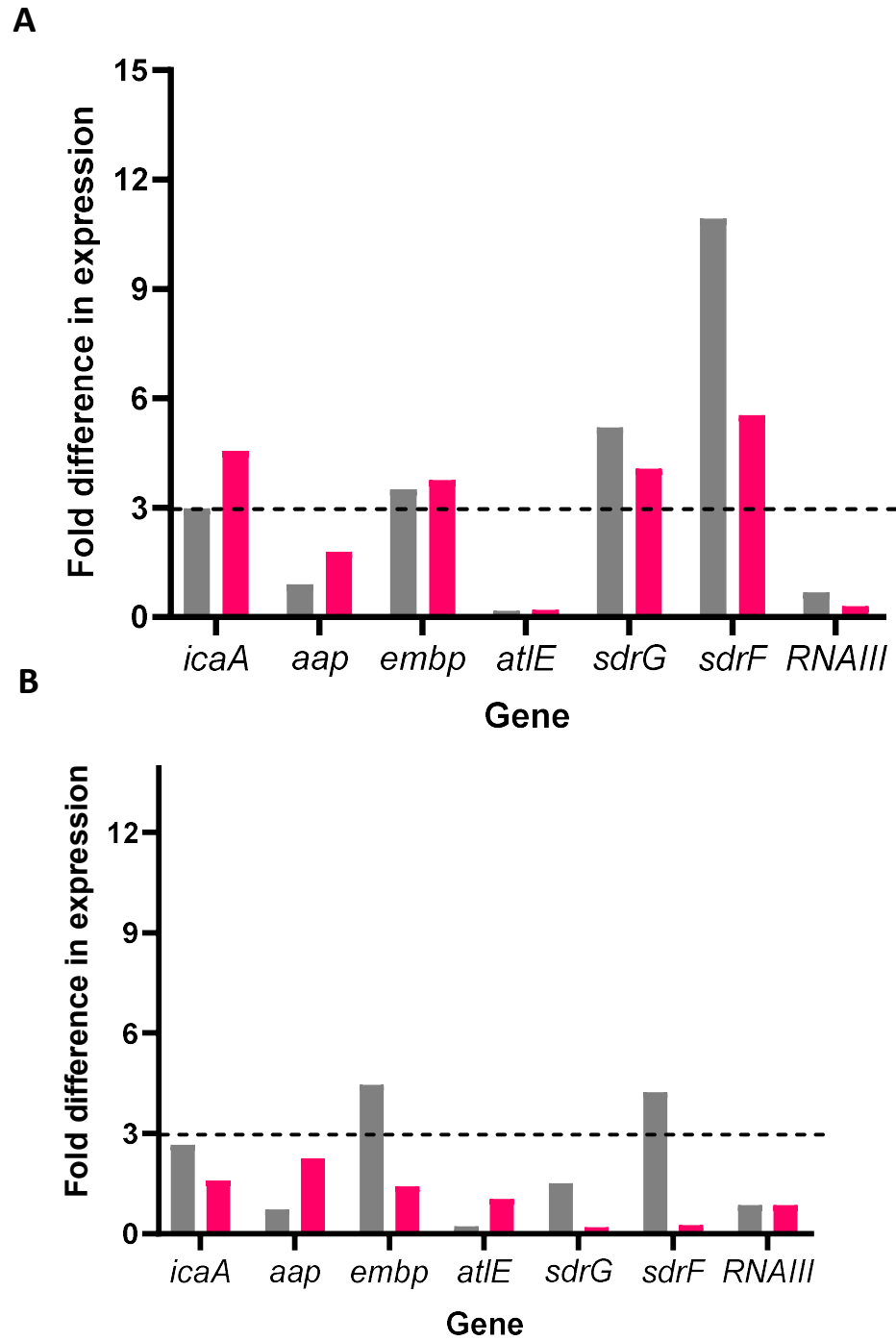
Figure 3.35. The mean fold difference in *S. epidermidis* gene expression between 6 h and 24 h on blood coated Ti and TiAlV in mono- or co-culture with 1BR.3.G fibroblasts. The mean fold difference in expression of *S. epidermidis* genes; *icaA, aap, embp, atlE, sdrG, sdrF* and *RNAIII*, between 6 h and 24 h when cultured on A) whole blood coated Ti or B) whole blood coated TiAlV discs in mono-culture (grey) or co-culture with THP-1 macrophages (pink; n= 1 biological replicates). Results show the mean average and hashed line represents the 3-fold threshold.
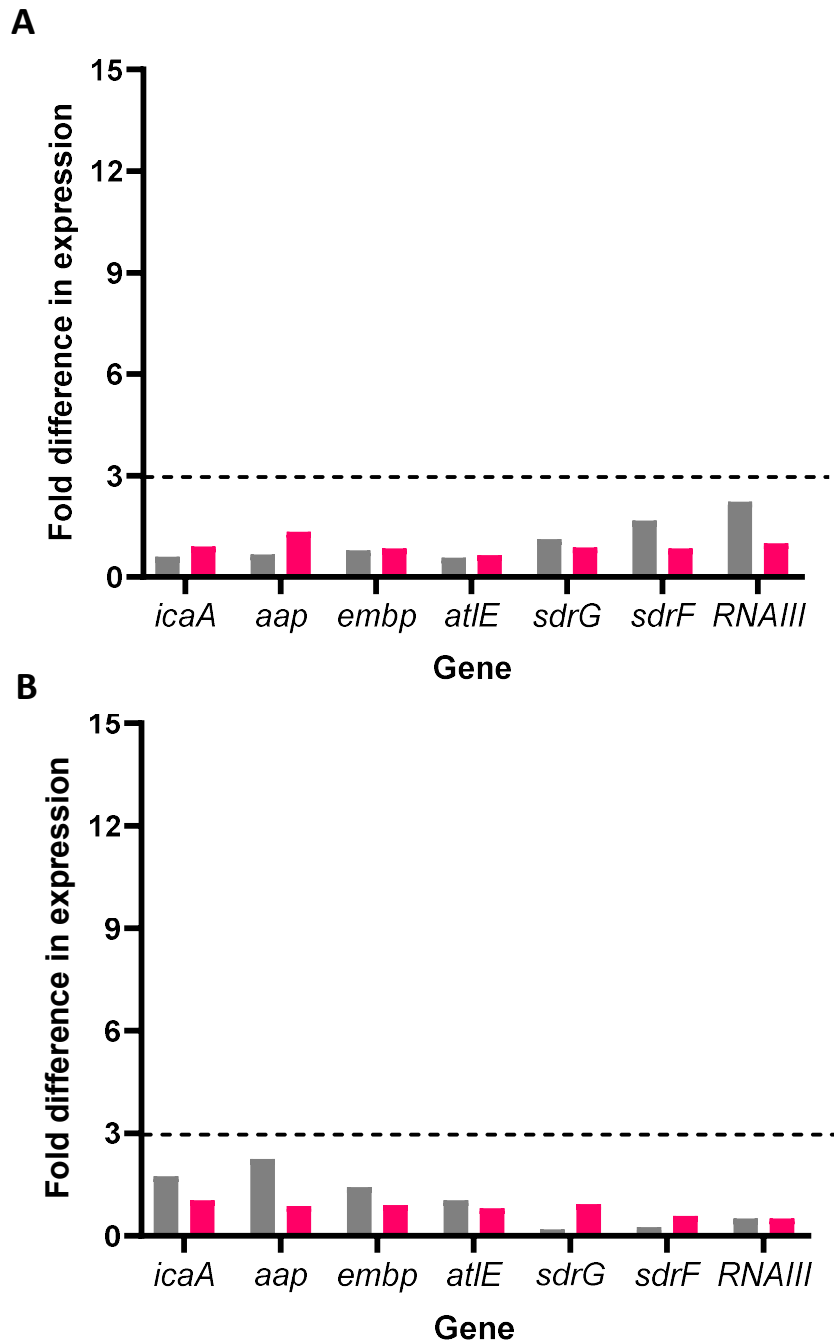
Figure 3.36. The mean fold difference in *S. epidermidis* gene expression between mono-culture and co-culture with 1BR.3.G fibroblasts on blood coated Ti and TiAlV. The mean fold difference in expression of *S. epidermidis* genes; *icaA, aap, embp, atlE, sdrG, sdrF* and *RNAIII*, between mono-culture and co-culture with 1BR.3.G fibroblasts A) whole blood coated Ti or B) whole blood coated TiAlV discs at 6 h (grey) or 24 h (pink; n=1 biological replicates). Results show the mean average and hashed line represents the 3-fold threshold.

3.4.3 Cytokine analysis

To investigate the effect of *S. epidermidis* 5179-R1 and whole blood coated Ti or TiAlV discs on the expression of IL-8 by 1BR.3.G fibroblasts, a DuoSet IL-8 ELISA was carried out as described in Section 2.11.2.

Results show a ten-fold increase in expression of IL-8 by mono-cultured 1BR.3.G fibroblasts on pre-coated Ti and TiAlV discs, compared to those cultured without a metal disc (Figure 3.37.). In mono-culture, no obvious difference was observed between IL-8 expression on Ti and TiAlV discs. In contrast, at both 6 h and 24 h in co-culture, IL-8 expression increased approximately 2-fold on Ti compared to TiAlV discs. On Ti, 1BR.3.G fibroblast expression of IL-8 was similar in mono-culture and co-culture at both 6 h and 24 h. However, on TiAlV, 1BR.3.G expression of IL-8 decreased in co-culture compared to mono-culture but was similar at both 6 h and 24 h.
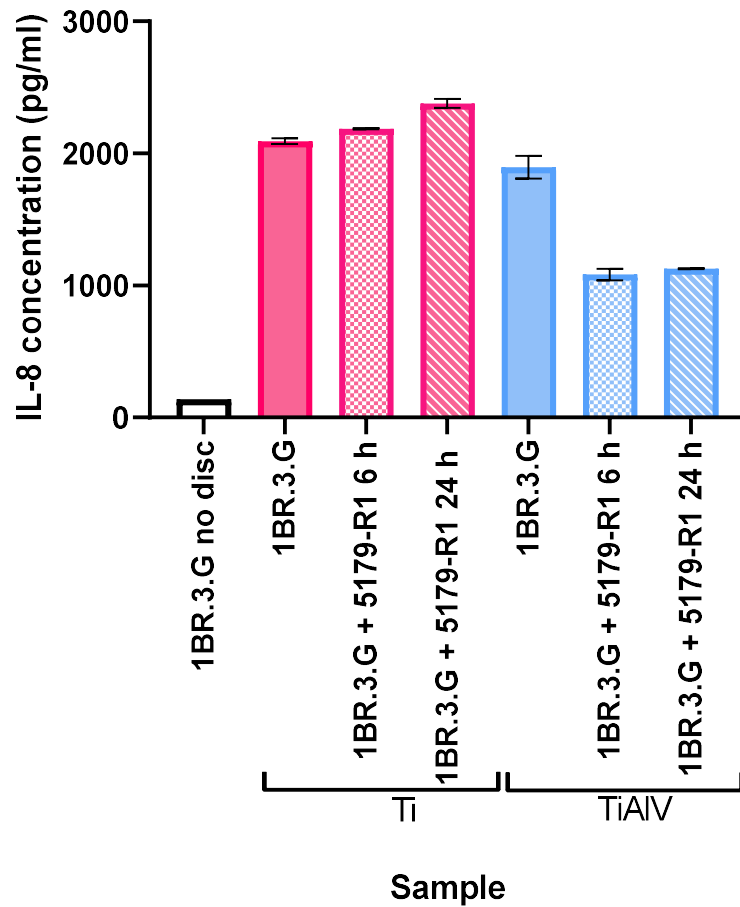
Figure 3.37. The effects of culture condition on 1BR.3.G fibroblast expression of IL-8 in mono-culture or co-culture with _S. epidermidis_ on pre-coated discs. The expression of IL-8 by 1BR.3.G fibroblasts grown with/without _S. epidermidis_ 5179-R1 is shown in the presence or absence of Ti and TiAlV discs pre-coated with whole blood. (n=1 biological sample, 2 technical replicates). Results show the mean average +/- the standard error of the mean.

To further investigate the expression of cytokines by 1BR.3.G fibroblasts in mono-culture or co-culture with _S. epidermidis_ 5179-R1 on Ti discs pre-coated with whole blood was determined using human proteome profiler arrays (Section 2.11.1 and Appendix B). Results are shown in Figure 3.38., and on all membranes positive control spots (orange circles) with high pixel density, and negative control spots (blue circles) showing no change in pixel density were seen, confirming that the membranes were successful.
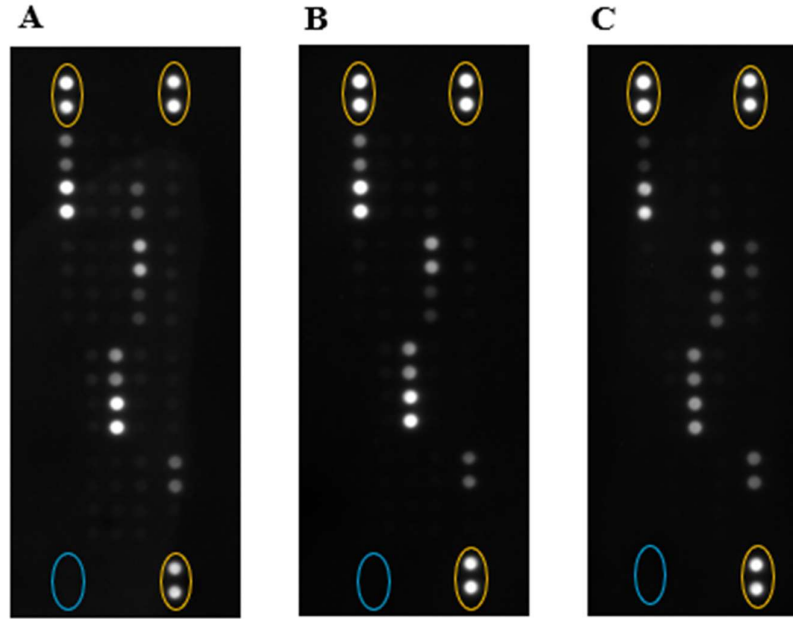
Figure 3.38. Human Proteome Profiler Array membranes of 1BR.3.G fibroblasts in mono-culture or co-culture with *S. epidermidis* on whole blood coated Ti. Membranes show the expression of 36 human cytokines for samples A) 1BR.3.G fibroblasts cultured on blood coated Ti, B) 1BR.3.G fibroblasts co-cultured with *S. epidermidis* 5179-R1 for 6 h on blood coated Ti, C) 1BR.3.G fibroblasts co-cultured with *S. epidermidis* 5179-R1 for 24 h on blood coated Ti. Positive and negative control spots are circled in orange and blue respectively.

Of the 36 cytokines tested, 17 cytokines were expressed by 1BR.3.G fibroblasts in one or more culture condition and are presented in Appendix E. 1BR.3.G fibroblasts cultured in mono-culture on pre-coated Ti showed expression of all 17 cytokines. However, in co-culture on blood coated Ti, fewer cytokines were expressed by 1BR.3.G fibroblasts. Co-culture with *S. epidermidis* for 6 h on blood coated Ti resulted in decreased expression of IL-1α, MCP-1 and SDF-1α was decreased by 1BR.3.G fibroblasts (Table 3.4). Similarly, when compared to mono-culture, 24 h co-culture conditions decreased the 1BR.3.G cytokine expression of IL-1α, IL-16, MCP-1, MIF and SDF-1α.

Table 3.4. The effect of *S. epidermidis* 5179-R1 and blood coated Ti discs on cytokine expression by 1BR.3.G fibroblasts in mono- or co-culture conditions (n=1). Detected with the or Human Proteome Profiler Array Kit.

Cytokine	1BR.3.G Blood Coated Ti	1BR.3.G + 5179-R1 6 h Blood Coated Ti	1BR.3.G + 5179-R1 24 h Blood Coated Ti
IL-1α	+	×	×
IL-2	+	+	×
IL-16	+	+	×
MCP-1	+	×	×
MIF	+++	+++	+
SDF-1α	++	+	×

× = no expression (mean pixel density <10), + = low expression (mean pixel density = 10-50), ++ = positive expression (meal pixel density = 51-100), +++ = High expression (mean pixel density >101)

4. Discussion

Medical device infections have a high burden not only on patient health, being associated with morbidity and mortality, but also on the NHS, costing £27.4 million for total knee arthroplasty revision surgery alone in 2012 (Kallala *et al*., 2015; Harris *et al*., 2016). In a recent study by Street *et al*. (2017), the opportunistic pathogen, *S. epidermidis* was present in 13% of PJIs. Few studies have yet investigated the impact of medical device surfaces and *S. epidermidis* on host cells in co-culture. Thus, this project was designed to investigate the interactions between *S.,* and host immune factors produced by cells such as 1BR.3.G fibroblasts and THP-1 macrophages in the presence of Ti and TiAlV surfaces. To achieve this, a culturing method was developed to co-culture THP-1 macrophages or 1BR.3.G fibroblasts with *S. epidermidis* cells on uncoated or whole blood coated Ti or TiAlV discs. The development of a co-staining technique allowed for the visualisation of both eukaryotic and prokaryotic cells on the Ti and TiAlV surfaces. Meanwhile the transcription of *S. epidermidis* genes was explored using RT-qPCR analysis and cytokine expression by THP-1 macrophages and 1BR.3.G fibroblasts was determined using human proteome profiler arrays and ELISA.

4.1 Optimisation

This project successfully developed a model to co-culture *S. epidermidis* with fibroblasts or macrophages on Ti or TiAlV discs. Bacterial cell components and the secretion of cytokines such as GM-CSF or IL-4 are known to be triggers for monocyte differentiation into macrophages (Ohradanova-Repic *et al*., 2016). For this reason, *S. epidermidis* was co-cultured with THP-1 monocytes before visualising cells for differentiation into adhesive macrophages. In this study, the presence of *S. epidermidis* cells did not stimulate the differentiation of THP-1 monocytes to macrophages (Figures 3.7 and 3.8). As PMA is known to trigger differentiation of THP-1 monocytes to macrophages (Lund *et al*., 2016), it was decided to add PMA to THP-1 monocyte cultures prior to the addition of *S. epidermidis*.

Cell culture media such as MEM or RPMI is essential for the growth of 1BR.3.G fibroblasts or THP-1 monocytes/macrophages respectively. Therefore, the growth and biofilm formation of *S. epidermidis* in both cell culture media was essential to develop a co-culturing method. Previous studies have successfully cultured *Staphylococcus* spp. in both MEM and RPMI cell culture media (Barcia-Macay *et al*., 2006; Spiliopoulou *et al*., 2012; Perez and Patel, 2018). This was confirmed by the current study in which, growth and biofilm formation of both *S. epidermidis* strains was demonstrated in both MEM and RMPI cell culture media (Figures 3.2, 3.3, 3.5 and 3.6). This was further corroborated by the visualisation and adhesion of *S. epidermidis* cells with SEM (Figure 3.7, 3.8 and 3.11). Despite this, difficulties arose with extracting sufficient yields of RNA from *S. epidermidis* 1457 in MEM. This may have been a result of weak biofilm formation on Ti (Figure 3.6), or due to the PIA-dependent biofilm phenotype, which is known to make RNA extractions more challenging (França *et al*., 2011).

4.2 Adherence of *S. epidermidis,* THP-1 Macrophages and 1BR.3.G Fibroblasts to Ti and TiAlV Discs.

The adherence of *S. epidermidis,* THP-1 macrophages and 1BR.3.G fibroblasts to Ti and TiAlV was visualised using CLSM and SEM. As expected, *S. epidermidis* cultured on Ti and TiAlV surfaces showed adherence and biofilm formation as reported in previous studies (Figure 3.16.; Shida *et al*., 2013; Kunrath *et al*., 2020). In mono-culture both THP-1 macrophages and 1BR.3.G fibroblasts also showed adherence to both surfaces, corresponding with previous studies (Figures 3.15. and 3.24.; Markhoff *et al*., 2017; Dai *et al*., 2015; Zwicker *et al*., 2022). Microscopy images showed that in 6 h co-culture, *S. epidermidis* and THP-1 macrophages or 1BR.3.G fibroblasts successfully adhered to the Ti and TiAlV surfaces (Figures 3.17. and 3.25.). However, at 24 h in co-culture, *S. epidermidis* biofilm formation and fibroblast detachment was evident on both Ti and TiAlV surfaces (Figure 3.26.). The mechanism or reason for fibroblast detachment from the surfaces was not identified in this study. However, it was determined that the detachment of 1BR.3.G fibroblasts was not dependent on the presence of Ti and TiAlV and instead was a result of co-culture with *S. epidermidis* strains. The detachment of fibroblasts in response to high

cytotoxicity has previously been reported by Reinhardt *et al*. (1985). Unlike *S. aureus* which produces a wealth of toxins to aid virulence and evade host defences, *S. epidermidis* toxins are far more limited, particularly to PSMs (reviewed by Otto, 2009). Some PSMs, specifically PSMδ, have been reported to demonstrate cytolytic activity, particularly against neutrophils (Cheung *et al*., 2010). However, cytotoxic effects of *S. epidermidis* PSMs against fibroblasts have not been widely explored. Adhesion molecules, intercellular adhesion molecule-1 (ICAM-1) and vascular cell adhesion molecule-1 (VCAM-1) expressed on fibroblast cell surfaces are known to be increased by inflammation (Pang *et al*., 1994). However, according to the human proteome profiler array, 1BR.3.G fibroblasts did not express ICAM-1 or VCAM-1 under any culture condition (Appendix D.). For this reason, ICAM-1 and VCAM-1 are unlikely to be involved in 1BR.3.G fibroblast detachment during this study. Dunlevy and Couchman (1995) observed that fibroblasts expressing high IL-8 exhibited decreased focal adhesions and an increase in motility. As displayed in Figure 3.28., 1BR.3.G fibroblasts in co-culture for 24 h with *S. epidermidis* on Ti or TiAlV expressed increased IL-8 compared to mono-cultured fibroblasts. Similarly, Wong *et al*. (2012) noted that damage or injury to the skin can stimulate fibroblast production of focal adhesion kinase thus allowing the induction of fibrosis. Therefore, the inflammatory response to *S. epidermidis* which results in increased IL-8 expression may lead to decreased 1BR.3.G fibroblast focal adhesion and thus detachment from the Ti or TiAlV surfaces.

When co-cultured with 1BR.3.G fibroblasts, *S. epidermidis* cells adhered to Ti and TiAlV discs at both time points (Figures 3.25. and 3.26.). To aid their function in wound healing, fibroblasts are known to produce an ECM containing proteins such as collagen, fibrinogen and vitronectin (Tracy *et al*., 2016). *Staphylococcus* spp. attach to the protein components of the ECM or host tissue through the expression of MSCRAMMs on *Staphylococcus* cell surfaces (Foster and Höök, 1998). In this study the expression of *S. epidermidis* MSCRAMMs were found to be expressed across co-culture conditions with 1BR.3.G fibroblasts, corresponding with *S. epidermidis* adherence (Figures 2.37. and 3.28). Therefore, it is likely that the expression of MSCRAMM proteins aids *S. epidermidis* adherence to the medical device when in the presence of ECM components.

In comparison to 1BR.3.G fibroblasts, THP-1 macrophages in co-culture with *S. epidermidis* for 24 h remained attached to the Ti surface but detached from the TiAlV surface (Figure 3.18.). Comparable to the fibroblasts, THP-1 macrophage detachment may be related to cytotoxicity by *S. epidermidis* cells, however, a study by Zwicker *et al* (2022) reported the adhesion of THP-1 macrophages in co-culture with *S. epidermidis* for 24 h on TiAlV when *S. epidermidis* was seeded at a higher OD_{600} of 0.3, suggesting that *S. epidermidis* presence may not be responsible for lack of THP-1 macrophage adhesion in this study. As detachment was only observed on the TiAlV surface and not on the Ti surface the metal composition may play a larger role in cellular detachment. Vallabani *et al*. (2022) identified little cytotoxic effects of TiAlV surfaces on macrophages, however, the release of aluminium and vanadium from the TiAlV surface is known to have cytotoxic effects on host cells (Haydar *et al*., 2021). It is therefore possible that the surface composition of TiAlV may be responsible for the THP-1 macrophage detachment in this current study.

From the CLSM images, it was difficult to identify whether *S. epidermidis* cells were intracellularly fluorescing within host cells, or extracellularly fluorescing on host cells. Macrophages are well known to phagocytose bacteria as part of the immune response (Greenberg and Grinstein, 2002). As reported by Schommer *et al*. (2011), macrophages can engulf and phagocytose both *S. epidermidis* 1457 and 5179-R1 strains. However, the protective effect of both Aap- and PIA-dependent biofilms aid *S. epidermidis* in reducing this immune clearance mechanism (Schommer *et al*., 2011). Similarly, a study by Parez and Patel, (2018) discussed the ability of *S. epidermidis* to persist intracellularly within human fibroblasts, as an immune evasion tactic. From this, it is therefore possible that *S. epidermidis* cells in this study may be present intracellularly in addition to extracellularly in co-culture with both THP-1 macrophages and 1BR.3.G cells.

Upon implantation, medical device surfaces are coated with patient blood, allowing the adherence of host cells and the establishment of a host ECM (Anderson *et al*., 2008). In this study, the coating of medical devices and establishment of an ECM during implantation was simulated by coating the Ti surfaces with whole blood prior to cell culture. SEM showed adherence of both *S. epidermidis* and 1BR.3.G fibroblast cells to the pre-coated Ti surfaces in monoculture and co-culture at 6 h (Figures 3.32., 3.33. and 3.34.). Despite detaching from the uncoated Ti surface, fibroblasts remained

adherent to the pre-coated Ti surface in 24 h co-culture, although their confluency decreased (Figures 3.26. and 3.34.). The attachment of fibroblasts to the host ECM is mediated by focal adhesions, which as a collection of integrins act as receptors for the ECM and mediate the attachment of cells to host ECM proteins (Burridge, K. and Chrzanowska-Wodnicka, 1996). Palkowitz *et al*. (2021) identified that fibroblast adhesion to TiAlV surfaces benefits from the presence of ECM components including fibronectin and laminin. Therefore, the establishment of the host ECM on the pre-coated Ti surfaces may allow increased and stronger fibroblast attachment to the Ti surface, which in turn may have allowed for decreased detachment of fibroblast cells following 24 h in co-culture with *S. epidermidis* cells. As discussed above, the presence of MSCRAMMs on the surface of *S. epidermidis* cells increases cellular attachment to host ECM proteins, and therefore, the attachment of *S. epidermidis* to pre-coated Ti surfaces is likely enhanced by the presence of the ECM.

4.3 Gene Expression of *S. epidermidis*

While previous studies have investigated the gene expression of *S. epidermidis* strains on various surfaces, no study has yet investigated the gene expression of *S. epidermidis* 5179-R1 in co-culture with THP-1 macrophages or 1BR.3.G fibroblasts on Ti or TiAlV surfaces. Due to difficulty extracting RNA, PCR analysis could not be completed for the PIA-dependent biofilm strain, *S. epidermidis* 1457. Despite this, RNA was successfully extracted from the Aap-dependent biofilm strain, *S. epidermidis* 5179-R1, and was then used for RT-qPCR analysis. In keeping with previous work by Harris *et al*. (2017) *gyrB* was selected as the housekeeping gene for this study. Due to its essential role as a catalyst for the hydrolysis of ATP in bacteria, *gyrB* is consistently expressed in *S. epidermidis,* therefore making it a good housekeeping gene for PCR analysis (Mizuuchi *et al*., 1978).

The genes used in this study were selected due to their roles in *S. epidermidis* attachment, biofilm formation or quorum sensing. According to Götz (2002), the establishment of a biofilm on any surface is divided into two main phases. In the first phase, planktonic *S. epidermidis* cells attach to the surface (Götz, 2002). For this study, primary attachment was investigated by analysing *embp, atlE, sdrG* and *sdrF* expression. As previously mentioned, *S. epidermidis* surface proteins, Embp, AtlE,

SdrG and SdrF bind to extracellular matrix proteins such as fibronectin (Williams *et al*., 2002), vitronectin (Heilmann *et al*., 1997), fibrinogen (Hartford *et al*., 2001) and collagen (Arrecubieta *et al*., 2007) respectively. Research by Vandecasteele *et al*. (2003) has shown that *S. epidermidis* 10b expression of *altE* remained constant in biofilms throughout the stages of biofilm development. This was corroborated by the current study where *S. epidermidis* 5179-R1 displayed no upregulated expression of *atlE* between 6 h and 24 h on both metal surfaces (Figures 3.19., 3.27. and 3.35.). In contrast, the expression of *embp*, *sdrG* and *sdrF* varied depending on culture condition and duration. Binding through Embp, SdrF and SdrG is thought to play an important role in attachment to medical devices, particularly in early stages of infection (Yao *et al.,* 2005; Sellman *et al*., 2008; Fey and Olson, 2010). A study by Linnes *et al*. (2014) identified that *embp* expression by PIA-dependent *S. epidermidis* strain 1457 was not upregulated between 4 h and 24 h in biofilms on the surface of culture flasks, however, inducing osmotic stress caused *S. epidermidis* 1457 expression of *embp* to increase. It is possible that increased *S. epidermidis* 5179-R1 expression of *embp* in this study could be related to increased stress caused by the presence of eukaryotic cells or the Ti and TiAlV surfaces themselves. Alternatively, in some PIA independent strains, *embp* also plays a role in biofilm accumulation in addition to attachment (Christner *et al*., 2010). As *S. epidermidis* 5179-R1 is a PIA-independent strain, *embp* may have a larger role in biofilm formation than in the PIA-dependent *S. epidermidis* strain 1457, accounting for increased transcription between timepoints. Sellman *et al*. (2008) reported that in a murine model, *sdrG* expression by *S. epidermidis* strains was increased during the first hour of infection. The current project identified a similar pattern whereby *sdrG* expression was increased in the early hours of biofilm formation compared to at 24 h when a more established biofilm was formed. Overall, the expression of *embp*, *sdrG* and *sdrF* supports previous studies and confirms the role of these MSCRAMM proteins in the primary attachment of *S. epidermidis* 5179-R1 to medical device surfaces (Yao *et al*., 2005).

Following attachment, the second step of biofilm formation is the accumulation of *S. epidermidis* cells and the development of intercellular adhesions (Götz, 2002). To investigate this, *S. epidermidis 5179-R1* expression of *icaA* and *aap* was explored under different culture conditions. The gene *icaA* is part of the *icaADBC* gene operon (Heilmann *et al*., 1996). This gene operon is responsible for the production of PIA, an

important intercellular adhesin in some *S. epidermidis* biofilms (Heilmann *et al*., 1996). Within this gene operon, *icaA* acts as a catalytic enzyme, *N*-acetylglucosaminyltransferase which is required for the activity of *icaD* (Gerke *et al*., 1998). Despite *S. epidermidis* 5179-R1 being an Aap-dependent biofilm producer, it still possesses the *icaA* gene (Rhode *et al*., 2005). However, the presence of the IS*257* insertion sequence in *icaA* is known to prevent functional *icaADBC* transcription and PIA production (Rohde *et al*., 2005). Although IS257 prevents PIA production, many strains with the IS257 insertion sequence still show positive *icaA* expression (Nasaj *et al*., 2021). For this reason, *icaA* expression was still recorded across *S. epidermidis* 5179-R1 samples but was not representative of PIA production or intercellular adhesion. In the absence of PIA, *S. epidermidis* 5179-R1 is well known to use proteinaceous factors such as Aap for intercellular adhesion (Rhode *et al*., 2005). In PIA-dependent strains such as *S. epidermidis* 1457 and *S. epidermidis* 10b where Aap is not a factor in intercellular adhesion, biofilm expression of *aap* was noted to decrease over time (Vandecasteele *et al*., 2003; Yao *et al*., 2005). However, this study determined that *aap* expression by *S. epidermidis* 5179-R1 was consistent across all conditions at both 6 h and 24 h. This finding supports the role of Aap as an intercellular adhesion throughout the development of the 5179-R1 biofilm. However, as Aap is also involved in initial attachment, it is possible that expression may be upregulated at an earlier time point.

In *S. epidermidis,* the *agr* quorum sensing system plays an important role not only in crosstalk between microbial communities but also in virulence, PSM production and biofilm production (Mack *et al*., 2007). Within the *agr* system the effector molecule, *RNAIII,* regulates the co-transcription of the *agr* genes (Van Wamel *et al*., 1998). For this reason, this study investigated the expression of *RNAIII* to explore *agr* activity in conjunction with biofilm formation and was seen to remain constant across all culture conditions except in co-culture with THP-1 macrophages on Ti at 24 h (Figures 3.19., 3.27., and 3.35.). Previous studies have shown that the *agr* system can negatively regulate primary adhesion of *S. epidermidis* cells and decrease biofilm formation (Vuong *et al*., 2003; Vuong *et al*., 2004; Dai *et al*., 2012). Studies have shown that the *agr* system downregulates the expression of *atlE* but does not impact upon *icaADBC* or *aap* expression (Vuong *et al*., 2003; Dai *et al*., 2012). However, this study did not show any correlation between *RNAIII* and *atlE* or *icaA* upregulation. It has also been

shown that *RNAIII* expression is decreased in *S. epidermidis* biofilms over time compared to planktonic cells (Yao *et al*., 2005). Although *RNAIII* expression did not decrease between 6 h and 24 h in this study, earlier timepoints such as 2 h or 4 h may have shown increased expression and should therefore be explored in the future to identify expression changes during earlier biofilm establishment.

The presence of THP-1 macrophages in co-culture was shown to have an impact on *S. epidermidis* 5179-R1 gene expression, particularly at 24 h on the Ti surface (Figure 3.20.). In contrast, the presence of 1BR.3.G fibroblasts did not alter *S. epidermidis* 5179-R1 gene expression on any surface (Figures 3.28. and 3.36.). *S. epidermidis* strains including *S. epidermidis* 5179-R1 use biofilm formation mechanisms to interfere with macrophage phagocytosis and activation (Christner *et al*., 2010; Schommer *et al*., 2011). Upregulated gene expression in the presence of THP-1 macrophages could therefore be related to immune evasion strategies involving biofilm proteins such as Embp, AtlE and SdrG. In this study, *embp, atlE* and *sdrF* expression was upregulated at 24 h between mono- and co-culture on Ti discs but not on TiAlV discs (Figure 3.20.). As shown in CLSM, the adherence of macrophages was decreased at 24 h on the TiAlV surface compared to Ti (Figure 3.18.). Corresponding samples showed no difference in *S. epidermidis* gene expression between mono-culture and co-cultured samples at 24 h (Figure 20). This is likely due to the absence of host cells for *S. epidermidis* to adhere to, which in turn makes *S. epidermidis* attachment and biofilm formation similar to that of the mono-culture. In keeping with this, *S. epidermidis* co-cultured with 1BR.3.G fibroblasts at 24 h also showed no upregulated gene expression in comparison to mono-culture, which may also be a result of 1BR.3.G fibroblast detachment (Figures 3.26. and 3.28.).

The effects of pre-coating the Ti and TiAlV surfaces with whole blood on *S. epidermidis* gene expression had not yet been explored prior to this study. Pre-coating of the surfaces had little effect on *S. epidermidis* 5179-R1 gene upregulation compared to *S. epidermidis* 5179-R1 on uncoated surfaces (Figures 3.28. and 3.36.). The uncoated and pre-coated surfaces showed no differences in gene upregulation between mono- and co-cultured samples at 6 h or 24 h. However, gene upregulation of *aap* and *embp* differed between pre-coated and uncoated Ti, while gene upregulation of *icaA, embp, sdrG* and *sdrF* differed between pre-coated and uncoated TiAlV (Figures 3.27. and 3.35.). Upon implantation, host proteins and host cells coat the medical device

surface, allowing for the attachment of *S. epidermidis* cells using MSCRAMM adhesions (original papers in Vuong and Otto, 2002). Pre-coating the Ti and TiAlV surfaces allows for the establishment of a host ECM on the metal surfaces to which *S. epidermidis* MSCRAMM proteins can attach. Therefore, the differences in the expression of MSCRAMM genes such as *embp, sdrG* and *sdrF* between uncoated and pre-coated discs is likely a result of increased ECM coating the Ti and TiAlV surfaces.

4.4 Cytokine Expression by THP-1 Macrophages and 1BR.3.G Fibroblasts

Human proteome profiler arrays and ELISAs were used to analysed cytokine expression in cell culture supernatant. Due to cytokine analysis being completed using the supernatant from RNA extraction cultures, the effect of *S. epidermidis* 1457 on cytokine expression was not explored.

As IL-8 is a common mediator of inflammation (Baggiolini and Clark-Lewis, 1992), the expression of IL-8 by THP-1 macrophages and 1BR.3.G fibroblasts was investigated using ELISA. Despite the human proteome profiler arrays showing little difference in IL-8 expression (Appendices C. and D.), ELISA analysis identified variation in THP-1 macrophage and 1BR.3.G fibroblast IL-8 expression between culture conditions (Figures 3.21., 3.22., 3.29., 3.30. and 3.37.). As Lipopolysaccharide (LPS) is known to stimulate IL-8 expression in both fibroblasts and macrophages (Pang *et al*., 1994; Dentener *et al*., 1993), LPS positive controls were included to demonstrate successful IL-8 expression. Corresponding with previous work by Kaufman *et al*. (2008) on TiAlV, the presence of Ti and TiAlV discs in this study caused an increase in expression of IL-8 by THP-1 macrophages. Similarly, THP-1 monocyte IL-8 expression also increased in the presence of the Ti and TiAlV surfaces, thus confirming that this expression was not related to cell differentiation. Comparable to THP-1 macrophages, 1BR.3.G fibroblast expression of IL-8 also increased in the presence of both pre-coated and uncoated Ti and TiAlV surfaces. Collectively, this corroborates previous work by Markhoff *et al*. (2017) which showed increased IL-8 expression by both macrophages and fibroblasts in the presence of TiAlV surfaces. Although increases in IL-8 expression by THP-1 macrophages and 1BR.3.G fibroblasts with Ti and TiAlV were observed, these increases were not significant. This has also been reported in osteoblasts, which showed increased IL-8 expression in

the presence of Ti but no statistical differences (Fritz *et al*., 2002). It has been noted by Spiliopoulou *et al*. (2012) that the expression of IL-8 by macrophages increases in culture with biofilm-phase *S. epidermidis*. In support of this, our results also identified increased expression of IL-8 by THP-1 macrophages in co-culture with *S. epidermidis* 5179-R1 compared to mono-culture in the absence of a Ti surface. 1BR.3.G fibroblast expression of IL-8 was also similar in mono- and co-culture at 6 h both in absence and presence of surfaces. However, at 24 h fibroblast co-cultures on Ti and TiAlV surfaces demonstrated increased expression of IL-8. As previously discussed, this increase in IL-8 expression could correspond with the detachment of the fibroblasts from the metal surfaces (Dunlevy and Couchman, 1995). This current study did not investigate 1BR.3.G fibroblast cytotoxicity in the presence of *S. epidermidis* 5179-R1, however, it is possible that increased IL-8 could be due to cytotoxic effects of *S. epidermidis* 5179-R1 during the 24 h co-culture period.

Finally, in comparison to uncoated surfaces, 1BR.3.G fibroblast expression of IL-8 was increased on Ti and TiAlV surfaces pre-coated with whole blood. Fredriksson *et al*. (2003) found that the presence of red blood cells causes increased IL-8 expression by fibroblast. In keeping with this, the adherence of red blood cells to the pre-coated Ti or TiAlV surfaces in this current study may be a factor in increased IL-8 expression on pre-coated surfaces (Figures 3.32. and 3.37.). Similar to other cytokines identified using the human proteome profiler array, fibroblast expression of IL-8 on the pre-coated Ti surface was high across all culture conditions and was not increased in the presence of *S. epidermidis* 5179-R1 (Appendix E.). In comparison, the expression of IL-8 by fibroblasts on pre-coated TiAlV surfaces was decreased in co-culture compared to monoculture samples (Figure 3.37). This suggests that metal composition of pre-coated surfaces may be a factor in 1BR.3.G fibroblast IL-8 expression in co-culture conditions. Alternatively, it could be possible that the adhesion of red blood cells may differ between Ti and TiAlV surface, however, as only Ti surfaces were visualised, this could not be confirmed.

Due to limited availability of human proteome profiler arrays, cytokine expression in the presence of *S. epidermidis* 1457 or TiAlV discs was not explored during this study. Despite implant surfaces being defined as biocompatible (Pennen *et al*., 1991), the implantation of medical devices into the body is known to trigger a host inflammatory response due to injury and the detection of a 'foreign' body (Thomsen and Gretzer,

2001; Hamlet and Ivanovski, 2017). This response allows the body to repair damage at the implant site and identify possible microbial threats (Thomsen and Gretzer, 2001; Refai *et al*., 2004). Therefore, a high biocompatibility of medical device surfaces is essential to allow for equilibrium between the host inflammatory response and the presence of the device (Refai *et al*., 2004). The effects of biomaterials including Ti and TiAlV and their surface topography on the inflammatory response by host cells has been well explored (Refai *et al.,* 2004; Tan *et al*., 2006; Anderson *et al*., 2008; Hamlet *et al*., 2012; Schwartz-Filho *et al*., 2012). Previous studies have shown that the presence of Ti can increase the expression of pro-inflammatory cytokines by both THP-1 macrophages and 1BR.3.G fibroblasts (Li *et al*, 2005; Andrukhov *et al*., 2020). In keeping with previous studies, the presence of Ti surfaces in this study had a clear influence on cytokine expression by both THP-1 macrophages and 1BR.3.G fibroblasts. Specifically, THP-1 macrophages exhibited increased expression of pro-inflammatory cytokines and chemokines such as TNF-α, MCP-1, MIP-1α/1β which are known to increase following implantation (Table 3.1.; Refai *et al*., 2004). The increased expression of CD14, GROα, ICAM-1, MIF and SDF-1α is further evidence to recognition of the Ti surface as foreign and thus the initiation of the host immune response. However, the expression of anti-inflammatory IL-1 receptor antagonist (IL-1ra), which inhibits the action of IL-1α and IL-1β, displays the fine balance between inflammation and device survival within the host (Arend, 2002). The increased expression of both pro-inflammatory and anti-inflammatory cytokines suggests that THP-1 macrophages are being activated to both M1 and M2 macrophages, however, as macrophage activation was not explored in this study, this cannot be said with certainty.

Compared to macrophages, 1BR.3.G fibroblasts showed increased expression of fewer cytokines in the presence of the Ti surface (Table 3.3.). A previous study by Alali *et al*. (2021) identified increased expression of FGF-basic and VEGF, which are involved in wound healing and angiogenesis by gingival fibroblasts in response to Ti surfaces (Alali *et al*., 2021). However, in this current study, expression of FGF-basic and VEGF by skin fibroblasts was only induced in the presence of *S. epidermidis* 5179-R1 on Ti. Despite this, it was clear that the Ti surface was recognised as foreign due to increased expression of IFN-γ, MIF and Pentraxin 3. In addition, the increased expression of angiopoietin-2 demonstrates the ability of fibroblasts to recognise

damage caused by the foreign Ti disc and to reduce this by initiating angiogenesis and wound repair (Staton *et al*., 2010).

Studies investigating the effects of *Staphylococcus* spp. on macrophages have identified increased expression of pro-inflammatory cytokines during infection (Jones *et al*., 2005; Kasraie *et al*., 2010). However, few studies have specifically focussed on the effects of *S. epidermidis* and Ti surfaces on cytokine expression by THP-1 macrophages. Previous studies have shown that in co-culture with biofilm *S. epidermidis* macrophages display increased expression of TNF-α, IFN-γ, IL-1, IL-6, IL-8, GM-CSF and IL-13 (Cerca *et al.,* 2011; Spiliopoulou *et al*., 2012). Even in the absence of bacterial cells, *S. epidermidis* products such as lipoteichoic acid and peptidoglycan have been found to induce macrophage expression of pro-inflammatory cytokines such as IL-6, TNF-α and IL-1β (Jones *et al*., 2005). Comparable to previous studies, this current work also identified increased expression of IL-1β and TNF-α, suggesting an inflammatory response of THP-1 macrophages in response to *S. epidermidis* alone and with Ti, however, the presence of *S. epidermidis* did not induce the expression of IL-6 or IL-13 (Table 3.2.; Appendix C.). Previous studies have investigated cytokine expression using murine macrophages or human peripheral macrophages (Jones *et al*., 2005; Cerca *et al.,* 2011; Spiliopoulou *et al*., 2012). It has been reported that THP-1 cell line derived macrophages may show less notable differences in gene expression or cytokine expression, compared to macrophages derived from human blood monocytes (Tedesco *et al*., 2018). Of note, Tedesco *et al*. (2018) identified that polarised THP-1 macrophages demonstrated lower, or no expression of IL-6 compared to polarised human derived macrophages. As the polarisation of THP-1 macrophages was not investigated in this study, it is possible that the lack of IL-6 and IL-13 expression could be due to the THP-1 macrophage cell line, or due to the polarisation of THP-1 macrophage cells.

When cultured on the Ti surface with *S. epidermidis* 5179-R1, THP-1 macrophages showed increased expression of CD40 ligand, endoglin, G-CSF, GM-CSF, GROα, IL-1α, IL-1β, IL-4, IL-24, IL-27 and TNF-α (Table 3.2.). This supports previous work which also identified increased expression of the pro-inflammatory cytokine TNF-α in the presence of both *S. epidermidis* and a Ti6Al4V biomaterial surface (Zwicker *et al*., 2022). Together, this suggests the activation of THP-1 macrophages to M1 macrophages and the initiation of an innate immune response as a result of *S.*

epidermidis infection. Increased cytokine production by THP-1 macrophages on the Ti disc may suggest that the presence of the Ti surface augments the inflammatory and immune responses during *S. epidermidis* infection. This could be due to the detection of the 'foreign' surface and the initiation of a pro-inflammatory response prior to the addition of *S. epidermidis,* thus resulting in increased cytokine expression at 24 h.

In a model of sepsis caused by *S. epidermidis,* the expression of NF-κB by THP-1 monocytes was found to be induced by *S. epidermidis* PSMs (Mehlin *et al*., 1999). A study by Schommer *et al.* (2011) identified that while biofilm-negative *S. epidermidis* induced a strong NF-κB response by macrophages, biofilm-positive *S. epidermidis* strain strongly reduced NF- κB expression. The expression of IL-1β is understood to be controlled by NF- κB and can therefore provide an indication to NF-κB activity (Schommet *et al*., 2011). Schommer *et al.* (2011) identified IL-1β and NF-κB expression by macrophages stimulated with *S. epidermidis*. Consistent with these findings, the current study identified that IL-1β expression by THP-1 macrophages was induced by the presence of *S. epidermidis* both with and without Ti surfaces (Tables 3.1. and 3.2.). Despite the expression of NF-κB not being explored through this study, THP-1 macrophage expression of IL-1β suggests that could be activated and expressed in co-culture with *S. epidermidis* 5179-R1.

In comparison to macrophages, the expression of cytokines by dermal fibroblasts during *S. epidermidis* infection has been far less explored. Overall, 1BR.3.G fibroblasts expressed fewer cytokines than THP-1 macrophages on the human proteome profiler array when challenged with *S. epidermidis* presence (Table 3.3. and Appendix D.). In the immune response, fibroblasts play important roles in the recognition of micro-organisms, the initiation of inflammation and the recruitment of other immune cells to the site of infection (Smith *et al*., 1997). Following activation, fibroblasts are known to express pro-inflammatory cytokines, chemokines and growth factors in response to microbial infection (Bautista-Hernández *et al*., 2017). In support of this, this project identified increased expression of GROα, IL-17A, MIC-1, MIF, uPAR and FGF basic by 1BR.3.G fibroblasts co-cultured with *S. epidermidis* 5179-R1 on Ti surfaces (Table 3.3.). In response to *S. aureus* infection, fibroblasts have been reported to increase expression of VEGF, a growth factor involved in cellular growth (Kirker *et al*., 2012). In keeping with this, our study also identified increased VEGF expression by 1BR.3.G fibroblasts in the presence of *S. epidermidis* and a Ti

surface (Table 3.3.). Research by Baranoi *et al.* (1998) identified increased expression of hepatocyte growth factor (HGF) by fibroblasts in co-culture with *S. aureus* lipoteichoic acid and protein A. However, the lack of HGF expression by 1BR.3.G fibroblasts in co-culture with *S. epidermidis* in this study suggests that HGF expression may be strain specific to *S. aureus.*

On Ti surfaces pre-coated with whole blood, the expression of cytokines by 1BR.3.G fibroblasts differed greatly to that of 1BR.3.G fibroblasts on uncoated surfaces (Appendices D. and E.). Compared to uncoated Ti cultures, 1BR.3.G fibroblasts cultured on pre-coated Ti surfaces expressed numerous cytokines involved in immune responses. On pre-coated surfaces only, 1BR.3.G fibroblasts expressed the adhesion molecule ICAM-1 under both mono- and co-culture conditions (Table 3.4). As ICAM-1 is an adhesion molecule that promotes the adhesion of lymphocytes to fibroblasts, increased expression of ICAM-1 in the presence of pre-coated surfaces could allow for increased cellular adhesion (Dustin *et al.*, 1986) Therefore, ICAM-1 expression may be responsible for decreased 1BR.3.G fibroblast detachment from the pre-coated Ti surface at 24 h in co-cultured samples.

Similar to ICAM-1, cytokines such as G-CSF, GM-CSF, IL-6, MIP-1α/MIP-1β, RANTES and TNF-α were expressed by 1BR.3.G fibroblasts cultured on pre-coated surfaces but were not on uncoated surfaces (Tables 3.3. and 3.4 and Appendices D. and E.). Previous studies have noted that red blood cells interact with fibroblasts to induce the expression of pro-inflammatory cytokines and modulate the expression of ECM proteins (Fredriksson *et al.*, 2003; Fredriksson *et al.*, 2006; Akbari *et al.*, 2012). As identified in Figures 3.32., 3.33. and 3.34., pre-coating the Ti surfaces with whole blood left visible cellular debris and red blood cells on the Ti surface during monoculture and co-culture. It is therefore possible that the remaining red blood cells may interact with 1BR.3.G fibroblasts in culture to influence cytokine expression. This may contribute to the expression of pro-inflammatory cytokines such as TNF-α or IL-6 which were not expressed by 1BR.3.G fibroblasts on uncoated surfaces. In contrast to 1BR.3.G fibroblasts cultured on uncoated Ti, on pre-coated Ti surfaces fibroblasts in co-culture with *S. epidermidis* 5179-R1 at both 6 h and 24 h did not display increased expression of any recorded cytokines (Table 3.4. and Appendix E.). Specifically, the expression of IL-1α, IL-2, IL-16, MCP-1, MIF and SDF-1α by 1BR.3.G fibroblasts decreased over time in co-culture with *S. epidermidis* 5179-R1

on the pre-coated surfaces. This suggests that 1BR.3.G fibroblasts may have decreased pro-inflammatory and immune responses to *S. epidermidis* infection in the presence of whole-blood coated Ti.

4.5 Conclusions

This study successfully created a model to investigate the interactions between *S. epidermidis,* host cells and relevant medical device surfaces. The thesis found that the presence of Ti and TiAlV biomaterial discs had an impact on both *S. epidermidis* and 1BR.3.G fibroblast or THP-1 macrophage activity. In addition, results suggested that the interactions between *S. epidermidis* and macrophages or fibroblasts influenced cellular attachment and gene or cytokine expression of both bacterial and host cells respectively. Coating the Ti disc with whole blood affected the attachment and immune response of 1BR.3.G fibroblasts, while also having an impact on *S. epidermidis* pathogenesis. Overall, this work has provided an insight into the initial interactions that occur between host cells, medical device surfaces and *S. epidermidis* and how this influences the pathogenicity of *S. epidermidis* in medical device infections. These results are clinically relevant and could be applied to the development of new therapeutics to combat the difficulty in treating medical device infections. Understanding the host response to both the device surfaces and infections could allow patient responses to medical device infections to be predicted and thus could be translated to the development of new diagnostic methods.

4.6 Limitations and Future Work.

While this study has successfully developed a 3D model and investigated effects on *S. epidermidis* and host cells, it has also identified limitations which could be explored in future work. As described in 'the race for the surface', bacteria and host cells compete to be the first colonisers of the surface following implantation of the medical device (Gristina *et al*., 1988). For this project, macrophages and fibroblasts were exposed to the Ti or TiAlV surface for 24 or 48 h prior to the addition of *S. epidermidis* cells, thus allowing host cells to be the first colonisers of the surface. While this considers one possible method of infection, it does not account for the possibility of

S. epidermidis colonisation prior to the presence of host cells. For this reason, future work could involve altering the 3D culturing method to allow *S. epidermidis* to establish a biofilm on the Ti or TiAlV surfaces for 6 h or 24 h prior to the co-culture with the eukaryotic cells, or to initiate the culture both eukaryotic and prokaryotic cells at the same time. This would allow for further investigation into the cell adhesion to medical device surfaces and would also give further evidence to the expression of cytokines by macrophages and fibroblasts when co-cultured with established *S. epidermidis* biofilms. As the 3D culturing method developed in this study allowed only for the investigation of one host cell at a time, it did not characterise the interactions between immune cells and therefore, did not provide the full picture of host response as is often achieved with *in vivo* studies. To account for this, a further 3D culturing could be developed which would allow for the culture of both fibroblasts and macrophages or whole blood with *S. epidermidis* on the Ti or TiAlV surface in one cell culture well. This 3D culturing method could be adapted to further investigate a wealth of host infections and could reduce the requirement for *in vivo* mouse infection studies.

Due to difficulty extracting RNA from *S. epidermidis* 1457, only *S. epidermidis* 5179-R1 was utilised for both the RT-qPCR and cytokine analysis. *S. epidermidis* 1457 forms PIA-dependent biofilms, and the presence of such biofilms has been known to make RNA extractions more challenging (França *et al*., 2011). Therefore, the presence of PIA in the *S. epidermidis* 1457 biofilm might be responsible for the difficulty extracting RNA from this strain. For this reason, it would be beneficial to explore methods such as bead-beating or sonication to disrupt the polysaccharide and aid biofilm breakdown for successful RNA extraction (Zhang *et al*., 2003; França *et al*., 2012). As biofilm assay results showed decreased biofilm formation of *S. epidermidis* 1457 in MEM compared to TSB (Figure 3.5.), it could also be beneficial to determine the effect of cell culture media on *S. epidermidis* 1457 RNA extractions. A further limitation of the study was the use of only two *S. epidermidis* isolates, and thus the use of a wider selection of both PIA-dependent and PIA-independent strains could be considered for future work.

Cytokine analysis using the human proteome profiler arrays was limited to the semi-quantitative analysis of a generic subset of human cytokines. For deeper investigation into host cell responses, it would be beneficial to investigate the cytokines showing

interesting responses or cytokines specific to fibroblasts and macrophages using ELISAs which provide more sensitive, quantitative data. Due to time constraints and the availability of blood, RT-qPCR and cytokine analysis of mono- and co-cultures on whole blood coated Ti discs was only carried out one time, so it would be of interest to gain a larger collection of biological replicates in order to obtain higher reliability.

As discussed in the result chapters, 1BR.3.G fibroblasts on both Ti and TiAlV surfaces and THP-1 macrophages on TiAlV displayed detachment from the surfaces in the presence of *S. epidermidis* strains for 24 h. It would therefore be of interest to investigate this detachment. Firstly, as cutaneous damage and high IL-8 concentrations are known to induce focal adhesion kinase expression, this expression by fibroblasts should be explored under different culture conditions using ELISA as described by Ahmed *et al.* (2018). Secondly, to investigate whether *S. epidermidis* and Ti or TiAlV surfaces are having cytotoxic effects on fibroblasts or macrophages, a lactate dehydrogenase (LDH) cytotoxicity assay could be conducted and adapted from Matter *et al*, (2011). Finally, the presence and expression of *S. epidermidis* proteinases and proteinaceous factors could be identified through genomic analysis and RT-qPCR to identify their impact on host cell attachment in co-culture conditions.

In this study, the CLSM images did not differentiate between intracellular and extracellular *S. epidermidis* for co-cultures with macrophages or fibroblasts. To improve upon this, future work could involve the completion of a lysostaphin-daptomycin protection assay (Perez and Patel, 2018) or *Staphylococcus* invasion assay (Yokota *et al*., 2021) alongside the CLSM work to determine the proportion of bacteria within eukaryotic cells. Additionally, the co-transcription of genes expressed by macrophages or fibroblasts in co-culture with *S. epidermidis* could be investigated to further explore the interactions between host cells and bacteria during medical device infections.

Bibliography

Aderem, A. and Underhill, D.M., 1999. Mechanisms of phagocytosis in macrophages. *Annual review of immunology*, *17*(1), pp.593-623.

Ahmed, M., Ramos, T., Wieringa, P., Blitterswijk, C.V., Boer, J.D. and Moroni, L., 2018. Geometric constraints of endothelial cell migration on electrospun fibres. *Scientific reports*, *8*(1), pp.1-10.

Alhajj, M. and Goyal, A., 2021. Physiology, granulation tissue. In *StatPearls [Internet]*. StatPearls Publishing.

Akbari, A., Li, Y., Kilani, R.T. and Ghahary, A., 2012. Red blood cell lysate modulates the expression of extracellular matrix proteins in dermal fibroblasts. *Molecular and cellular biochemistry*, *370*(1), pp.79-88.

Alali, A.Q., Abdal-Hay, A., Gulati, K., Ivanovski, S., Fournier, B.P. and Lee, R.S., 2021. Influence of Bioinspired Lithium-Doped Titanium Implants on Gingival Fibroblast Bioactivity and Biofilm Adhesion. *Nanomaterials*, *11*(11), p.2799.

Anderson, J.M., 2000. Multinucleated giant cells. *Current opinion in hematology*, *7*(1), pp.40-47.

Anderson, J.M., Rodriguez, A. and Chang, D.T., 2008, April. Foreign body reaction to biomaterials. In *Seminars in immunology* (Vol. 20, No. 2, pp. 86-100). Academic Press.

Andrukhov, O., Behm, C., Blufstein, A., Wehner, C., Gahn, J., Pippenger, B., Wagner, R. and Rausch-Fan, X., 2020. Effect of implant surface material and roughness to the susceptibility of primary gingival fibroblasts to inflammatory stimuli. *Dental Materials*, *36*(6), pp.e194-e205.

Arrecubieta, C., Lee, M.H., Macey, A., Foster, T.J. and Lowy, F.D., 2007. SdrF, a Staphylococcus epidermidis surface protein, binds type I collagen. *Journal of Biological Chemistry*, *282*(26), pp.18767-18776.

Baker, B.S., Ovigne, J.M., Powles, A.V., Corcoran, S. and Fry, L., 2003. Normal keratinocytes express Toll-like receptors (TLRs) 1, 2 and 5: modulation of TLR expression in chronic plaque psoriasis. *British Journal of Dermatology*, *148*(4), pp.670-679.

Baggiolini, M. and Clark-Lewis, I., 1992. Interleukin-8, a chemotactic and inflammatory cytokine. *FEBS letters*, *307*(1), pp.97-101.

Barcia-Macay, M., Seral, C., Mingeot-Leclercq, M.P., Tulkens, P.M. and Van Bambeke, F., 2006. Pharmacodynamic evaluation of the intracellular activities of antibiotics against Staphylococcus aureus in a model of THP-1 macrophages. *Antimicrobial agents and chemotherapy*, *50*(3), pp.841-851.

Baroni, A., Perfetto, B., Ruocco, E. and Rossano, F., 1998. Lipoteichoic acid and protein-A from Staphylococcus aureus stimulate release of hepatocyte growth factor

(HGF) by human dermal fibroblasts. *Archives of dermatological research*, *290*(4), pp.211-214.

Barker, R.N., Erwig, L.P., Hill, K.S.K., Devine, A., Pearce, W.P. and Rees, A.J., 2002. Antigen presentation by macrophages is enhanced by the uptake of necrotic, but not apoptotic, cells. *Clinical & Experimental Immunology*, *127*(2), pp.220-225.

Bautista-Hernández, L.A., Gómez-Olivares, J.L., Buentello-Volante, B. and Bautista-de Lucio, V.M., 2017. Fibroblasts: the unknown sentinels eliciting immune responses against microorganisms. *European Journal of Microbiology and Immunology*, *7*(3), pp.151-157.

Becker, K., Heilmann, C. and Peters, G., 2014. Coagulase-negative staphylococci. *Clinical microbiology reviews*, *27*(4), pp.870-926.

Begun, J., Gaiani, J.M., Rohde, H., Mack, D., Calderwood, S.B., Ausubel, F.M. and Sifri, C.D., 2007. Staphylococcal biofilm exopolysaccharide protects against Caenorhabditis elegans immune defenses. *PLoS pathogens*, *3*(4), p.e57.

Berbari, E.F., Hanssen, A.D., Duffy, M.C., Steckelberg, J.M., Ilstrup, D.M., Harmsen, W.S. and Osmon, D.R., 1998. Risk factors for prosthetic joint infection: case-control study. *Clinical Infectious Diseases*, *27*(5), pp.1247-1254.

Bierbaum, G., Götz, F., Peschel, A., Kupke, T., van de Kamp, M. and Sahl, H.G., 1996. The biosynthesis of the lantibiotics epidermin, gallidermin, Pep5 and epilancin K7. *Antonie Van Leeuwenhoek*, *69*(2), pp.119-127.

Bitschar, K., Wolz, C., Krismer, B., Peschel, A. and Schittek, B., 2017. Keratinocytes as sensors and central players in the immune defense against Staphylococcus aureus in the skin. *Journal of dermatological science*, *87*(3), pp.215-220.

Burridge, K. and Chrzanowska-Wodnicka, M., 1996. Focal adhesions, contractility, and signaling. *Annual review of cell and developmental biology*, *12*(1), pp.463-519.

Cao, Y., Su, B., Chinnaraj, S., Jana, S., Bowen, L., Charlton, S., Duan, P., Jakubovics, N.S. and Chen, J., 2018. Nanostructured titanium surfaces exhibit recalcitrance towards Staphylococcus epidermidis biofilm formation. *Scientific reports*, *8*(1), pp.1-13.

Cerca, F., Andrade, F., França, Â., Andrade, E.B., Ribeiro, A., Almeida, A.A., Cerca, N., Pier, G., Azeredo, J. and Vilanova, M., 2011. Staphylococcus epidermidis biofilms with higher proportions of dormant bacteria induce a lower activation of murine macrophages. *Journal of medical microbiology*, *60*(12), pp.1717-1724.

Cerca, N., Jefferson, K.K., Oliveira, R., Pier, G.B. and Azeredo, J., 2006. Comparative antibody-mediated phagocytosis of Staphylococcus epidermidis cells grown in a biofilm or in the planktonic state. *Infection and immunity*, *74*(8), pp.4849-4855.

Cheung, G.Y., Rigby, K., Wang, R., Queck, S.Y., Braughton, K.R., Whitney, A.R., Teintze, M., DeLeo, F.R. and Otto, M., 2010. Staphylococcus epidermidis strategies to avoid killing by human neutrophils. *PLoS pathogens*, *6*(10), p.e1001133.

Christensen, G.J.M. and Brüggemann, H., 2014. Bacterial skin commensals and their role as host guardians. *Beneficial microbes*, *5*(2), pp.201-215

Christner, M., Franke, G.C., Schommer, N.N., Wendt, U., Wegert, K., Pehle, P., Kroll, G., Schulze, C., Buck, F., Mack, D. and Aepfelbacher, M., 2010. The giant extracellular matrix-binding protein of Staphylococcus epidermidis mediates biofilm accumulation and attachment to fibronectin. *Molecular microbiology*, *75*(1), pp.187-207.

Chrzanowska-Wodnicka, M. and Burridge, K., 1996. Rho-stimulated contractility drives the formation of stress fibers and focal adhesions. *The Journal of cell biology*, *133*(6), pp.1403-1415.

Chung, C.Y., Funamoto, S. and Firtel, R.A., 2001. Signaling pathways controlling cell polarity and chemotaxis. *Trends in biochemical sciences*, *26*(9), pp.557-566.

Clark, W.I., 1926. Guarding Against Infection. *The ANNALS of the American Academy of Political and Social Science*, *123*(1), pp.168-171.

Coates, M., Blanchard, S. and MacLeod, A.S., 2018. Innate antimicrobial immunity in the skin: A protective barrier against bacteria, viruses, and fungi. *PLoS pathogens*, *14*(12), p.e1007353.

Cogen, A.L., Yamasaki, K., Sanchez, K.M., Dorschner, R.A., Lai, Y., MacLeod, D.T., Torpey, J.W., Otto, M., Nizet, V., Kim, J.E. and Gallo, R.L., 2010a. Selective antimicrobial action is provided by phenol-soluble modulins derived from Staphylococcus epidermidis, a normal resident of the skin. *Journal of Investigative Dermatology*, *130*(1), pp.192-200.

Cogen, A.L., Yamasaki, K., Muto, J., Sanchez, K.M., Alexander, L.C., Tanios, J., Lai, Y., Kim, J.E., Nizet, V. and Gallo, R.L., 2010b. Staphylococcus epidermidis antimicrobial δ-toxin (phenol-soluble modulin-γ) cooperates with host antimicrobial peptides to kill group A Streptococcus. *PloS one*, *5*(1), p.e8557.

Collado, M.C., Rautava, S., Aakko, J., Isolauri, E. and Salminen, S., 2016. Human gut colonisation may be initiated in utero by distinct microbial communities in the placenta and amniotic fluid. *Scientific reports*, *6*, p.23129.

Comerford, I. and McColl, S.R., 2011. Mini-review series: focus on chemokines. *Immunology and cell biology*, *89*(2), pp.183-184.

Conlan, S., Mijares, L.A., Becker, J., Blakesley, R.W., Bouffard, G.G., Brooks, S., Coleman, H., Gupta, J., Gurson, N., Park, M. and Schmidt, B., 2012. Staphylococcus epidermidis pan-genome sequence analysis reveals diversity of skin commensal and hospital infection-associated isolates. *Genome biology*, *13*(7), pp.1-13.

Corradetti, B., Scarritt, M.E., Londono, R., Badylak, S.F. and Hildebrandt, M., 2017. *The immune response to implanted materials and devices.* Springer. Swizerland.

Correa-Gallegos, D., Jiang, D. and Rinkevich, Y., 2021. Fibroblasts as confederates of the immune system. *Immunological reviews*, *302*(1), pp.147-162.

Cruickshank, R., 1937. Staphyloeoagulase. *Journal of Pathology and Bacteriology*, *45*, pp.295-303.

Currey, H.L.F., 1962. Staphylococcal septicaemia and pyaemia. *South African Medical Journal*, *36*(12).

Dai, L., Yang, L., Parsons, C., Findlay, V.J., Molin, S. and Qin, Z., 2012. Staphylococcus epidermidis recovered from indwelling catheters exhibit enhanced biofilm dispersal and "self-renewal" through downregulation of agr. *BMC microbiology*, *12*(1), pp.1-9.

Dai, X., Wei, Y., Zhang, X., Meng, S., Mo, X., Liu, X., Deng, X., Zhang, L. and Deng, X., 2015. Attenuating immune response of macrophage by enhancing hydrophilicity of Ti surface. *Journal of Nanomaterials*, *2015*.

Damiati, L., Eales, M.G., Nobbs, A.H., Su, B., Tsimbouri, P.M., Salmeron-Sanchez, M. and Dalby, M.J., 2018. Impact of surface topography and coating on osteogenesis and bacterial attachment on titanium implants. *Journal of Tissue Engineering*, *9*, p.2041731418790694.

Darouiche, R.O., Dhir, A., Miller, A.J., Landon, G.C., Raad, I.I. and Musher, D.M., 1994. Vancomycin penetration into biofilm covering infected prostheses and effect on bacteria. *Journal of Infectious Diseases*, *170*(3), pp.720-723.

de Vor, L., Rooijakkers, S.H. and van Strijp, J.A., 2020. Staphylococci evade the innate immune response by disarming neutrophils and forming biofilms. *FEBS letters*, *594*(16), pp.2556-2569.

den Haan, J.M., Arens, R. and van Zelm, M.C., 2014. The activation of the adaptive immune system: cross-talk between antigen-presenting cells, T cells and B cells. *Immunology letters*, *162*(2), pp.103-112.

Dentener, M.A., Bazil, V., Von Asmuth, E.J., Ceska, M. and Buurman, W.A., 1993. Involvement of CD14 in lipopolysaccharide-induced tumor necrosis factor-alpha, IL-6 and IL-8 release by human monocytes and alveolar macrophages. *The Journal of Immunology*, *150*(7), pp.2885-2891.

Diamond, M.S., Staunton, D.E., Marlin, S.D. and Springer, T.A., 1991. Binding of the integrin Mac-1 (CD11b/CD18) to the third immunoglobulin-like domain of ICAM-1 (CD54) and its regulation by glycosylation. *Cell*, *65*(6), pp.961-971.

Diekema, D.J., Pfaller, M.A., Schmitz, F.J., Smayevsky, J., Bell, J., Jones, R.N., Beach, M. and SENTRY Participants Group, 2001. Survey of infections due to Staphylococcus species: frequency of occurrence and antimicrobial susceptibility of isolates collected in the United States, Canada, Latin America, Europe, and the Western Pacific region for the SENTRY Antimicrobial Surveillance Program, 1997–1999. *Clinical Infectious Diseases*, *32*(Supplement_2), pp.S114-S132.

Dobbins, J.J., Seligson, D. and Raff, M.J., 1988. Bacterial colonization of orthopedic fixation devices in the absence of clinical infection. *The Journal of infectious diseases*, *158*(1), pp.203-205.

Dominguez-Bello, M.G., Costello, E.K., Contreras, M., Magris, M., Hidalgo, G., Fierer, N. and Knight, R., 2010. Delivery mode shapes the acquisition and structure of the initial microbiota across multiple body habitats in newborns. *Proceedings of the National Academy of Sciences*, *107*(26), pp.11971-11975.

Driskell, R.R., Lichtenberger, B.M., Hoste, E., Kretzschmar, K., Simons, B.D., Charalambous, M., Ferron, S.R., Herault, Y., Pavlovic, G., Ferguson-Smith, A.C. and Watt, F.M., 2013. Distinct fibroblast lineages determine dermal architecture in skin development and repair. *Nature*, *504*(7479), pp.277-281.

Dunlevy, J.R. and Couchman, J.R., 1995. Interleukin-8 induces motile behavior and loss of focal adhesions in primary fibroblasts. *Journal of Cell Science*, *108*(1), pp.311-321.

Dunne, W.M., Mason, E.O. and Kaplan, S.L., 1993. Diffusion of rifampin and vancomycin through a Staphylococcus epidermidis biofilm. *Antimicrobial agents and chemotherapy*, *37*(12), pp.2522-2526.

Dustin, M.L., Rothlein, R., Bhan, A.K., Dinarello, C.A. and Springer, T.A., 1986. Induction by IL 1 and interferon-gamma: tissue distribution, biochemistry, and function of a natural adherence molecule (ICAM-1). *The Journal of Immunology*, *137*(1), pp.245-254.

Eckert, R.L. and Rorke, E.A., 1989. Molecular biology of keratinocyte differentiation. *Environmental health perspectives*, *80*, pp.109-116.

Elices, M.J., Osborn, L., Takada, Y., Crouse, C., Luhowskyj, S., Hemler, M.E. and Lobb, R.R., 1990. VCAM-1 on activated endothelium interacts with the leukocyte integrin VLA-4 at a site distinct from the VLA-4/fibronectin binding site. *Cell*, *60*(4), pp.577-584.

Engh, G.A., Dwyer, K.A. and Hanes, C.K., 1992. Polyethylene wear of metal-backed tibial components in total and unicompartmental knee prostheses. *The Journal of Bone and Joint Surgery. British volume*, *74*(1), pp.9-17.

Evans, C.A., Smith, W.M., Johnston, E.A. and Giblett, E.R., 1950. Bacterial flora of the normal human skin. *Journal of Investigative Dermatology*, *15*(4), pp.305-324.

Fernandes, I.R., Russo, F.B., Pignatari, G.C., Evangelinellis, M.M., Tavolari, S., Muotri, A.R. and Beltrão-Braga, P.C.B., 2016. Fibroblast sources: Where can we get them?. *Cytotechnology*, *68*(2), pp.223-228.

Fey, P.D. and Olson, M.E., 2010. Current concepts in biofilm formation of Staphylococcus epidermidis. *Future microbiology*, *5*(6), pp.917-933.

Fisk, A., 1940. The technique of the coagulase test for staphylococci. *British Journal of Experimental Pathology*, *21*(5), p.311.

Foster, T.J. and Höök, M., 1998. Surface protein adhesins of Staphylococcus aureus. *Trends in microbiology*, *6*(12), pp.484-488.

Fournier, B. and Philpott, D.J., 2005. Recognition of Staphylococcus aureus by the innate immune system. *Clinical microbiology reviews*, *18*(3), pp.521-540.

França, A., Melo, L.D. and Cerca, N., 2011. Comparison of RNA extraction methods from biofilm samples of Staphylococcus epidermidis. *BMC research notes*, *4*(1), pp.1-5.

França, A., Freitas, A.I., Henriques, A.F. and Cerca, N., 2012. Optimizing a qPCR gene expression quantification assay for S. epidermidis biofilms: a comparison between commercial kits and a customized protocol. *PloS one*, *7*(5), p.e37480.

Francois, P., Tu Quoc, P.H., Bisognano, C., Kelley, W.L., Lew, D.P., Schrenzel, J., Cramton, S.E., Götz, F. and Vaudaux, P., 2003. Lack of biofilm contribution to bacterial colonisation in an experimental model of foreign body infection by

Staphylococcus aureus and Staphylococcus epidermidis. *FEMS Immunology & Medical Microbiology*, *35*(2), pp.135-140.

Fredriksson, K., Lundahl, J., Palmberg, L., Romberger, D.J., Liu, X.D., Rennard, S.I. and Skold, C.M., 2003. Red blood cells stimulate human lung fibroblasts to secrete interleukin-8. *Inflammation*, *27*(2), pp.71-78.

Fredriksson, K., Liu, X.D., Lundahl, J., Klominek, J., Rennard, S.I. and Skold, C.M., 2006. Red blood cells increase secretion of matrix metalloproteinases from human lung fibroblasts in vitro. *American Journal of Physiology-Lung Cellular and Molecular Physiology*, *290*(2), pp.L326-L333.

Fritz, E.A., Glant, T.T., Vermes, C., Jacobs, J.J. and Roebuck, K.A., 2002. Titanium particles induce the immediate early stress responsive chemokines IL-8 and MCP-1 in osteoblasts. *Journal of orthopaedic research*, *20*(3), pp.490-498.

Gaga, M., Ong, Y.E., Benyahia, F., Aizen, M., Barkans, J. and Kay, A.B., 2008. Skin reactivity and local cell recruitment in human atopic and nonatopic subjects by CCL2/MCP-1 and CCL3/MIP-1α. *Allergy*, *63*(6), pp.703-711.

Gallo, R.L. and Nakatsuji, T., 2011. Microbial symbiosis with the innate immune defense system of the skin. *Journal of Investigative Dermatology*, *131*(10), pp.1974-1980.

Ganapathy, P., Manivasagam, G., Rajamanickam, A. and Natarajan, A., 2015. Wear studies on plasma-sprayed Al2O3 and 8mole% of Yttrium-stabilized ZrO2 composite coating on biomedical Ti-6Al-4V alloy for orthopedic joint application. *International Journal of Nanomedicine*, *10*(Suppl 1), p.213.

Gao, Z., Tseng, C.H., Pei, Z. and Blaser, M.J., 2007. Molecular analysis of human forearm superficial skin bacterial biota. *Proceedings of the National Academy of Sciences*, *104*(8), pp.2927-2932.

Gasteiger, G., D'osualdo, A., Schubert, D.A., Weber, A., Bruscia, E.M. and Hartl, D., 2017. Cellular innate immunity: an old game with new players. *Journal of innate immunity*, *9*(2), pp.111-125.

Geetha, M., Singh, A.K., Asokamani, R. and Gogia, A.K., 2009. Ti based biomaterials, the ultimate choice for orthopaedic implants–a review. *Progress in materials science*, *54*(3), pp.397-425.

Geissmann, F., Manz, M.G., Jung, S., Sieweke, M.H., Merad, M. and Ley, K., 2010. Development of monocytes, macrophages, and dendritic cells. *Science*, *327*(5966), pp.656-661.

Georgel, P., Crozat, K., Lauth, X., Makrantonaki, E., Seltmann, H., Sovath, S., Hoebe, K., Du, X., Rutschmann, S., Jiang, Z. and Bigby, T., 2005. A toll-like receptor 2-responsive lipid effector pathway protects mammals against skin infections with gram-positive bacteria. *Infection and immunity*, *73*(8), pp.4512-4521.

Gerke, C., Kraft, A., Süßmuth, R., Schweitzer, O. and Götz, F., 1998. Characterization of theN-Acetylglucosaminyltransferase Activity Involved in the Biosynthesis of the Staphylococcus epidermidisPolysaccharide Intercellular Adhesin. *Journal of Biological Chemistry*, *273*(29), pp.18586-18593.

Gillespie, S. and Hawkey, P.M. eds., 2006. *Principles and practice of clinical bacteriology*. John Wiley & Sons.

Girardin, S.E., Boneca, I.G., Viala, J., Chamaillard, M., Labigne, A., Thomas, G., Philpott, D.J. and Sansonetti, P.J., 2003. Nod2 is a general sensor of peptidoglycan through muramyl dipeptide (MDP) detection. *Journal of Biological Chemistry*, *278*(11), pp.8869-8872.

Gomes, F., Teixeira, P., Cerca, N., Ceri, H. and Oliveira, R., 2011. Virulence gene expression by Staphylococcus epidermidis biofilm cells exposed to antibiotics. *Microbial Drug Resistance*, *17*(2), pp.191-196.

Götz, F., 2002. Staphylococcus and biofilms. *Molecular microbiology*, *43*(6), pp.1367-1378.

Götz, F., Verheij, H.M. and Rosenstein, R., 1998. Staphylococcal lipases: molecular characterisation, secretion, and processing. *Chemistry and physics of lipids*, *93*(1-2), pp.15-25.

Greenberg, S. and Grinstein, S., 2002. Phagocytosis and innate immunity. *Current opinion in immunology*, *14*(1), pp.136-145.

Grice, E.A., Kong, H.H., Conlan, S., Deming, C.B., Davis, J., Young, A.C., Bouffard, G.G., Blakesley, R.W., Murray, P.R., Green, E.D. and Turner, M.L., 2009. Topographical and temporal diversity of the human skin microbiome. *science*, *324*(5931), pp.1190-1192.

Gristina, A.G., Naylor, P. and Myrvik, Q., 1988. Infections from biomaterials and implants: a race for the surface. *Medical progress through technology*, *14*(3-4), pp.205-224.

Guillemot, F., Prima, F., Bareille, R., Gordin, D., Gloriant, T., Porté-Durrieu, M.C., Ansel, D. and Baquey, C., 2004. Design of new titanium alloys for orthopaedic applications. *Medical and Biological Engineering and Computing*, *42*(1), pp.137-141.

Gurtner, G.C., Werner, S., Barrandon, Y. and Longaker, M.T., 2008. Wound repair and regeneration. *Nature*, *453*(7193), pp.314-321.

Gushiken, L.F.S., Beserra, F.P., Bastos, J.K., Jackson, C.J. and Pellizzon, C.H., 2021. Cutaneous wound healing: An update from physiopathology to current therapies. *Life*, *11*(7), p.665.

Hamels, S., Gala, J.L., Dufour, S., Vannuffel, P., Zammatteo, N. and Remacle, J., 2001. Consensus PCR and microarray for diagnosis of the genus Staphylococcus, species, and methicillin resistance. *Biotechniques*, *31*(6), pp.1364-1372.

Hamlet, S., Alfarsi, M., George, R. and Ivanovski, S., 2012. The effect of hydrophilic titanium surface modification on macrophage inflammatory cytokine gene expression. *Clinical oral implants research*, *23*(5), pp.584-590.

Hamlet, S.M. and Ivanovski, S., 2017. Inflammatory cytokine response to titanium surface chemistry and topography. In *The Immune Response to Implanted Materials and Devices* (pp. 151-167). Springer, Cham.

Hammer, B.K. and Bassler, B.L., 2003. Quorum sensing controls biofilm formation in Vibrio cholerae. *Molecular microbiology*, *50*(1), pp.101-104.

Hanssen, A.D. and Rand, J.A., 1998. Evaluation and treatment of infection at the site of a total hip or knee arthroplasty. *Journal of Bone and Joint Surgery*, *80*(6), p.910.

Harris, L.G. and Richards, R.G., 2004. Staphylococcus aureus adhesion to different treated titanium surfaces. *Journal of Materials Science: Materials in Medicine*, *15*(4), pp.311-314.

Harris, L.G. and Richards, R.G., 2006. Staphylococci and implant surfaces: a review. *Injury*, *37*(2), pp.S3-S14.

Harris, L.G., Murray, S., Pascoe, B., Bray, J., Meric, G., Magerios, L., Wilkinson, T.S., Jeeves, R., Rohde, H., Schwarz, S. and De Lencastre, H., 2016. Biofilm morphotypes and population structure among Staphylococcus epidermidis from commensal and clinical samples. *PLoS One*, *11*(3), p.e0151240.

Harris, L.G., Dudley, E., Rohde, H., Frommelt, L., Siemssen, N., Wilkinson, T.S. and Mack, D., 2017. Limitations in the use of PSMγ, agr, RNAIII, and biofilm formation as biomarkers to define invasive Staphylococcus epidermidis from chronic biomedical device-associated infections. *International Journal of Medical Microbiology*, *307*(7), pp.382-387.

Hart, R. and Greaves, D.R., 2010. Chemerin contributes to inflammation by promoting macrophage adhesion to VCAM-1 and fibronectin through clustering of VLA-4 and VLA-5. *The Journal of Immunology*, *185*(6), pp.3728-3739.

Hartford, O., O'Brien, L., Schofield, K., Wells, J. and Foster, T.J., 2001. The Fbe (SdrG) protein of Staphylococcus epidermidis HB promotes bacterial adherence to fibrinogen. *Microbiology*, *147*(9), pp.2545-2552.

Haydar, H.J., Al-Deen, J., AbidAli, A.K. and Mahmoud, A.A., 2021, August. Improved performance of Ti6Al4V alloy in Biomedical applications-Review. In *Journal of Physics: Conference Series* (Vol. 1973, No. 1, p. 012146). IOP Publishing.

Heilmann, C., Schweitzer, O., Gerke, C., Vanittanakom, N., Mack, D. and Götz, F., 1996. Molecular basis of intercellular adhesion in the biofilm-forming Staphylococcus epidermidis. *Molecular microbiology*, *20*(5), pp.1083-1091.

Heilmann, C., Hussain, M., Peters, G. and Götz, F., 1997. Evidence for autolysin-mediated primary attachment of Staphylococcus epidermidis to a polystyrene surface. *Molecular microbiology*, *24*(5), pp.1013-1024.

Heilmann, C., Thumm, G., Chhatwal, G.S., Hartleib, J., Uekötter, A. and Peters, G., 2003. Identification and characterization of a novel autolysin (Aae) with adhesive properties from Staphylococcus epidermidis. *Microbiology*, *149*(10), pp.2769-2778.

Hermanowicz, S.W., 2001. A simple 2D biofilm model yields a variety of morphological features. *Mathematical biosciences*, *169*(1), pp.1-14.

Hernandez-Pando, R., Bornstein, Q.L., Aguilar Leon, D., Orozco, E.H., Madrigal, V.K. and Martinez Cordero, E., 2000. Inflammatory cytokine production by immunological and foreign body multinucleated giant cells. *Immunology*, *100*(3), pp.352-358.

Hoekman, P., Van de Perre, P., Nelissen, J., Kwisanga, B., Bogaerts, J. and Kanyangabo, F., 1991. Increased frequency of infection after open reduction of

fractures in patients who are seropositive for human immunodeficiency virus. *The Journal of Bone and Joint surgery. American Volume*, *73*(5), pp.675-679.

Hoffmann, M. and Schwarz, U.S., 2013. A kinetic model for RNA-interference of focal adhesions. *BMC Systems Biology*, *7*(1), pp.1-18.

Hudetz, D., Hudetz, S.U., Harris, L.G., Luginbühl, R., Friederich, N.F. and Landmann, R., 2008. Weak effect of metal type and ica genes on staphylococcal infection of titanium and stainless steel implants. *Clinical microbiology and infection*, *14*(12), pp.1135-1145.

Italiani, P. and Boraschi, D., 2014. From monocytes to M1/M2 macrophages: phenotypical vs. functional differentiation. *Frontiers in immunology*, *5*, p.514.

Iwase, T., Uehara, Y., Shinji, H., Tajima, A., Seo, H., Takada, K., Agata, T. and Mizunoe, Y., 2010. Staphylococcus epidermidis Esp inhibits Staphylococcus aureus biofilm formation and nasal colonization. *Nature*, *465*(7296), pp.346-349.

Izzard, C.S. and Lochner, L.R., 1976. Cell-to-substrate contacts in living fibroblasts: an interference reflexion study with an evaluation of the technique. *Journal of cell science*, *21*(1), pp.129-159.

Janeway Jr, C.A., Travers, P., Walport, M. and Shlomchik, M.J., 2001. The complement system and innate immunity. In *Immunobiology: The Immune System in Health and Disease. 5th edition*. Garland Science.

Jang, I.T., Yang, M., Kim, H.J. and Park, J.K., 2020. Novel Cytoplasmic Bacteriocin Compounds Derived from Staphylococcus epidermidis Selectively Kill Staphylococcus aureus, Including Methicillin-Resistant Staphylococcus aureus (MRSA). *Pathogens*, *9*(2), p.87.

Jones, K.J., Perris, A.D., Vernallis, A.B., Worthington, T., Lambert, P.A. and Elliott, T.S., 2005. Induction of inflammatory cytokines and nitric oxide in J774. 2 cells and murine macrophages by lipoteichoic acid and related cell wall antigens from Staphylococcus epidermidis. *Journal of medical microbiology*, *54*(4), pp.315-321.

Kaiko, G.E., Horvat, J.C., Beagley, K.W. and Hansbro, P.M., 2008. Immunological decision-making: how does the immune system decide to mount a helper T-cell response?. *Immunology*, *123*(3), pp.326-338.

Kallala, R.F., Vanhegan, I.S., Ibrahim, M.S., Sarmah, S. and Haddad, F.S., 2015. Financial analysis of revision knee surgery based on NHS tariffs and hospital costs: does it pay to provide a revision service?. *The bone & joint journal*, *97*(2), pp.197-201.

Kalluri, R. and Zeisberg, M., 2006. Fibroblasts in cancer. *Nature Reviews Cancer*, *6*(5), pp.392-401.

Kaplan, J.B., Ragunath, C., Velliyagounder, K., Fine, D.H. and Ramasubbu, N., 2004. Enzymatic detachment of Staphylococcus epidermidis biofilms. *Antimicrobial agents and chemotherapy*, *48*(7), pp.2633-2636.

Kasraie, S., Niebuhr, M. and Werfel, T., 2010. Interleukin (IL)-31 induces pro-inflammatory cytokines in human monocytes and macrophages following stimulation with staphylococcal exotoxins. *Allergy*, *65*(6), pp.712-721.

Kaufman, A.M., Alabre, C.I., Rubash, H.E. and Shanbhag, A.S., 2008. Human macrophage response to UHMWPE, TiAlV, CoCr, and alumina particles: analysis of multiple cytokines using protein arrays. *Journal of biomedical materials research Part A*, *84*(2), pp.464-474.

Kaverina, I., Krylyshkina, O. and Small, J.V., 2002. Regulation of substrate adhesion dynamics during cell motility. *The international journal of biochemistry & cell biology*, *34*(7), pp.746-761.

Kirker, K.R., James, G.A., Fleckman, P., Olerud, J.E. and Stewart, P.S., 2012. Differential effects of planktonic and biofilm MRSA on human fibroblasts. *Wound Repair and Regeneration*, *20*(2), pp.253-261.

Khoury, A.E., Lam, K., Ellis, B. and Costerton, J.W., 1992. Prevention and control of bacterial infections associated with medical devices. *ASAIO journal (American Society for Artificial Internal Organs: 1992)*, *38*(3), pp.M174-8.

Kloos, W.E. and Schleifer, K.H., 1975. Simplified scheme for routine identification of human Staphylococcus species. *Journal of clinical Microbiology*, *1*(1), pp.82-88.

Knafl, D., Tobudic, S., Cheng, S.C., Bellamy, D.R. and Thalhammer, F., 2017. Dalbavancin reduces biofilms of methicillin-resistant Staphylococcus aureus (MRSA) and methicillin-resistant Staphylococcus epidermidis (MRSE). *European Journal of Clinical Microbiology & Infectious Diseases*, *36*(4), pp.677-680.

Knobloch, J.K.M., Jäger, S., Horstkotte, M.A., Rohde, H. and Mack, D., 2004. RsbU-dependent regulation of Staphylococcus epidermidis biofilm formation is mediated via the alternative sigma factor σB by repression of the negative regulator gene icaR. *Infection and immunity*, *72*(7), pp.3838-3848.

Kocianova, S., Vuong, C., Yao, Y., Voyich, J.M., Fischer, E.R., DeLeo, F.R. and Otto, M., 2005. Key role of poly-γ-DL-glutamic acid in immune evasion and virulence of Staphylococcus epidermidis. *The Journal of clinical investigation*, *115*(3), pp.688-694.

Kong, H.H., 2011. Skin microbiome: genomics-based insights into the diversity and role of skin microbes. *Trends in molecular medicine*, *17*(6), pp.320-328.

Kozitskaya, S., Cho, S.H., Dietrich, K., Marre, R., Naber, K. and Ziebuhr, W., 2004. The bacterial insertion sequence element IS256 occurs preferentially in nosocomial Staphylococcus epidermidis isolates: association with biofilm formation and resistance to aminoglycosides. *Infection and immunity*, *72*(2), pp.1210-1215.

Kristian, S.A., Birkenstock, T.A., Sauder, U., Mack, D., Götz, F. and Landmann, R., 2008. Biofilm formation induces C3a release and protects Staphylococcus epidermidis from IgG and complement deposition and from neutrophil-dependent killing. *The Journal of infectious diseases*, *197*(7), pp.1028-1035.

Kuehl, R., Brunetto, P.S., Woischnig, A.K., Varisco, M., Rajacic, Z., Vosbeck, J., Terracciano, L., Fromm, K.M. and Khanna, N., 2016. Preventing implant-associated infections by silver coating. *Antimicrobial agents and chemotherapy*, *60*(4), pp.2467-2475.

Kunrath, M.F., Monteiro, M.S., Gupta, S., Hubler, R. and de Oliveira, S.D., 2020. Influence of titanium and zirconia modified surfaces for rapid healing on adhesion and biofilm formation of Staphylococcus epidermidis. *Archives of Oral Biology*, *117*, p.104824.

Kurtz, S.M., Lau, E., Watson, H., Schmier, J.K. and Parvizi, J., 2012. Economic burden of periprosthetic joint infection in the United States. *The Journal of arthroplasty*, *27*(8), pp.61-65.

Lai, Y., Villaruz, A.E., Li, M., Cha, D.J., Sturdevant, D.E. and Otto, M., 2007. The human anionic antimicrobial peptide dermcidin induces proteolytic defence mechanisms in staphylococci. *Molecular microbiology*, *63*(2), pp.497-506.

Lai, Y., Cogen, A.L., Radek, K.A., Park, H.J., MacLeod, D.T., Leichtle, A., Ryan, A.F., Di Nardo, A. and Gallo, R.L., 2010. Activation of TLR2 by a small molecule produced by Staphylococcus epidermidis increases antimicrobial defense against bacterial skin infections. *Journal of Investigative Dermatology*, *130*(9), pp.2211-2221.

Lai, Y., Di Nardo, A., Nakatsuji, T., Leichtle, A., Yang, Y., Cogen, A.L., Wu, Z.R., Hooper, L.V., Schmidt, R.R., Von Aulock, S. and Radek, K.A., 2009. Commensal bacteria regulate Toll-like receptor 3–dependent inflammation after skin injury. *Nature medicine*, *15*(12), p.1377.

Lamers, R.P., Muthukrishnan, G., Castoe, T.A., Tafur, S., Cole, A.M. and Parkinson, C.L., 2012. Phylogenetic relationships among Staphylococcus species and refinement of cluster groups based on multilocus data. *BMC evolutionary biology*, *12*(1), p.171.

Le, K.Y., Park, M.D. and Otto, M., 2018. Immune evasion mechanisms of Staphylococcus epidermidis biofilm infection. *Frontiers in microbiology*, *9*, p.359.

Le, K.Y., Villaruz, A.E., Zheng, Y., He, L., Fisher, E.L., Nguyen, T.H., Ho, T.V., Yeh, A.J., Joo, H.S., Cheung, G.Y. and Otto, M., 2019. Role of phenol-soluble modulins in Staphylococcus epidermidis biofilm formation and infection of indwelling medical devices. *Journal of molecular biology*, *431*(16), pp.3015-3027.

Lenguerrand, E., Whitehouse, M.R., Beswick, A.D., Jones, S.A., Porter, M.L. and Blom*, A.W., 2017b. Revision for prosthetic joint infection following hip arthroplasty: Evidence from the National Joint Registry. *Bone & joint research*, *6*(6), pp.391-398.

Lenguerrand, E., Whitehouse, M.R., Beswick, A.D., Toms, A.D., Porter, M.L. and Blom, A.W., 2017a. Description of the rates, trends and surgical burden associated with revision for prosthetic joint infection following primary and revision knee replacements in England and Wales: an analysis of the National Joint Registry for England, Wales, Northern Ireland and the Isle of Man. *BMJ open*, *7*(7), p.e014056.

Li, Y., Schutte, R.J., Abu-Shakra, A. and Reichert, W.M., 2005. Protein array method for assessing in vitro biomaterial-induced cytokine expression. *Biomaterials*, *26*(10), pp.1081-1085.

device-associated biofilms. *Coatings*, *11*(3), p.294.

Licitra, G., 2013. Etymologia: Staphylococcus. *Emerging Infectious Diseases*, *19*(9), p.1553.

Linnes, J.C., Ma, H. and Bryers, J.D., 2013. Giant extracellular matrix binding protein expression in Staphylococcus epidermidis is regulated by biofilm formation and osmotic pressure. *Current microbiology*, *66*(6), pp.627-633.

Livak, K.J. and Schmittgen, T.D., 2001. Analysis of relative gene expression data using real-time quantitative PCR and the 2− ΔΔCT method. *methods*, *25*(4), pp.402-408.

Lorenzetti, M., Dogša, I., Stošicki, T., Stopar, D., Kalin, M., Kobe, S. and Novak, S., 2015. The influence of surface modification on bacterial adhesion to titanium-based substrates. *ACS applied materials & interfaces*, *7*(3), pp.1644-1651.

Lund, M.E., To, J., O'Brien, B.A. and Donnelly, S., 2016. The choice of phorbol 12-myristate 13-acetate differentiation protocol influences the response of THP-1 macrophages to a pro-inflammatory stimulus. *Journal of immunological methods*, *430*, pp.64-70.

Ma, J., Chen, T., Mandelin, J., Ceponis, A., Miller, N.E., Hukkanen, M., Ma, G.F. and Konttinen, Y.T., 2003. Regulation of macrophage activation. *Cellular and Molecular Life Sciences CMLS*, *60*(11), pp.2334-2346.

Ma, Y., Chen, M., Jones, J.E., Ritts, A.C., Yu, Q. and Sun, H., 2012. Inhibition of Staphylococcus epidermidis biofilm by trimethylsilane plasma coating. *Antimicrobial agents and chemotherapy*, *56*(11), pp.5923-5937.

Ma, R., Qiu, S., Jiang, Q., Sun, H., Xue, T., Cai, G. and Sun, B., 2017. AI-2 quorum sensing negatively regulates rbf expression and biofilm formation in Staphylococcus aureus. *International Journal of Medical Microbiology*, *307*(4-5), pp.257-267.

Mack, D., Siemssen, N. and Laufs, R., 1992. Parallel induction by glucose of adherence and a polysaccharide antigen specific for plastic-adherent Staphylococcus epidermidis: evidence for functional relation to intercellular adhesion. *Infection and immunity*, *60*(5), pp.2048-2057.

Mack, D., Fischer, W., Krokotsch, A., Leopold, K., Hartmann, R., Egge, H. and Laufs, R., 1996. The intercellular adhesin involved in biofilm accumulation of Staphylococcus epidermidis is a linear beta-1, 6-linked glucosaminoglycan: purification and structural analysis. *Journal of bacteriology*, *178*(1), pp.175-183.

Mack, D., Riedewald, J., Rohde, H., Magnus, T., Feucht, H.H., Elsner, H.A., Laufs, R. and Rupp, M.E., 1999. Essential functional role of the polysaccharide intercellular adhesin of Staphylococcus epidermidis in hemagglutination. *Infection and Immunity*, *67*(2), pp.1004-1008.

Mack, D., Davies, A.P., Harris, L.G., Rohde, H., Horstkotte, M.A. and Knobloch, J.K.M., 2007. Microbial interactions in Staphylococcus epidermidis biofilms. *Analytical and Bioanalytical Chemistry*, *387*(2), pp.399-408.

Matter, L.B., Barbieri, N.L., Nordhoff, M., Ewers, C. and Horn, F., 2011. Avian pathogenic Escherichia coli MT78 invades chicken fibroblasts. *Veterinary microbiology*, *148*(1), pp.51-59.

Marang-Van de Mheen, P.J., Bragan Turner, E., Liew, S., Mutalima, N., Tran, T., Rasmussen, S., Nelissen, R.G. and Gordon, A., 2017. Variation in Prosthetic Joint Infection and treatment strategies during 4.5 years of follow-up after primary joint

arthroplasty using administrative data of 41397 patients across Australian, European and United States hospitals. *BMC musculoskeletal disorders*, *18*(1), pp.1-8.

Markhoff, J., Krogull, M., Schulze, C., Rotsch, C., Hunger, S. and Bader, R., 2017. Biocompatibility and inflammatory potential of titanium alloys cultivated with human osteoblasts, fibroblasts and macrophages. *Materials*, *10*(1), p.52.

Marlin, S.D. and Springer, T.A., 1987. Purified intercellular adhesion molecule-1 (ICAM-1) is a ligand for lymphocyte function-associated antigen 1 (LFA-1). *Cell*, *51*(5), pp.813-819.

Mass, E., Ballesteros, I., Farlik, M., Halbritter, F., Günther, P., Crozet, L., Jacome-Galarza, C.E., Händler, K., Klughammer, J., Kobayashi, Y. and Gomez-Perdiguero, E., 2016. Specification of tissue-resident macrophages during organogenesis. *Science*, *353*(6304), p.aaf4238.

McAnulty, R.J., 2007. Fibroblasts and myofibroblasts: their source, function and role in disease. *The international journal of biochemistry & cell biology*, *39*(4), pp.666-671.

McCann, M.T., Gilmore, B.F. and Gorman, S.P., 2008. Staphylococcus epidermidis device-related infections: pathogenesis and clinical management. *Journal of Pharmacy and Pharmacology*, *60*(12), pp.1551-1571.

McCrea, K.W., Hartford, O., Davis, S., Eidhin, D.N., Lina, G., Speziale, P., Foster, T.J. and Höök, M., 2000. The serine-aspartate repeat (Sdr) protein family in Staphylococcus epidermidisThe GenBank accession numbers for the sequences determined in this work are AF245041 (sdrF), AF245042 (sdrG) and AF245043 (sdrH). *Microbiology*, *146*(7), pp.1535-1546.

Mehlin, C., Headley, C.M. and Klebanoff, S.J., 1999. An inflammatory polypeptide complex from Staphylococcus epidermidis: isolation and characterization. *The Journal of experimental medicine*, *189*(6), pp.907-918.

Metschnikoff, E., 1887. Ueber den Kampf der Zellen gegen Erysipel-kokken. *Archiv für pathologische Anatomie und Physiologie und für klinische Medicin*, *107*(2), pp.209-249.

Metsemakers, W.J., Kuehl, R., Moriarty, T.F., Richards, R.G., Verhofstad, M.H.J., Borens, O., Kates, S. and Morgenstern, M., 2018. Infection after fracture fixation: current surgical and microbiological concepts. *Injury*, *49*(3), pp.511-522.

Mitra, S.K., Hanson, D.A. and Schlaepfer, D.D., 2005. Focal adhesion kinase: in command and control of cell motility. *Nature reviews Molecular cell biology*, *6*(1), pp.56-68.

Mizel, S.B., West, A.P. and Hantgan, R.R., 2003. Identification of a sequence in human toll-like receptor 5 required for the binding of Gram-negative flagellin. *Journal of Biological Chemistry*, *278*(26), pp.23624-23629.

Monzón, M., Oteiza, C., Leiva, J., Lamata, M. and Amorena, B., 2002. Biofilm testing of Staphylococcus epidermidis clinical isolates: low performance of vancomycin in relation to other antibiotics. *Diagnostic microbiology and infectious disease*, *44*(4), pp.319-324.

Mosser, D.M., 2003. The many faces of macrophage activation. *Journal of leukocyte biology*, *73*(2), pp.209-212.

Mizuuchi, K., O'Dea, M.H. and Gellert, M., 1978. DNA gyrase: subunit structure and ATPase activity of the purified enzyme. *Proceedings of the National Academy of Sciences*, *75*(12), pp.5960-5963.

Nakatsuji, T., Kao, M.C., Zhang, L., Zouboulis, C.C., Gallo, R.L. and Huang, C.M., 2010. Sebum free fatty acids enhance the innate immune defense of human sebocytes by upregulating β-defensin-2 expression. *Journal of Investigative Dermatology*, *130*(4), pp.985-994.

Nasaj, M., Hosseini, S.M., Saeidi, Z., Dehbashi, S., Tahmasebi, H. and Arabestani, M.R., 2021. Analysis of phenotypic and genotypic methods for determining the biofilm-forming abilities of CoNS isolates: Association with hemolysin production and the bacterial insertion sequence elements IS256/257. *Gene Reports*, *23*, p.101036.

Navegantes, K.C., de Souza Gomes, R., Pereira, P.A.T., Czaikoski, P.G., Azevedo, C.H.M. and Monteiro, M.C., 2017. Immune modulation of some autoimmune diseases: the critical role of macrophages and neutrophils in the innate and adaptive immunity. *Journal of translational medicine*, *15*(1), pp.1-21.

Nguyen, T.H., Park, M.D. and Otto, M., 2017. Host response to Staphylococcus epidermidis colonization and infections. *Frontiers in cellular and infection microbiology*, *7*, p.90.

Nich, C., Takakubo, Y., Pajarinen, J., Ainola, M., Salem, A., Sillat, T., Rao, A.J., Raska, M., Tamaki, Y., Takagi, M. and Konttinen, Y.T., 2013. Macrophages—key cells in the response to wear debris from joint replacements. *Journal of biomedical materials research Part A*, *101*(10), pp.3033-3045.

Nickel, J.C., Ruseska, I., Wright, J.B. and Costerton, J.W., 1985. Tobramycin resistance of Pseudomonas aeruginosa cells growing as a biofilm on urinary catheter material. *Antimicrobial agents and chemotherapy*, *27*(4), pp.619-624.

Nilsson, M., Frykberg, L., Flock, J.I., Pei, L., Lindberg, M. and Guss, B., 1998. A fibrinogen-binding protein ofStaphylococcus epidermidis. *Infection and immunity*, *66*(6), pp.2666-2673.

Nostro, A., Roccaro, A.S., Bisignano, G., Marino, A., Cannatelli, M.A., Pizzimenti, F.C., Cioni, P.L., Procopio, F. and Blanco, A.R., 2007. Effects of oregano, carvacrol and thymol on Staphylococcus aureus and Staphylococcus epidermidis biofilms. *Journal of medical microbiology*, *56*(4), pp.519-523.

O'Gara, J.P., 2007. ica and beyond: biofilm mechanisms and regulation in Staphylococcus epidermidis and Staphylococcus aureus. *FEMS microbiology letters*, *270*(2), pp.179-188.

Ogston, A., Witte, W., 1984. On abscesses. *Reviews of Infectious Diseases*, *6*(1), pp.122-128.

Ohradanova-Repic, A., Machacek, C., Fischer, M.B. and Stockinger, H., 2016. Differentiation of human monocytes and derived subsets of macrophages and dendritic cells by the HLDA10 monoclonal antibody panel. *Clinical & translational immunology*, *5*(1), p.e55.

Oliveira, V., Chaves, R.R., Bertazzoli, R. and Caram, R., 1998. Preparation and characterization of Ti-Al-Nb alloys for orthopedic implants. *Brazilian Journal of Chemical Engineering*, *15*, pp.326-333.

Oliveira, W.F., Silva, P.M.S., Silva, R.C.S., Silva, G.M.M., Machado, G., Coelho, L.C.B.B. and Correia, M.T.S., 2018. Staphylococcus aureus and Staphylococcus epidermidis infections on implants. *Journal of Hospital Infection*, *98*(2), pp.111-117.

Olson, M.E., Todd, D.A., Schaeffer, C.R., Paharik, A.E., Van Dyke, M.J., Büttner, H., Dunman, P.M., Rohde, H., Cech, N.B., Fey, P.D. and Horswill, A.R., 2014. Staphylococcus epidermidis agr quorum-sensing system: signal identification, cross talk, and importance in colonization. *Journal of bacteriology*, *196*(19), pp.3482-3493.

Opal, S.M. and DePalo, V.A., 2000. Anti-inflammatory cytokines. *Chest*, *117*(4), pp.1162-1172.

Orekhov, A.N., Orekhova, V.A., Nikiforov, N.G., Myasoedova, V.A., Grechko, A.V., Romanenko, E.B., Zhang, D. and Chistiakov, D.A., 2019. Monocyte differentiation and macrophage polarization. *Vessel Plus*, *3*, p.10.

Otto, M., 2009. Staphylococcus epidermidis—the'accidental'pathogen. *Nature reviews microbiology*, *7*(8), pp.555-567.

Otto, M., 2010. Staphylococcus colonization of the skin and antimicrobial peptides. *Expert review of dermatology*, *5*(2), pp.183-195.

Otto, M., Süßmuth, R., Vuong, C., Jung, G. and Götz, F., 1999. Inhibition of virulence factor expression in Staphylococcus aureus by the Staphylococcus epidermidis agr pheromone and derivatives. *FEBS letters*, *450*(3), pp.257-262.

Paital, S.R. and Dahotre, N.B., 2009. Calcium phosphate coatings for bio-implant applications: Materials, performance factors, and methodologies. *Materials Science and Engineering: R: Reports*, *66*(1-3), pp.1-70.

Palkowitz, A.L., Tuna, T., Bishti, S., Böke, F., Steinke, N., Müller-Newen, G., Wolfart, S. and Fischer, H., 2021. Biofunctionalization of Dental Abutment Surfaces by Crosslinked ECM Proteins Strongly Enhances Adhesion and Proliferation of Gingival Fibroblasts. *Advanced Healthcare Materials*, *10*(10), p.2100132.

Pang, G., Couch, L., Batey, R., Clancy, R. and Cripps, A., 1994. GM-CSF, IL-1α, IL-β, IL-6, IL-8, IL-10, ICAM-1 and VCAM-1 gene expression and cytokine production in human duodenal fibroblasts stimulated with lipopolysaccharide, IL-1α and TNF-α. *Clinical & Experimental Immunology*, *96*(3), pp.437-443.

Patti, J.M., Allen, B.L., McGavin, M.J. and Höök, M., 1994. MSCRAMM-mediated adherence of microorganisms to host tissues. *Annual Reviews in Microbiology*, *48*(1), pp.585-617.

Pennen, Allgöwer, M., Klaue, K., Küng, R., Mast, J., Matter, P., Monney, G., Pohler, O., Rahn, B.A., Rüedi, T., Schatzker, J., Steinemann, S., Brunner, H., Tepic, M., Weber, B.C., Z'Brun, P., Burch, H.B., Cordey, J., Ganz, R., Gasser, B., Gerber, H., Gisin, P., Höntzsch, D., 1991. The concept of biological plating using the limited contact-dynamic compression plate (LC-DCP): scientific background, design and application. *Injury*, *22*, pp.1-2.

Perez, K. and Patel, R., 2018. Survival of Staphylococcus epidermidis in fibroblasts and osteoblasts. *Infection and immunity*, *86*(10), pp.e00237-18.

Perrin, J.C. and McLaurin, R.L., 1967. Infected ventriculoatrial shunts: a method of treatment. *Journal of neurosurgery*, *27*(1), pp.21-26.

Pidwill, G.R., Gibson, J.F., Cole, J., Renshaw, S.A. and Foster, S.J., 2021. The role of macrophages in Staphylococcus aureus infection. *Frontiers in Immunology*, p.3506.

Pier-Francesco, A., Adams, R.J., Waters, M.G. and Williams, D.W., 2006. Titanium surface modification and its effect on the adherence of Porphyromonas gingivalis: an in vitro study. *Clinical oral implants research*, *17*(6), pp.633-637.

Pivarcsi, A., Kemény, L. and Dobozy, A., 2004. Innate immune functions of the keratinocytes. *Acta microbiologica et immunologica Hungarica*, *51*(3), pp.303-310.

Post, V., Harris, L.G., Morgenstern, M., Mageiros, L., Hitchings, M.D., Méric, G., Pascoe, B., Sheppard, S.K., Richards, R.G. and Moriarty, T.F., 2017. Comparative genomics study of Staphylococcus epidermidis isolates from orthopedic-device-related infections correlated with patient outcome. *Journal of Clinical Microbiology*, *55*(10), pp.3089-3103.

Prieto, J., Eklund, A. and Patarroyo, M., 1994. Regulated expression of integrins and other adhesion molecules during differentiation of monocytes into macrophages. *Cellular immunology*, *156*(1), pp.191-211.

Public Health England, NHS., 2020a, Identification of *Staphylococcus* species, Micrococcus species and *Rothia* species. *UK Standards for Microbiology Invesitgation.* ID 07, Issue number 4. Public health England, London.

Public Health England, NHS., 2020b, Investigation of orthopaedic implant associated infections. *UK Standards for Microbiology Invesitgation.* B 44, Issue number 2.1. Public health England, London.

Qin, Z., Ou, Y., Yang, L., Zhu, Y., Tolker-Nielsen, T., Molin, S. and Qu, D., 2007. Role of autolysin-mediated DNA release in biofilm formation of Staphylococcus epidermidis. *Microbiology*, *153*(7), pp.2083-2092.

Rand, A.I., Armstrong, J., Gregory, M., O'Hara, M., Phiri, K., Harris, L.G., Rohde, H., Siemssen, N., Frommelt, L., Mack, D. and Wilkinson, T.S., 2015. Effects of polysaccharide intercellular adhesin (PIA) in an ex vivo model of whole blood killing and in prosthetic joint infection (PJI): a role for C5a. *International Journal of Medical Microbiology*, *305*(8), pp.948-956.

Rani, S.A., Pitts, B. and Stewart, P.S., 2005. Rapid diffusion of fluorescent tracers into Staphylococcus epidermidis biofilms visualized by time lapse microscopy. *Antimicrobial agents and chemotherapy*, *49*(2), pp.728-732.

Refai, A.K., Textor, M., Brunette, D.M. and Waterfield, J.D., 2004. Effect of titanium surface topography on macrophage activation and secretion of proinflammatory cytokines and chemokines. *Journal of Biomedical Materials Research Part A: 70*(2), pp.194-205.

Reinhardt, C.A., Pelli, D.A. and Sandvold, M., 1985. Cell detachment and growth of fibroblasts as parameters for cytotoxicity of inorganic metal saltsin Vitro. *Cell Biology and Toxicology*, *1*(2), pp.33-43.

Reinke, J.M. and Sorg, H., 2012. Wound repair and regeneration. *European surgical research*, *49*(1), pp.35-43

Ren, X.D., Kiosses, W.B., Sieg, D.J., Otey, C.A., Schlaepfer, D.D. and Schwartz, M.A., 2000. Focal adhesion kinase suppresses Rho activity to promote focal adhesion turnover. *Journal of cell science*, *113*(20), pp.3673-3678.

Richards, R.G., Owen, G.R., Rahn, B.A. and Ap Gwynn, I., 1997. A quantitative method of measuring cell-substrate adhesion areas. *Cells and Materials*, *7*(1), p.2.

Rohde, H., Knobloch, J.K.M., Horstkotte, M.A. and Mack, D., 2001. Correlation of biofilm expression types of Staphylococcus epidermidis with polysaccharide intercellular adhesin synthesis: evidence for involvement of icaADBC genotype-independent factors. *Medical microbiology and immunology*, *190*(3), pp.105-112.

Rohde, H., Kalitzky, M., Kröger, N., Scherpe, S., Horstkotte, M.A., Knobloch, J.K.M., Zander, A.R. and Mack, D., 2004. Detection of virulence-associated genes not useful for discriminating between invasive and commensal Staphylococcus epidermidis strains from a bone marrow transplant unit. *Journal of clinical microbiology*, *42*(12), pp.5614-5619.

Rohde, H., Burdelski, C., Bartscht, K., Hussain, M., Buck, F., Horstkotte, M.A., Knobloch, J.K.M., Heilmann, C., Herrmann, M. and Mack, D., 2005. Induction of Staphylococcus epidermidis biofilm formation via proteolytic processing of the accumulation-associated protein by staphylococcal and host proteases. *Molecular microbiology*, *55*(6), pp.1883-1895.

Rohde, H., Burandt, E.C., Siemssen, N., Frommelt, L., Burdelski, C., Wurster, S., Scherpe, S., Davies, A.P., Harris, L.G., Horstkotte, M.A. and Knobloch, J.K.M., 2007. Polysaccharide intercellular adhesin or protein factors in biofilm accumulation of Staphylococcus epidermidis and Staphylococcus aureus isolated from prosthetic hip and knee joint infections. *Biomaterials*, *28*(9), pp.1711-1720.

Rosenbach, A.J.F., 1884. *Mikro-organismen bei den Wund-infections-krankheiten des Menschen*. JF Bergmann.

Ross, T.D., Coon, B.G., Yun, S., Baeyens, N., Tanaka, K., Ouyang, M. and Schwartz, M.A., 2013. Integrins in mechanotransduction. *Current opinion in cell biology*, *25*(5), pp.613-618.

Sabaté Brescó, M., Harris, L.G., Thompson, K., Stanic, B., Morgenstern, M., O'Mahony, L., Richards, R.G. and Moriarty, T.F., 2017. Pathogenic mechanisms and host interactions in Staphylococcus epidermidis device-related infection. *Frontiers in microbiology*, *8*, p.1401.

Sah, S., Bordoloi, P., Vijaya, D., Amarnath, S.K., Devi, C.S., Indumathi, V.A. and Prashanth, K., 2018. Simple and economical method for identification and speciation of Staphylococcus epidermidis and other coagulase negative Staphylococci and its validation by molecular methods. *Journal of Microbiological Methods*, *149*, pp.106-119.

Sahl, H.G. and Brandis, H., 1981. Production, purification and chemical properties of an antistaphylococcal agent produced by Staphylococcus epidermidis. *Microbiology*, *127*(2), pp.377-384.

Saleh, K., Olson, M., Resig, S., Bershadsky, B., Kuskowski, M., Gioe, T., Robinson, H., Schmidt, R. and McElfresh, E., 2002. Predictors of wound infection in hip and knee joint replacement: results from a 20 year surveillance program. *Journal of Orthopaedic Research*, *20*(3), pp.506-515.

Sanzen, L. and Carlsson, A.S., 1989. The diagnostic value of C-reactive protein in infected total hip arthroplasties. *The Journal of Bone and Joint Surgery. British volume*, *71*(4), pp.638-641.

Schittenhelm, L., Hilkens, C.M. and Morrison, V.L., 2017. β2 integrins as regulators of dendritic cell, monocyte, and macrophage function. *Frontiers in immunology*, p.1866.

Schoenwaelder, S.M. and Burridge, K., 1999. Bidirectional signaling between the cytoskeleton and integrins. *Current opinion in cell biology*, *11*(2), pp.274-286.

Schommer, N.N., Christner, M., Hentschke, M., Ruckdeschel, K., Aepfelbacher, M. and Rohde, H., 2011. Staphylococcus epidermidis uses distinct mechanisms of biofilm formation to interfere with phagocytosis and activation of mouse macrophage-like cells 774A. 1. *Infection and immunity*, *79*(6), pp.2267-2276.

Schwartz-Filho, H.O., Morandini, A.C.F., Ramos-Junior, E.S., Jimbo, R., Santos, C.F., Marcantonio Jr, E., Wennerberg, A. and Marcantonio, R.A.C., 2012. Titanium surfaces with nanotopography modulate cytokine production in cultured human gingival fibroblasts. *Journal of Biomedical Materials Research Part A*, *100*(10), pp.2629-2636.

Sellman, B.R., Timofeyeva, Y., Nanra, J., Scott, A., Fulginiti, J.P., Matsuka, Y.V. and Baker, S.M., 2008. Expression of Staphylococcus epidermidis SdrG increases following exposure to an in vivo environment. *Infection and immunity*, *76*(7), pp.2950-2957.

Sheikh, Z., Brooks, P.J., Barzilay, O., Fine, N. and Glogauer, M., 2015. Macrophages, foreign body giant cells and their response to implantable biomaterials. *Materials*, *8*(9), pp.5671-5701.

Shiau, A.L. and Wu, C.L., 1998. The inhibitory effect of Staphylococcus epidermidis slime on the phagocytosis of murine peritoneal macrophages is interferon-independent. *Microbiology and immunology*, *42*(1), pp.33-40.

Shida, T., Koseki, H., Yoda, I., Horiuchi, H., Sakoda, H. and Osaki, M., 2013. Adherence ability of Staphylococcus epidermidis on prosthetic biomaterials: an in vitro study. *International journal of nanomedicine*, *8*, p.3955.

Shiels, S.M., Mangum, L.H. and Wenke, J.C., 2020. Revisiting the" race for the surface" in a pre-clinical model of implant infection. *European Cells and Materials*, *39*, pp.77-95.

Sidambe, A.T., 2014. Biocompatibility of advanced manufactured titanium implants—A review. *Materials*, *7*(12), pp.8168-8188.

Simon, J.P. and Fabry, G., 1991. An overview of implant materials. *Acta Orthop Belg*, *57*(1), pp.1-5.

Singh, H., Rana, P.K., Singh, J., Singh, S., Prakash, C. and Królczyk, G., 2020. Plasma Spray Deposition of HA–TiO 2 Composite Coating on Ti–6Al–4V Alloy for

Orthopedic Applications. In *Advances in Materials Processing* (pp. 13-20). Springer, Singapore.

Siverino, C., Freitag, L., Arens, D., Styger, U., Richards, R.G., Moriarty, T.F., Stadelmann, V.A. and Thompson, K., 2021. Titanium wear particles exacerbate S. epidermidis-induced implant-related osteolysis and decrease efficacy of antibiotic therapy. *Microorganisms*, *9*(9), p.1945.

Smith, R.S., Smith, T.J., Blieden, T.M. and Phipps, R.P., 1997. Fibroblasts as sentinel cells. Synthesis of chemokines and regulation of inflammation. *The American journal of pathology*, *151*(2), p.317.

Snyder, S., DeJulius, C. and Willits, R.K., 2017. Electrical stimulation increases random migration of human dermal fibroblasts. *Annals of Biomedical Engineering*, *45*(9), pp.2049-2060.

Spiliopoulou, A.I., Kolonitsiou, F., Krevvata, M.I., Leontsinidis, M., Wilkinson, T.S., Mack, D. and Anastassiou, E.D., 2012. Bacterial adhesion, intracellular survival and cytokine induction upon stimulation of mononuclear cells with planktonic or biofilm phase Staphylococcus epidermidis. *FEMS microbiology letters*, *330*(1), pp.56-65.

Spink, W.W. and Vivino, J.J., 1942. The coagulase test for staphylococci and its correlation with the resistance of the organisms to the bactericidal action of human blood. *The Journal of clinical investigation*, *21*(3), pp.353-356.

Stacy, A. and Belkaid, Y., 2019. Microbial guardians of skin health. *Science*, *363*(6424), pp.227-228.

Staton, C.A., Valluru, M., Hoh, L., Reed, M.W.R. and Brown, N.J., 2010. Angiopoietin-1, angiopoietin-2 and Tie-2 receptor expression in human dermal wound repair and scarring. *British Journal of Dermatology*, *163*(5), pp.920-927.

Stewart, P.S., 1998. A review of experimental measurements of effective diffusive permeabilities and effective diffusion coefficients in biofilms. *Biotechnology and bioengineering*, *59*(3), pp.261-272.

Steinhauser, M.L., Kunkel, S.L., Hogaboam, C.M., Evanoff, H., Strieter, R.M. and Lukacs, N.W., 1998. Macrophage/fibroblast coculture induces macrophage inflammatory protein-1a production mediated by intercellular adhesion molecule-1 and oxygen radicals. *Journal of leukocyte biology*, *64*(5), pp.636-641.

Stoakes, L., John, M.A., Lannigan, R., Schieven, B.C., Ramos, M., Harley, D. and Hussain, Z., 1994. Gas-liquid chromatography of cellular fatty acids for identification of staphylococci. *Journal of Clinical Microbiology*, *32*(8), pp.1908-1910.

Street, T.L., Sanderson, N.D., Atkins, B.L., Brent, A.J., Cole, K., Foster, D., McNally, M.A., Oakley, S., Peto, L., Taylor, A. and Peto, T.E., 2017. Molecular diagnosis of orthopedic-device-related infection directly from sonication fluid by metagenomic sequencing. *Journal of clinical microbiology*, *55*(8), pp.2334-2347.

Subbiahdoss, G., Kuijer, R., Grijpma, D.W., van der Mei, H.C. and Busscher, H.J., 2009. Microbial biofilm growth vs. tissue integration:"the race for the surface" experimentally studied. *Acta biomaterialia*, *5*(5), pp.1399-1404.

Takeda, K. and Akira, S., 2005. Toll-like receptors in innate immunity. *International immunology*, *17*(1), pp.1-14.

Tan, K.S., Qian, L., Rosado, R., Flood, P.M. and Cooper, L.F., 2006. The role of titanium surface topography on J774A. 1 macrophage inflammatory cytokines and nitric oxide production. *Biomaterials*, *27*(30), pp.5170-5177.

Tedesco, S., De Majo, F., Kim, J., Trenti, A., Trevisi, L., Fadini, G.P., Bolego, C., Zandstra, P.W., Cignarella, A. and Vitiello, L., 2018. Convenience versus biological significance: are PMA-differentiated THP-1 cells a reliable substitute for blood-derived macrophages when studying in vitro polarization? *Frontiers in pharmacology*, *9*, p.71.

Thomsen, P. and Gretzer, C., 2001. Macrophage interactions with modified material surfaces. *Current Opinion in Solid State and Materials Science*, *5*(2-3), pp.163-176.

Thurlow, L.R., Hanke, M.L., Fritz, T., Angle, A., Aldrich, A., Williams, S.H., Engebretsen, I.L., Bayles, K.W., Horswill, A.R. and Kielian, T., 2011. Staphylococcus aureus biofilms prevent macrophage phagocytosis and attenuate inflammation in vivo. *The Journal of Immunology*, *186*(11), pp.6585-6596.

Tracy, L.E., Minasian, R.A. and Caterson, E.J., 2016. Extracellular matrix and dermal fibroblast function in the healing wound. *Advances in wound care*, *5*(3), pp.119-136.

Trampuz, A. and Zimmerli, W., 2005. Prosthetic joint infections: update in diagnosis and treatment. *Swiss medical weekly*, *135*(17-18), pp.243-251.

Tsuchiya, S., Yamabe, M., Yamaguchi, Y., Kobayashi, Y., Konno, T. and Tada, K., 1980. Establishment and characterization of a human acute monocytic leukemia cell line (THP-1). *International journal of cancer*, *26*(2), pp.171-176.

Turnbaugh, P.J., Ley, R.E., Hamady, M., Fraser-Liggett, C.M., Knight, R. and Gordon, J.I., 2007. The human microbiome project. *Nature*, *449*(7164), pp.804-810.

Turvey, S.E. and Broide, D.H., 2010. Innate immunity. *Journal of Allergy and Clinical Immunology*, *125*(2), pp.S24-S32.

Underhill, D.M., Bassetti, M., Rudensky, A. and Aderem, A., 1999. Dynamic interactions of macrophages with T cells during antigen presentation. *The Journal of experimental medicine*, *190*(12), pp.1909-1914

Vacheethasanee, K., Temenoff, J.S., Higashi, J.M., Gary, A., Anderson, J.M., Bayston, R. and Marchant, R.E., 1998. Bacterial surface properties of clinically isolated Staphylococcus epidermidis strains determine adhesion on polyethylene. *Journal of Biomedical Materials Research: An Official Journal of The Society for Biomaterials, The Japanese Society for Biomaterials, and the Australian Society for Biomaterials*, *42*(3), pp.425-432.

Vallabani, N.S., Alijagic, A., Persson, A., Odnevall, I., Särndahl, E. and Karlsson, H.L., 2022. Toxicity evaluation of particles formed during 3D-printing: cytotoxic, genotoxic, and inflammatory response in lung and macrophage models. *Toxicology*, p.153100.

Van De Kamp, M., Horstink, L.M., Van Den Hooven, H.W., Konings, R.N., Hilbers, C.W., Frey, A., Sahl, H.G., Metzger, J.W. and Van De Ven, F.J., 1995. Sequence analysis by NMR spectroscopy of the peptide lantibiotic epilancin K7 from Staphylococcus epidermidis K7. *European journal of biochemistry*, *227*(3), pp.757-771.

Van Hove, R.P., Sierevelt, I.N., van Royen, B.J. and Nolte, P.A., 2015. Titanium-nitride coating of orthopaedic implants: a review of the literature. *BioMed research international*, *2015*.

Van Wamel, W.J., van Rossum, G., Verhoef, J., Vandenbroucke-Grauls, C.M. and Fluit, A.C., 1998. Cloning and characterization of an accessory gene regulator (agr)-like locus from Staphylococcus epidermidis. *FEMS microbiology letters*, *163*(1), pp.1-9.

Vandecasteele, S.J., Peetermans, W.E., Merckx, R. and Eldere, J.V., 2003. Expression of biofilm-associated genes in Staphylococcus epidermidis during in vitro and in vivo foreign body infections. *The Journal of infectious diseases*, *188*(5), pp.730-737.

Vergidis, P., Rouse, M.S., Euba, G., Karau, M.J., Schmidt, S.M., Mandrekar, J.N., Steckelberg, J.M. and Patel, R., 2011. Treatment with linezolid or vancomycin in combination with rifampin is effective in an animal model of methicillin-resistant Staphylococcus aureus foreign body osteomyelitis. *Antimicrobial agents and chemotherapy*, *55*(3), pp.1182-1186.

Vuong, C. and Otto, M., 2002. Staphylococcus epidermidis infections. *Microbes and infection*, *4*(4), pp.481-489.

Vuong, C., Gerke, C., Somerville, G.A., Fischer, E.R. and Otto, M., 2003. Quorum-sensing control of biofilm factors in Staphylococcus epidermidis. *The Journal of infectious diseases*, *188*(5), pp.706-718.

Vuong, C., Voyich, J.M., Fischer, E.R., Braughton, K.R., Whitney, A.R., DeLeo, F.R. and Otto, M., 2004a. Polysaccharide intercellular adhesin (PIA) protects Staphylococcus epidermidis against major components of the human innate immune system. *Cellular microbiology*, *6*(3), pp.269-275.

Vuong, C., Kocianova, S., Yao, Y., Carmody, A.B. and Otto, M., 2004b. Increased colonization of indwelling medical devices by quorum-sensing mutants of Staphylococcus epidermidis in vivo. *The Journal of infectious diseases*, *190*(8), pp.1498-1505.

Wang, X., Qiu, S., Yao, X., Tang, T., Dai, K. and Zhu, Z.A., 2009. Berberine inhibits Staphylococcus epidermidis adhesion and biofilm formation on the surface of titanium alloy. *Journal of Orthopaedic Research*, *27*(11), pp.1487-1492.

Wang, X., Wang, Y., Bosshardt, D.D., Miron, R.J. and Zhang, Y., 2018. The role of macrophage polarization on fibroblast behavior-an in vitro investigation on titanium surfaces. *Clinical oral investigations*, *22*(2), pp.847-857.

Weintraub, S., Harris, L.G., Thevissen, K. and Lewitus, D.Y., 2018. Polyastaxanthin-based coatings reduce bacterial colonization in vivo. *Materialia*, *3*, pp.15-20.

Welch, W.H., 1891. CONDITIONS UNDERLYING THE INFECTION OF WOUNDS.'. *The American Journal of the Medical Sciences (1827-1924)*, *102*(5), p.439.

West, H.C. and Bennett, C.L., 2018. Redefining the role of langerhans cells as immune regulators within the skin. *Frontiers in Immunology*, *8*, p.1941.

Wi, Y.M. and Patel, R., 2018. Understanding biofilms and novel approaches to the diagnosis, prevention, and treatment of medical device-associated infections. *Infectious Disease Clinics*, *32*(4), pp.915-929.

Wieser, M. and Busse, H.J., 2000. Rapid identification of Staphylococcus epidermidis. *International Journal of Systematic and Evolutionary Microbiology*, *50*(3), pp.1087-1093.

Wiesolek, H.L., Bui, T.M., Lee, J.J., Dalal, P., Finkielsztein, A., Batra, A., Thorp, E.B. and Sumagin, R., 2020. Intercellular adhesion molecule 1 functions as an efferocytosis receptor in inflammatory macrophages. *The American journal of pathology*, *190*(4), pp.874-885.

Willekens, F.L., Werre, J.M., Kruijt, J.K., Roerdinkholder-Stoelwinder, B., Groenen-Döpp, Y.A., van den Bos, A.G., Bosman, G.J. and van Berkel, T.J., 2005. Liver Kupffer cells rapidly remove red blood cell–derived vesicles from the circulation by scavenger receptors. *Blood*, *105*(5), pp.2141-2145.

Williams, R.J., Henderson, B., Sharp, L.J. and Nair, S.P., 2002. Identification of a fibronectin-binding protein from Staphylococcus epidermidis. *Infection and immunity*, *70*(12), pp.6805-6810.

Williams, M.R. and Gallo, R.L., 2015. The role of the skin microbiome in atopic dermatitis. *Current allergy and asthma reports*, *15*(11), p.65.

Winans, S.C. and Bassler, B.L., 2002. Mob psychology. *Journal of bacteriology*, *184*(4), pp.873-883.

Winslow, C.E., Rothberg, W. and Parsons, E.I., 1920. Notes on the classification of the white and orange staphylococci. *Journal of bacteriology*, *5*(2), p.145.

Wong VW, Rustad KC, Akaishi S, Sorkin M, Glotzbach JP, Januszyk M, Nelson ER, Levi K, Paterno J, Vial IN, Kuang AA. Focal adhesion kinase links mechanical force to skin fibrosis via inflammatory signaling. Nature medicine. 2012 Jan;18(1):148-52.

Yao, C., Oh, J.H., Lee, D.H., Bae, J.S., Jin, C.L., Park, C.H. and Chung, J.H., 2015. Toll-like receptor family members in skin fibroblasts are functional and have a higher expression compared to skin keratinocytes. *International Journal of Molecular Medicine*, *35*(5), pp.1443-1450.

Yao, Y., Sturdevant, D.E. and Otto, M., 2005. Genomewide analysis of gene expression in Staphylococcus epidermidis biofilms: insights into the pathophysiology of S. epidermidis biofilms and the role of phenol-soluble modulins in formation of biofilms. *Journal of Infectious Diseases*, *191*(2), pp.289-298.

Yoda, I., Koseki, H., Tomita, M., Shida, T., Horiuchi, H., Sakoda, H. and Osaki, M., 2014. Effect of surface roughness of biomaterials on Staphylococcus epidermidis adhesion. *BMC microbiology*, *14*(1), pp.1-7.

Yokota, M., Häffner, N., Kassier, M., Brunner, M., Shambat, S.M., Brennecke, F., Schniering, J., Marques Maggio, E., Distler, O., Zinkernagel, A.S. and Maurer, B., 2021. Staphylococcus aureus impairs dermal fibroblast functions with deleterious effects on wound healing. *The Federation of American Societies for Experimental Biology Journal*, *35*(7), p.e21695.

Zamir, E. and Geiger, B., 2001. Molecular complexity and dynamics of cell-matrix adhesions. *Journal of cell science*, *114*(20), pp.3583-3590.

Zhang, L., Foxman, B., Gilsdorf, J.R. and Marrs, C.F., 2005. Bacterial genomic DNA isolation using sonication for microarray analysis. *Biotechniques*, *39*(5), pp.640-644.

Zheng, Y., He, L., Asiamah, T.K. and Otto, M., 2018. Colonization of medical devices by staphylococci. *Environmental microbiology*, *20*(9), pp.3141-3153.

Zhou, W., Wang, T., Gan, Y., Yang, J., Zhu, H., Wang, A., Wang, Y. and Xi, W., 2020. Effect of micropore/microsphere topography and a silicon-incorporating modified titanium plate surface on the adhesion and osteogenic differentiation of BMSCs. *Artificial cells, nanomedicine, and biotechnology*, *48*(1), pp.230-241.

Zhu, J., Kamiya, A., Yamada, T., Shi, W. and Naganuma, K., 2003. Influence of boron addition on microstructure and mechanical properties of dental cast titanium alloys. *Materials Science and Engineering: A*, *339*(1-2), pp.53-62.

Zwicker, P., Schmidt, T., Hornschuh, M., Lode, H., Kramer, A. and Müller, G., 2022. In vitro response of THP-1 derived macrophages to antimicrobially effective PHMB-coated Ti6Al4V alloy implant material with and without contamination with S. epidermidis and P. aeruginosa. *Biomaterials Research*, *26*(1), pp.1-13.

Appendices

Appendix A. Human Proteome Profiler XL Array membrane cytokines, abbreviations and spot positions.

Position	Cytokine	Abbreviations
A1/A2	Positive Reference Spot	----
A3/A4	Adiponectin	----
A5/A6	Apolipoprotein A-I	----
A7/A8	Angiogenin	----
A9/A10	Angiopoietin-1	----
A11/A12	Angiopoietin-2	----
A13/A14	B-cell Activating Factor	BAFF
A15/A16	Brain-derived neurotrophic factor	BDNF
A17/A18	Complement component C5/C5a	C5/C5a
A19/A20	Cluster of Differentiation 14	CD14
A21/A22	Cluster of Differentiation 30	CD30
A23/A24	Positive Reference Spot	----
B3/B4	Cluster of Differentiation 40 Ligand	CD40 ligand
B5/B6	Chitinase 3-Like 1	----
B7/B8	Complement Factor D	----
B9/B10	C-Reactive Protein	CRP

B11/B12	Cripto-1	----
B13/B14	Cystatin C	----
B15/B16	Dickkopf-1	Dkk-1
B17/B18	Dipeptidyl Peptidase-4 Inhibitor	DPPIV
B19/B20	Epidermal Growth Factor	EGF
B21/B22	Extracellular Matrix Metalloproteinase Inducer	EMMPRIN
C3/C4	Epithelial Neutrophil-Activating Peptide	ENA-78
C5/C6	Endoglin	----
C7/C8	Fas ligand	----
C9/C10	Fibroblast Growth Factor Basic	FGF basic
C11/C12	Fibroblast Growth Factor 7	FGF-7
C13/C14	Fibroblast Growth Factor 19	FGF-19
C15/C16	FMS-like Tyrosine Kinase 3 Ligand	FLT-3 ligand
C17/C18	Granulocyte Colony-Stimulating Factor	G-CSF
C19/C20	Growth/Differentiation Factor 15 or Macrophage Inhibitory Cytokine	GDF-15/MIC-1
C21/C22	Granulocyte-Macrophage Colony-Stimulating Factor	GM-CSF
D1/D2	Growth Related Oncogene-α	GRO-α/CXCL1
D3/D4	Growth Hormone	GH
D5/D6	Hepatocyte Growth Factor	HGF
D7/D8	Intercellular Adhesion Molecule-1	ICAM-1
D9/D10	Interferon γ	IFN-γ
D11/D12	Insulin Like Growth Factor Binding Protein 2	IGFBP-2
D13/D14	Insulin Like Growth Factor Binding Protein 3	IGFBP-3
D15/D16	Interleukin 1α	IL-1α
D17/D18	Interleukin 1β	IL-1 β
D19/D20	Interleukin 1 Receptor Antagonist	IL-1ra
D21/D22	Interleukin 2	IL-2
D23/24	Interleukin 3	IL-3
E1/E2	Interleukin 4	IL-4
E3/E4	Interleukin 5	IL-5
E5/E6	Interleukin 6	IL-6
E7/E8	Interleukin 8	IL-8/ CXCL8
E9/E10	Interleukin 10	IL-10
E11/E12	Interleukin 11	IL-11
E13/E14	Interleukin 12 p70	IL-12 p70
E15/E16	Interleukin 13	IL-13
E17/E18	Interleukin 15	IL-15
E19/E20	Interleukin 16	IL-16
E21/E22	Interleukin 17A	IL-17A
E23/24	Interleukin 18 Binding Protein	IL-18 Bpa
F1/F2	Interleukin 19	IL-19
F3/F4	Interleukin 22	IL-22
F5/F6	Interleukin 23	IL-23

F7/F8	Interleukin 24	IL-24
F9/F10	Interleukin 27	IL-27
F11/F12	Interleukin 31	IL-31
F13/F14	Interleukin 32	IL-32
F15/F16	Interleukin 33	IL-33
F17/F18	Interleukin 34	IL-34
F19/F20	Interferon Gamma-Induced Protein 10	IP-10/CXCL10
F21/F22	Interferon-Inducible T-cell alpha Chemoattractant	I-TAC/CXCL11
F23/F24	Kallikrein 3	----
G1/G2	Leptin	----
G3/G4	Leukaemia Inhibitory Factor	LIF
G5/G6	Lipocalin-2	----
G7/G8	Macrophage Chemoattractant Protein-1	MCP-1
G9/G10	Monocyte Chemotactic Protein 3	MCP-3
G11/G12	Macrophage Colony-Stimulating Factor	M-CSF
G13/G14	Macrophage Migration Inhibitory Factor	MIF
G15/G16	Monokine Induced by Gamma Interferon	MIG/ CXCL9
G17/G18	Macrophage Inflammatory Protein 1α/1β	MIP-1α/1β
G19/G20	Macrophage Inflammatory Protein 3α	MIP-3α
G21/G22	Macrophage Inflammatory Protein 3β	MIP-3β
G23/G24	Matrix Metalloprotease	MMP-9
H1/H2	Myeloperoxidase	----
H3/H4	Osteopontin	----
H5/H6	Platelet Derived Growth Factor AA	PDGF-AA
H7/H8	Platelet Derived Growth Factor AB/BB	PDGF-AB/BB
H9/H10	Pentraxin 3	----
H11/H12	Platelet Factor 4	PF4
H13/H14	Receptor for Advanced Glycation Endproducts	RAGE
H15/H16	Regulated Upon Activation, Normal T cell Expressed, and Secreted	RANTES/CCL5
H17/H18	Retinol Binding Protein 4	RBP-4
H19/H20	Relaxin-2	----
H21/H22	Resistin	----
H23/H24	Stromal Cell-Derived Factor 1α	SDF-1α
I1/I2	Serpin E1	----
I3/I4	Sex Hormone-Binding Globulin	SHBG
I5/I6	Interleukin 1 Receptor-Like 1	ST2/ IL1RL1
I7/I8	Thymus- and Activation-Regulation Chemokine	TARC/CCL17
I9/I10	Trefoil Factor 3	TFF3
I11/I12	Transferrin Receptor	TfR/ CD71
I13/I14	Transforming Growth Factor α	TGF-α
I15/I16	Thrombospondin-1	----
I17/I18	Tumour Necrosis Factor α	TNF-α
I19/I20	Urokinase Plasminogen Activator Receptor	uPAR

Position	Cytokine	Abbreviations
I21/I22	Vascular Endothelial Growth Factor	VEGF
J1/J2	Positive Reference Spots	----
J5/J6	Vitamin D BP	----
J7/J8	Platelet Endothelial Cell Adhesion Molecule	PECAM-1/CD31
J9/J10	T-cell Immunoglobulin and Mucin-Domain Containing-3	TIM-3
J11/J12	Vascular Cell Adhesion Molecule 1	VCAM-1
J23/24	Negative Reference Spots	----

Appendix B. Human Proteome Profiler Array membrane cytokines, abbreviations and spot positions.

Position	Cytokine	Abbreviations
A1/A2	Positive Reference Spot	----
A3/A4	CCL1	TCA-3
A5/A6	Macrophage Chemoattractant Protein-1	MCP-1
A7/A8	Macrophage Inflammatory Protein 1α/1β	MIP-1α/1β
A9/A10	Regulated Upon Activation, Normal T cell Expressed, and Secreted	RANTES/CCL5
A11/A12	Cluster of Differentiation 40 Ligand	CD40 ligand
A13/A14	Complement component C5/C5a	C5/C5a
A15/A16	Growth Related Oncogene-α	GRO-α/CXCL1
A17/A18	Interferon Gamma-Induced Protein 10	IP-10/CXCL10
A19/A20	Reference Spots	----
B3/B4	Interferon-Inducible T-cell alpha Chemoattractant	I-TAC/CXCL11
B5/B6	Stromal Cell-Derived Factor 1	SDF-1/CXCL12
B7/B8	Granulocyte Colony-Stimulating Factor	G-CSF
B9/B10	Granulocyte-Macrophage Colony-Stimulating Factor	GM-CSF
B11/B12	Intercellular Adhesion Molecule-1	ICAM-1
B13/B14	Interferon γ	IFN-γ
B15/B16	Interleukin 1α	IL-1α
B17/B18	Interleukin 1β	IL-1 β

C3/C4	Interleukin 1 Receptor Antagonist	IL-1ra
C5/C6	Interleukin 2	IL-2
C7/C8	Interleukin 4	IL-4
C9/C10	Interleukin 5	IL-5
C11/C12	Interleukin 6	IL-6
C13/C14	Interleukin 8	IL-8/ CXCL8
C15/C16	Interleukin 10	IL-10
C17/C18	Interleukin 12 p70	IL-12 p70
D3/D4	Interleukin 13	IL-13
D5/D6	Interleukin 16	IL-16
D7/D8	Interleukin 17A	IL-17A
D9/D10	Interleukin 17E	IL-17E
D11/D12	Interleukin 18	IL-18
D13/D14	Interleukin 21	IL-21
D15/D16	Interleukin 27	IL-27
D17/D18	Interleukin 32α	IL-32α
E1/E2	Positive Reference Spots	----
E3/E4	Macrophage Migration Inhibitory Factor	MIF
E5/E6	Serpin E1	----
E7/E8	Tumour Necrosis Factor α	TNF-α
E9/E10	Triggering Receptor Expressed on Myeloid Cells	TREM-1
E19/E20	Negative Reference Spots	----

Appendix C. A table displaying the cytokines expressed by THP-1 macrophages in mono-culture or co-culture with *S. epidermidis* 5179-R1 in the absence or presence of Ti discs (n=1).

Cytokine	THP-1 No Ti	THP-1 + 5179-R1 24 h No Ti	THP-1 With Ti	THP-1 + 5179-R1 6 h With Ti	THP-1 + 5179-R1 24 h With Ti
Angiopectin-2	×	n/a	×	×	+
CD14	×	n/a	+	×	×
CD40 ligand	×	×	×	×	+
Chitinase 3-like 1	+++	n/a	+++	+++	+++
Complement factor D	+++	n/a	++	+	+++
Cystatin C	++	n/a	++	×	+
Dkk-1	×	n/a	×	×	+
EMMPRIN	+	n/a	++	+	+++
Endoglin	×	n/a	×	×	+
FGF-19	+	n/a	+	+	+++
G-CSF	×	×	×	×	+
GDF-15	+++	n/a	+++	+++	+++
GM-CSF	×	×	×	×	+
GROα	×	+	+	++	+++
ICAM-1	×	+	+	×	+++
IGFBP-2	+	×	×	×	×
IGFBP-3	+	n/a	+++	×	×
IL-1α	×	×	×	×	+++
IL-1β	×	+	×	+	+++
IL-1ra	+	×	++	×	++
IL-4	×	×	×	×	+
IL-8	+++	++	+++	+++	+++
IL-17A	+	×	+	×	+

IL-24	×	n/a	×	×	+
IL-27	×	×	×	×	+
IP-10	×	++	++	×	+
MCP-1	×	×	+++	×	+
MIF	+	+	+++	+++	+++
MIP-1α/MIP-1β	+	+++	+++	+++	+++
MIP-3α	×	n/a	+++	+++	+++
MMP-9	+++	n/a	+++	+++	+++
Osteopontin	+++	n/a	+++	+++	+++
PDGF-AA	+++	n/a	+++	+++	+++
RANTES	+++	+	+++	+++	+++
SDF-1α	×	×	+	×	+
Serpin E1	×	×	+++	×	+
SHBG	×	n/a	×	×	+
TNF-α	×	+	++	+++	+++
uPAR	+++	n/a	+++	+++	+++
VEGF	×	n/a	+++	+++	+++
Vitamin D BP	×	n/a	×	×	+
CD31	+++	n/a	+++	++	+++
TIM-3	+++	n/a	+++	+++	+++

× = no expression (mean pixel density <10), + = low expression (mean pixel density = 10-50), ++ = positive expression (meal pixel density = 51-100), +++ = High expression (mean pixel density >101) and n/a= not present on cytokine array.

Appendix D. A table displaying the cytokines expressed by 1BR.3.G fibroblasts in mono-culture or co-culture with *S. epidermidis* 5179-R1 in the absence or presence of Ti discs (n=1).

Cytokine	1BR.3.G No Ti	1BR.3.G With Ti	1BR.3.G + 5179-R1 6 h With Ti	1BR.3.G + 5179-R1 24 h With Ti
Angiogenin	++	+	×	+
Angiopoietin-2	×	+	+	×
BDNF	+	+	×	×
Cystatin C	+	+	×	×
Dkk-1	+++	+++	+++	+++
DPPIV	×	×	×	+
EMMPRIN	×	×	×	++
Endoglin	×	×	×	++
FGF basic	×	×	×	++
FGF-19	+	+	+	+
MIC-1	×	×	×	+
GROα	×	×	×	+
IFN-γ	×	+	+	×
IL-8	+++	+++	+++	+++
IL-17A	+	×	×	+
MIF	×	+	+	+++
Osetopontin	+	+	+	+
Pentraxin 3	+	++	+	++
SDF-1α	++	++	+	+
Serpin E1	+++	+++	+++	+++
SHBG	+	+	+	+
Thrombospondin-1	+	+	×	×
uPAR	×	×	×	++
VEGF	×	×	×	+
Vitamin D BP	×	+	×	×

× = no expression (mean pixel density <10), + = low expression (mean pixel density = 10-50), ++ = positive expression (meal pixel density = 51-100), +++ = High expression (mean pixel density >101).

Appendix E. A table displaying the cytokines expressed by 1BR.3.G fibroblasts in mono-culture or co-culture with *S. epidermidis* 5179-R1 in the absence or presence of blood coated Ti discs (n=1).

Cytokine	1BR.3.G Blood Coated Ti	1BR.3.G + 5179-R1 6 h Blood Coated Ti	1BR.3.G + 5179-R1 24 h Blood Coated Ti
GROα	++	++	++
G-CSF	+++	+++	+++
GM-CSF	+	+	+
ICAM-1	+	+	+
IL-1α	+	×	×
IL-2	+	+	×
IL-6	+++	+++	+++
IL-8	+++	+++	+++
IL-16	+	+	×
IL-18	+	+	+
MCP-1	+	×	×
MIF	+++	+++	+
MIP-1α/MIP-1β	+	+	+
RANTES	+	+	+
SDF-1α	++	+	×
Serpin E1	+++	+++	+++
TNF-α	+	+	+

× = no expression (mean pixel density <10), + = low expression (mean pixel density = 10-50), ++ = positive expression (meal pixel density = 51-100), +++ = High expression (mean pixel density >101)